



Dipl.-Ing. Konstantin Weller, BSc

# **Emission Models for Heavy Duty Vehicles Based on On-road Measurements**

## **DISSERTATION**

to achieve the university degree of  
Doktor der technischen Wissenschaften

submitted to

**Graz University of Technology**

Supervisor

Ao.Univ.-Prof. Dipl.-Ing. Dr.techn. Stefan Hausberger  
Institute of Internal Combustion Engines and Thermodynamics

Prof. Mech. Eng. PhD Leonidas Ntziachristos  
Laboratory of Applied Thermodynamics, Aristotle University of Thessaloniki

Graz, April 2020

The author would like to thank the independent laboratories in Europe that provided important measurement data for this project. The work would not have been possible without support from “Umweltbundesamt Deutschland” and “Umweltbundesamt Österreich”. Further thanks also go to the funding organisations of the ERMES Group, “BAFU” from Switzerland, “ADEME” from France, “Trafikverket” from Sweden and “SFT” from Norway.

## Vorwort

Die Arbeit ist im Rahmen meiner wissenschaftlichen Tätigkeit in der Forschungsgesellschaft für Verbrennungskraftmaschinen und Thermodynamik entstanden. Ich möchte mich ganz herzlich für diese Möglichkeit und die hervorragende Betreuung bei Prof. Stefan Hausberger bedanken. Außerdem möchte ich mich bei der TU Graz bedanken, an der ich mein Maschinenbaustudium erfolgreich abschließen durfte sowie die Möglichkeit der Dissertation nutzen konnte.

Mein weiterer Dank gilt:

Prof. Leonidas Ntziachristos für die Begutachtung meiner Arbeit,

Dr. Martin Rexeis für die tolle Unterstützung bei jeglichen Fragestellungen zu Messung oder Simulation,

ganz besonders meinen Bürokollegen Martin, Lukas und FJ, die immer für eine herausragende Stimmung im Büro gesorgt haben,

natürlich dem Team der LKW Rolle mit Thomas, Werner und Mario, die jeden Messauftrag sehr gewissenhaft durchgeführt haben und praktisch jedes Problem gelöst haben,

Bernhard für die unermüdliche Programmierarbeit am ERMES Tool,

Pipa für die Unterstützung bei jeglichen EDV-Problemen,

und natürlich auch bei Alexandra, Silke, Claus, Martin O., Martin D., Gérard, Markus und Gerald, für die tolle Zusammenarbeit und das entspannte Arbeitsklima.

Mein ganz besonderer Dank gilt meiner Frau Sigrid, die mich immer unterstützt hat und mir in jeder Lage mit Rat und Tat zur Seite gestanden hat.

Auch bei meinen Eltern möchte ich mich ganz herzlich für die Möglichkeit bedanken, diesen Lebensweg einzuschlagen.

Ein ganz großer Dank gilt auch meiner Oma für Ihre Unterstützung und Ihr Vertrauen in mich.

Mein Dank gilt auch meinen Schwiegereltern, Monika und Werner, die mich stetig ermutigt und unterstützt haben.

Schließlich bedanke ich mich bei meinen Freundinnen und Freunden, die mich während dieser Zeit begleitet haben.

## **Eidesstattliche Erklärung**

Ich erkläre an Eides statt, dass ich die vorliegende Arbeit selbstständig verfasst, andere als die angegebenen Quellen/Hilfsmittel nicht benutzt, und die den benutzten Quellen wörtlich und inhaltlich entnommenen Stellen als solche kenntlich gemacht habe. Das in TUGRAZonline hochgeladene Textdokument ist mit der vorliegenden Dissertation identisch.

I declare that I have authored this thesis independently, that I have not used other than the declared sources/resources, and that I have explicitly indicated all material which has been quoted either literally or by content from the sources used. The text document uploaded to TUGRAZonline is identical to the present dissertation.

Konstantin Weller

Graz, 16.04.2020

---

## Table of contents

Vorwort .....	III
Eidesstattliche Erklärung.....	IV
Table of contents .....	V
Formula symbols, abbreviations and indices .....	VII
Zusammenfassung.....	X
Abstract .....	XI
1 Introduction .....	1
2 Objective of work.....	3
3 Background .....	5
3.1 Emission Standards for Heavy Duty Vehicles .....	5
3.2 Emission Reduction Systems .....	6
3.2.1 Internal Engine Modifications.....	6
3.2.2 Exhaust After-treatment System .....	7
3.3 Handbook Emission Factors for Road Transport.....	9
4 Measurement Program for the HBEFA.....	12
4.1 Chassis Dyno.....	12
4.2 On-road Testing.....	13
4.3 Measurement Results .....	15
4.3.1 Regulated Pollutants.....	16
4.3.2 Non-Regulated Pollutants .....	22
5 Evaluation of Emission Measurements .....	23
5.1 Main Effects which Distort Instantaneous Data from Emission Testing .....	23
5.2 Algorithms for Emission Mass Calculation from the Analysers to the Engine .....	26
5.2.1 Analyse Response and Dead Time Correction.....	26
5.2.2 Correction of Transport Time in the Diluted Measurement System .....	26
5.2.3 Correction of Variable Transport Time in the Undiluted Measurement System ..	27
5.3 Practical Applications .....	32
5.3.1 Application to Test Measurements with Known Reference Signal .....	32
5.3.2 Application to Full Vehicle Tests.....	33
5.3.3 “Short Test” for Calibration of Volume of Vehicles’ Exhaust System.....	35
5.3.4 Influence of Differences in the Response Characteristics of Exhaust Mass Flow and Concentration Measurement on the Results of the Variable Time Shift Method .....	37
6 Simulation Model PHEM.....	38
6.1 Standard Simulation Process .....	38
6.2 Exhaust After-treatment Model.....	40
6.2.1 Temperature Model.....	40

---

6.2.2	SCR Simulation.....	42
6.3	Gear Shift Model.....	49
6.3.1	HGV .....	50
6.3.2	City Busses.....	53
7	Heavy Duty Emission Model .....	57
7.1	Database .....	57
7.1.1	Database of New Vehicle Registration EU-28.....	57
7.1.2	HDV Emission Database.....	57
7.2	Vehicle Data.....	58
7.3	Engine Maps for Fuel Consumption .....	60
7.4	Models for Pollutant Emissions .....	61
7.5	Adjustment of NO <sub>x</sub> Emission Models.....	69
7.5.1	Heavy Goods Vehicles – NO <sub>x</sub> Emission Model.....	70
7.5.2	City busses – NO <sub>x</sub> Emission Model .....	74
7.5.3	Vehicles below 7.5 Tons – NO <sub>x</sub> Emission Model.....	75
7.6	Deterioration Function .....	77
7.7	Elaboration of N <sub>2</sub> O and NH <sub>3</sub> EFAs for HDVs.....	82
8	HDV Results for the HBEFA 4.1 .....	87
8.1	Introduction of New Driving and Preconditioning Cycles.....	87
8.2	Comparison between Simulation Models for HBEFA 3.3 and HBEFA 4.1 .....	88
8.3	Results HBEFA 4.1 .....	92
8.3.1	34–40t Tractor Semi-trailer Combination .....	93
8.3.2	< 7.5 Tons Rigid Truck .....	96
8.3.3	Coach.....	97
8.3.4	3-Axle City Bus.....	99
9	Conclusion and Outlook.....	101
	References .....	104
	Annex .....	108
	Index of figures .....	118
	Index of tables .....	122

## Formula symbols, abbreviations and indices

### Latin formula symbols

A	m <sup>2</sup>	Cross Sectional Area
AF	-	Adjustment Factor
BSE	g/kWh	Brake Specific Emissions
Cd	-	Drag Coefficient
CR	-	Conversion Rate
EC	ppm	Emission Concentration
EFA	g/km	Emission Factor
EM	kg	Emission Mass
EMF	kg/s	Emission Mass Flow
EnC	kWh/km	Energy Consumption
ExMF	kg/s	Exhaust Mass Flow
ExVF	m <sup>3</sup> /s	Exhaust Volume Flow
Factor	-	Factor for the Adjustment of the Conversion Rate
M	g/mol	Molar Mass
n	rpm	Engine Speed
NH <sub>3</sub> dosing	mol/s	Dosing Level of NH <sub>3</sub>
NH <sub>3</sub> stor.	kg	NH <sub>3</sub> -mass Stored in the SCR Catalyst
NO <sub>x</sub> EO	g	NO <sub>x</sub> Engine Out
NO <sub>x</sub> TP	g	NO <sub>x</sub> Tailpipe
P	kW	Engine Power
p	Pa	Pressure
RRC	N/kN	Rolling Resistance Coefficient
SV	1/s	Space Velocity
T	K	Temperature
TT	s	Transport Time
t	s	Time
V	m <sup>3</sup>	Volume
VF	m <sup>3</sup> /s	Volume Flow

### Constants

$R_{Air} = 287.1$	J/(kg*K)	Specific gas constant of air
-------------------	----------	------------------------------

### Operators

$\Delta$		Difference between two values
----------	--	-------------------------------

### Abbreviations and indices

adj	Adjusted
AMT	Automated Manual Transmission
artic	Articulated
AT	Automatic Transmission
AT	Articulated Truck
CAN	Controller Area Network
cat	Catalyst
CB	City Bus
CF	Conformity Factor
CO	Coach
CO	Carbon Monoxide

CO <sub>2</sub>	Carbon Dioxide
CPC	Condensation Particle Counter
CR	Conversion Rate
Cu	Copper
CUC	Clean-up Catalyst
CVS	Constant Volume Sampling
det	Deterioration
DOC	Diesel Oxidation Catalyst
diff	Difference
DPF	Diesel Particle Filter
EGR	Exhaust Gas Recirculation
EFA	Emission Factor
EFM	Exhaust Flow Meter
ELR	European Load Ramp
EM	Emission Mass
EO	Engine Out
ERMES	European Research for Mobile Emission Sources
ESC	European Stationary Cycle
ETC	European Transient Cycle
EU	European Union
FC	Fuel Consumption
Fe	Iron
FTIR	Fourier-Transform Infrared Spectroscopy
GPS	Global Positioning System
grd	gradient
GVM	Gross Vehicle Mass
HBEFA	Handbook Emission Factors for Road Transport
HC	Hydrocarbons
HDV	Heavy Duty Vehicle
HGV	Heavy Goods Vehicle
HNCO	Isocyanic acid
ICE	Internal Combustion Engine
int	Intervention
ISC	In-service Conformity
IVT	Institute for Internal Combustion Engines and Thermodynamics
LCV	Light Commercial Vehicle
LDV	Light Duty Vehicle
max	Maximum
MAW	Moving Average Window
meas	Measurement
min	Minimum
MT	Manual Transmission
n	Index for Time Step
(NH <sub>2</sub> ) <sub>2</sub> CO	Urea
NH <sub>3</sub>	Ammonia
NO	Nitrogen Monoxide
NO <sub>2</sub>	Nitrogen Dioxide
NO <sub>x</sub>	Nitrogen Oxides
norm	Normalised
N <sub>2</sub> O	Nitrous Oxide
OBD	On-board Diagnosis

---

OCE	Off-cycle Emissions
OEM	Original Equipment Manufacturer
PC	Passenger Car
PEMS	Portable Emission Measurement System
PHEM	Passenger Car and Heavy Duty Emission Model
PM	Particulate Matter
PN	Particle Number
res	Result
RDE	Real Drive Emissions
RRC	Rolling Resistance Coefficient
RT	Rigid Truck
RWC	Real World Cycle
SCR	Selective Catalytic Reduction
sim	Simulation
Std	Standard
stor	Storage
TC	Turbocharger
temp	Temperature
TP	Tailpipe
TPMLM	Technically Permissible Maximum Laden Mass
TT	Tractor Trailer
TUG	Graz University of Technology
TU Graz	Graz University of Technology
Ubus	Urban Bus
VECTO	Vehicle Energy Consumption Simulation Tool
WHSC	World Harmonized Stationary Cycle
WHTC	World Harmonized Transient Cycle
WHVC	World Harmonized Vehicle Cycle

## Zusammenfassung

Die Schadstoffemissionen des Verkehrssektors haben einen großen Einfluss auf die Luftqualität in Europa. Um in diesem Bereich Verbesserungen zu erzielen, wird der maximale Schadstoffausstoß pro Fahrzeug durch die Verschärfung der Emissionsgesetzgebung immer stärker begrenzt. Natürlich müssen Datenbanken wie zum Beispiel das Handbuch Emissionsfaktoren (HBEFA), das Emissionswerte für alle Emissionsklassen und Fahrzeugkategorien für alle relevanten Verkehrssituationen beinhaltet, somit auch ständig auf den neuesten Stand gebracht werden. Aus diesem Grund wurde die neue Version, das HBEFA 4.1, im September 2019 veröffentlicht. Diese Dissertation beschreibt die Arbeiten beginnend mit den Messungen bis hin zur Erstellung von Simulationsmodellen und die Berechnung der finalen Emissionsfaktoren im Bereich der schweren Nutzfahrzeuge.

Das Messprogramm am Rollenprüfstand wurde auf die speziellen Eigenschaften von Euro<sup>o</sup>VI schweren Nutzfahrzeugen angepasst und um Messungen im realen Straßenverkehr ergänzt. Dabei wurde auch darauf geachtet, dass neben den Standardbetriebsbedingungen auch Niederlastzyklen gemessen werden. Insgesamt wurden im Rahmen der Arbeiten für das HBEFA 35 Nutzfahrzeuge vermessen, wobei neben Fahrzeugen mit geringer Laufleistung auch speziell Fahrzeuge mit einer Laufleistung von mindestens 500 000 km vermessen wurden, um mögliche Alterungseffekte hinsichtlich des Emissionsverhaltens erkennen zu können. Für die Zuordnung von Emissionen zu ihren jeweiligen Motorbetriebspunkten wurde eine neue Auswertemethodik entwickelt, die die variablen Gaslaufzeiten vom Motor bis zu den verschiedenen Analysatoren in Abhängigkeit vom Massenstrom korrigiert. Bei der auf diesen Messdaten basierenden Simulationsmodellentwicklung stellte sich die Abbildung der NO<sub>x</sub>-Konvertierungsraten im SCR-Katalysator, vor allem in langanhaltenden Niederlastphasen, als größte Herausforderung dar. Um diese möglichst genau darstellen zu können, wurde die gesamte Abgasnachbehandlung modelliert und die SCR-Konvertierung wird in Abhängigkeit von Temperatur, Raumgeschwindigkeit und Ammoniakspeicherstand berechnet. Zudem erhöhen neue Fahrzeug- und Gangschaltmodelle die Genauigkeit der Leistungs- und Drehzahlberechnung auf Basis der Längsdynamik.

Die finalen Emissionsfaktoren zeigen, dass Fahrzeuge mit der Abgasnorm Euro<sup>o</sup>VI im realen Straßenverkehr eine deutliche Emissionsreduzierung, speziell bei Partikelanzahl und Stickoxiden, im Vergleich zu früheren Emissionsstufen mit sich bringen. Da die Verbesserungen im Niederlastbereich am größten sind, wirken sich diese bei Stadtbussen aufgrund des städtischen Standardlastprofils am stärksten aus. Zudem ist zu beachten, dass sich die NO<sub>x</sub>-Emissionen von Euro<sup>o</sup>VI Fahrzeugen mit steigender Laufleistung bis zum 2,5-fachen des Werts bei 50 000 km erhöhen.

## Abstract

Pollutant emissions from the transport sector have a major impact on air quality in Europe. In order to achieve improvements in this area, legislation stipulates increasingly stringent emission limits per vehicle. Of course, databases such as the Handbook for Emission Factors for Road Transport (HBEFA), which contains the emission factors for every emission class and vehicle category in all relevant traffic situations, must be regularly updated. For this reason, the new version, HBEFA 4.1, was published in September 2019. This dissertation describes the work in the field of heavy duty vehicles starting with the measurements up to the creation of simulation models and the calculation of the final emission factors.

The measurement program on the chassis dynamometer was adapted to the special characteristics of Euro<sup>o</sup>VI heavy duty vehicles and supplemented by measurements in real road traffic. In addition to the standard operating conditions also low-load cycles were measured. The whole campaign for the HBEFA comprised 35 vehicles; in addition to vehicles with low mileage, it also included the measurement of special vehicles with a mileage of at least 500 000 km in order to identify possible deterioration effects on the emission behaviour. Another point was the development of a new evaluation methodology to assign emissions to their respective engine operating points. This feature corrects the variable gas transport times from the engine to the various analysers as a function of exhaust mass flow. In the simulation model development based on these measurement data, the calculation of the NO<sub>x</sub> conversion rates in the SCR catalytic converter, especially in long-lasting low-load phases, proved to be the greatest challenge. In order to be able to represent these rates as accurately as possible, the entire exhaust after-treatment was modelled and the SCR conversion is simulated as a function of temperature, space velocity and ammonia storage level. In addition, new vehicle and gear shift models increase the accuracy of engine power and speed calculations based on longitudinal dynamics.

The final emission factors show that vehicles complying with the Euro<sup>o</sup>VI emission standard are on a low emission level in real road traffic, especially in terms of particle numbers and nitrogen oxides, compared with earlier emission levels. Since improvements are greatest in the low-load range, they have the biggest effect on city buses due to the standard urban load profile. It should also be noted that NO<sub>x</sub> emissions of Euro<sup>o</sup>VI vehicles raise up to 2.5 times with increasing mileage as compared to the value at 50 000 km.



# 1 Introduction

Humans have always had the desire to move freely without any boundaries. In the last century, the passenger transport sector took an important step towards satisfying human demands by the comprehensive introduction of vehicles driven by internal combustion engines. But, of course, this achievement also creates problems—as is always the case with new developments. Beside noise, congestion, water pollution and other impacts, the formation of emissions during the combustion process of fossil fuels is a main issue. On the one hand, there is the natural combustion product CO<sub>2</sub>, which has a big impact on the greenhouse gas effect, and on the other hand, there are the unintended pollutant emissions like CO, HC, NO<sub>x</sub> or particles [1]. These components have a negative influence on human health, which is especially critical in large cities due to the big amount of traffic in a relatively small area [2].

Engine driven vehicles do not only play a major role in the passenger transport sector, but also in the commercial vehicle sector. Further economic developments and the ongoing globalisation came along with progress in the on-road transport of goods. Of course, there are other possibilities like trains or ships, but, for example, in Germany, the share of on-road transport in the commercial sector is more than 70 percent and there is no trend towards a reduction in the coming years [3]. However, this leads to problems focusing on the emission situation. The CO<sub>2</sub> emissions produced by heavy duty vehicles account for approximately a quarter of the total CO<sub>2</sub> in the on-road sector [4] and also the majority of NO<sub>x</sub>-emissions can be attributed to diesel driven vehicles [5].

As a consequence, the current discussion about air quality in urban areas deals a lot with bans for vehicles with diesel engines as propulsion system. But some people disregard the fact that diesel engines are much more efficient compared to petrol driven vehicles. Thus, a ban of diesel vehicles is not reasonable regarding the CO<sub>2</sub> issue. Of course, the logical trend is towards alternative propulsion systems, which currently focus on battery electric and hydrogen fuel cell vehicles. However, both categories also bring some problems besides their major advantages of zero tailpipe emissions, high efficiency and a clear reduction of noise. Regarding battery electric vehicles, the production is very energy consuming and, of course, daily operation also needs electric power. If it is not produced in a renewable way, e.g. sun or wind power, the CO<sub>2</sub>-benefit is more or less negligible. When it comes to general usage, the limited travel range is also an issue, especially for heavy duty vehicles. Fuel cell vehicles have almost the same refuelling performance as conventional diesel or petrol driven vehicles and consequently do not face any problems in this particular area; however, the production of hydrogen requires high amounts of electrical energy, which can result in corresponding CO<sub>2</sub> emissions, if produced from natural gas, as is usual today. Of course, the only reasonable way to save CO<sub>2</sub> is to produce hydrogen in a renewable way. Another issue for fuel cell vehicles are the asset costs, which are currently very high and pose a problem especially for the mass market. A summary of all these challenges leads to the conclusion, that the total changeover to alternative propulsion systems is not to be expected in the coming years. Especially the commercial vehicle sector sets a big challenge because of the huge energy demand due to high vehicle masses and long daily distances driven by a large share of the fleet. However, the long-term development of shares of the various systems will be an interesting topic in the future, influenced by environmental, economic and also political aspects. [6] [7]

Since diesel will remain a main fuel for trucks and busses in the next years, further development of fuel saving and emission reduction technologies in this field is requested for improving air quality and limiting greenhouse gases. The last years showed that checking of real drive emissions is mandatory to gain information about the development of the entire emission situation and possible effects of single measures like stricter emission regulations. This is mainly done by vehicle measurements based on a focused test program, which covers

all relevant driving situations and boundary conditions. In doing so, on-road testing with portable emission measurement systems has turned out to be a reasonable supplement to chassis dyno measurements. Of course, measuring every vehicle is not possible, but a well-balanced mix of single vehicle measurements of different brands and vehicle categories can provide a clear picture regarding the entire fleet. Furthermore, this data can also be used as a base for simulation tools, which have become more and more important in recent years. As shown in the present thesis, simulation tools are relevant for putting test data from different on-board tests onto a comparable basis, since loading, route, traffic conditions etc. are different and cause different emission levels.

Simulation tools are also relevant for assessing impacts of various measures in the transport sector; actions like a ban of single vehicle categories or different speed limits can be investigated without big effort by using such tools. Contrary to that, measuring these effects would be very expensive and time consuming. Consequently, simulation tools are important, but a reasonable combination of simulation and vehicle or engine testing is the best way for future emission research work and the resulting improvement of air quality and effective CO<sub>2</sub> reduction.

## 2 Objective of work

Stricter emission limits and new boundary conditions lead to new versions of the Handbook of Emission Factors for Road Transport, in this case the HBEFA 4.1. These periodic updates guarantee state-of-the-art emission factors and consequently provide actual information about on-road emission behaviour. The previous version HBEFA 3.3 already includes data of the current emission level Euro<sup>o</sup>VI, but this data only comprises chassis dyno measurements of a small number of vehicles. In particular, regulatory real-drive emission (RDE) tests with on board emission measurements in real operation are not covered by any measurement data in HBEFA 3.3. As a consequence, the Euro<sup>o</sup>VI emission factors had to be reworked for the HBEFA 4.1 to serve as a reasonable database for further use (e.g. in air quality models), for identifying possible remaining shortcomings in the real world emission behaviour of Euro<sup>o</sup>VI HDVs or for deciding about bans for single vehicle categories in urban areas.

The related research questions for the present thesis are:

- How can the emission behaviour in any driving situation be assessed based on a limited number of on-road tests per vehicle?
- Do recorded signals from a PEMS system need post-processing to be used as a model input?
- Can a proper method for the use of PEMS data be implemented in the vehicle simulation tool PHEM, which in the past was used for the calculation of emission factors?
- Does the simulation of current EURO<sup>o</sup>VI vehicles need additional or different methods to reflect the real world emission behaviour?

The first section of this thesis implies the main task of this work: the generation of emission factors for the new version of the HBEFA with a focus on Euro<sup>o</sup>VI heavy duty vehicles. Since mainly Euro<sup>o</sup>V and VI vehicles are currently on the road in Central European Countries and, of course, there is a clear future trend towards a majority of Euro<sup>o</sup>VI vehicles, these are the main relevant categories. The HBEFA 3.3 already provides a sufficient database for Euro<sup>o</sup>V vehicles, but, as already mentioned, the database for Euro<sup>o</sup>VI had to be extended by on-road tests in particular. The following sections explain the most relevant subtasks for the creation of new emission factors.

The first step is the setup of a measurement program which includes both on-road and chassis dyno tests. Here, the main challenge is the variability of on-road tests. The question is how to design the tests in order to gain comparable results and how to combine all data in a reasonable way.

Before the measurement data is processed, it has to be evaluated. Focusing on this point, the main challenge is the correct time alignment of emissions to their engine operating points. Time alignment becomes important when emissions shall be allocated to special engine operating points or states of the after-treatment system. For this purpose, an approach was developed for correcting the variable transport times in the undiluted part of the measurement system and the not ideal response characteristic of the analysers.

The next step is the setup of a comprehensive emission model based on the prepared measurement data. This simulation model shall provide fuel consumption and the main emission components for all relevant traffic situations. For that reason, some special features were developed and integrated such as a SCR catalyst model, deterioration functions dependent on the vehicle mileage and an updated gear shift model for trucks and urban busses for an improvement of the engine speed simulation.

The last step is the generation of the final emission factors for every heavy duty vehicle category and every emission level for all different traffic situations.

### 3 Background

This thesis deals mainly with emissions of heavy duty vehicles (HDV), which include heavy goods vehicles (HGV), city busses (CB) and coaches (CO). For that reason, this chapter first gives an overview of the development of the emission regulation for HDVs in Europe and the state of the art regarding emission reduction strategies. As a last point, this chapter explains the Handbook Emission Factors for Road Transport, which provides information about the real world emission behaviour of all relevant on-road vehicle categories.

#### 3.1 Emission Standards for Heavy Duty Vehicles

Emission testing for heavy duty diesel engines started in 1992 (Euro I) with steady-state tests following the regulation ECE R-49. With the introduction of Euro III in 1999/2000, the ECE R-49 was replaced by the European stationary cycle (ESC) and complemented with the European transient cycle (ETC). There has not been any change regarding the test cycles up to and including Euro<sup>o</sup>V, but the emission limits have decreased. Euro<sup>o</sup>VI emission standards were introduced by Regulation 595/2009 and became effective from 2013 on. [8]

Table 1 shows an overview of the different regulations for heavy duty vehicles.

**Table 1: Emission limits for HDVs [9]**

Limit	Introduction	Test
Euro I	7/1993	ESC R-49
Euro II	10/1996	ESC R-49
Euro III	10/2001	ESC & ELR/ETC
Euro IV	10/2006	ESC & ELR/ETC
Euro <sup>o</sup> V	10/2009	ESC & ELR/ETC
Euro <sup>o</sup> VI	12/2013	WHSC/WHTC + on-road testing

The current regulation Euro<sup>o</sup>VI is split into two different parts:

- Type approval testing
  - o World Harmonized Stationary Cycle (WHSC) + World Harmonized Transient Cycle (WHTC)
  - o Off-cycle emission (OCE) testing
- In-service conformity (ISC)

Some Euro<sup>o</sup>VI provisions, like on-board diagnosis (OBD) requirements and OCE/ISC testing, are phased in over a period of several years with different steps of Euro<sup>o</sup>VI<sup>1</sup>. Due to measurement uncertainties in on-road testing, the emission limits are multiplied with a conformity factor of 1.5 in this part. The emission value used for comparison with the on-road regulatory limits is calculated as the 90 percentile of all valid moving average window (MAW) values from emissions measured on-board during a real-world trip. One MAW represents the entire time it takes before the work of one WHTC has been carried out and a new MAW is started each second of the cycle. To be valid, the average engine power of such a window has to be a minimum of 20 % of the rated engine power. This value was lowered to 10 % with the introduction of Euro<sup>o</sup>VI step D (9/2018 for new models, 9/2019 for all vehicles). [10]

<sup>1</sup> Euro<sup>o</sup>VI is divided into different steps (step A to current step D and future step E). Details are listed in Table 17 in the annex.

Although the WHTC is close to real driving including different driving conditions, high load range, transient profile and cold start conditions, the on-road tests represented by OCE and ISC extend the test standards. Variability in loading, unknown track profile, driver variability and different ambient conditions challenge the vehicles on a high level. Considering measurement results for Euro<sup>o</sup>VI step A to C, the regulations decrease the emissions in an effective way compared to former Euro classes. However, the reduction of the power threshold to 10 % and the upcoming inclusion of the cold start raise the requirements regarding thermal management of the exhaust after-treatment system to a much higher level. [8]

## 3.2 Emission Reduction Systems

The perfect combustion process of a  $C_xH_yO_y$ -fuel produces an exhaust gas which consists of  $O_2$ ,  $N_2$ ,  $CO_2$  and  $H_2O$ ; however, in reality it contains additional pollutants as a result of incomplete combustion (e.g. CO, HC and particles) and of  $N_2$  oxidation ( $NO_x$ ). Since  $CO_2$  does not have a direct influence on human health, it is not treated as a pollutant, but as a greenhouse gas due to its impact on the climate.  $CO_2$  is the product of every complete oxidation process of HCs and consequently the only way to reduce it is to decrease fuel consumption. [11]

Heavy duty vehicles almost exclusively use Diesel combustion engines as a propulsion system [12]. The big advantage of Diesel engines lies in the lean burning process ( $\lambda > 1$ ) and the high engine efficiency linked with this. However, Diesel engines also implicate disadvantages primarily for the exhaust after-treatment system. While a stoichiometric combustion process (common for gasoline vehicles) allows both oxidation (CO, HC) and reduction ( $NO_x$ ) at the same time by using a Three-Way-Catalyst, the treatment of  $NO_x$  emissions sets a significant challenge for lean Diesel combustion.

This section describes the two main possibilities to reduce emissions for a Diesel engine concept: internal engine modifications and exhaust after-treatment.

### 3.2.1 Internal Engine Modifications

The possible internal engine modifications are exhaust gas recirculation, variable valve timing and increase of injection pressure. They will be explained in the following part.

#### 3.2.1.1 Exhaust Gas Recirculation

The primary aim of exhaust gas recirculation (EGR) is to prevent  $NO_x$  generation during the combustion process by reducing the combustion temperature. There are a lot of different possibilities to return burned exhaust gas to the engine. On the one hand, exhaust gas can be held in the cylinder or sucked back from the engine exhaust channel and, on the other hand, a recirculation outside the cylinder is possible. This can be realized by taking the exhaust gas upstream of the turbocharger and recirculating it downstream of the compressor (high pressure EGR) or by proceeding in the same way in the low pressure part of the system (low pressure EGR).

The recirculated exhaust gas influences the combustion process due to chemical, thermal and dilution effects. Higher heat capacities of  $CO_2$  and  $H_2O$  compared to the intake air lead to a decrease in combustion temperature. Another point is the dissociation of water to O and OH radicals, this increase of radicals should actually influence  $NO_x$  emissions. However, the dissociation reactions are endotherm and therefore the exhaust gas temperature and consequently  $NO_x$  emissions will decrease. The biggest effect is based on dilution. Oxygen concentration goes down according to the recirculation of exhaust gas and as a consequence, the mixture, which has to be heated up for the combustion process, is much bigger than without EGR. This has a big impact both on combustion temperature and thermal  $NO_x$

creation. In addition, lower  $O_2$  concentration reduces the  $NO_x$  formation also from the perspective of reaction kinetics. [11] [13]

At the Euro IV and V stages, some original equipment manufacturers (OEM) provided engines with EGR as the only emission control system and thus could reach the respective limits without any  $NO_x$  catalyst. The much stricter Euro<sup>o</sup>VI limits cannot be achieved without a SCR catalyst (see 3.2.2.3), but most engines additionally use EGR to reduce engine-out emissions as a first step. Primarily, this strategy helps to decrease cold start emissions, when the SCR catalyst has not reached its light off temperature, and reduces AdBlue consumption in normal operation.

### **3.2.1.2 Variable Valve Timing**

Variable valve timing is also an effective possibility to reduce emissions directly in the engine. This can be realized by using the Miller or Atkinson cycle. While the Miller cycle reduces the combustion cylinder charge and consequently the process temperature by closing the inlet valve early, the Atkinson cycle achieves the same effect by using longer valve opening times. [14]

Another option regarding the valves is the deactivation of single inlet valves or the aimed control of their stroke. This can optimize the swirl effect in the engine and leads to an improved burning process. As a consequence, soot and particle emissions will decrease. [15]

The internal EGR process (described in 3.2.1.1) is also controlled by variable valve timing. Special opening and closing times help to keep the exhaust gas in the cylinder or to suck it back from the exhaust channel. [11]

### **3.2.1.3 Increase of the Injection Pressure**

An increase of the injection pressure leads to a higher outlet speed of the fuel. Rising the relative speed between air and fuel reduces the drop diameter and thus improves evaporation [16]. Another advantage is the higher spray impulse, which makes for an enhanced mixture formation.

The improved mixture leads to a reduction of soot and particle emissions, while  $NO_x$  emissions can increase due to higher combustion temperatures. However, the biggest advantage is the enhanced mixture during EGR phases, which allows for higher EGR rates without raising soot emissions. [11]

## **3.2.2 Exhaust After-treatment System**

This section illustrates the possibility to reduce emissions by using an exhaust after-treatment system and explains the single components of the system. Figure 1 shows the principle scheme of the common structure of a Euro<sup>o</sup>VI HDV exhaust after-treatment system. The exhaust gas produced in the engine flows to the exhaust after-treatment box, which contains all catalyst modules to generate an appropriate thermal situation. The gas first passes the diesel oxidation catalyst (DOC) and a diesel particle filter (DPF) before AdBlue is injected. Next, the mixture of exhaust gas and AdBlue enters the selective catalytic reduction catalyst (SCR) and the clean-up catalyst (CUC) before leaving the system.

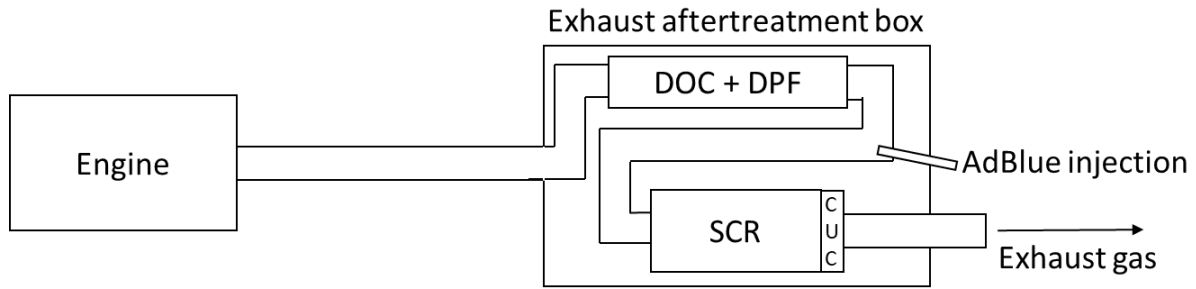


**Figure 1: Principle scheme of an exhaust after-treatment system of HDVs**

### 3.2.2.1 Diesel Oxidation Catalyst

On the one hand, Diesel oxidation catalysts (DOC) oxidize partly oxidized components as CO to CO<sub>2</sub> and NO to NO<sub>2</sub> and, on the other hand, unburned hydrocarbons. This catalyst type is mostly used for lean burning engines (e.g. Diesel engines). An important indicator for proper functionality is the fuel quality regarding the contamination with sulphur and lead. [11]

### 3.2.2.2 Diesel Particulate Filter

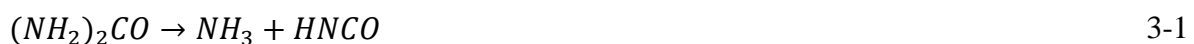
Diesel particulate filters (DPF) have the task to reduce both particulate number and mass generated during the combustion process. Since the temperature of the exhaust gas at normal operation points is too low to burn the soot in the filter, a regeneration process is needed to consistently clean the catalyst in order to limit the backpressure of the filter. To generate these high temperatures for the regeneration process, heavy duty vehicles often use extern fuel injectors. Another possibility is passive regeneration which uses NO<sub>2</sub> to oxidize the soot and starts to proceed already above 250°C. This method is also called continuous regeneration trap. [11]

Particulate filters are mainly built as wall flow filters, which force the exhaust gas to flow through the filter. There are different mechanisms to separate particulates in a filter. The main processes are impact due to inertia, diffusion, interception and electrostatic effects. If the filter loading is rather low, the main deposition is in the filtrate medium; however, with higher loading, the deposition shifts towards the soot cake resulting in higher efficiency. [11]

### 3.2.2.3 Selective Catalytic Reduction

Selective catalytic reduction (SCR) with ammonia is one of the most effective possibilities to reduce NO<sub>x</sub> in the exhaust gas. The first comprehensive use of this technology came along with the introduction of EURO IV and V for HDVs. Regarding Euro<sup>o</sup>VI, there is no reasonable alternative to SCR and consequently all European manufacturers use SCR catalysts for HDVs. [17]

The ammonia used for the reduction of NO<sub>x</sub> is produced by thermolysis (see equation 3-1) and hydrolysis (see equation 3-2) out of AdBlue. The minimum temperature for this process is approximately 200°C. AdBlue is a brand name in Europe and it contains urea (32.5 %) and water [18].



As these formulas illustrate, CO<sub>2</sub> is produced during this AdBlue conversion process as well. The production of 2 mole NH<sub>3</sub> results in 1 mole CO<sub>2</sub>.

To keep AdBlue consumption at a low level, its dispersion and consequently a homogeneous mixture of AdBlue and air is important. For that reason, the injection uses a compressed-air boost or works with high pressures. [11]

At high temperatures the produced  $\text{NH}_3$  can react with oxygen in the exhaust gas and is not available for  $\text{NO}_x$ -conversion, which drops as a consequence. [11]

Besides vanadium also copper- or iron-zeolite are used as catalyst material. Cu-zeolite catalysts have the best efficiency at low temperatures, while Fe-zeolite shows the best performance at high temperatures. In general, Zeolites have high thermal stability, whereas the characteristic of Vanadium catalysts is a relatively low thermal stability beyond  $550^\circ\text{C}$ . [11]

In principal, both zeolites and vanadium catalysts have the feature to store ammonia, whereas the storage performance of zeolites is enhanced compared to vanadium catalysts. However, independent of the material, storage capacity is reliant on the catalyst temperature and decreases when the temperature increases. [11]

$\text{NO}_x$  can be reduced by different reactions, but a  $\text{NO}_2/\text{NO}_x$  ratio of 0.5 leads to the preferred fast SCR reaction:



This reaction is split into different single steps with ammonium nitrate as an intermediate product. Additionally,  $\text{N}_2\text{O}$  can be produced as a side product even at low temperatures. [19]

Finally, the exhaust after-treatment system contains a clean-up catalyst downstream of the SCR. Again, this is an oxidation catalyst which is used for the oxidation of  $\text{NH}_3$  to  $\text{N}_2$  and  $\text{H}_2\text{O}$ . Excess  $\text{NH}_3$  can occur while overdosing and refilling the ammonia storage of the SCR. Ammonia is toxic and stinks; therefore it is limited in the regulation. [20] [21]

### 3.3 Handbook Emission Factors for Road Transport

The Handbook Emission Factors for Road Transport provides emission factors (EFA) for every on-road vehicle category and every emission class for all relevant traffic situations. Emission factors in general represent emissions masses per travelled distance (e.g. gram per kilometre). The HBEFA includes EFAs for all regulated and the most important unregulated emission components and, additionally, it delivers values for fuel consumption and  $\text{CO}_2$ . For a more precise specification, the different vehicle categories (passenger cars, light duty vehicles, heavy good vehicles, urban busses, coaches and motorcycles) are divided into subcategories (e.g. different propulsion systems or vehicle size). The wide range of traffic situations covers urban, rural and motorway driving with road gradients from -6 to 6 percent in 1911 different driving cycles (example for HGVs). [22]

Regarding this huge amount of different traffic situations (for the other vehicle categories the number of traffic situations is in a similar range), calculation of the emission factors is based on a simulation tool. Measuring all these various cycles would be too complex and expensive. Of course, the simulation models are based on a continuous ongoing measurement campaign for in-use heavy duty emissions. [23]

Figure 2 shows an example for  $\text{NO}_x$  emission factors of a 34-40 tons EURO<sup>o</sup>VI tractor trailer combination (half loaded, gradient 0 percent). Each point represents the result for a single cycle and consequently one traffic situation.

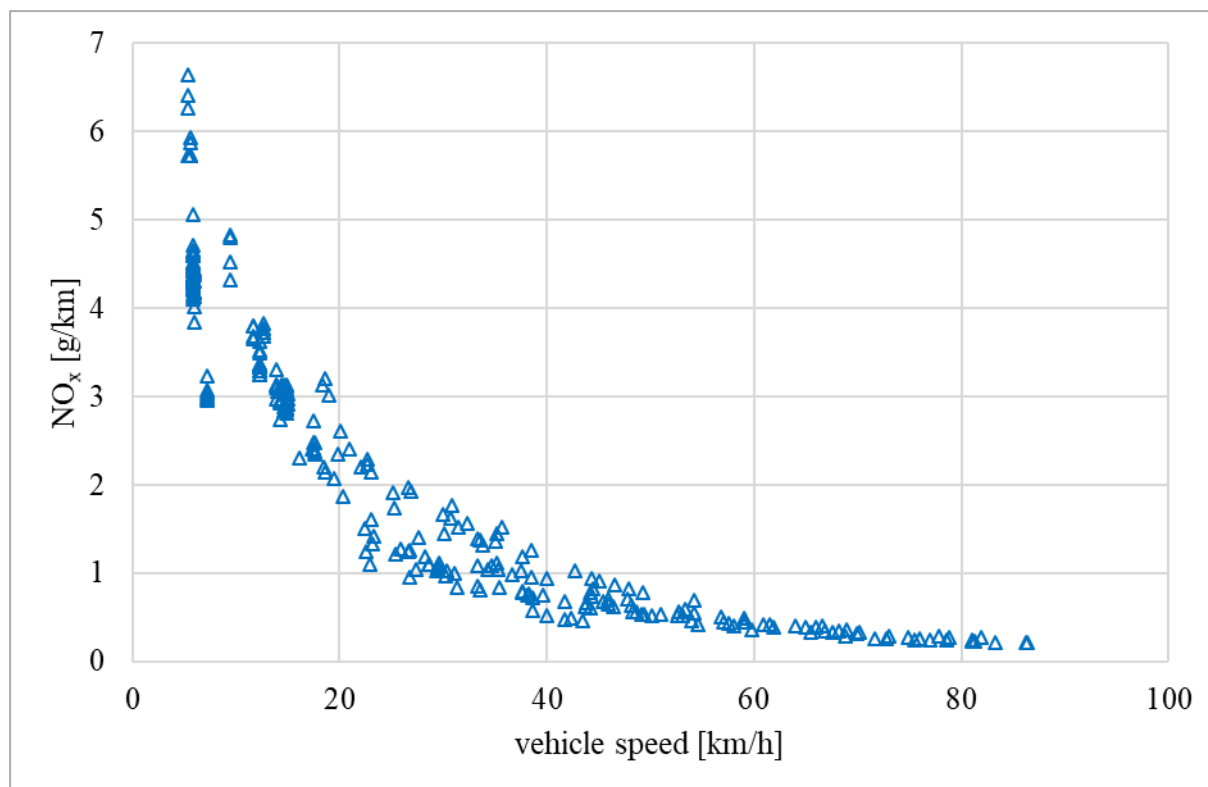


**Figure 2: NO<sub>x</sub> emission factors for a EURO<sup>o</sup>VI tractor trailer combination 34-40t HL**

The first HBEFA (version 1.1) was published in December 1995. Since that date, the development of legislation and consequently of vehicle technology has proceeded calling for a continuous update of the HBEFA. The latest version was released in April 2017 (version 3.3) [24], with no updates regarding HDVs. The last version containing HDV updates is HBEFA 3.2 released in 2014 [25]. In September 2019, HBEFA version 4.1 [23] was published and includes the final emission factors worked out in the present thesis. [22]

This version of the HBEFA will provide new emission factors for all HDV subcategories. Figure 3 shows the comprehensive workflow for the creation of emission factors for the HBEFA 4.1. Besides the measurement data from the roller test bench and the engine test bed, additional data from PEMS tests is available for the database. All this data is used for the creation of simulation models which are applied in all different traffic situations to gain single emission factors as a next step. Finally, these results are summarized in HBEFA 4.1.

This dissertation deals with the handling of additional on-road measurements for HDVs and bringing together all measurement data into comprehensive emission models. Consequently, the main challenge is the variability of driving profiles of on-road tests compared to standard cycles on the test bench. Another topic is the further development of the simulation tool PHEM [26], which is used for all the simulation work, due to the new technical developments introduced with emission standard Euro<sup>o</sup>VI.

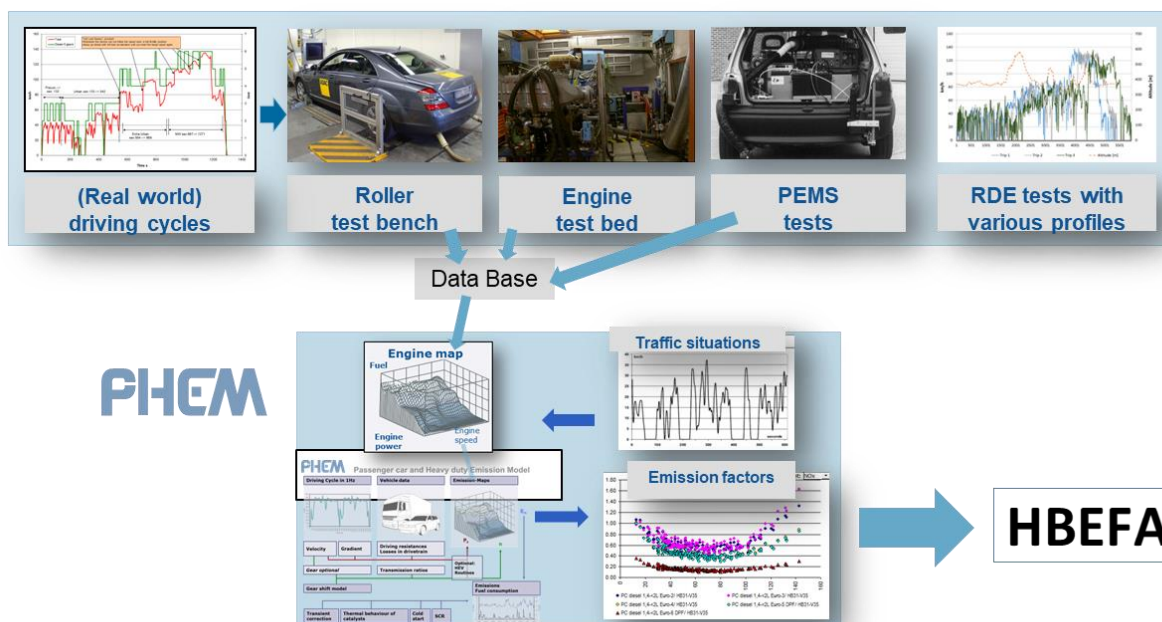


**Figure 3: Workflow for the creation of emission factors for the HBEFA**

Besides the HBEFA itself, the emission factors may further be used in the COPERT model and consequently in the EMEP/EEA air emission inventory guidebook, which provides data for emission inventory for 30 different countries [27].

## 4 Measurement Program for the HBEFA

The HBEFA is based on continuous measurement campaigns for the collection of in-use test data for HDVs. The environmental protection agencies of Austria [28] [29] and Germany [30] [31] financed different campaigns to gain a widespread measurement database regarding the distribution of vehicle sizes, mileages and emission technologies of all relevant HDV categories.

For a long time, emission research was based on chassis dyno and engine test bed measurements. Consequently, until now this data has also been the base for the creation of emission factors, which shall represent the emission behaviour in real drive conditions. However, research results in the last few years showed a difference between vehicle behaviour on the chassis dyno and in on-road testing for passenger cars [31]. Of course, LCVs have to do their certification tests on the chassis dyno, which led to low emitting strategies optimised for the chassis dyno test procedure; however, due to this discussion, questions arose regarding the HDV chassis dyno measurement data as well. Do the test cycles represent the real driving behaviour? Do vehicles behave the same way on the chassis dyno as in on-road conditions? For that reason, the measurement program for the HBEFA 4.1 at TUG was extended to cover both chassis dyno and on-road measurements for the same vehicles. This allows a comparison and consequently a validation of the chassis dyno results.

These findings lead to a combined use of measurements from roller test benches as well as from on-road tests with PEMS. The results cover a huge array of relevant driving conditions due to on-road tests, whereas the tests on the chassis dyno can be repeated and offer the possibility to use special measurement technology for exhaust components not covered by PEMS on HDVs (e.g. PN, NH<sub>3</sub>, N<sub>2</sub>O), which can only be used in the laboratory. In addition, the use of both types of emission tests leads to a much broader database as part of the data collection campaign by the ERMES member labs.

### 4.1 Chassis Dyno

Of course, measurements on the engine test bench would allow exact comparisons with emission limits for the WHTC and the WHSC, but dismounting the engines and setting them up on an engine test bed would be expensive and time consuming. The main aim of the measurements for the HBEFA is to gain average values for the fleet on the roads in Europe. Thus, the focus is set on relatively fast measurements and consequently the coverage of a representative number of different vehicles. Measurements on the engine test bed do not meet this requirement.

Although the certification process for HDVs does not cover chassis dyno measurements, they take an important part in research work. First, tests can be repeated with different vehicles allowing for good comparison between the vehicles. Another advantage is the possibility of various preconditioning cycles for the same test cycle. In this way, the effect on the emission behaviour can be investigated, e.g. for cold start, traffic jam or motorway driving before the cycle starts. But what is most important is that these tests are done in the laboratory; thus special measurement equipment like FTIR or CPC can be used on the chassis dyno for additional emission components.

The measurement program on the chassis dyno is not exactly the same for all vehicles, but in any case, the TUG tests comprise the World Harmonized Vehicle Cycle and the HBEFA Stop&Go cycle. For some vehicles additional tests like real world cycles have been tested. The measurement program for the chassis dyno is shown in Table 2.

**Table 2: Chassis dyno test program at TU Graz**

Driving cycle	Preconditioning	Enforcement
WHVC 2 phases	Cold start	Mandatory
WHVC	10 minutes at 80 km/h	Mandatory
HBEFA Stop&Go hot	10 minutes at 80 km/h	Mandatory
HBEFA Stop&Go int.	30 minutes idling	Mandatory
RWC urban	Real world	Optional
RWC motorway	Real world	Optional

The WHVC is measured in the form of a cold start test with two phases; the second phase is a repetition of the first phase after ten minutes soak time in between. For the final emission result the first phase is weighted by 14 % and the second phase by 86 %. This cycle allows an indicative comparison of the emission behaviour of the vehicle with the WHTC emission limits, which is driven on the engine test bed for the certification process. This method was developed while working on the Global Technical Regulation for the emission certification of hybrid HDVs [32]. To fit the engine load resulting from the WHVC to the WHTC, the vehicle mass and the driving resistance coefficients on the chassis dyno are calculated based on the rated engine power. Additionally, the gradient profile for the WHVC is calculated. This leads to an engine speed and power course, which is close to the one of the WHTC [33].

A “hot” WHVC is tested as well, with the preconditioning illustrating a motorway drive for ten minutes.

The Stop&Go cycle represents the “worst case” regarding low load and consequently low temperature operating and is suitable for the analysis of the SCR catalyst under these special conditions. The cycle is driven two times, first preconditioned “hot” (ten minutes motorway driving) and the second time “intermediate” (30 minutes idling). This means that the engine is hot, but the exhaust after-treatment system is more or less “cold”. On the one hand, these two cycles show the emission behaviour of the vehicle during cooling down conditions and, on the other hand, for an eventual heating up to improve the performance of the exhaust after-treatment system.

A combination of these cycles and different preconditioning conditions makes a perfect database for the PHEM simulation models, because they cover the main load, engine speed and exhaust temperature range.

The optional real world cycles represent the real world behaviour. They shall mainly answer the question, if it is possible to repeat real world cycles on the chassis dyno and if the emission behaviour of the vehicle is the same on the chassis dyno and in on-road conditions.

## 4.2 On-road Testing

The aim of the HBEFA is to provide emission factors, which represent the real driving behaviour of the different vehicle types. For this purpose, it is certainly relevant to include on-road measurements in the measurement campaign. Indeed, the WHVC covers a wide range of different operating points (urban, road and motorway driving); however, comparison with an ISC cycle shows a difference between chassis dyno and on-road testing (see Figure 4). Especially driving at high engine speeds is not perfectly rebuilt by the WHVC on the chassis dyno.

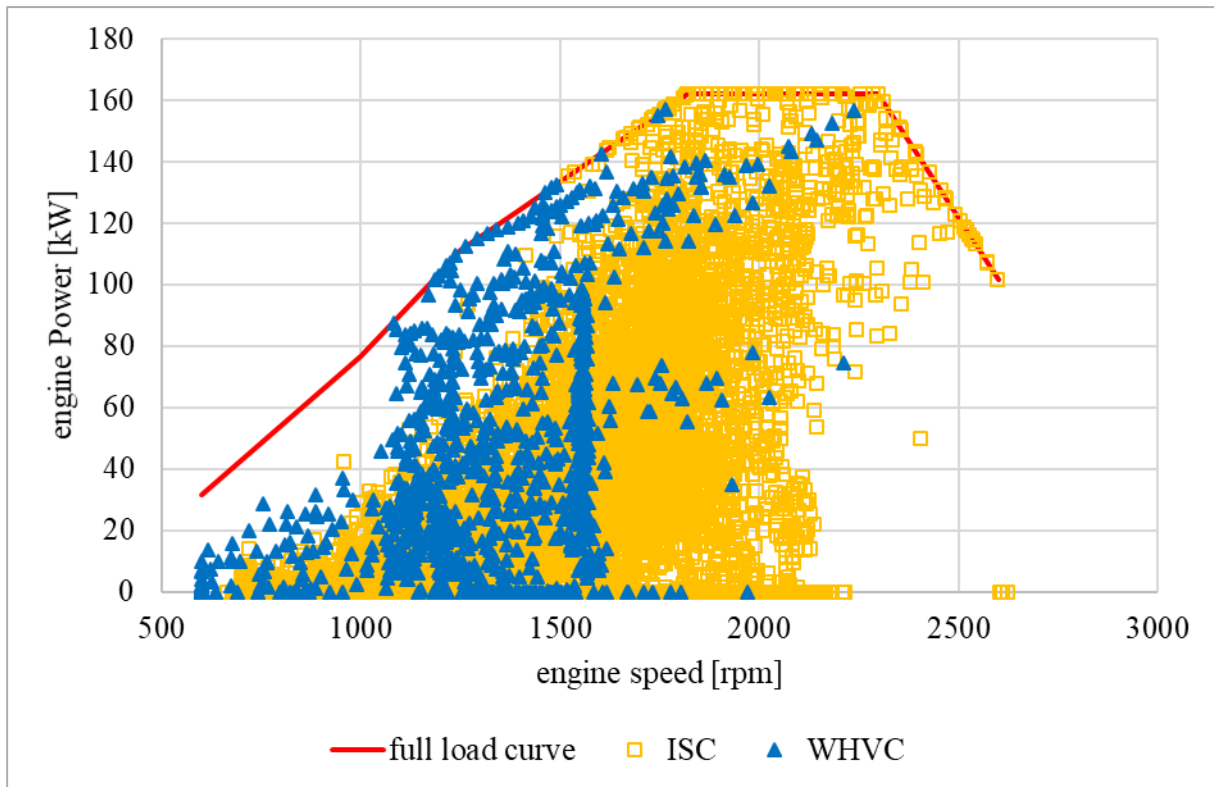


**Figure 4: Engine operating points – WHVC and ISC cycle**

Another issue is the operating mode of the vehicles on the chassis dyno. Some vehicles change their gear shift routines on the chassis dyno compared to on-road driving. For example, automatic gear shifting may not work anymore. Consequently, on-road driving is mandatory to compare the principle emission level of the chassis dyno and on-road behaviour for validation reasons. Only if they fit together, the emissions of the chassis dyno can be used for further research work.

Table 3 gives an overview on the different on-road measurement cycles in the HBEFA measurement campaigns.

**Table 3: On-road test program at TU Graz**

Driving cycle	Preconditioning	Enforcement
Warm-up cycle	Cold start	For all vehicles
ISC cycle	Follow up warm-up cycle	For all vehicles
On-road Stop&Go cycle	Follow up warm-up cycle	Optional

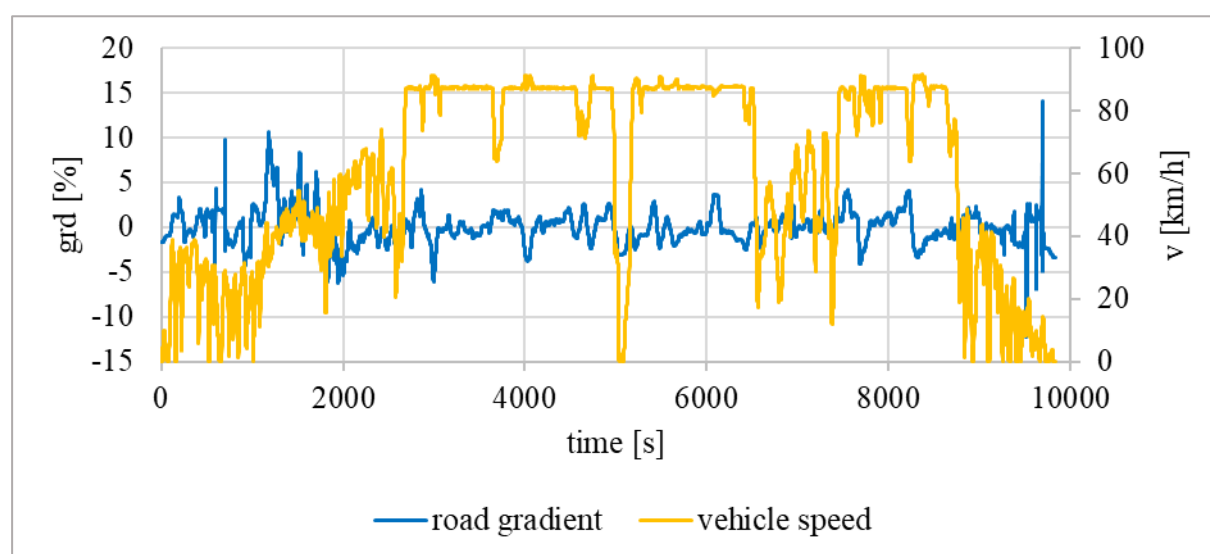
First, the on-road measurement starts with a warm-up cycle in the morning. This cycle is used to heat up the engine and the exhaust after-treatment system, but also to record the cold start emissions, of course.

After this, an ISC cycle according to the ISC provisions in Regulation (EU) 582/2011 and its amendments is measured. Table 4 shows the time shares for the different vehicle and road categories. For a valid ISC test, the deviation must not exceed five percent in any part.

**Table 4: ISC trip – share of road categories [10]**

Category	Urban	Road	Motorway
Time share – N2	45 %	25 %	30 %
Time share – N3	20 %	25 %	55 %
Speed range	0–50 km/h	50–75 km/h	Above 75 km/h

Based on these criteria, two different cycles in the Graz area were selected. After the first measurements the routes were adapted. Each trip takes up to three hours and the distance is about 160 km with a positive elevation gain of about 650 meters per 100 km. Due to the versatility of the routes, the measured engine operating points cover more or less the whole engine map. Consequently, these ISC cycles are suitable for the model creation in PHEM. Figure 5 shows the road gradient and the vehicle speed on the ISC route “Ries” as an example.

**Figure 5: Vehicle speed and road gradient – ISC measurement on the “Ries” route**

The first Stop&Go measurements on the chassis dyno showed high  $\text{NO}_x$  emissions compared to the first measurement results of the ISC cycles. The main reason for this is the SCR temperature, which decreased in the low load phases of the Stop&Go cycles, while the SCR performed on a high level in all phases in the ISC cycles. Based on these findings, another on-road test, the Stop&Go cycle, was designed. This route leads through the city of Graz and is ideally driven during rush hour to illustrate on-road low load driving. This cycle can be used to identify any kind of temperature management of the test vehicle in real drive conditions and completes the on-road measurement program.

### 4.3 Measurement Results

This part illustrates measurement results for HDVs for the HBEFA 4.1 and highlights the main findings of the laboratory work split into regulated and non-regulated pollutants.

Table 5 gives an overview on all measured vehicles of TU Graz, AVL MTC and TÜV Nord for the HBEFA. AVL MTC operates test facilities for HDV both in test beds and on-road in Scandinavia. TÜV Nord conducts engine test bed and on-road measurements in Germany.

**Table 5: Number of conventional HDVs with instantaneous test data used for setup and calibration of PHEM models (numbers: new data for HBEFA 4.1, numbers in brackets: measured HDV already included in HBEFA 3.2 [25])**

Laboratory	Number of vehicles				
	Total	Euro <sup>°5</sup> <sup>2</sup>	Euro <sup>°V</sup>	Euro <sup>°6</sup> <sup>2</sup>	Euro <sup>°VI</sup> <sup>3</sup>
Total	34 (15)	1 (-)	1 (11)	1 (-)	31 (4)
TUG	16 (10)	1 (-)	1 (7)	1 (-)	12 (3)
AVL MTC	18 (3)	- (-)	- (3)	- (-)	18 (-)
TÜV Nord	- (2)	- (-)	- (1)	- (-)	1 (1)

The TU Graz data in total consists of both chassis dyno and on-road measurements<sup>4</sup>, while AVL MTC and TÜV Nord provided only on-road test data. Details regarding the measured vehicles can be found in the annex (Table 18 to Table 23).

### 4.3.1 Regulated Pollutants

Figure 6 shows results of WHVC laboratory measurements of Euro<sup>°VI</sup> vehicles and compares them with the regulatory limits in the WHTC, which are shown in Table 6. TUG was the only laboratory which measured vehicles on the chassis dyno and therefore this chassis dyno data only contains TUG data.

**Table 6: Overview of Euro<sup>°VI</sup> regulatory emission limits in the WHTC**

CO [g/kWh]	HC [g/kWh]	NO <sub>x</sub> [g/kWh]	PM [g/kWh]	PN [#kWh]
4.00	0.16	0.46	0.01	6.00 E11

The WHVC is a chassis dyno cycle which represents an engine speed and load collective close to the one of the WHTC measured on the engine test bed [34]. For comprehensive comparison with the emission limits, all emission results were normalised by division by the corresponding limit value (see Figure 6). The mean results for all WHVC measurements are illustrated using blue bars for the different emission components. The error bars represent the minimum and maximum value and the red line gives the normalised emission limit, which logically is 1 due to the working method for all different components.

For CO, HC, PM and PN, the mean values are below the limit value. Even the maximum measurement results do not reach the limit but for one test for PN. Consequently, all vehicles can be regarded as “clean” considering these components. However, focusing on NO<sub>x</sub> we get a different picture. Some single measurements were within the regulatory limits, but the mean value exceeds this limit. The maximum result is actually more than 6 times higher than the limit.

<sup>2</sup> Vehicles above 3.5t TPMLM which use an engine certified in the NEDC (up to EURO<sup>°6b</sup>) on the chassis dyno. Roman numbers indicate a HD engine certification. Detailed explanations can be found in 7.5.3.

<sup>3</sup> All measured Euro<sup>°VI</sup> vehicles follow the regulations Euro<sup>°VI</sup> a or b.

<sup>4</sup> Some TU Graz vehicles are measured only on on-road trips and others only on the chassis dyno.

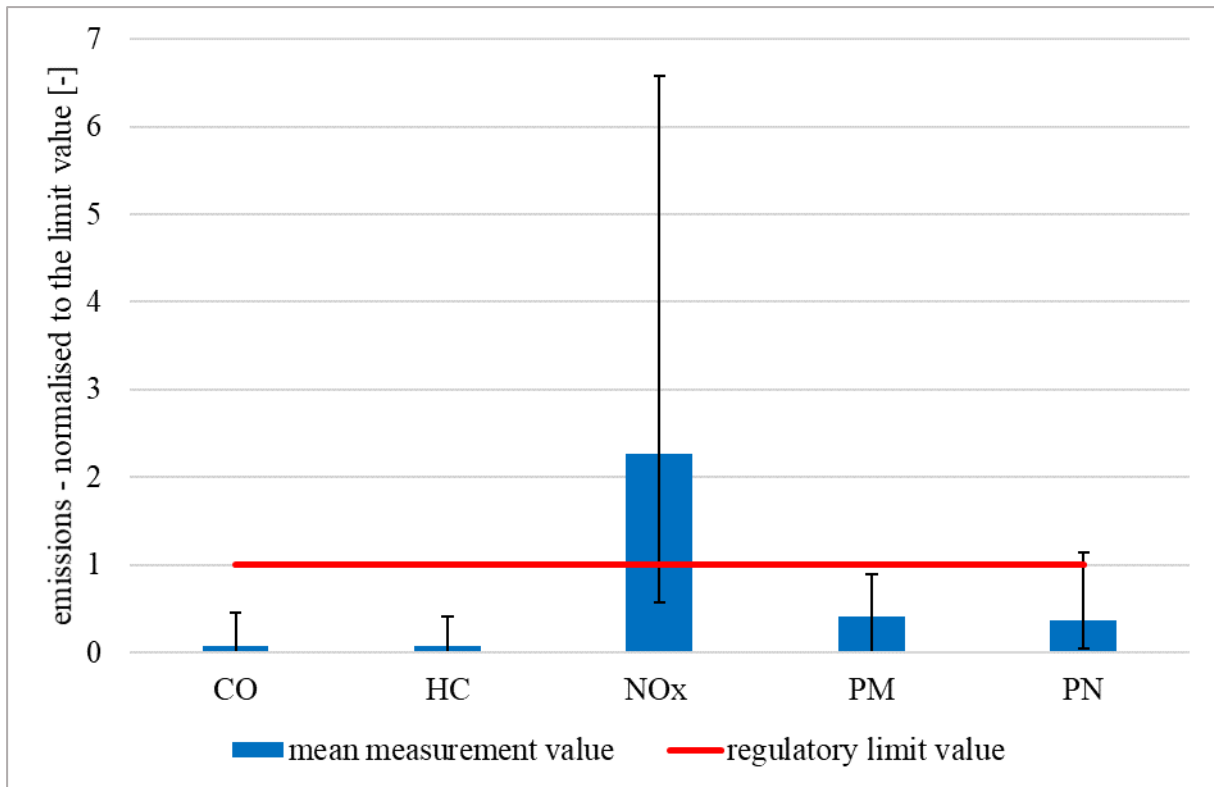


**Figure 6: Regulated pollutants compared to the respective limit value – WHVC measurement results of 8 Euro<sup>o</sup>VI vehicles**

The results of all single vehicles and tests can be found in the annex (see Table 23).

As a consequence of the chassis dyno results, the following part focuses on the NO<sub>x</sub> emissions in real driving conditions. In this case, on-road test data contains data of TUG and AVL MTC. Figure 7 shows the NO<sub>x</sub> TP results and their average normalised engine power<sup>5</sup> for all Euro<sup>o</sup>VI HDV measurements on ISC tests. Most of the vehicles emit on a low level (smaller than 0.69 g/kWh<sup>6</sup>), but some tests show NO<sub>x</sub> emissions even up to 1.6 g/kWh. In general, the results seem to be independent of the laboratory (TUG = blue, AVL MTC = yellow).

For a better understanding of the following charts, it must be remarked that all ISC measurement results are illustrated as mean values and not as 90 percentile as required for a regulatory test. Additionally, the cold start phase (first 30 minutes) was cut off for respective tests.

<sup>5</sup> Normalised engine power means engine power divided by rated engine power (see equation 6-1).

<sup>6</sup> For ISC cycles, the regulatory limits are multiplied by a conformity factor of 1.5 due to measurement uncertainties.

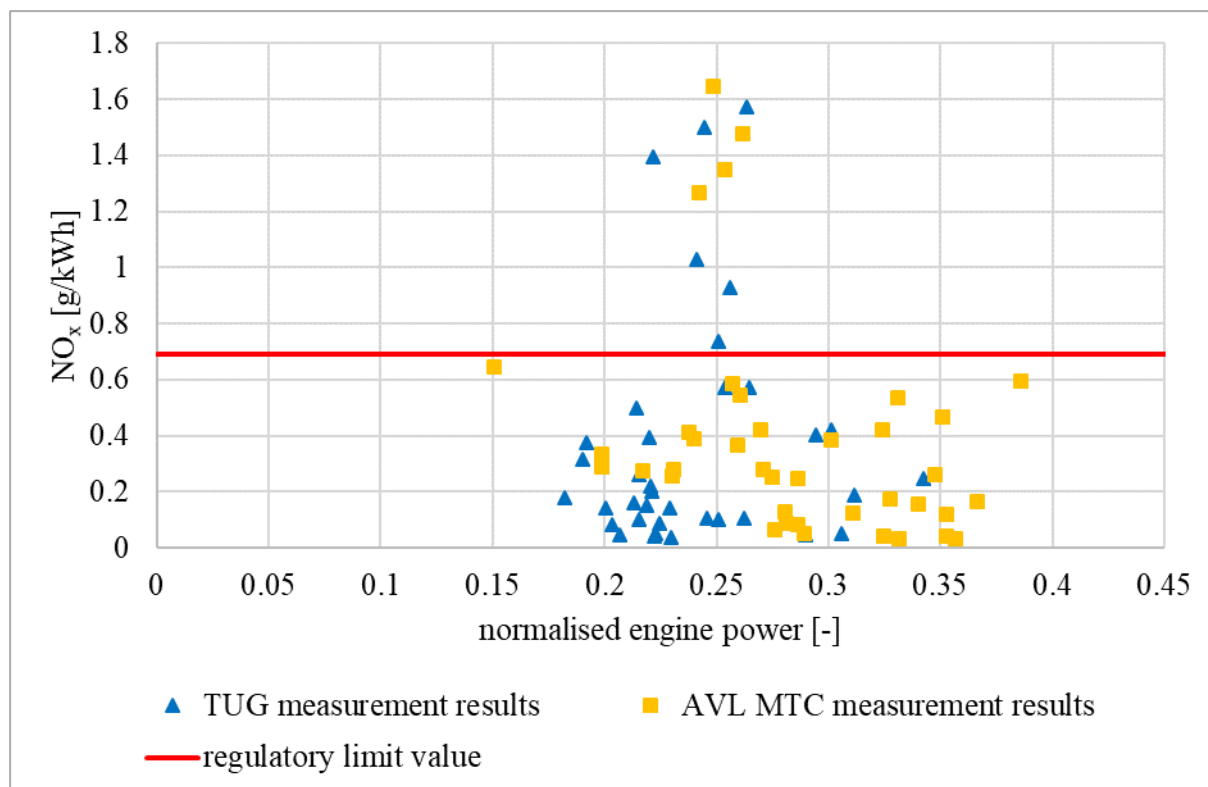


**Figure 7: NO<sub>x</sub> TP emissions and normalised engine power of EURO<sup>o</sup>VI HDVs – total ISC**

Figure 8 illustrates the NO<sub>x</sub> TP emissions dependency on the vehicle mileage. This view gives more details regarding the origin of high emitters. A few vehicles have high tailpipe emissions (more than 0.69 g/kWh) although their mileage is rather low (lower than 120 000 km), but emissions of “new” vehicles are generally on a low level, whereas the mean NO<sub>x</sub> TP emissions for high mileage vehicles (more than 500 000 km) are principally on a higher level. These results show that durability poses a challenge for manufacturers. The basic emission factors for the HBEFA are elaborated only with “new” data and the data of “old” vehicles is used for the creation of an average deterioration function for Euro<sup>o</sup>VI HDVs (see section 7.6).

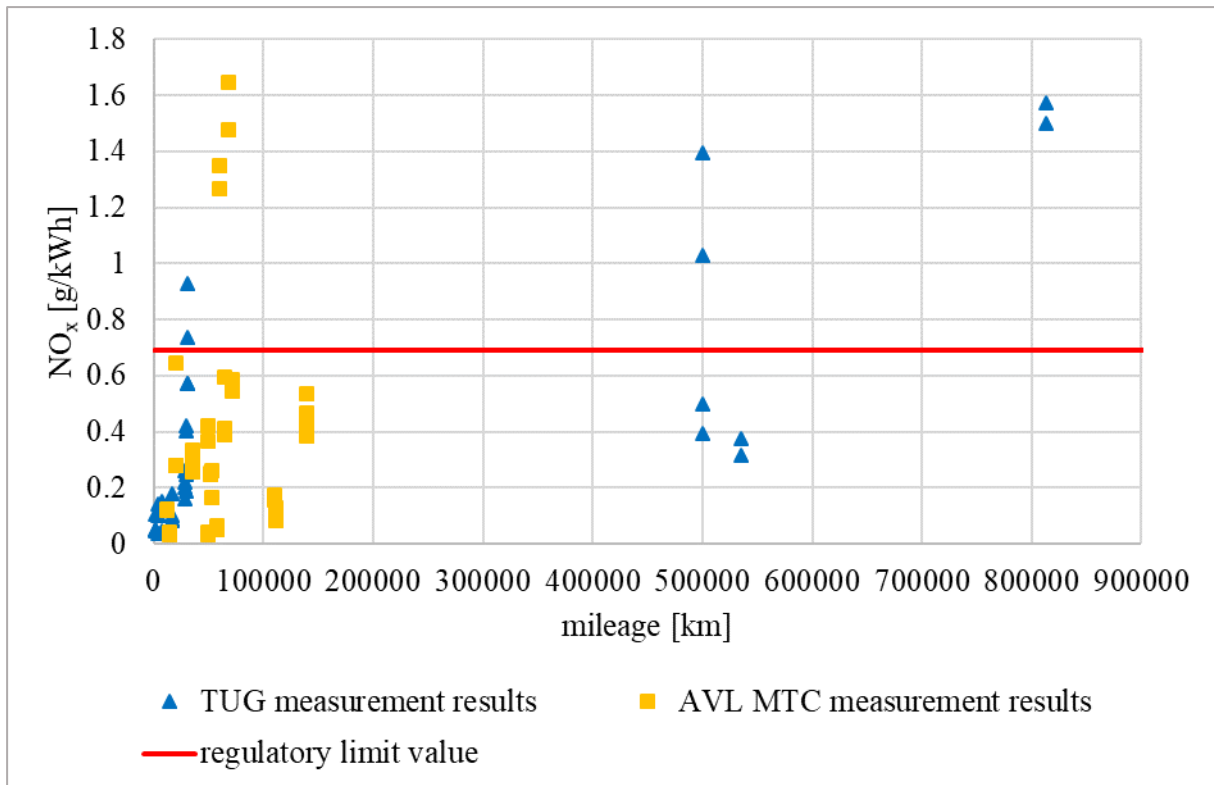


**Figure 8: NO<sub>x</sub> TP emissions and vehicle mileage of EURO<sup>o</sup>VI HDVs – total ISC**

Focusing on the split into different parts of the single trips shows interesting details regarding the spread of NO<sub>x</sub> TP emission mass. Figure 9 shows NO<sub>x</sub> TP emissions separated for the urban part of the same ISC cycles as seen before. These results illustrate an increase of emissions with decreasing average engine power as an effect of longer low load periods and consequently a drop in temperature in the exhaust after-treatment system. Details for these effects can be found in section 6.2.2. Compared to the total ISC, the emissions are on a much higher level for all vehicles (up to 3 g/kWh).

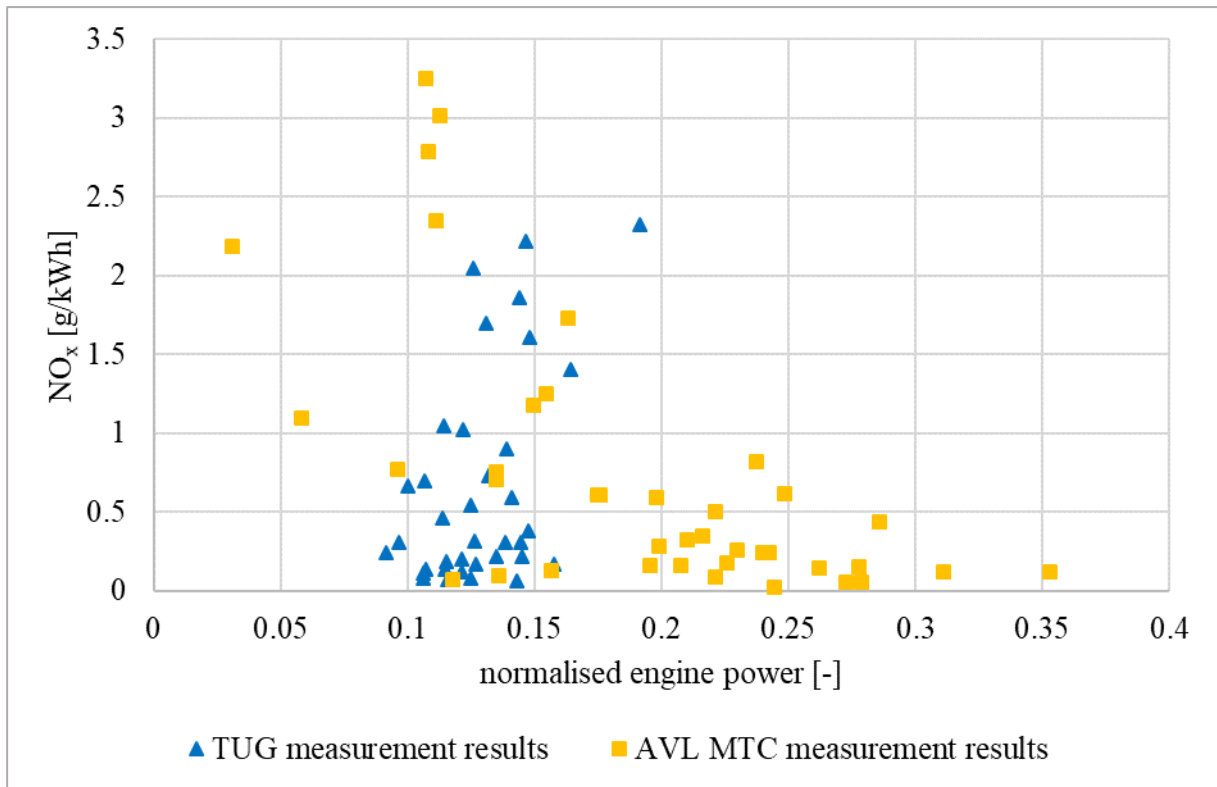


Figure 9: NO<sub>x</sub> TP emissions and normalised engine power of EURO<sup>o</sup>VI HDVs – urban part of ISC

Figure 10 shows more or less the opposite regarding operating conditions, that is results for the motorway part of these ISC cycles. Due to higher average loads the emission level is clearly lower. NO<sub>x</sub> TP emissions of high emitting vehicles rise up to 1.2 g/kWh, while the average remains on a much lower level compared to the urban results shown before.

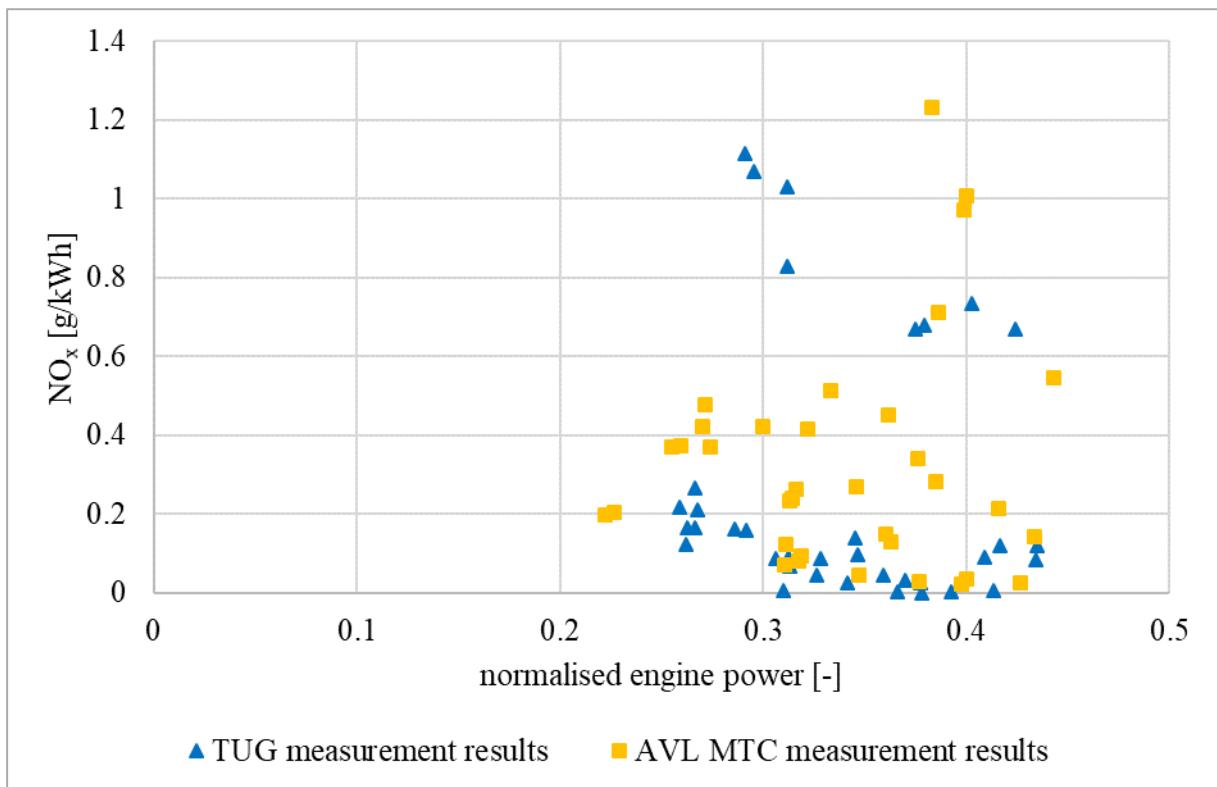
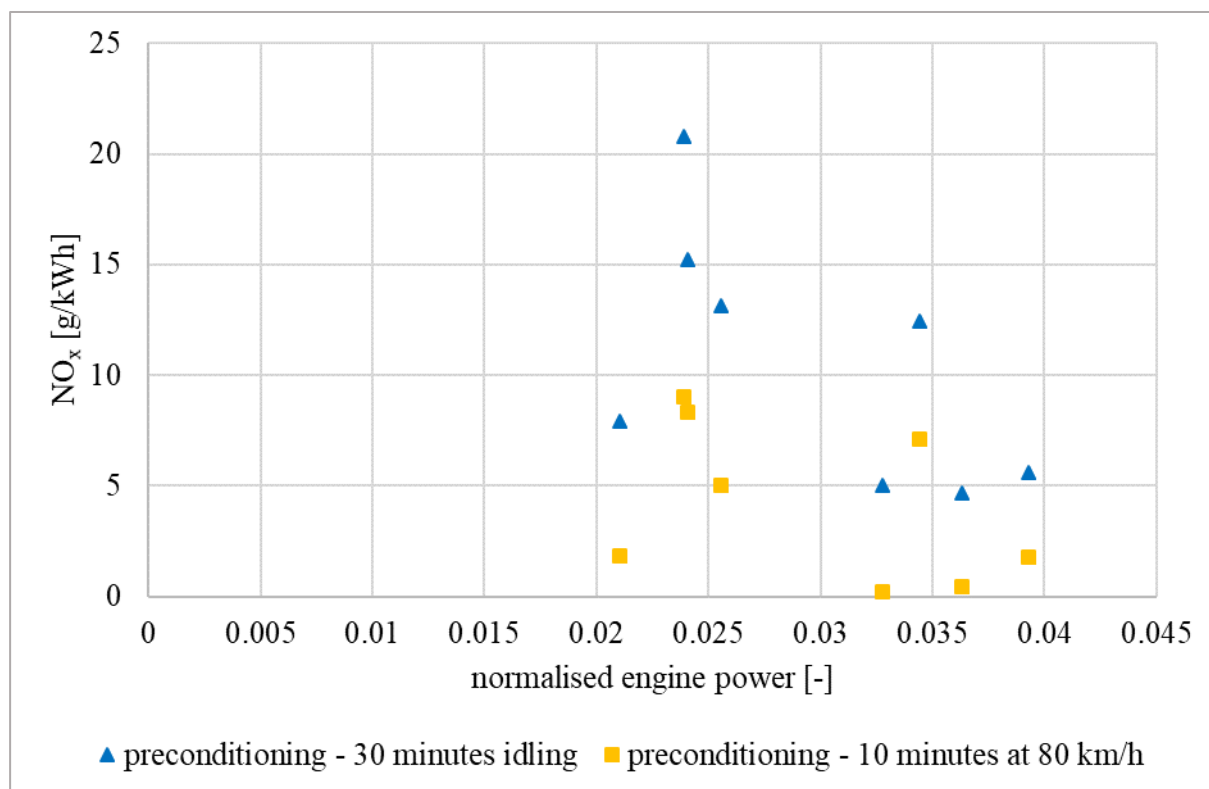


Figure 10: NO<sub>x</sub> TP emissions and normalised engine power of EURO<sup>o</sup>VI HDVs – motorway part of ISC

The results for the HBEFA Stop&Go cycle (see Figure 11) illustrate the effect of extra-low load driving conditions (average vehicle speed 7 km/h) measured on the chassis dyno. The mean normalised engine power (see equation 6-1) for these cycles is much lower (smaller than 0.05) compared to the urban ISC parts. Dependent on the preconditioning, this leads to NO<sub>x</sub> TP emissions of more than 10 g/kWh. Of course, 30 minutes idling causes the temperature of the catalytic system to fall below the optimal operating area and leads to a performance drop of the SCR catalyst before cycle start (blue points); however, this HBEFA Stop&Go low load cycle itself also leads to high tailpipe emissions even with hot preconditioning (yellow points, up to 10 g/kWh).

As TUG is the only laboratory which provides chassis dyno measurements, it is of course the only institute which comes up with results for this Stop&Go cycle.



**Figure 11: NO<sub>x</sub> TP emissions and normalised engine power of 8 different EURO<sup>VI</sup> HDVs – HBEFA Stop&Go measurements, 30 minutes idling and 10 minutes at 80 km/h as preconditioning**

To highlight the effect of these low load parts on the performance of the exhaust after-treatment system, Figure 12 illustrates both engine-out and tailpipe NO<sub>x</sub> emissions for these Stop&Go measurements with 30 minutes idling as preconditioning. In fact, the tailpipe emissions account for more than half of the engine-out emissions for the first 3 vehicles; in particular, the last 4 vehicles (number 4 to 7) do not reduce the engine-out emission effectively. Each of these 4 vehicles has a mileage of more than 500 000 km, which is much higher compared to all others. Deterioration effects dependent on the vehicle mileage seem to be significant especially for these low load phases.

Not all vehicles have been equipped with a sensor for the measurement of NO<sub>x</sub> EO emissions and consequently this data set covers fewer vehicles than shown in the figures before.

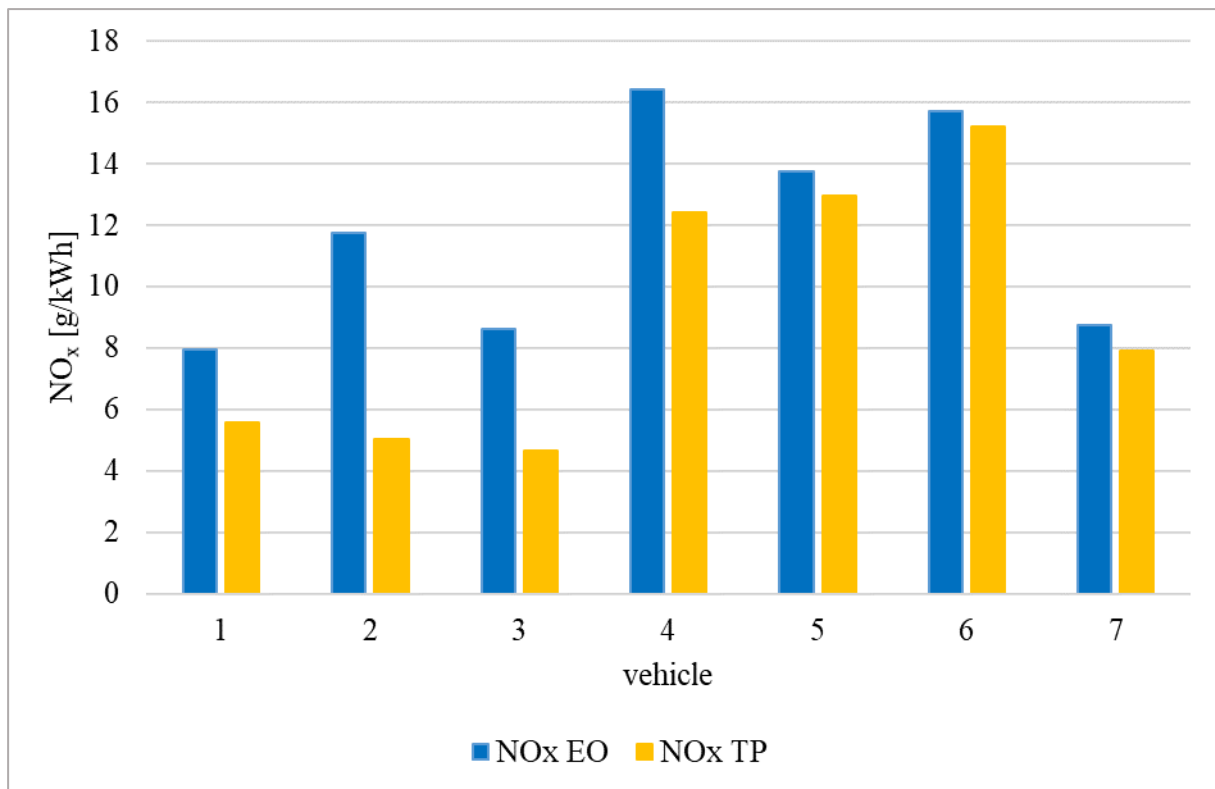


**Figure 12: NO<sub>x</sub> EO and TP emissions of EURO<sup>o</sup>VI HDVs – HBEFA Stop&Go measurements, 30 minutes idling as preconditioning**

#### 4.3.2 Non-Regulated Pollutants

As mentioned before, the measurements comprise also non-regulated pollutants. The most important ones are CO<sub>2</sub>, NO, N<sub>2</sub>O, and NH<sub>3</sub>. While a PEMS can only measure CO<sub>2</sub> and NO as unregulated pollutants in on-road conditions, the FTIR can measure all 4 emission components mentioned on the chassis dynamometer. However, 8 Euro<sup>o</sup>VI vehicles were measured on the chassis dynamometer, all of them with standard laboratory equipment and 6 of them additionally with FTIR. Table 7 gives an overview of the WHVC results for the most relevant unregulated pollutants of all vehicles measured on the chassis dynamometer for the HBEFA 4.1. The spread between the minimum and maximum value is relatively high for all different components. However, CO<sub>2</sub> will be regulated in the future [35]. Another interesting issue is N<sub>2</sub>O, because it has a greenhouse gas potential of 298 [36] leading to CO<sub>2</sub> equivalent emissions of 95.6 g/kWh for the highest emitting vehicle in the WHVC. This case increases total greenhouse gas emissions approximately by 15 percent (details in section 7.7). Consequently, N<sub>2</sub>O is part of the discussion regarding emission components to be limited in regulations post Euro<sup>o</sup>VI.

**Table 7: Unregulated pollutants – WHVC measurement results**

	CO <sub>2</sub> [g/kWh]	NO [g/kWh]	N <sub>2</sub> O [g/kWh]	NH <sub>3</sub> [g/kWh]
Mean value	720.475	0.815	0.16330	0.00605
Max. value	771.6	1.945	0.32084	0.02200
Min. value	636.7	0.083	0.03848	0.00092

## 5 Evaluation of Emission Measurements

Some parts of this chapter were already published in [37] and are repeated in this part of the work.

High quality data from emission testing is a key factor for the development and simulation of complex internal combustion engines and exhaust after-treatment systems. A crucial point in the evaluation of data from any kind of emission test system is to provide a correct temporal allocation of modal emission mass signal to the correlated engine operating point. Especially the consideration of variable transports times of the exhaust gas in the exhaust pipe and the emission measurement system is a well-known challenge, for which no common scientific method has been established so far. Provisions as defined in different emission legislations (e.g. UNECE R49.06) only foresee a constant time shift for modal measured emissions which considers the average transport time over an emission test. This is acceptable as only the averaged results per cycle (or per phase of the cycle) count as relevant results from legislative emission testing. However, for research and development purposes, there is a much higher demand on the quality of data from emission testing; e.g. for the HBEFA the instantaneous data is used for the setup of emission maps (see chapter 6). Over the last two decades, several methods on the post-processing of modal emission data have been published. For example, the method as developed by Franco V. [38] uses CO<sub>2</sub> as tracer gas allowing for a “reconstruction” of emission behaviour at the engine via correlation of CO<sub>2</sub> as measured on the test bed with the fuel consumption signal as measured at the engine. Other papers (e.g. [39] or [40]) use methods from signal theory to correct for transport dynamics in the emission measurement system.

In this work, a novel algorithm was developed, which allows for compensation of variable gas transport times based on a physical model. Main input data for the correction algorithm are the measured exhaust mass flow and volumes and temperatures in the measurement system. Consequently, this method provides an approach that—compared to other approaches—can be applied without great effort and expenditure of time for different vehicles. The comprehensive method is implemented into the software “ERMES tool” which is capable of performing evaluations of measurement data from any kind of emission test systems (diluted from CVS, undiluted from engine dyno or PEMS measurement). The tool now provides methods to correct emission test results for effects of analyser response behaviour and transport times in diluted and undiluted parts of the measurement equipment. This chapter shall give an overview of the methods developed by providing:

- An introduction to the main effects which distort instantaneous data from emission testing,
- A description of the correction algorithms as implemented in the “ERMES tool”, and
- Examples for applying the method.

### 5.1 Main Effects which Distort Instantaneous Data from Emission Testing

This section gives an introduction to the main effects which cause a distortion and a time shift of instantaneous emissions as measured on a test bed compared to the emissions at the engine outlet. The explanations are given by using the example of a diluted measuring system in which the sampling of modal emissions is performed at the end of the dilution tunnel of a CVS system. A scheme of such a system is given in Figure 13. The exhaust system of the vehicle ranges from the engine (position E) to the beginning of the undiluted part of the CVS system at position D. From this point the exhaust gas flows through the CVS undiluted pipe until it reaches the mixing point (position C) and enters the diluted part of the system. At

position B, a sample of the diluted exhaust is extracted and flows towards the analysers (position A).

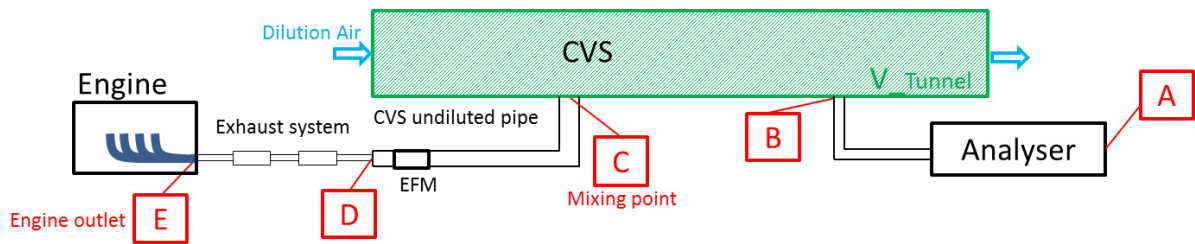


**Figure 13: CVS system of the dynamometer of the IVT Graz**

In the following, a synthetic “test case” is used to demonstrate the course of emissions for a rectangular signal (“low” – “high” – “low” step both for emission concentrations and exhaust mass flow) originating at the engine and flowing downwards the emission measurement system. This test case correlates to a sudden change in the engine operation point, where total exhaust volume flow (“ExVF”), the concentration of a certain emission component (“EC”) and – as a consequence – the mass flow of the emission component (“EMF”) are varied. Figure 14 shows all three quantities of this test case at the engine outlet position E.

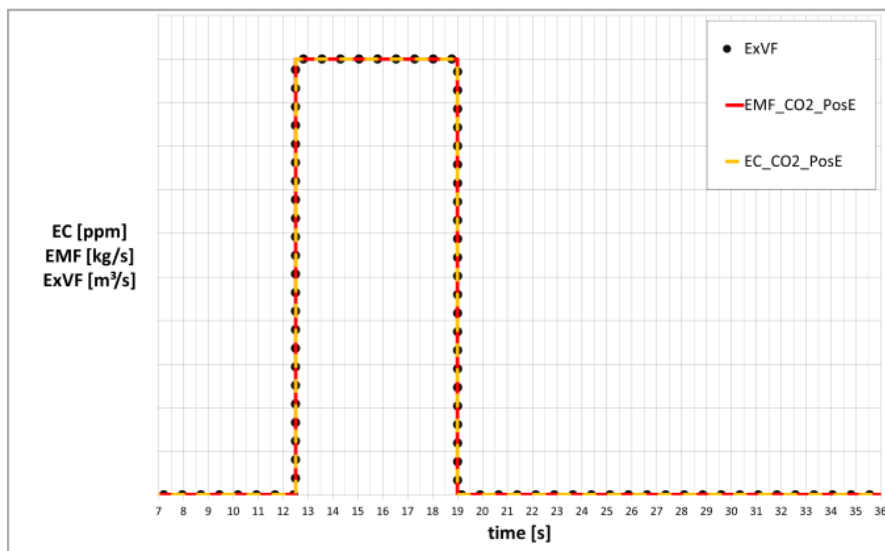


**Figure 14: Test case, emission mass flow at position E (engine outlet)**

From position E, the exhaust gas flows downwards the vehicle’s exhaust system (passing position D) and the CVS undiluted part to the “mixing point” with the dilution air at position C. Position C can also be interpreted as a sampling point of an undiluted measurement system. This signal behaviour is shown in Figure 15. At the mixing point C, the changes of volume flow and emission concentration arrive at different time steps: The change of the volume flow spreads with the velocity of sound, while the step of emission concentration flows with the exhaust flow velocity in the undiluted system. Consequently, the emission mass flow of the exhaust component under consideration rises in two steps: first, with the rising volume flow (1: concentration remains low, but exhaust flow goes up) and second, with the rising emission concentration (2: high volume flow and high emission concentration). When the exhaust flow falls back to “low” level again, the undiluted pipe is still filled with high emission concentration. Because of the low volume flow, this remaining high concentration needs a long time to leave the exhaust pipe (3).

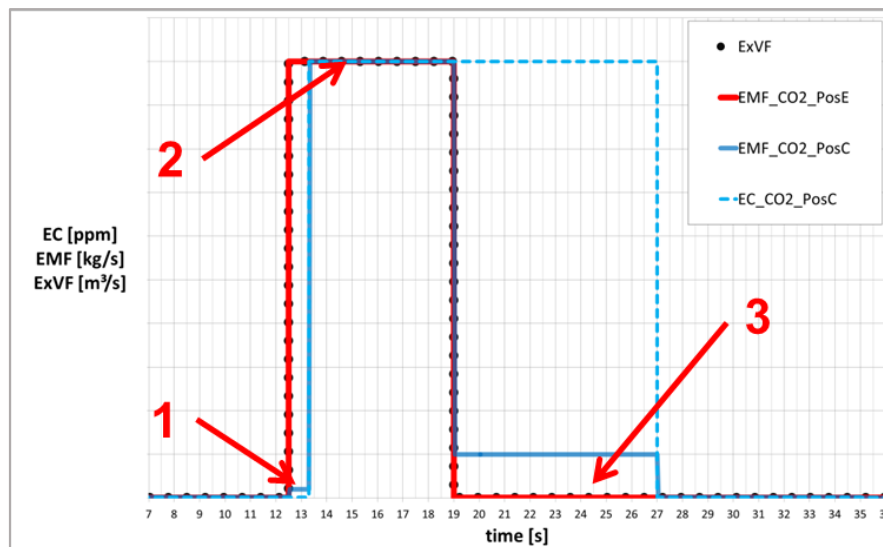


**Figure 15: Test case, emission mass flow at position C (mixing point with dilution air)**

When entering the CVS tunnel, the exhaust gas gets diluted by background air achieving a nearly constant volume flow. The dilution does not change the emission mass flow of the pollutant, but lowers the associated emission concentration in the CVS tunnel. This emission concentration gets time shifted by an almost constant transport time through the CVS tunnel towards position B (sampling point), see Figure 16.

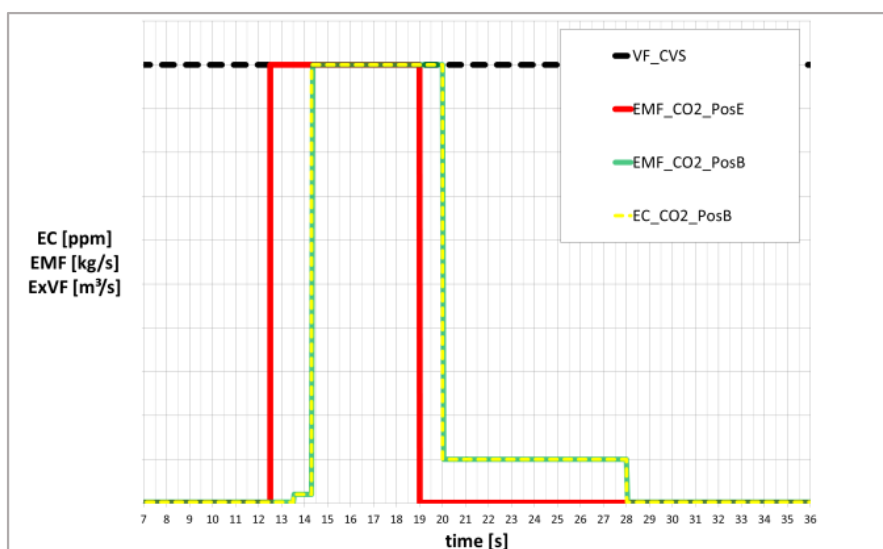


**Figure 16: Test case, emission mass flow at position B (sampling point in CVS tunnel)**

At sampling point B, a constant probe of the CVS volume flow is taken and sucked towards the analysers with constant volume flow. Because of the transport time through the sampling line and limitations in the response behaviour of the analysers (position A), the signal for emission concentrations is again time shifted and distorted resulting in the purple signal as shown in Figure 17. If the mass flow of the emission component would be calculated without applying any corrections just from the analyser signal and the constant CVS volume flow, the resulting course of emission mass flow would have a similar shape as the purple line in Figure 17. This signal is not only time shifted to the original signal in point E but also shows a remarkably different shape.

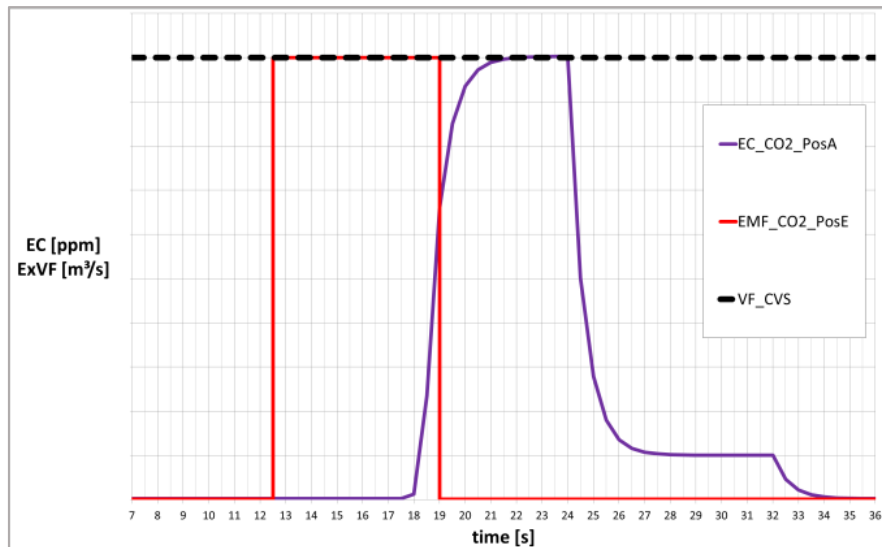


**Figure 17: Test case, emission concentration as measured by an analyser at position A**

The correction algorithms as presented in the next section aim to reconstruct the original signal at position E. The list of distorting effects as presented in this section only covers the main relevant mechanisms as identified for the test beds at TU Graz. Other mechanisms are e.g. the smoothening of emission concentrations by turbulent mixing effects. However, these effects are less important compared to the mechanisms which are corrected by the ERMES tool.

## 5.2 Algorithms for Emission Mass Calculation from the Analysers to the Engine

This section explains the different correction algorithms for calculating the signal for emission mass flow at the engine from the signal for emission concentration measured by the analyser.

### 5.2.1 Analyse Response and Dead Time Correction

Starting point is the correction of the response characteristics of the analysers, which is approximated by an inverse PT1 (first order low-pass) element. The resulting emission concentration signal is then subjected to a constant time shift, which comprises the constant transport time of the sample gas from position B to position A as well as an analyser specific dead time in the response characteristics. The applied parameters for PT1 time constant as well as analyser specific dead times were determined by test measurements, in which a distinctive rectangular signal for emission concentrations was injected at point B and the related valve position as well as the analyser signal were recorded.

Based on the PT1 and dead time corrected emission concentration signal at position B and the actual volume flow in the CVS system, in a next step, the emission mass flow for the component under consideration at point B is calculated. From this point on, any further algorithms are based on the emission mass flow but not on concentrations.

### 5.2.2 Correction of Transport Time in the Diluted Measurement System

For each time step the transport time in the diluted part of the measurement systems is calculated by division of the known volume of the CVS tunnel between point B and C with the actual value for CVS volume flow. This transport time is then applied as a time shift to calculate the emission mass signal at C. As the volume flow as well as the temperatures in the CVS tunnel are nearly constant, a simplified algorithm (see equation 5-1) is applied for

transport time correction compared to the method used for correction in the undiluted pipe system (see 5.2.3).

$$TT_{CVS\ tunnel} = \frac{V_{CVS\ tunnel}}{VF_{CVS\ tunnel}} \quad 5-1$$

Notation:

$TT_{CVS\ tunnel}$  ... Transport time in the CVS tunnel in s

$V_{CVS\ tunnel}$  ... Volume of the CVS tunnel in m<sup>3</sup>

$VF_{CVS\ tunnel}$  ... Volume flow in the CVS tunnel in m<sup>3</sup>/s

### 5.2.3 Correction of Variable Transport Time in the Undiluted Measurement System

The next and final step in the calculation procedure is the variable time shifting through the undiluted part of the measurement system until the emission mass reaches the engine at position E. For this purpose, the emission mass as calculated at position C for each time step gets shifted through the undiluted part which is split into different volume sections with varying temperatures and pressures.

#### 5.2.3.1 Main Calculation Principle

The calculation is performed reverse to the flow direction and is done for each “packet”. A packet denotes the properties:

- volume,
- the mass of the emission component as well as
- the total exhaust mass,

which correlates to a single data point in the emission mass flow calculated first at position C which is then virtually shifted “upstream” towards position E in the correction algorithm. The emission mass as well as the total exhaust mass of each packet are constant, independent of its position. The volume of each packet at a certain position depends on the temperature and the pressure at a certain time and position. At every time step, the current calculated packet at position C is virtually shifted into the undiluted system and “pushes” the packets located inside the system towards position E until they reach the end. Using this calculation, the individual transport time of each packet can be calculated. This principle is illustrated in Figure 18: every horizontal line represents a single time step and every coloured cell represents a packet. In this simplified example the transport time of packet 13 is calculated as 2 seconds by shifting packets 12, 11 and 10 backwards into the undiluted system.

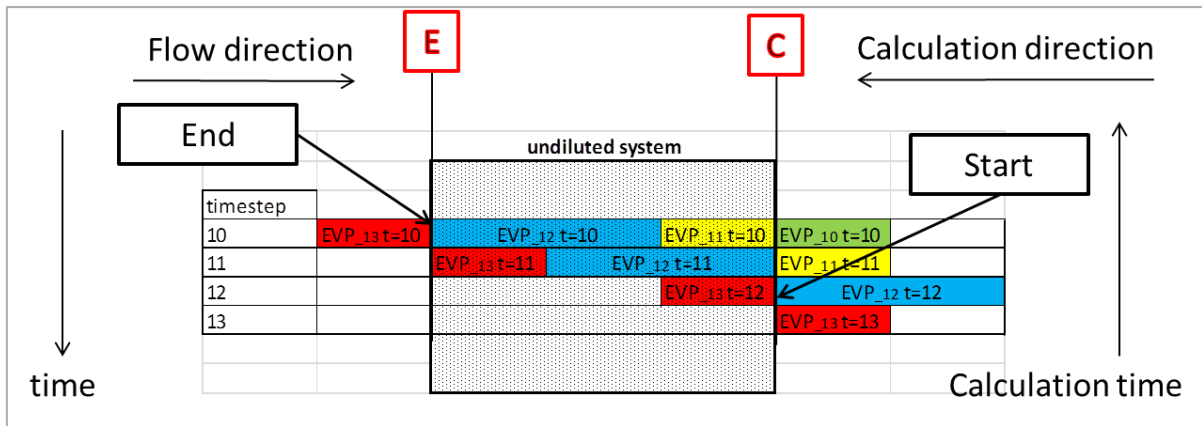


Figure 18: Principle of pushing packets through the undiluted section

### 5.2.3.2 Calculation of the Packet Position

The calculation of the position of a packet inside the undiluted system is based on the cumulative mass of exhaust gas inside the system with position C as zero-point. As already defined above, each packet has its specific values for mass of exhaust gas and for mass of each emission component. The exhaust mass represents the whole mass of the packet which is measured by an exhaust mass flow meter (EFM). Regarding gas properties, the exhaust gas of every packet is considered as ambient air.

The whole undiluted volume is divided into different volume sections. Each of them has its own size (equal in this example) and separate temperature and pressure at the beginning and at the end. Within these volume sections temperature and pressure are assumed to change linearly. These volume sections are divided into smaller partial volume sections (equally sized). Within a partial volume section pressure, temperature and consequently density are assumed to be constant and represent average values. The division explained above is illustrated in Figure 19.

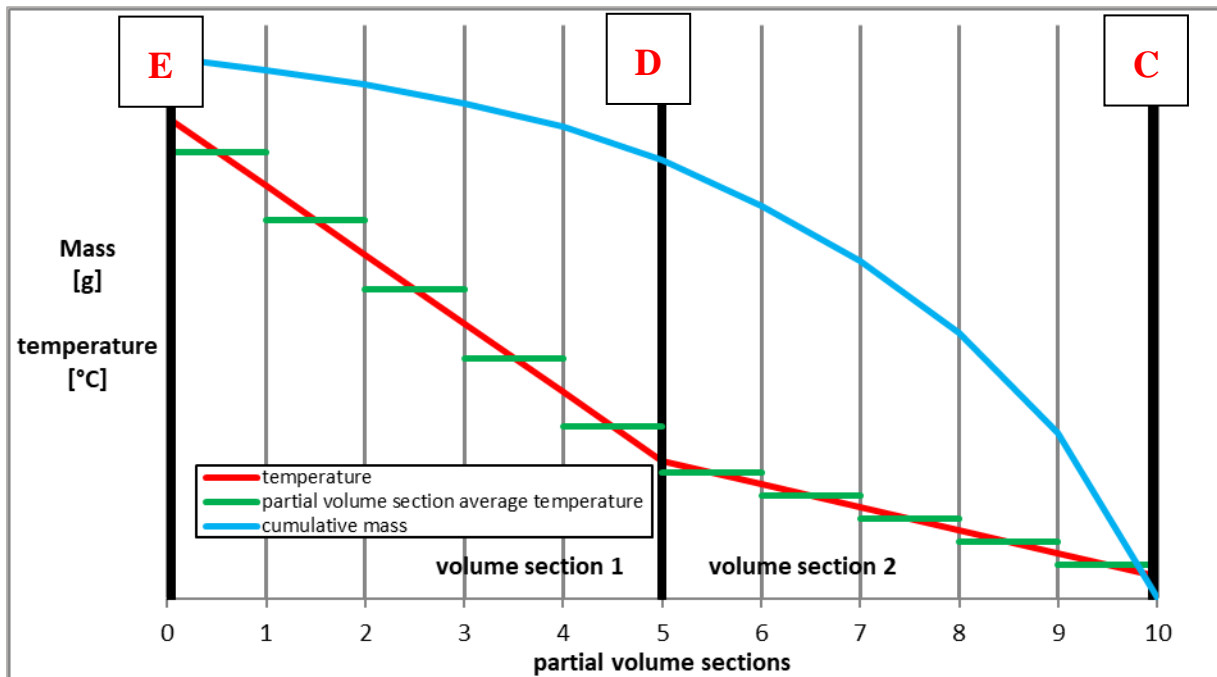


Figure 19: Division into partial volume sections

As a function of volume, temperature and pressure, each partial volume section can be filled linearly with a separate exhaust mass. The ideal gas equation is used for this calculation. By adding up the separate masses starting at position C, the course of the cumulative mass (blue

line in Figure 19) in the undiluted part of the system can be calculated. With varying pressure and temperature in the undiluted system over time, this cumulative curve has to be calculated once for every time step. With this function, the position and the size of a packet (starting at position C) can be calculated using the exhaust mass as a describing parameter. This approach is shown exemplarily in Figure 20.

The curve (blue, in the background of the entire graph) represents the cumulative mass of the partial volume sections. Due to the measured exhaust mass of the packets, their position can be calculated out of this cumulative mass function.

For every time step, the position calculation starts with the packet, which just entered the undiluted system at C (partial volume section 10 in this example). With its mass, the covered volume from the system border is computed. At the time of entering the system, the volume of the yellow packet (mass = 150 g) is 1.5 partial volume sections. For the calculation of the packet volume and position at the next time step (one line higher), the mass of the next packet entering the undiluted system at the considered time step (red packet) is added to the mass of the first packet and the covered volume for the whole mass is calculated. The red packet (mass = 200 g) was measured one time step earlier. With the reverse calculation direction, this packet is the next to enter the undiluted system with the volume 2.3 partial volume sections. The cumulative mass of these two packets is 350 g and consequently the volume for both packets is 7.4 partial volume sections. The new packet volume of the yellow one is calculated by subtracting the volume of the red packet from the cumulative volume of both packets. Therefore, the volume of the yellow packet increases from 1.5 to 5.1 partial volume sections. At every time step, this procedure is repeated until the packets have left the tunnel completely.

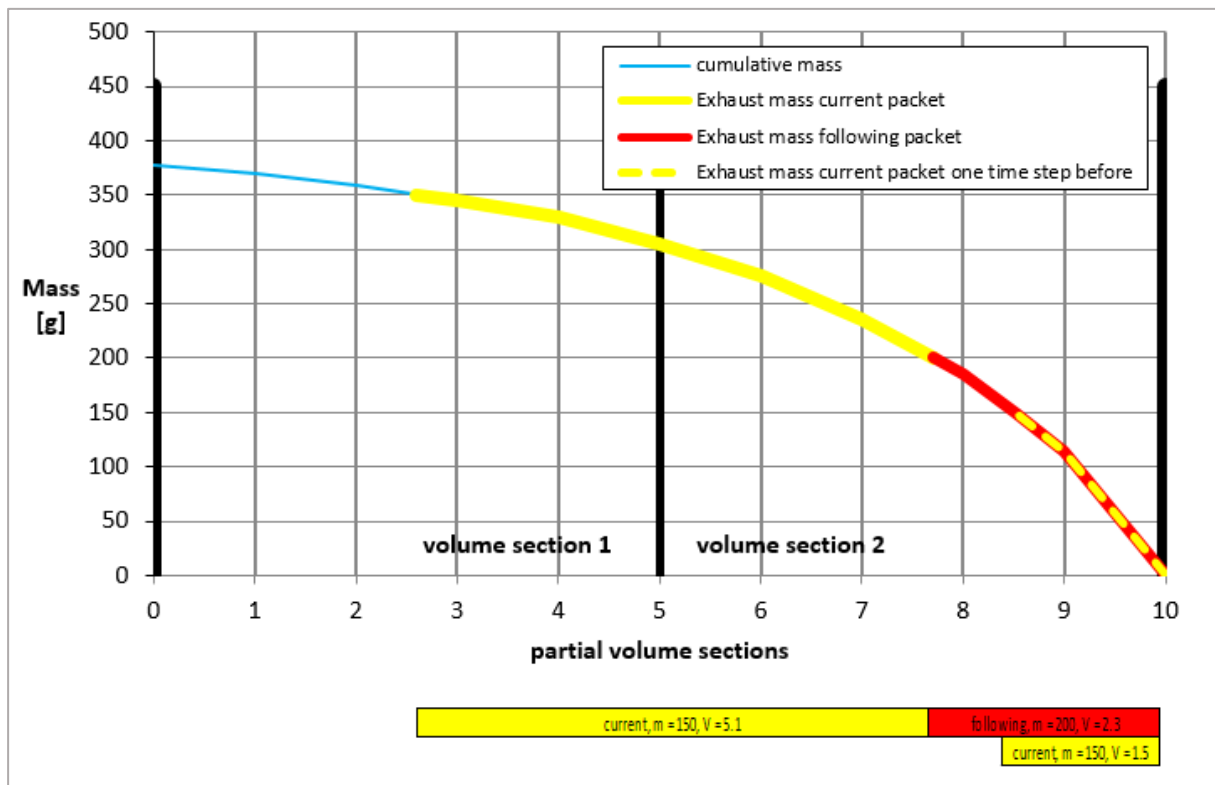


**Figure 20: Mass curve, illustration of various packet volumes in the undiluted system**

The number of partial volume sections per volume section can be decided manually regarding calculation time and accuracy. With an increasing number of partial volume sections, the accuracy of the calculation increases; however, calculation time is increasing as well.

### 5.2.3.3 Final Temporal Allocation of the Packets to Engine Operation Point

When a packet leaves the undiluted system, the emission mass gets assigned to this time step at position E, shown in Figure 18. However, in most cases, at the end of one time step a volume packet will overlap the system border as shown in Figure 21. This has to be considered by splitting and assigning the mass at different time steps.

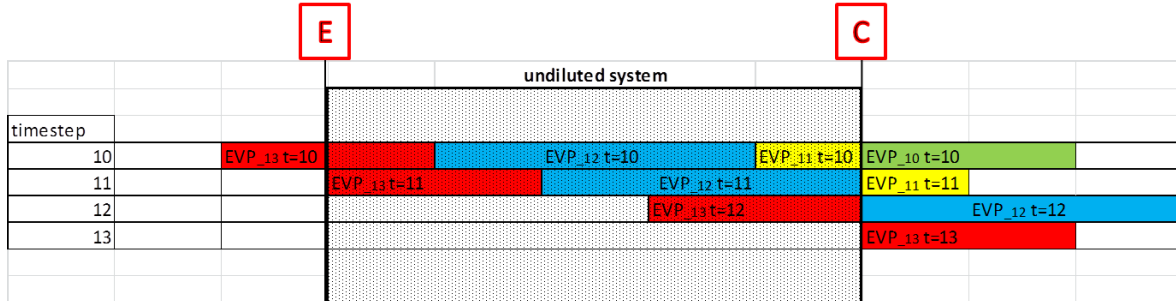


Figure 21: Overlapping of packets while dynamic time shift

Caused by the shift of packet 11 (yellow, allocated to point C at time step 11) into the undiluted system in time step 10, packet 13 (red) overlaps the border. As a consequence, the emission mass of this packet has to be allocated to two different time steps (10 and 9 in this example). Figure 22 and equations 5-2 to 5-5 describe the method applied. At every time step, the emission mass denoted with  $EM_{out}$  gets assigned to that engine operating point.  $EM_{in}$  represents the not assigned emission mass of the packet and will be assigned in the next time step(s). Depending on the variation of exhaust flow during the emission test, it is also possible that multiple packets are allocated to single time steps at engine out. The presented method is also able to depict this case correctly.

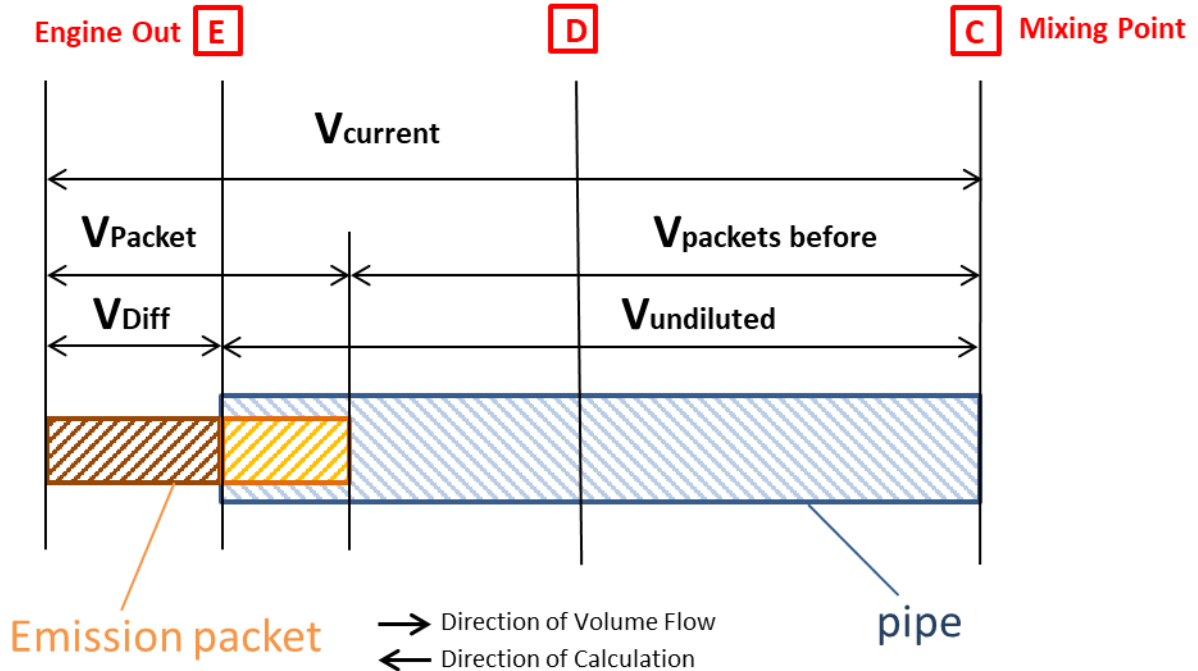


Figure 22: Assignment of emission masses for volume packets only partly released out of the pipe

$$V_{current} = V_{packet} + V_{packets\ before} \quad 5-2$$

$$V_{Diff} = V_{current} - V_{undiluted} \quad 5-3$$

$$EM_{out} = EM_{Packet} * \frac{V_{diff}}{V_{Packet}} \quad 5-4$$

$$EM_{in} = EM_{Packet} - EM_{out} \quad 5-5$$

Notation:

$EM_{in}$  ... Part of the emission mass of the considered packet which is still located in the tunnel in g

$EM_{out}$  ... Part of the emission mass of the considered packet which already left the tunnel in g

$EM_{Packet}$  ... Emission mass of the considered volume packet in g

$V_{current}$  ... Volume of considered volume packet and previous volume packets in m<sup>3</sup>

$V_{Diff}$  ... Part of considered volume packet which already left the tunnel in m<sup>3</sup>

$V_{Packet}$  ... Volume of the considered emission volume packet in m<sup>3</sup>

$V_{packets\ before}$  ... Aggregated Volume of all emission volume packets measured before and filled into the tunnel in m<sup>3</sup>

$V_{undiluted}$  ... Volume of undiluted pipe system in m<sup>3</sup>

### 5.2.3.4 Application Example

This section demonstrates the effect of the variable time shift method for the undiluted exhaust system for the synthetic test case as discussed in section 5.1. Figure 23 shows the temporal assignment of emission masses from position C (upper graph) to position E (lower graph). In the top diagram, the coloured boxes filling the area below the blue line represent the emission mass as allocated to time at position C. All these coloured boxes are shifted to different time steps at position E depending on their individual transport time. The emissions in the blue area (time step 19 to 27 at C) are shifted back to time step 18 to 19 at E because of the increasing transport time caused by the low exhaust mass flow during the last phase of the test. All emissions as represented in the yellow box are shifted from C to E by about the same transport time because of the constant mass flow during this phase of the test. The first box on the left side (around time step 13 at position C dark green) is shifted to the first “low” phase of the test at position E (higher emission mass is distributed to more time steps). Consequently, the gap between the long-time shifted normal idling emissions and the short shifted high phase (running time 8 seconds before throttling and 0.8 seconds while throttling) is filled up. As a consequence, in this test case, the emission mass flow signal at E is correctly calculated by the method.

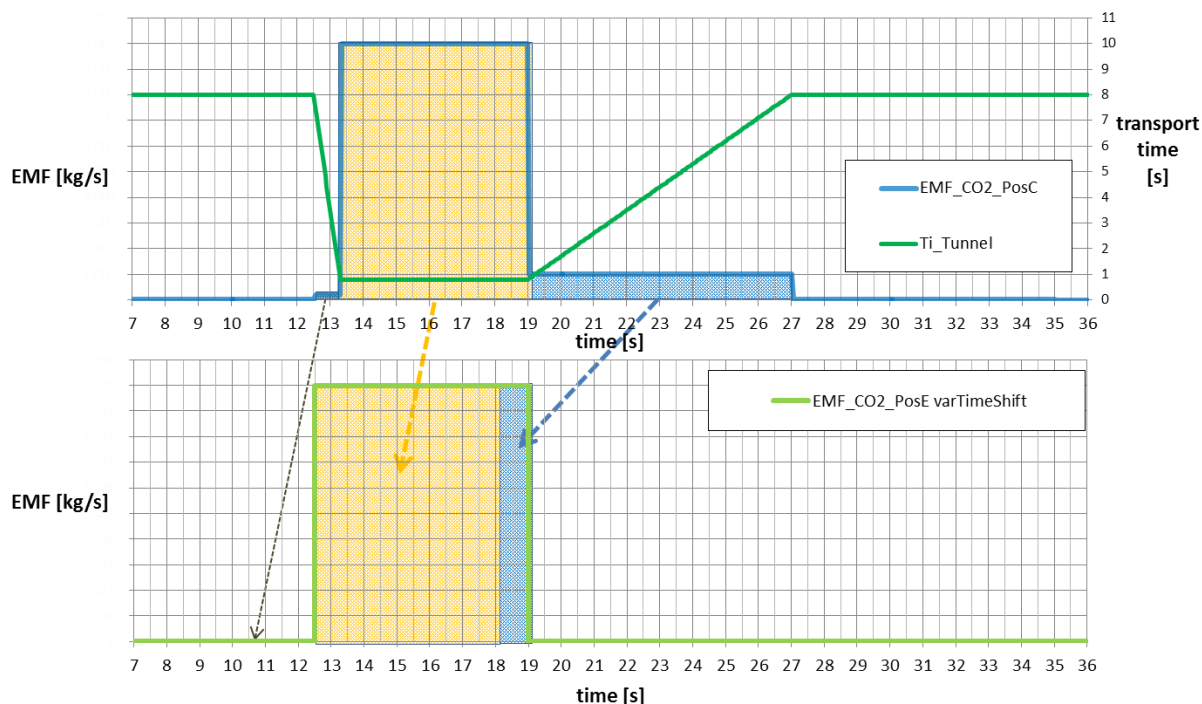


**Figure 23: Assignment of emission masses with variable time shift**

It is important to note that the method of correction of variable transport time as introduced in this work only changes the allocation of emission mass flow over time but does not change the cumulative emission mass over an entire emission test.

### 5.3 Practical Applications

In this section, practical applications of the variable time shift method are demonstrated. These results show the benefit of using the method. Therefore, these results are compared with the constant time shift method currently used. First, the result of a test measurement is shown followed by results for vehicle emission tests. Furthermore, some special cases important for the parametrisation of the evaluation methods are discussed.

#### 5.3.1 Application to Test Measurements with Known Reference Signal

Figure 24 shows a test measurement representing a step response test performed at the CVS system at the IVT in Graz. The object of the test is to check the entire signal correction methods as implemented in the ERMES tool by a test measurement with known reference result. The exhaust mass flow is generated by a fan and CO<sub>2</sub> gas from a calibration gas bottle is injected into measurement system at tailpipe position. The exhaust mass flow and the CO<sub>2</sub> concentration are changed at the same time from “low” to “high” and back to “low” again similar to the synthetic test case as discussed in the previous sections. Figure 24 illustrates the results of the whole process of the ERMES tool with the measured CO<sub>2</sub> concentration at the analysers “EC CO<sub>2</sub> PosA NbcNrc” and the exhaust mass flow “ExMF” as input signals and the corrected emission mass flow at the engine “EMF CO<sub>2</sub> Var” as a result. Compared to the emission mass flow calculated by the simple constant time shift method “EMF CO<sub>2</sub> Const 1.5”, a much better temporal correlation of the emission mass flow can be achieved with the reference result.

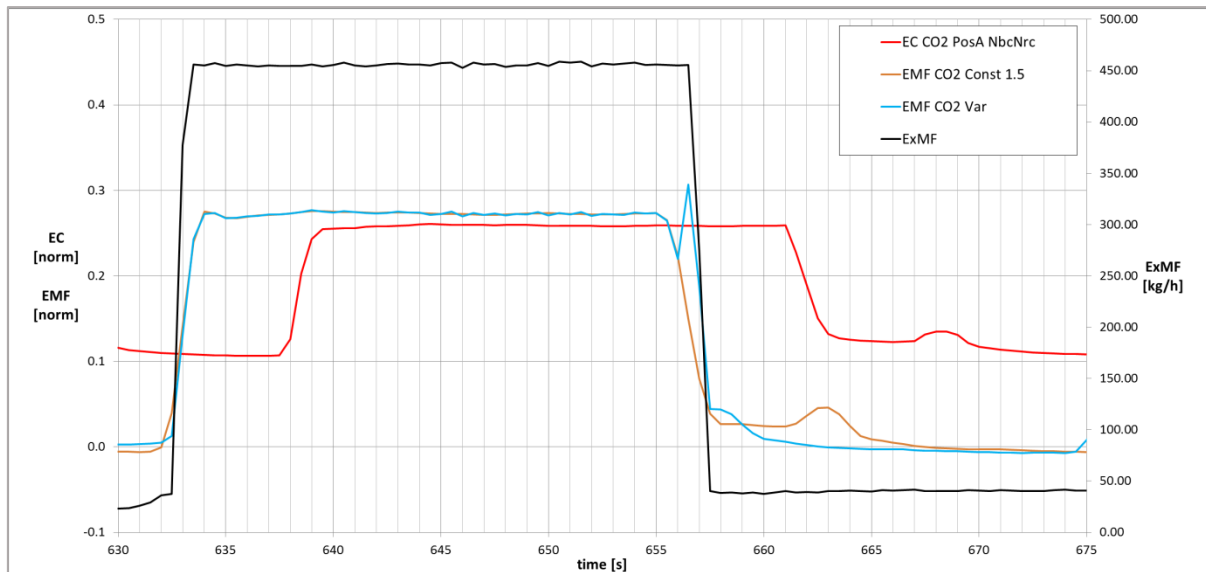


Figure 24: Evaluation of a test measurement representing a step response test

### 5.3.2 Application to Full Vehicle Tests

This section describes the application of the evaluation method to measurements with modal sampling in the diluted and the undiluted exhaust.

#### 5.3.2.1 Measurements with Modal Sampling in the Diluted Exhaust (CVS System)

In this section, the evaluation methods as implemented in the ERMES tool are demonstrated using data from a full vehicle measurement at a chassis dynamometer with modal sampling in the diluted exhaust. The results for mass flow of CO<sub>2</sub> emissions are compared to the results based on the constant time shift method. The engine power as calculated from vehicle dynamics and drivetrain efficiencies is used as a reference signal. An excerpt of the data is shown in Figure 25. A high quality signal for CO<sub>2</sub> mass flow is expected to follow the engine power signal (blue) qualitatively. Both CO<sub>2</sub> emission peaks and phases of low emissions correlate very well with the power signal using the ERMES tool method (green). This is obviously much less the case for the CO<sub>2</sub> signal obtained from the constant time shift method (red).

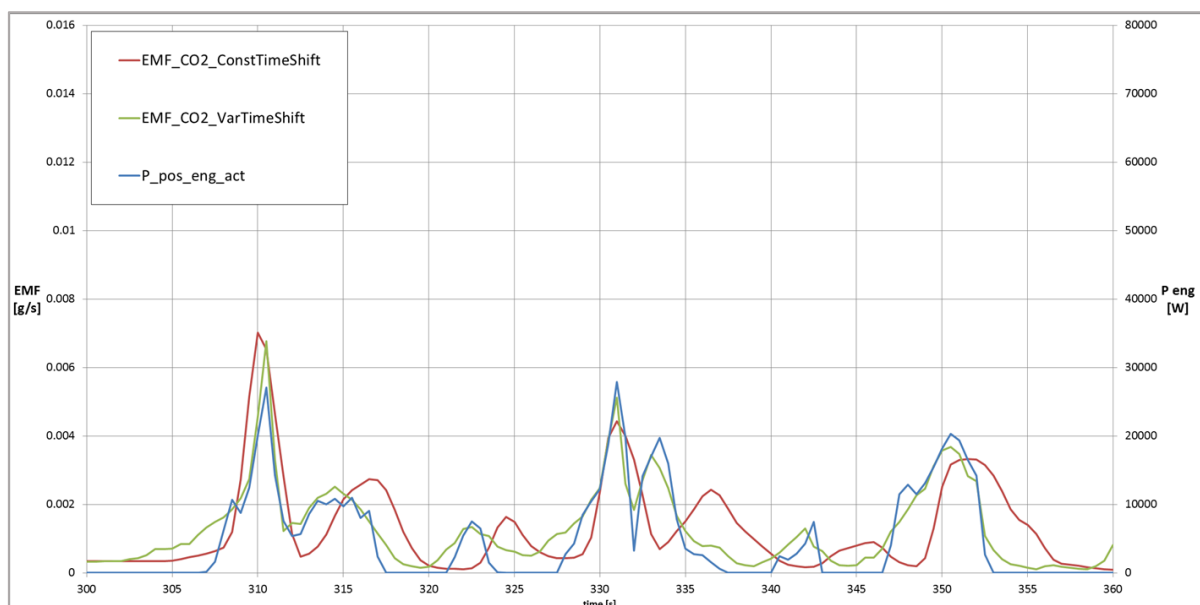
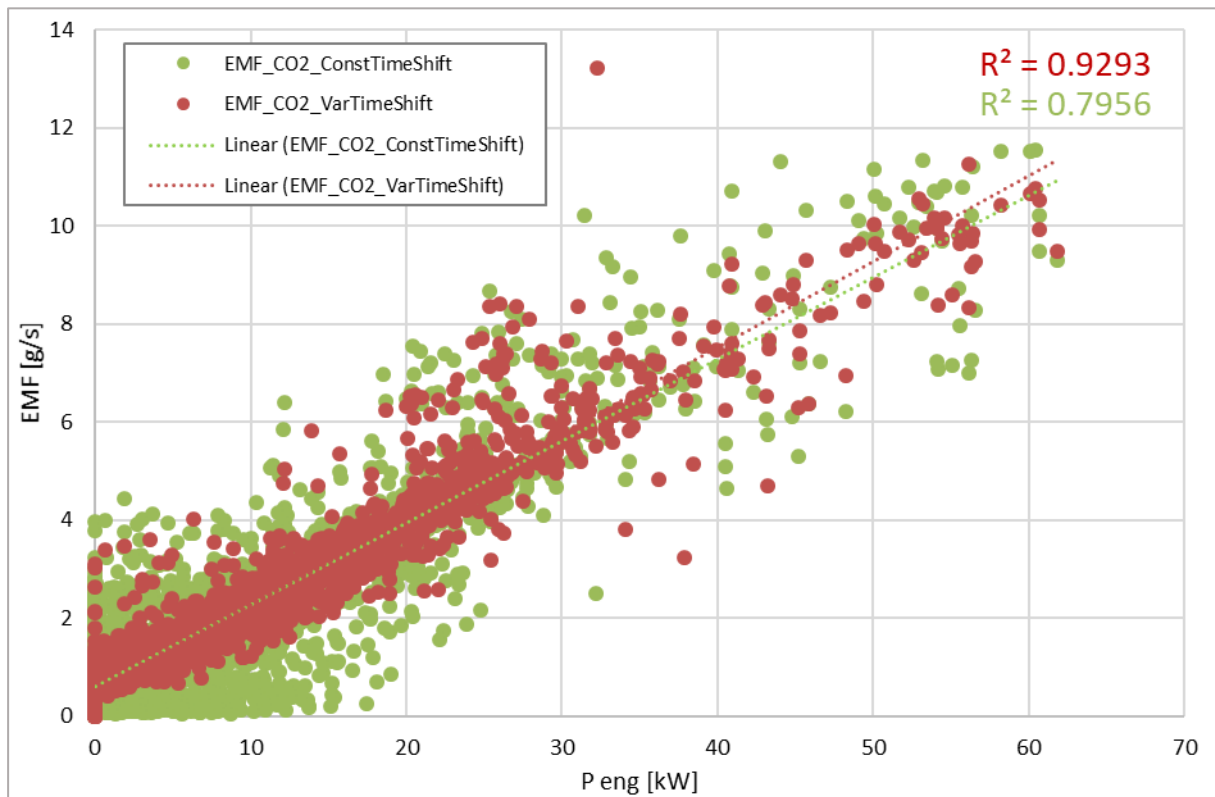


Figure 25: Comparison of CO<sub>2</sub> emission mass flow with engine power for an emission test at a chassis dynamometer with emission sampling in diluted exhaust (CVS system)

An engine power – CO<sub>2</sub> regression (Figure 26) can be used to quantify these results. The determination coefficient is higher for the signal post processed with the variable time shift method (0.9293) compared to the one post processed with the constant time shift method (0.7956) and consequently confirms the results of Figure 25.



**Figure 26: Engine power – CO<sub>2</sub> regression for an emission test at a chassis dyno with emission sampling in diluted exhaust (CVS system)**

Transient emission data with a higher signal quality improves the emission modelling in PHEM [41] as described in chapter 7. The model uses the information recorded in emission testing to set up engine emission maps, in which the emission mass flow or other engine relevant parameters are modelled over engine speed and engine power (details in chapter 6). The common method for setup of PHEM emission maps is to use emission data from transient real world cycles (e.g. WHVC). For creation of emission maps based on constant time shift data, the input signals for engine speed, power and emission mass flow were averaged over 3s to reduce the well-known temporal assignment problem. Using the ERMES tool data such an averaging procedure is no longer necessary. To demonstrate the benefit of the ERMES tool method, emission maps were created with both approaches. The quality of the resulting emission maps can be checked looking at the emission mass flow on the engine drag curve, which should be close to zero. Such a comparison of engine map data for CO<sub>2</sub> on the drag curve is shown in Figure 27. The emission map compiled based on the constant time shift method shows much higher emissions on the drag curve than the map created based on the ERMES tool data. However, also the variable time shift method cannot fully and perfectly correct all existing “distorting mechanisms” in the emission measurement setup. As a consequence, the emissions are not zero at the drag curve but obviously lower.

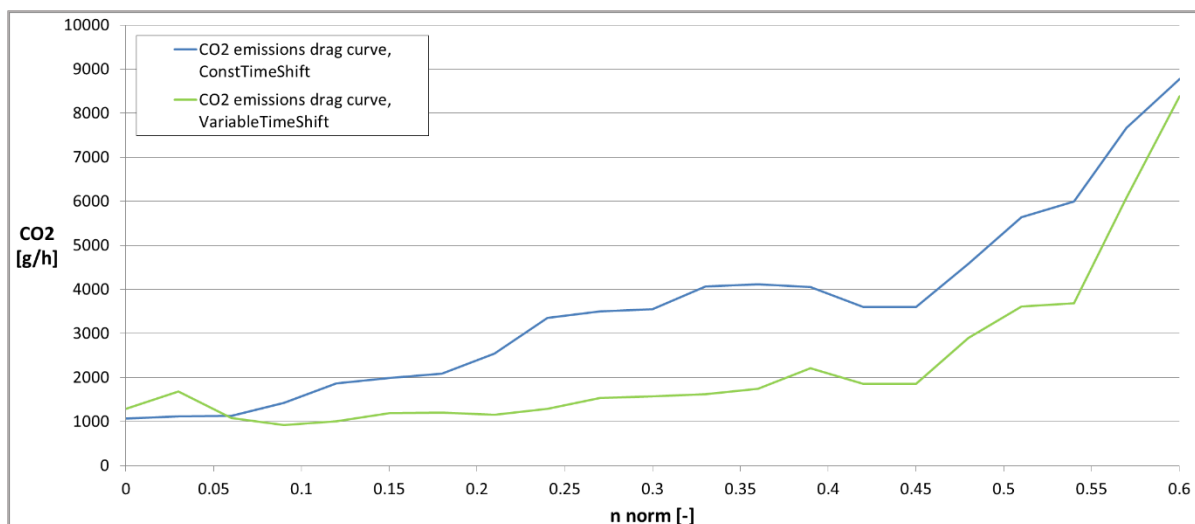


Figure 27: Comparison of CO<sub>2</sub> emissions on the drag curve

### 5.3.2.2 Measurements with Modal Sampling in Undiluted Exhaust

The ERMES tool correction methods can also be applied to test data from modal emission sampling in undiluted exhaust, e.g. from PEMS measurements. In most cases, due to the much smaller volume of the undiluted parts of the measurement system compared to CVS sampling, the variability of the gas transport time decreases. As a consequence, also the influence of the variable time shift method on the calculated mass flows from the constant time shift method is much less pronounced as for a CVS system (Figure 28).

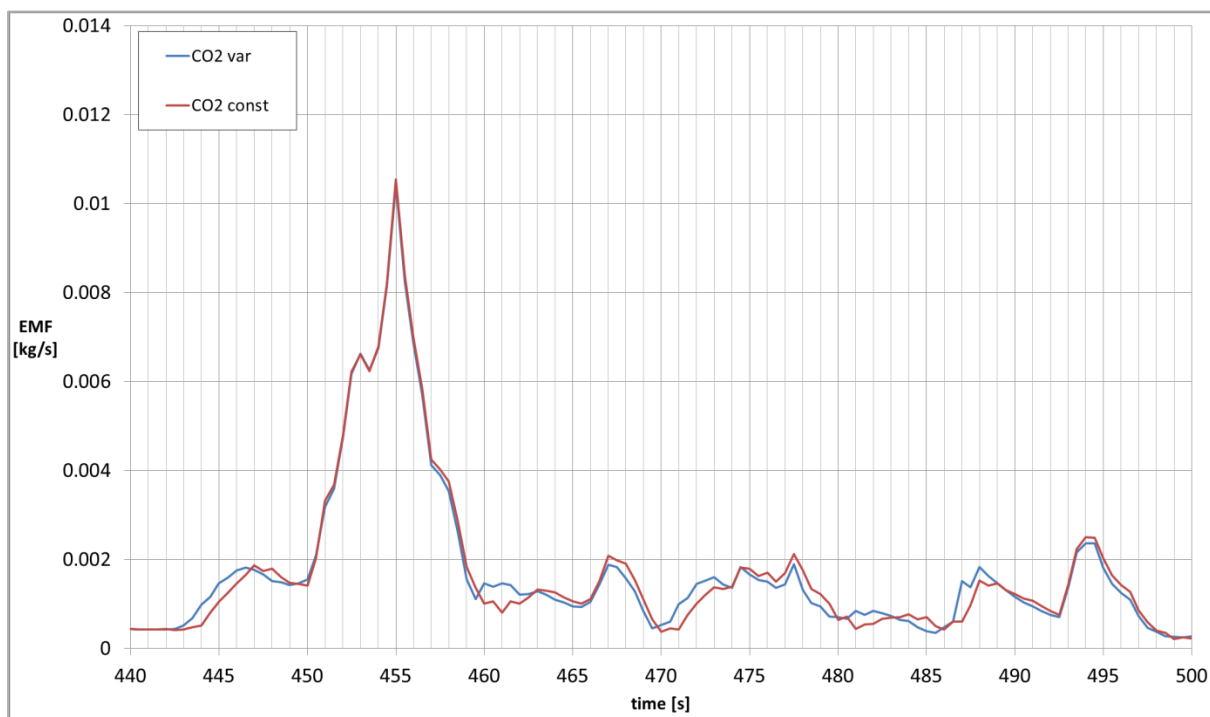


Figure 28: Comparison of variable and constant time shift method for a PEMS measurement

### 5.3.3 “Short Test” for Calibration of Volume of Vehicles’ Exhaust System

The parameterisation of the volumes in the exhaust system has a significant effect on the assignment of the emission masses to their right operating point. Consequently, exact information about the different volume sections is necessary. The volumes of test bench specific pipes (all pipes except the exhaust system of the vehicle) can be measured once and can then be defined as default values in the evaluation process. However, the volume of the

vehicle's exhaust system has to be determined for each tested vehicle. To avoid these measurement efforts, at the IVT a "short test" was developed which fulfils two purposes:

1. The implicit determination of the exhaust system volume (engine out to tailpipe)
2. Verification that the ERMES tool correction algorithms provide reasonable results for the tested vehicle.

This short test consists of the variation of engine speed from idling followed by a short phase of engine rated speed (target: approximately 10 seconds) and followed again by engine idling. The driver gets the instruction to perform engine speed changes as quickly as possible. Due to this simple test setup, such a short test can be performed both on the chassis dyno as well as in real world PEMS testing. In the test evaluation, the volume of the vehicles exhaust systems is varied within a reasonable range and the results for CO<sub>2</sub> mass flow are compared with the recorded engine speed signal. Figure 29 gives an example for the evaluation of a short test.

Accompanied by the beginning of gas pedal activation, the CO<sub>2</sub> emission mass and the engine speed rise at the same time. Following the acceleration phase, the engine speed is held close to the rated speed with a somewhat smaller CO<sub>2</sub> emission mass compared to the peak in the acceleration phase. Stopping the gas pedal activation leads to the stop of fuel injection until reaching the idling speed. With decreasing engine speed the exhaust volume flow is going down and, as a consequence, the zero CO<sub>2</sub> emissions from fuel cut-off are delayed in the measurement system due to low gas transport speed. This low CO<sub>2</sub> level should be at idling level again once the engine speed reaches idling speed, the point at which fuel injection starts again. According to the various volumes, which are shown in the legend of the diagram, both the assignment of the slope at the beginning of the gas pedal activation and the "filling up" of the zero CO<sub>2</sub> emission phase are solved differently. In this case, exhaust and undiluted volume of 68 litres (red line) provides the most reasonable result. The blue line representing a volume of 88 litres shifts the emission packets too far and the smaller ones cannot completely correct the zero emission phase. Especially the "filling" of the zero emission phase until the engine speed reaches the idling speed is the most valuable indication and shows the sensitivity of the correction methods to different volumes of the exhaust system.

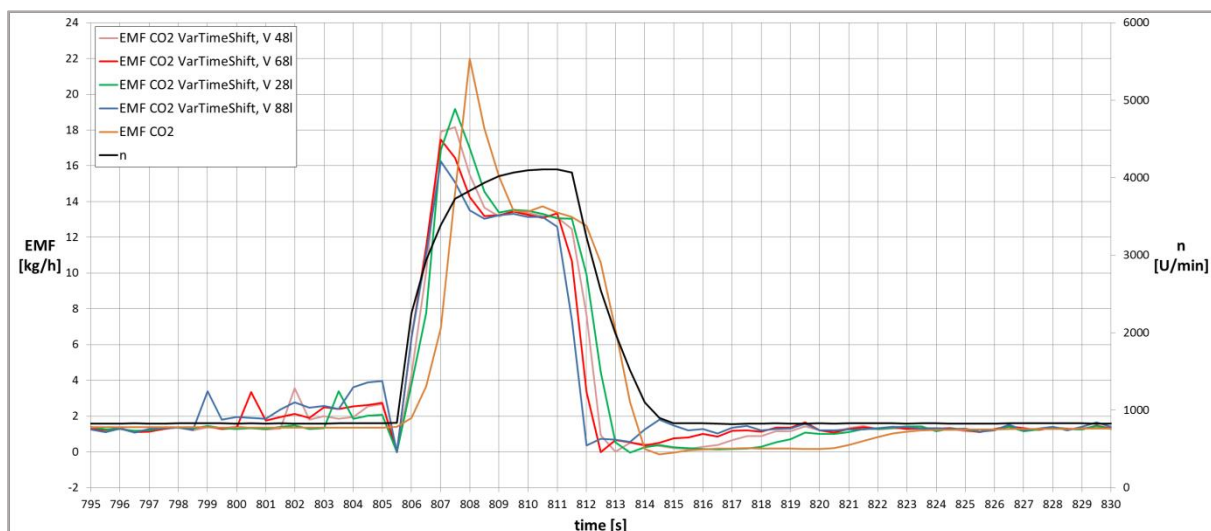


**Figure 29: Volume determination (exhaust system + CVS connection pipe) based on the results of the short test**

By evaluating the test in the ERMES tool, the volume of the exhaust system of the vehicle can be determined with very low effort.

### 5.3.4 Influence of Differences in the Response Characteristics of Exhaust Mass Flow and Concentration Measurement on the Results of the Variable Time Shift Method

The variable time shift method optimally corrects the signal when there is a match between the response characteristics (delay and duration) of the measurement of exhaust mass flow and emission concentration. To demonstrate this influence, Figure 30 shows the emission mass flow at position C (sampling point at the end of the undiluted system).

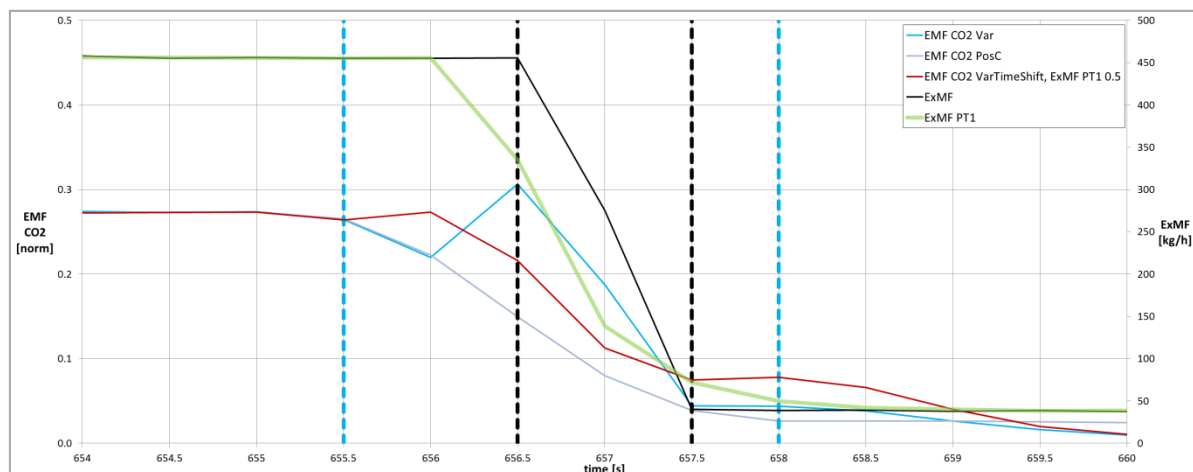


**Figure 30: Coherence of response characteristic**

This example represents the decrease from a high constant emission and mass flow level to a lower one. The dotted lines in the respective colours show the beginning and the end of the different signal changes. It is obvious that the change of the response corrected emission concentration (represented by the emission mass at position C “EMF CO2 PosC”, purple) takes longer than the turn of the mass flow (“ExMF”, black). For that reason, the different concentrations are inverse PT1 corrected, but the effect is limited and cannot completely compensate the difference of the response characteristics. This is a result of the slower response time of the analyser compared to the measured mass flow. Consequently, the variable time shift method does not work perfectly. The valley at second 656 is formed because of the falling concentration with the constant volume flow before the first black dotted line. The missing emission mass is shifted to second 656.5 resulting in a peak at that position. One possibility for the equalization of the different response characteristics – in addition to the inverse PT1 correction of the concentrations – could be a PT1 correction of the exhaust mass flow. With this flattened signal (“ExMF PT1”, green), the response delay would be extended and consequently the signals would match better regarding the peak at second 656.5 (“EMF CO2 VarTimeShift, ExMF PT1 0.5”, dark red signal). However, the long delay implies high idling emissions and the signal is just corrected to the “new” flattened exhaust mass flow. Despite the improvement of the response characteristic by the invers PT1 correction of the measured concentration, this method downgrades the fast measured exhaust mass flow. Moreover, the different concentration measuring sensors have different response characteristics. Consequently, the adaption of the PT1 correction of the exhaust mass flow has to be done for the average of these different response characteristic signals. This restricts the benefit for the single emission components.

Coherence of the response characteristic has to be checked for every test bed because of different sensors and mass flow measurement equipment. A decision concerning separate signal correction possibilities has to be made after having regarded the test results.

## 6 Simulation Model PHEM

The HBEFA provides such a huge amount of data (see section 3.3) that measuring the emissions for all these different traffic situations would be very costly and time-consuming. Consequently, using a simulation tool to create the final emission factors is the only reasonable way to handle this multiplicity of various traffic situations. The main purpose of this simulation tool is the trade-off between model accuracy (and consequently complexity) and reasonable handling for whole fleet applications. This means that, on the one hand, the final vehicle models for the HBEFA (e.g. HDV TT 34-40t Euro<sup>o</sup>VI) shall provide the main specific features and behaviours regarding the exhaust after-treatment system (e.g. cool down effects of the SCR catalyst) and, on the other hand, the model shall work on an accuracy level, which allows to merge different technologies (e.g. SCR only vehicles and EGR plus SCR vehicles) to one comprehensive vehicle. For that reason, the model PHEM seems to be most appropriate [41] and was also used to generate the emission factors for former versions of the HBEFA [25].

The following part gives a short description of the model PHEM and deals with some special functions which have been worked out in line with this dissertation. Some parts of this chapter are taken over from [23], but more details can be found in [42] and [43].

Equations 6-1 and 6-2 help to understand how PHEM works. They describe the normalisation of engine rated power and speed. This process allows comparing engines independent of size and power and simplifies the creation of average engine maps and consequently the setup of fleet models, one of the main aims of PHEM.

$$P_{norm} = \frac{P}{P_{rated}} \quad 6-1$$

$$n_{norm} = \frac{n - n_{idle}}{n_{rated} - n_{idle}} \quad 6-2$$

Notation:

$n$  ... Engine speed in rpm

$n_{idle}$  ... Idling engine speed in rpm

$n_{norm}$  ... Normalised engine speed

$n_{rated}$  ... Rated engine speed in rpm

$P$  ... Engine power in kW

$P_{norm}$  ... Normalised engine power

$P_{rated}$  ... Rated engine power in kW

### 6.1 Standard Simulation Process

The Passenger Car and Heavy Duty Emission Model was developed at the IVT at TU Graz in the early 1990s. Due to continuous further development of vehicle technologies, further development of the simulation processes in PHEM goes on as well.

PHEM calculates fuel consumption and emissions of road vehicles in 1 Hz for a given driving cycle based on the vehicle longitudinal dynamics and emission maps (Figure 31). Engine power demand for the cycles is calculated from driving resistances, losses in the transmission line and auxiliary power demand. The engine speed is simulated by the tire diameter, final

drive and transmission ratio as well as a driver gear shift model. Base exhaust emissions and fuel flow are then interpolated from engine maps. To increase the accuracy of the simulated emissions, transient correction functions are applied to consider different emission behaviour under transient engine loads. Since the vehicle longitudinal dynamics model calculates the engine power output and speed from physical interrelationships, any imaginable driving condition can be illustrated by this approach. The simulation of different payloads of vehicles in combination with road longitudinal gradients and variable speeds and accelerations can thus be illustrated by the model just like the effects of different gear shifting behaviour of drivers.

For the simulation of emission factors, a predefined set of “average vehicles” is elaborated for each update of the HBEFA representing average European vehicles for all relevant vehicle categories in terms of mass, driving resistances, etc. The engine emission maps and after-treatment system parameters are gained from the huge number of instantaneous measurements in the HBEFA database. From the test data, PHEM computes the engine power and then sorts the measured emissions according to engine speed and power into the engine map per vehicle. The map formats are normalized. This allows calculation of weighted average engine maps from all vehicles measured within a class (e.g. all EURO<sup>o</sup>VI TT 34-40t). Similarly, the efficiency maps from after-treatment systems are set up as functions of space velocity, temperature and ammonia storage.

To assess the engine power trajectories over a test, PHEM uses a novel approach calculating the actual engine power from CO<sub>2</sub> and engine speed recordings [44]. Besides engine and chassis dynamometer tests, all PEMS tests can thus be used for model development – as long as emissions and engine speed are recorded and the driving cycle covers the relevant engine load areas.

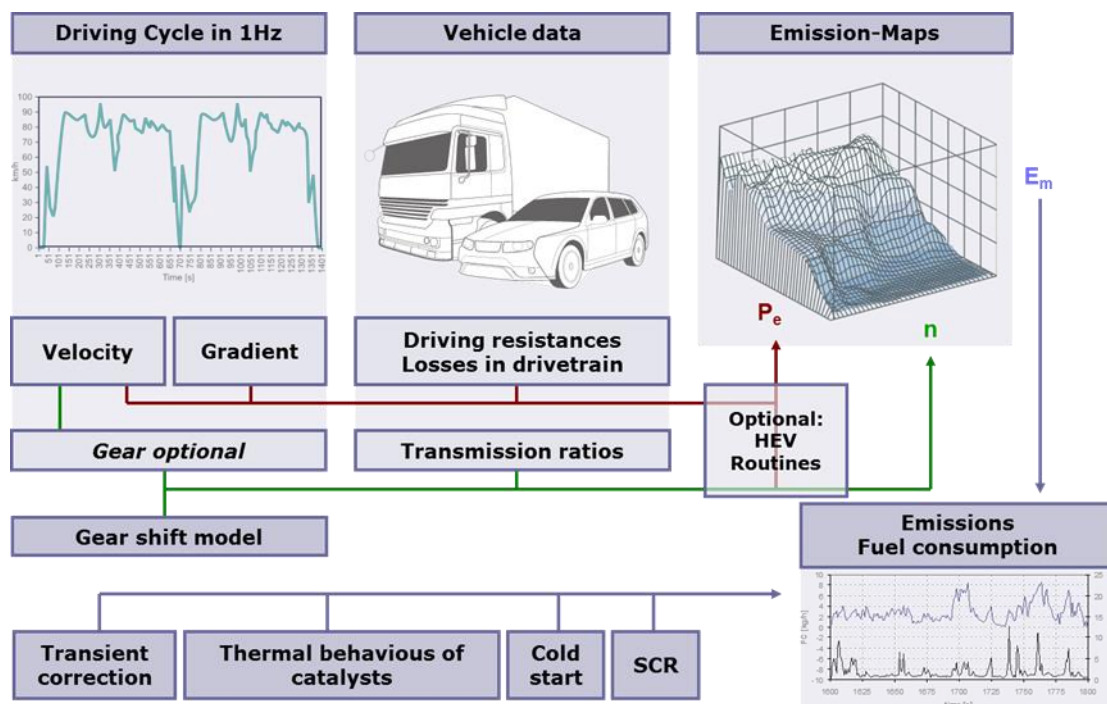


Figure 31: Scheme of the PHEM model

This engine speed and engine power related standard simulation works for all emission components in a similar way. Of course, e.g. CO and HC are not only dependent on these two parameters in modern Euro<sup>o</sup>VI vehicles, but statistical analysis showed that there is no other parameter which has more influence on these components. Moreover, the focus is not primarily on the accuracy of CO and HC simulation due to the low absolute emission level.

Consequently, this engine speed and power based approach, which fits well with former vehicle generations [42], is also applied to modern vehicle generations for these components.

## 6.2 Exhaust After-treatment Model

The  $\text{NO}_x$  conversion of a SCR catalyst (standard for an effective  $\text{NO}_x$  reduction in current EURO<sup>o</sup>VI vehicles) is dependent on exhaust gas temperature, space velocity inside the catalyst and the storage level of  $\text{NH}_3$ . In this case, PHEM includes a model for the simulation of temperatures in the exhaust after-treatment system [43]. An additional model for the simulation of the  $\text{NO}_x$  conversion rates was developed especially for this version of the HBEFA. The following section describes both parts of the exhaust after-treatment model.

### 6.2.1 Temperature Model

The simulation of temperatures uses a zero dimensional approach. To calculate the temperatures of single components, the heat transfer between exhaust and components and between components and ambient and a heat balance per component is calculated. The thermal inertia of the components is considered together with the masses and heat capacities. With this approach, the heat up and cool down effects down-stream of the engine can be simulated. This is especially relevant for the SCR catalysts in diesel vehicles, where the cool down in low load driving can reduce the  $\text{NO}_x$ -conversion significantly (see section 4.3). Figure 32 depicts the scheme of the model for the simulation of temperatures in the exhaust after-treatment system. The sensor signals are simulated also considering heat transfer and thermal inertia to allow comparison with measured temperature signals. Details of this model can be found in [43].

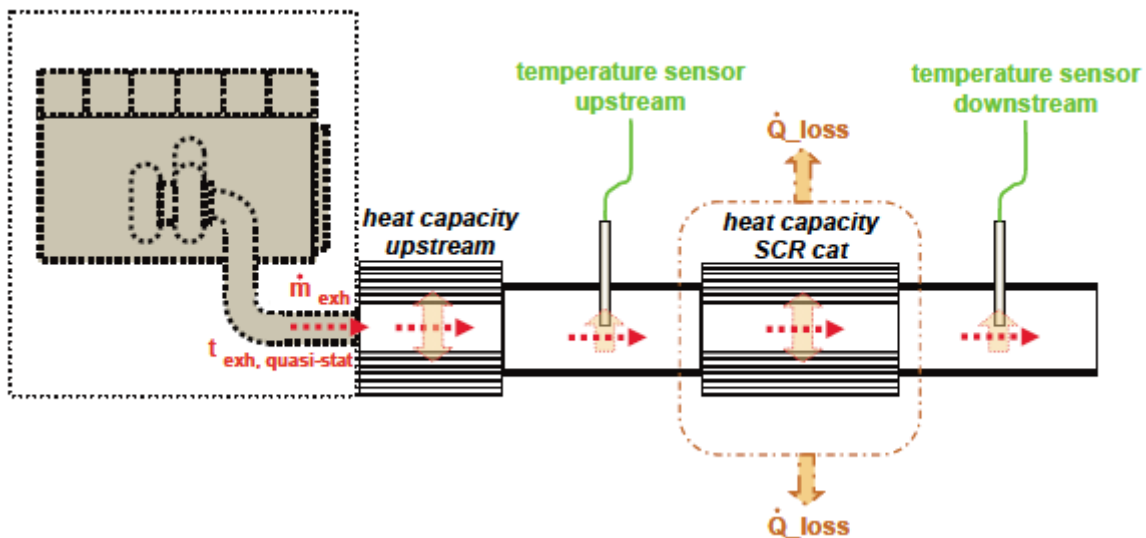


**Figure 32: Scheme of the PHEM model for temperature simulation in the exhaust after-treatment**

Within the scope of this work, the existing temperature model was parametrized and applied. The first step is to set up the models of the complete exhaust after-treatment system for each single vehicle measured in the test program. In this case, a big advantage is the similar construction of each exhaust after-treatment system independent on make and model of the vehicle. All contain a turbocharger, a pipe, which leads to the exhaust after-treatment box, a DOC-DPF combination and a SCR catalyst. Each module gets material and vehicle specific attributes like mass or external surface, which, for example, affect heat exchange or thermal conduction. The next step is to create the engine temperature map (dependent on engine power and speed) using the temperature recorded by a thermal element directly downstream of the turbocharger. Since the temperature map in PHEM represents quasi-stationary temperatures at the turbocharger, the measured temperatures have to be corrected by the

thermal inertia of the turbocharger. To gain data for the temperature map, some steady state points were measured on the chassis dyno. In principle, engine test bed measurements would be more appropriate, because for steady state points at high load the tyre temperatures reach a critical level on the chassis dyno since the operating point has to be held for some minutes until all temperatures in the exhaust system have reached constant conditions. As a consequence, just some points and not the complete matrix can be measured. Figure 33 shows the measured quasi-stationary temperatures for one single vehicle.

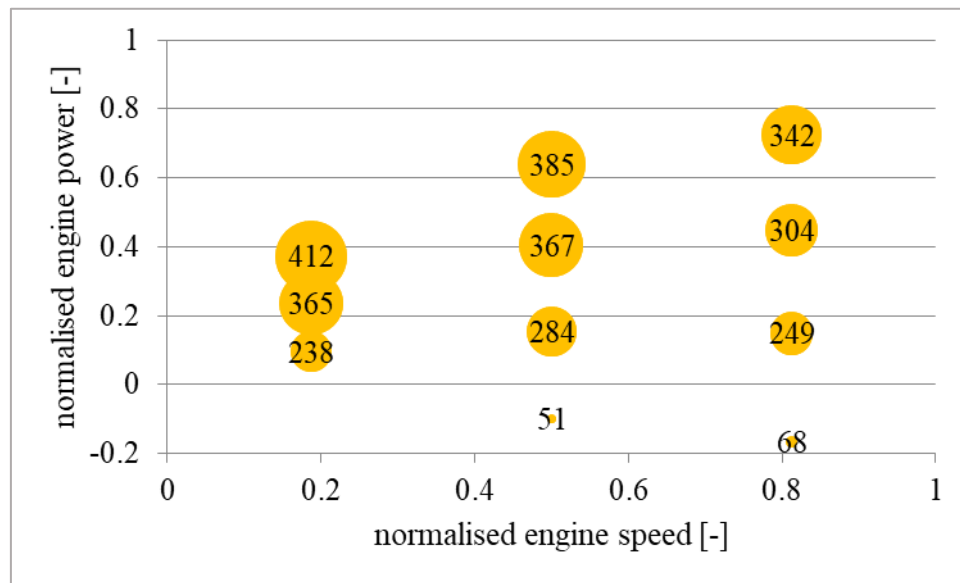


**Figure 33: Quasi-stationary temperatures at turbocharger**

After filling the standard grid for HDVs in PHEM by a Shepard based extrapolation of the measurement data, the next step is to check this generated map by comparison of the simulated and the measured temperature downstream of the turbocharger. Figure 34 shows that the simulation result (yellow line) fits to the measurement (blue line) for one on-road trip.

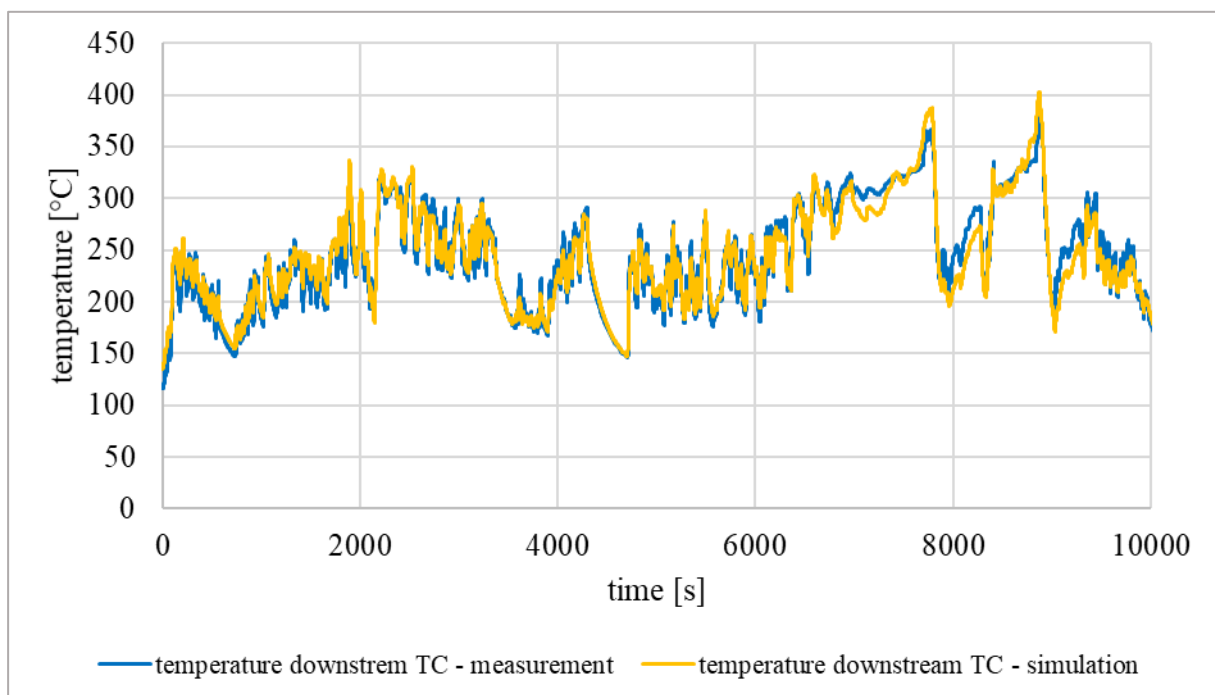


**Figure 34: Temperature downstream TC – simulation and measurement**

The complete exhaust gas temperature map can be seen in Figure 57.

The next step is to adjust the characteristics of the single modules of the exhaust after-treatment system (e.g. mass, heat transfer) in order to meet the measured temperature upstream of the SCR. Figure 35 shows a comparison between measured (blue line) and simulated (yellow line) temperature for one on-road trip. Also in this case, the two signals fit quite well.

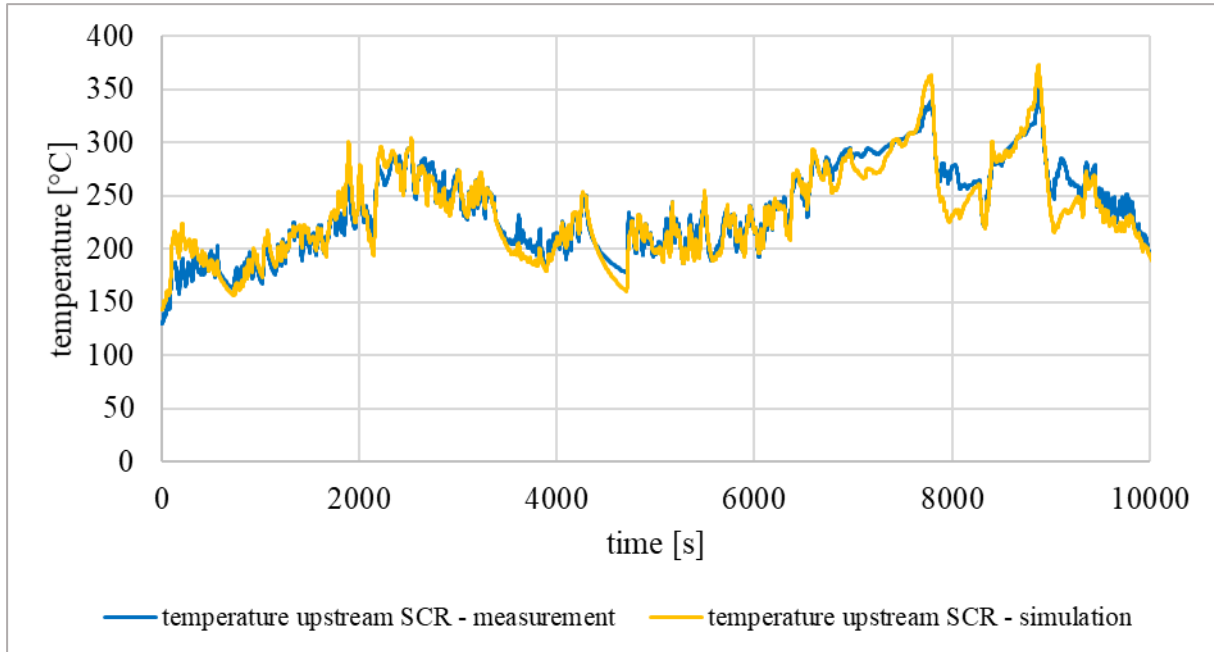


**Figure 35: Temperature upstream SCR – simulation and measurement**

## 6.2.2 SCR Simulation

The simulation of the  $\text{NO}_x$  Tailpipe emissions in PHEM is based on a  $\text{NO}_x$  Engine-out simulation, which is dependent on engine power and engine speed, and on the  $\text{NO}_x$  conversion in the SCR catalyst. The following section describes the basic SCR simulation model in PHEM and the further development regarding the special requirements of EURO<sup>o</sup>VI vehicles. This part of the work is based on 7 EURO<sup>o</sup>VI HDVs measured at TUG.

### 6.2.2.1 Basic $\text{NO}_x$ Conversion

As section 3.2.2.3 describes, the conversion in a SCR catalyst is mainly dependent on the temperature and the space velocity of a catalyst. A simple tailpipe emission simulation which uses emission maps based on engine power and engine speed does not consider these effects and consequently does not offer appropriate simulation accuracy. However, the standard SCR model in PHEM works with conversion efficiency maps according to these principles (Figure 36).

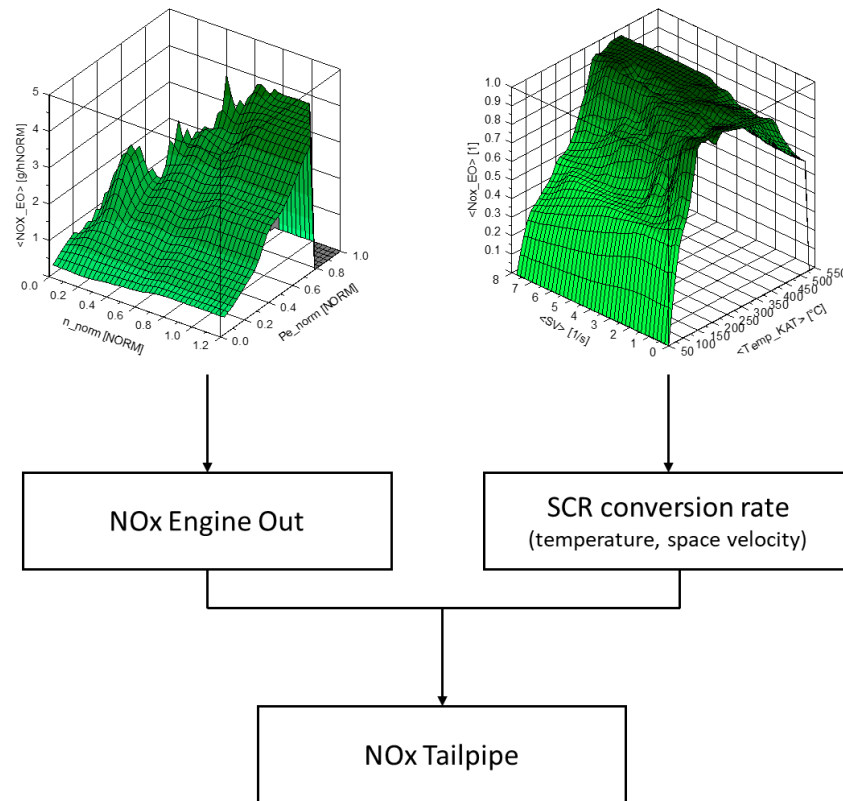


**Figure 36: Principle of the standard SCR model in PHEM**

As temperature for the SCR efficiency, the model uses the temperature directly upstream of the SCR catalyst. Investigations for single vehicles showed that this works more satisfactorily than the temperature downstream of the catalyst, which is obviously too inert and cannot rebuilt relevant load changes accurately.

The space velocity gives the ratio of exhaust gas volume flow at standard conditions to the catalyst volume. PHEM uses the properties of air at standard conditions (0 °C, 1.013 bar) for the diesel exhaust gas. Thus, the space velocity is:

$$SV = \frac{ExMF * R_{Air} * T_{norm}}{p_{norm} * V_{cat}} \quad 6-3$$

Notation:

$ExMF$  ... Exhaust mass flow in kg/s

$p_{norm}$  ... Pressure at normalised conditions in Pa

$R_{Air}$  ... Specific gas constant of air in J/(kg\*K)

$SV$  ... Space velocity in 1/s

$T_{norm}$  ... Temperature at normalised conditions in K

$V_{cat}$  ... Catalyst volume in m<sup>3</sup>

Figure 37 shows a comparison between measured and simulated NO<sub>x</sub> emissions for different cycles. The graph represents the mean results of all EURO<sup>o</sup>VI vehicles, which have been used for model development. ISC cycles are the base for the model parametrization and consequently the simulation fits these standard operating conditions very well. However, the

model has problems with predicting the on-road Stop&Go and the heavy Stop&Go cycle on the chassis dyno (preconditioning idling) in an accurate way because of the long low load phases. These phases lead to a temperature drop in the exhaust after-treatment system and this effects the reduction in the NO<sub>x</sub> conversion rate mainly due to slower chemical reactions [45]. Of course, the standard SCR model respects this temperature decrease and calculates higher NO<sub>x</sub> emissions for these low load cycles compared to the ISC cycle, but the results are clearly on a level that is too low. Obviously, the standard PHEM SCR model does not cover all relevant impacts on NO<sub>x</sub> emissions during low load phases.

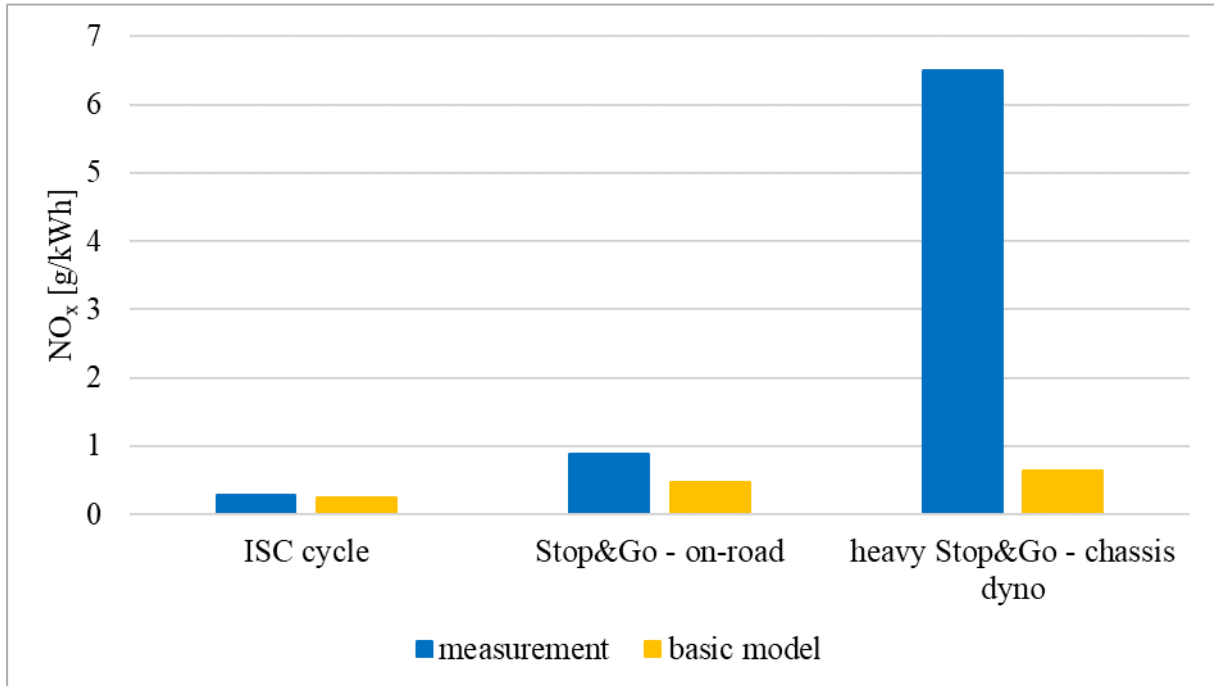


**Figure 37: Standard SCR model – comparison of measurement and simulation**

These results are illustrated in detail in the annex (see Table 24).

### 6.2.2.2 NH<sub>3</sub> Storage Model

As already described above, the temperature decrease in the exhaust after-treatment system during long low load phases (e.g. traffic jam) leads to a reduction of the NO<sub>x</sub> conversion rate due to slower chemical reactions at lower temperatures [45]. This effect is already respected in the standard SCR model. However, another relevant effect is the AdBlue injection cut off below approximately 180 to 200°C in the exhaust after-treatment system. Hydro- and thermolysis, which are used for the conversion of AdBlue to NH<sub>3</sub>, do no longer work in this low temperature area [46]. Details of this process have already been explained in 3.2.2.3. NH<sub>3</sub>-injection measurement data, which unfortunately was available for only one vehicle, and a sensitivity analysis of the NH<sub>3</sub> storage models for all vehicles treated confirmed the findings in literature in this field and resulted in a limit temperature of 190°C [20]. Figure 38 illustrates on-road measurement data showing this AdBlue cut off (AdBlue dosing is the blue line) when the temperature (yellow) drops below the limit temperature (red).

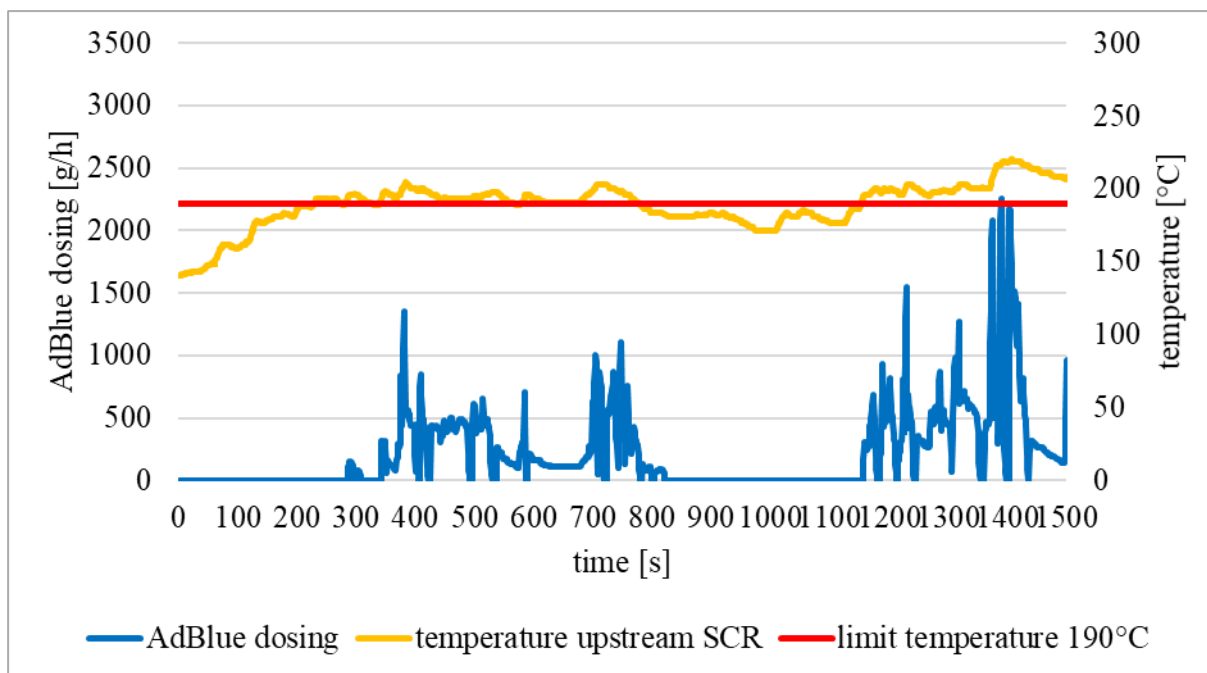


**Figure 38: On-road trip – AdBlue dosing and temperature upstream of the SCR**

During AdBlue injection phases, enough  $\text{NH}_3$  is stored in the SCR-catalyst and can be used for the reduction of  $\text{NO}_x$  in the cut off phases. However, this  $\text{NH}_3$ -consumption reduces the  $\text{NH}_3$  storage level and consequently deteriorates the  $\text{NO}_x$  conversion rate in addition to the slower chemical reactions at this low temperature level. The conversion rate finally falls to zero when the  $\text{NH}_3$  storage is completely empty. As soon as the temperature rises above the limit temperature again, the  $\text{NH}_3$  dosing is activated once more and storage gets filled up to approximately 50 % of the possible storage capacity. Equation 6-5 explains the calculation of the stored ammonia mass in the catalyst, which is mainly dependent on the catalyst volume and the temperature dependent  $\text{NH}_3$  storage capacity [45]. Measurements on vehicles with different engine sizes showed that the volume of the SCR catalyst changes approx. proportionally to the rated engine power. Consequently, the SCR catalyst volume of each single vehicle was normalised with the respective rated engine power and a mean value was set up for the general  $\text{NH}_3$  storage model (equation 6-4).

$$V_{cat} = V_{cat\ norm} * P_{rated} \quad 6-4$$

$$\text{NH}_3\text{stor.} = V_{cat} * \text{NH}_3\text{stor.}_{temp} * \text{NH}_3\text{stor.}_{\%} \quad 6-5$$

Notation:

$\text{NH}_3\text{stor.}$  ... Stored  $\text{NH}_3$  mass in g

$\text{NH}_3\text{stor.}_{\%}$  ...  $\text{NH}_3$  storage ratio in % of maximum storage capacity at the current temperature

$\text{NH}_3\text{stor.}_{temp}$  ... Temperature dependent  $\text{NH}_3$  storage capacity in g/l

$P_{rated}$  ... Rated engine power in kW

$V_{cat}$  ... Catalyst volume in l

$V_{cat\ norm}$  ... Normalised catalyst volume in l/kW

Measurement data from a EURO<sup>o</sup>VI truck with 152 kW rated engine power showed that the AdBlue injection rate (see equation 6-7) is dependent on the NH<sub>3</sub> storage ratio. It is higher for phases at a very low NH<sub>3</sub> storage level and decreases with a filling level above 40 percent. It illustrates an average AdBlue injection of 600 g/h at a high storage level; however, after long low load phases (consequently, the NH<sub>3</sub> storage level drops), the vehicle injects at the maximum rate of the installed system. In this case, this is 6800 g/h for the Bosch Denoxtronic [47]. The factor 2 in this equation can be explained by equations 3-1 and 3-2. Both reactions, thermolysis and hydrolysis, each produce 1 mole NH<sub>3</sub>, but in total only 1 mole Adblue/urea is used for both reactions. The factor 0.325 represents the share of urea in the AdBlue.

As all pollutant emissions, NO<sub>x</sub> EO emissions are normalised in the simulation method of PHEM based on the rated engine power (see section 7.4.1.1). That means that a vehicle with more engine power produces higher EO emissions. Since vehicle AdBlue injection systems have increasing injection mass flow capacities with increasing raw exhaust NO<sub>x</sub> emissions, i.e. with increasing engine sizes [47], the AdBlue injection is also normalised in PHEM according to the rated engine power (see equation 6-6):

$$\dot{m}_{AdBlue\ norm} = \frac{\dot{m}_{AdBlue}}{P_{rated}} \quad 6-6$$

$$NH_3\ dosing = \frac{\dot{m}_{AdBlue\ norm}(NH_3\ stor.\%) * 0.325}{M_{urea} * 3600} * 2 * P_{rated} \quad 6-7$$

Notation:

$\dot{m}_{AdBlue\ norm}$  ... Normalised AdBlue mass flow in g/(s\*kW)

$\dot{m}_{AdBlue}$  ... AdBlue mass flow in g/s

$M_{urea}$  ... Molar mass of urea in g/mol

$NH_3\ dosing$  ... Dosing level of NH<sub>3</sub> in mol/s

$NH_3\ stor.\%$  ... NH<sub>3</sub> storage ratio in % of maximum storage capacity at the current temperature

$P_{rated}$  ... Rated engine power in kW

Equation 6-8 describes the increase of the NH<sub>3</sub> storage level during AdBlue dosing.

$$NH_3\ stor.\_{n+1} = NH_3\ stor.\_n + NH_3\ dosing * \Delta t * M_{NH_3} \quad 6-8$$

Notation:

$M_{NH_3}$  ... Molar mass of NH<sub>3</sub> in g/mol

$n$  ... Index for time step

$NH_3\ dosing$  ... Dosing level of NH<sub>3</sub> in mol/s

$NH_3\ stor.$  ... Stored NH<sub>3</sub> mass in g

$\Delta t$  ... Time step duration in s

The PHEM exhaust after-treatment model for HDVs respects both effects, the decrease in conversion due to lower temperatures and the additional reduction of the conversion

efficiency caused by dropping NH<sub>3</sub> storage. Figure 39 shows the principle of the exhaust after-treatment system including the NH<sub>3</sub> storage model for HDVs in PHEM. Engine-out emissions are converted according to temperature and space-velocity in the SCR (basic NO<sub>x</sub> conversion, see section 6.2.2.1) as long as NH<sub>3</sub> storage and temperature are at the target level of 50%. Below the limit temperature for AdBlue injection, PHEM reduces NH<sub>3</sub> storage proportional to the conversion of NO<sub>x</sub> emissions (see equation 6-9).

$$NH_3stor.n = NH_3stor.n-1 - \left( \frac{NO_xEO_{n-1} - NO_xTP_{n-1}}{M_{NO_x}} \right) * M_{NH_3} \quad 6-9$$

Notation:

$M_{NH_3}$  ... Molar mass of NH<sub>3</sub> in g/mol

$M_{NO_x}$  ... Molar mass of NO<sub>x</sub> in g/mol

$n$  ... Index for time step

$NH_3stor.$  ... Stored NH<sub>3</sub> mass in g

$NO_xEO$  ... NO<sub>x</sub> engine out in g

$NO_xTP$  ... NO<sub>x</sub> tailpipe in g

This NH<sub>3</sub> storage reduction influences a correction factor, which is used as a multiplier for the conversion efficiency (calculated by using the basic method). This factor always lies between 0 (empty storage) and 1 (storage level is at 50 percent), but does not behave linearly in between. A decrease in ammonia storage at high storage levels has a lower effect on the SCR efficiency compared to a decrease at lower storage levels. The function for the correction factor has been created from and is empirically based on measurement data of EURO<sup>o</sup>VI vehicles. In this way PHEM respects the influence of the NH<sub>3</sub> storage level on the NO<sub>x</sub> conversion. This leads to an increase of NO<sub>x</sub> tailpipe emissions during longer low load phases. The whole principle is illustrated in Figure 39. [20]

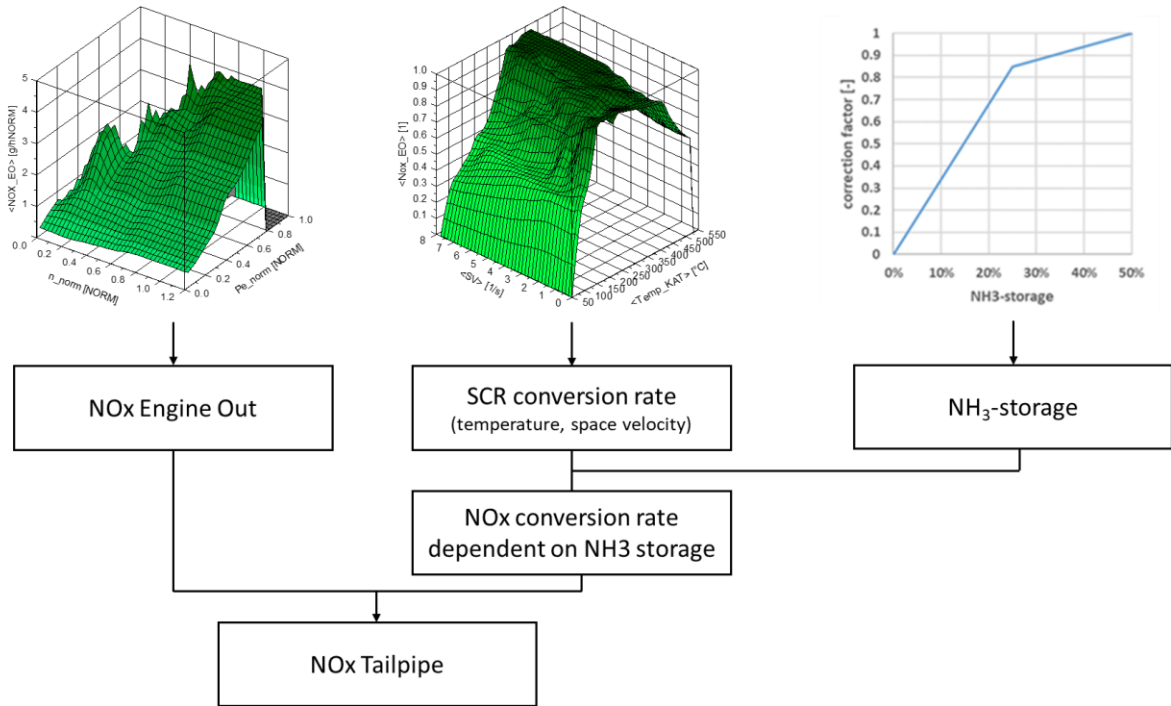


**Figure 39: Principle of the SCR model with NH<sub>3</sub> storage function in PHEM**

Figure 40 shows the same comparison as Figure 37, plus the simulation results using the NH<sub>3</sub> storage model. It is obvious that the NH<sub>3</sub> storage model does not have a big influence on simulations in standard conditions (see ISC cycle); however, for both low load cycles, the modified model provides much more accurate results than the standard SCR model.

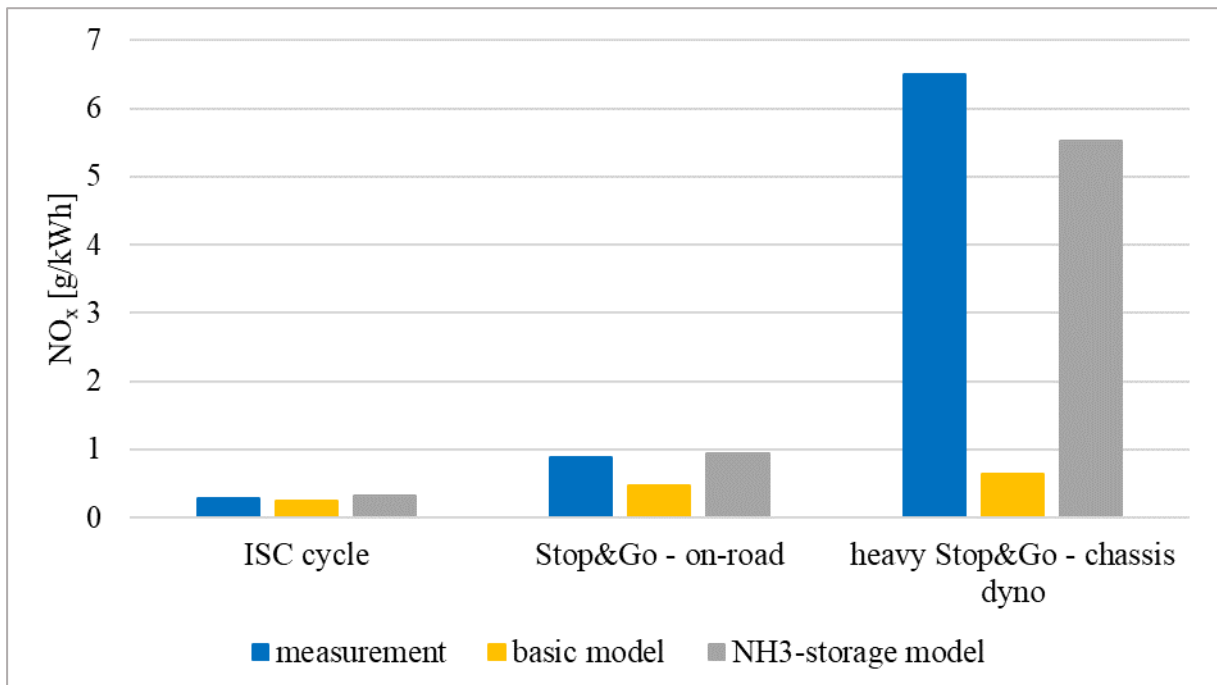


**Figure 40: Standard SCR and NH<sub>3</sub> storage model – comparison of measurement and simulation**

These results are illustrated in detail in the annex (see Table 24).

Figure 41 shows the temperatures simulated for an on-road Stop&Go cycle to illustrate the effect of the NH<sub>3</sub> storage model. The yellow line displays the vehicle speed and the blue line represents the exhaust gas temperature upstream the SCR catalyst. This example shows the special characteristic of this cycle. In some phases, the exhaust gas temperature is below the

limit temperature (red line), in other phases, it rises over  $190^{\circ}\text{C}$ . Consequently, in the simulation the cycle leads to a frequent change between emptying and refilling the ammonia storage. Since simulated  $\text{NO}_x$  emissions fit better with the measured emissions with the  $\text{NH}_3$  model engaged (Figure 40), the  $\text{NH}_3$  storage model seems to reflect the real behaviour in these driving conditions.

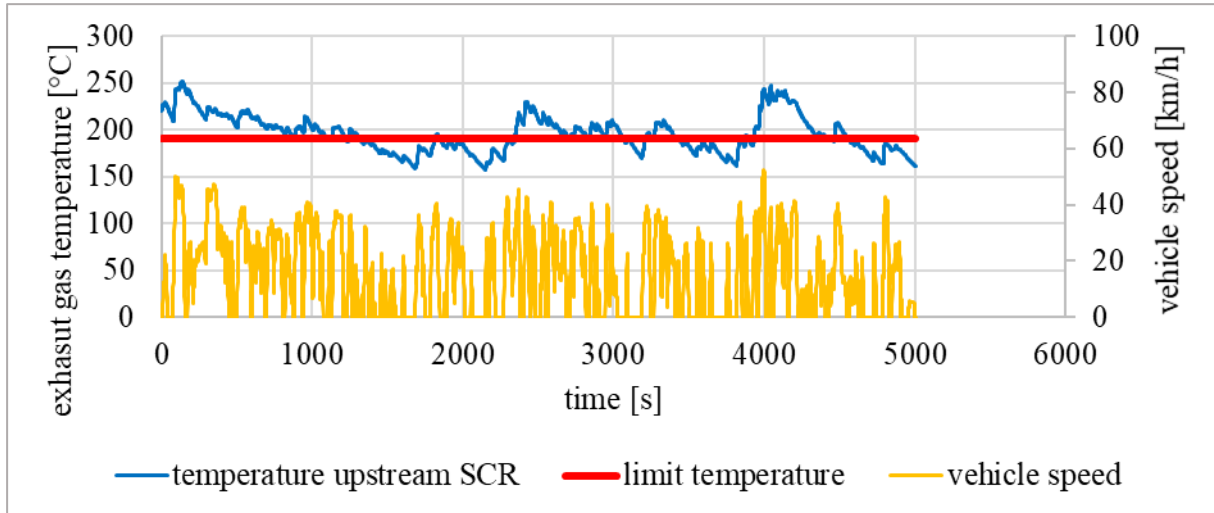


**Figure 41: Exhaust gas temperature and vehicle speed – on-road Stop&Go cycle**

Figure 42 shows simulation results for a HBEFA Stop&Go cycle with 30 minutes idling as preconditioning. The temperature upstream of the SCR stays below the limit temperature for the entire cycle time and consequently the ammonia storage continuously decreases without refilling. Again, the simulated  $\text{NO}_x$  emissions fit much better with the  $\text{NH}_3$  model; thus, the model shows a realistic performance (see Figure 40) also in Stop&Go conditions by using the correction factor function at low ammonia storage levels.

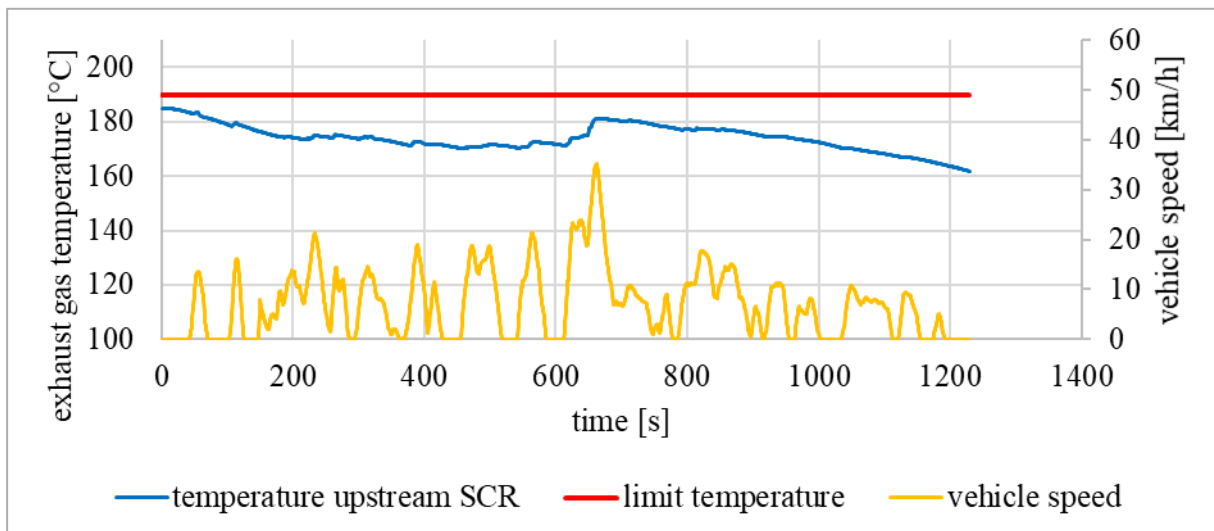


**Figure 42: Exhaust gas temperature and vehicle speed – HBEFA Stop&Go cycle**

### 6.3 Gear Shift Model

PHEM offers different simulation options: on the one hand, the engine only mode, which needs engine power and speed as input, and, on the other hand, the simulation of an entire vehicle by longitudinal dynamics. In this case, the engine speed is calculated using a gear shift model. This model is designed to reflect an average European driver employing a manual transmission system or an average automated transmission system. All in all, the model focuses on correct gear selection for all different driving situations in Europe. The

investigation of the PHEM gear selection for the HEBFA version 3 [41] partially shows a significant deviation between measurement and simulation for HDVs [48] and CBs [49]. The model does not distinguish between HDV and CB gear shift systems although CBs mostly use automatic transmission systems while HDVs use manual or automated manual transmissions [50]. Of course, these inaccuracies have an influence on the engine speed simulation and consequently on the emission simulation in PHEM.

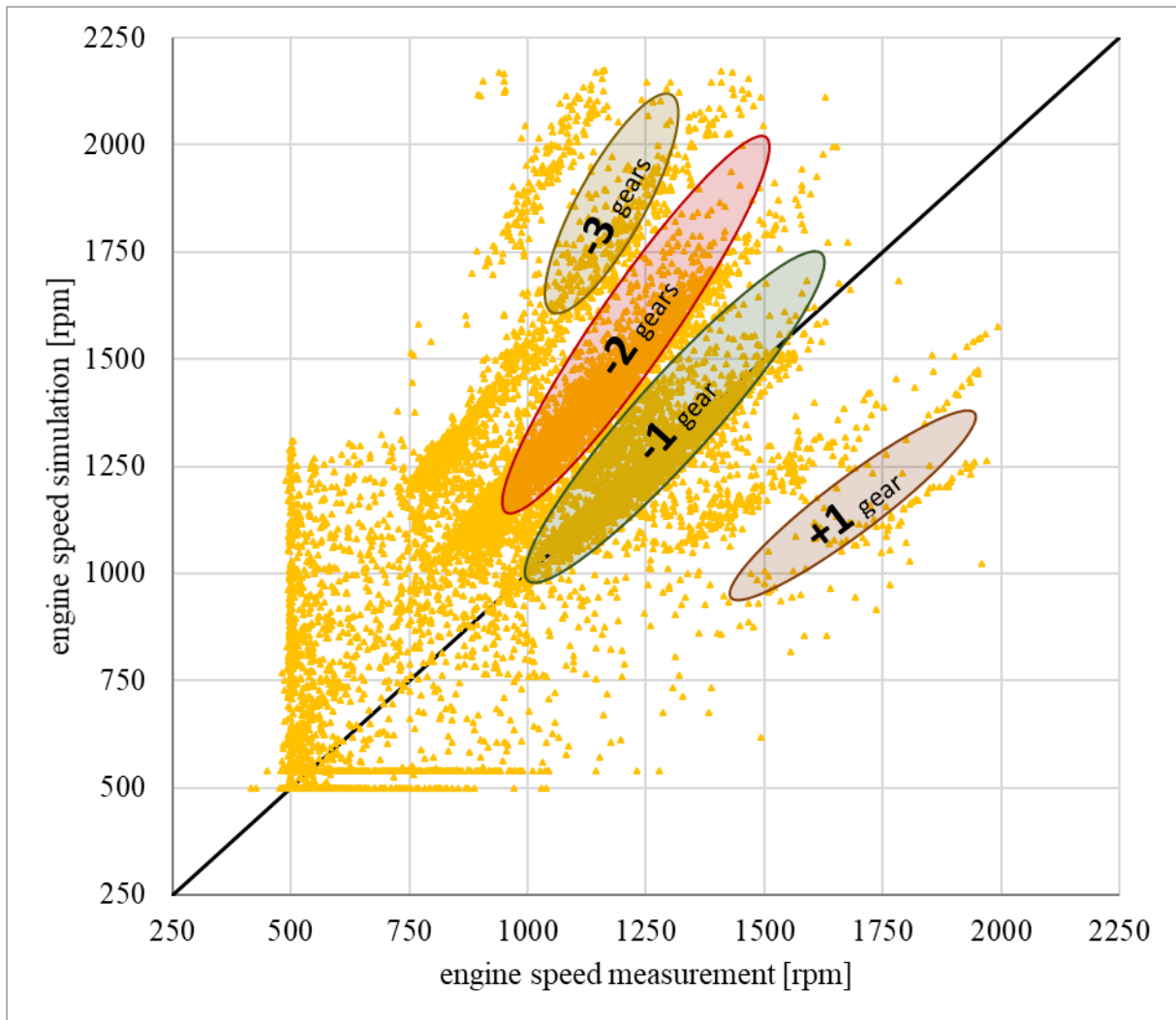
These results led to some research work regarding the gear shift model for HBEFA 4.1. This section illustrates the main findings and developments related to this topic.

### 6.3.1 HGVS

The HBEFA 3 gear shift model is divided into fast and economical driving with functions to calculate shift engine speeds. These gear shift curves themselves are not dependent on the engine power, but the “average” driving style mode mixes the two different modes according to the required engine power [41]. The model was developed for HDVs from Euro 0 up to Euro 3 and parametrized with corresponding data. The gear shift model of the HBEFA 3 has not been adapted for vehicles of the category Euro<sup>IV</sup> to Euro<sup>VI</sup>.

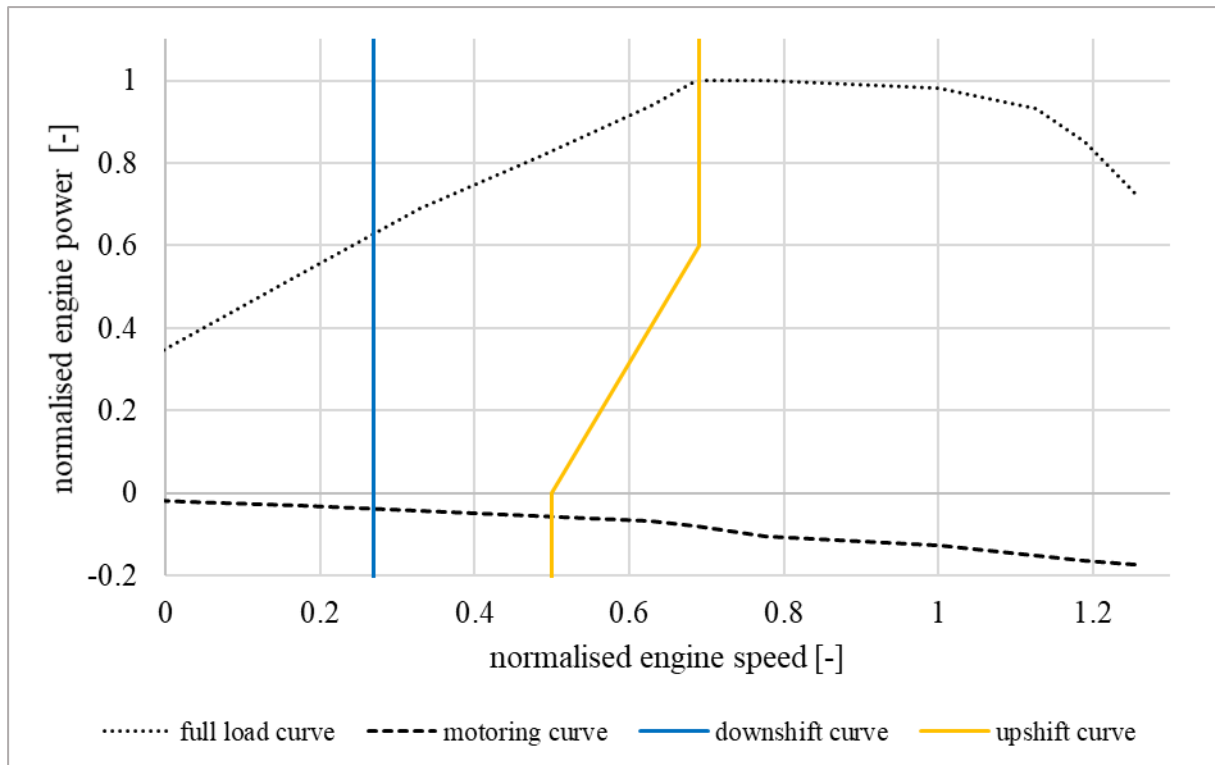
Most of the Euro<sup>IV</sup> to Euro<sup>VI</sup> HGVS use MT or AMT gear shift systems, because they offer good performance in traction and high speed phases [50]. For that reason, the database for research work regarding the gear shift model comprises 2 vehicles with MT and 2 vehicles with AMT gear shift systems. The selected vehicles also cover different size categories to obtain a comprehensive picture of the gear shift behaviour in the entire fleet.

Figure 43 illustrates a comparison for an on-road measurement, in which each yellow point represents one instantaneous measurement value. The engine speed simulation overestimates the measurement on average in this test. This means, the gears selected by PHEM are rather lower than they are in reality. The gears chosen by the HBEFA 3 PHEM gear shift model are up to 3 steps too low in some cases. Tests of other vehicles showed that this single test is representative for the general behaviour of vehicles in the current fleet.



**Figure 43: Comparison of engine speed – measurement and simulation**

The research work for VECTO done by the IVT [51] provided new findings on the design of gear shift curves. This knowledge was used to design the new gear shift curves for HDVs in PHEM, which are now based on engine power and engine speed (see Figure 44). The downshift happens at a fixed engine speed for all HGVs, while the upshift engine speed depends on the engine power demanded in the current time step. Some exception rules for special operating conditions are added, to allow higher engine speeds (e.g. if maximum engine power is needed to maintain the target vehicle speed in uphill driving). Comparison of measured and simulated engine speeds showed that PHEM keeps the engine operating points in the typical operating area for HDV engines by using these new gear shift curves. [48]



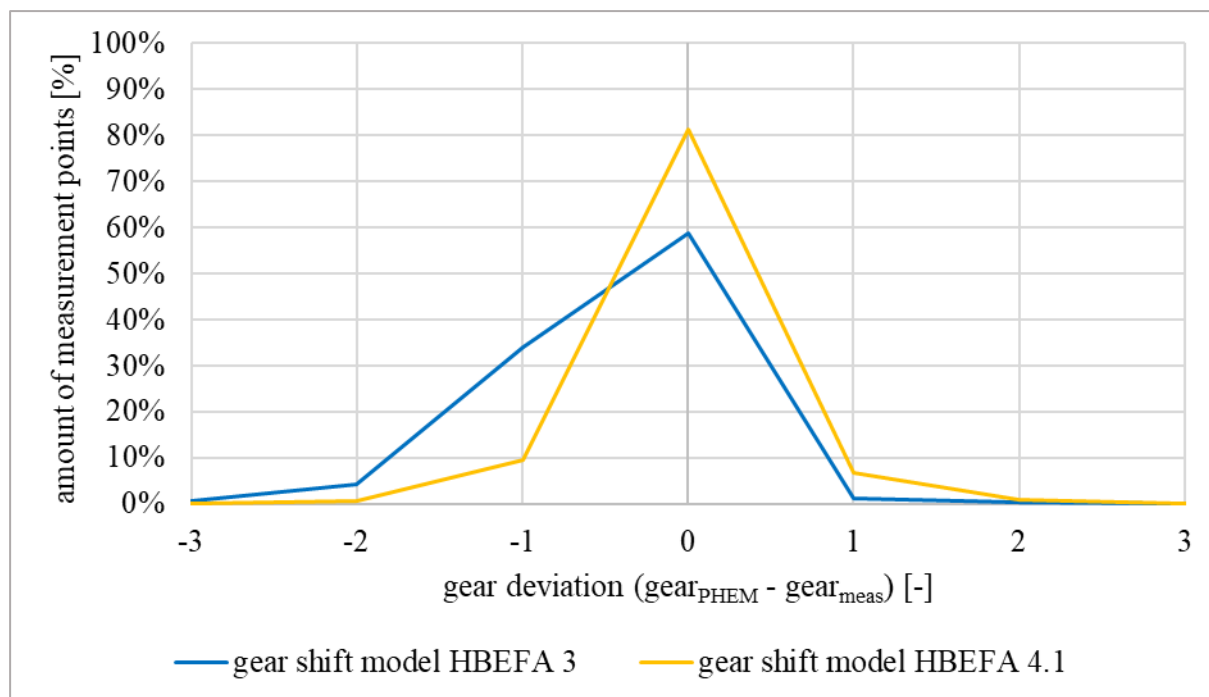
**Figure 44: Gear shift curves – gear shift model HBEFA 4.1**

Table 8 shows the numerical details regarding these new gear shift curves.

**Table 8: Definition of the gear shift curves for the HBEFA 4.1**

Point no.	Standardized engine power [-]	Standardized engine speed downshift curve [-]	Standardized engine speed upshift curve [-]
1	0.0	0.27	0.50
2	0.6	0.27	0.69

Figure 45 compares the deviation between measurement and simulation of the gear shift models for HEBFA 3 and HBEFA 4.1 regarding the measurement of a Euro<sup>o</sup>VI vehicle. As already described in Figure 43, the calculated gears are often too low when using the old model (blue line), whereas the new model provides the correct gear (yellow line) in more than 80 percent of the time steps and the distribution of wrong selections is more or less uniform around zero. Of course, this improvement influences the quality of engine speed simulation and consequently the accuracy in emission simulation in a positive way.



**Figure 45: Deviation in gear selection – gear shift model HBEFA 3 and 4.1**

Coaches have more or less the same requirements for their transmission systems regarding similar applications and consequently they use mostly MT and AMT systems [52] as well. Thus, PHEM employs the same gear shift model for coaches as for HGVs.

### 6.3.2 City Busses

The PHEM gear shift model for HBEFA 3 provides the same gear shift logics for all different kinds of HDVs. As mentioned before, HGVs mostly have MT or AMT transmission systems, but city busses normally use automatic transmission systems. Although they are quite expensive, they provide advantages for special urban driving conditions (e.g. gear shifts without traction interruption) [50] [52]. The AT systems for CBs in Europe have 4 or 6 gear ratios in most cases and use a hydrodynamic torque converter. A power junction based on converter and planetary gear set offers a continuous drive off where other systems have to switch gears repeatedly. An opened converter lock up clutch also leads to different drive train losses [49].

The research work described in this section is based on on-road city bus measurements. For this reason, 2 different busses (both of the same make and model) were measured on different test tracks.

PHEM does not provide the possibility to include a torque converter in the gear shift model, but VECTO does [51]. In PHEM every gear and axle has its own efficiency map and consequently the difference in performance has to be expressed in this way. A VECTO simulation delivered the efficiencies for different driving conditions (e.g. urban, heavy urban, suburban), which build the base for the mean efficiency maps of each gear. This is the final input for the gear efficiencies in PHEM. It improves the simulation of the required engine power and consequently the emission simulation. [49]

Regarding the principal gear shift logics for a city bus, it is reasonable to use a model which is reliant on engine speed and power, too, as it is also taken in VECTO. Thus, the development of the CB gear shift strategy is based on the logics of the new HGV model. Figure 46 shows that the HGV simulation model works more accurate for CBs than the HBEFA 3 gear shift model regarding the average deviation between measurement and simulation. The results represent the mean values for 4 on-road measurements with 2 different vehicles. Both the

mean and the absolute mean deviation are smaller for the engine power dependent HGV model compared to the HBEFA 3 gear shift model. However, it is also obvious that this new model calculates engine speeds that are too high, which is caused by the determination of gears that are too small.

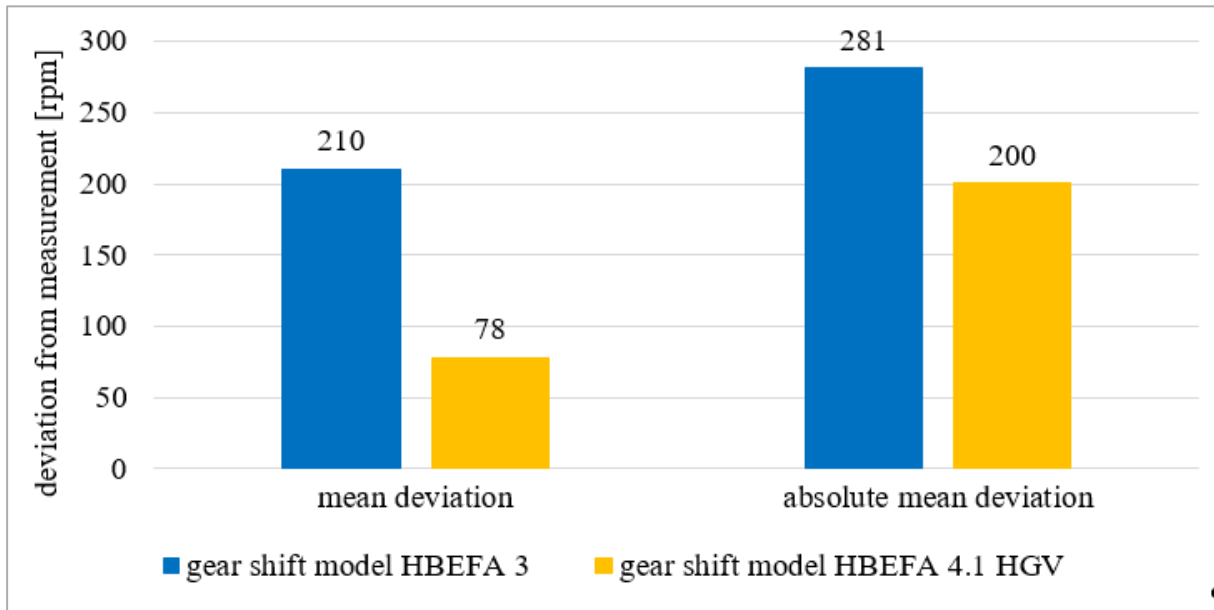


**Figure 46: Engine speed simulation – comparison of existing gear shift methods for CBs**

An investigation of the position and design of the gear shift curves resulted in different possible adaptations for improvement of the gear selection. Figure 47 illustrates the measured engine operating points on different on-road measurements and the investigated gear shift curves for the same tests as were already shown in Figure 46. It is important to mention that special functions allow to exceed the curves (e.g. full load acceleration). The red line represents the upshift and the red dotted line the downshift curve of the new HGV model. The downshift curve has not been changed due to the independence of the engine power. As Figure 46 shows, the mean deviation between simulation and measurement for four on-road cycles is about 80 rpm regarding the new HGV model. As a consequence, the first adaptation was a parallel shift of the HGV curve by these 80 rpm (blue dotted line). Looking at the data and assuming a possible upshift curve lead to type 2 (blue dashed line) and type 3 (blue line), whereas type 2 is shifted by another 80 rpm compared to type 1, and type 3 has a different shape.

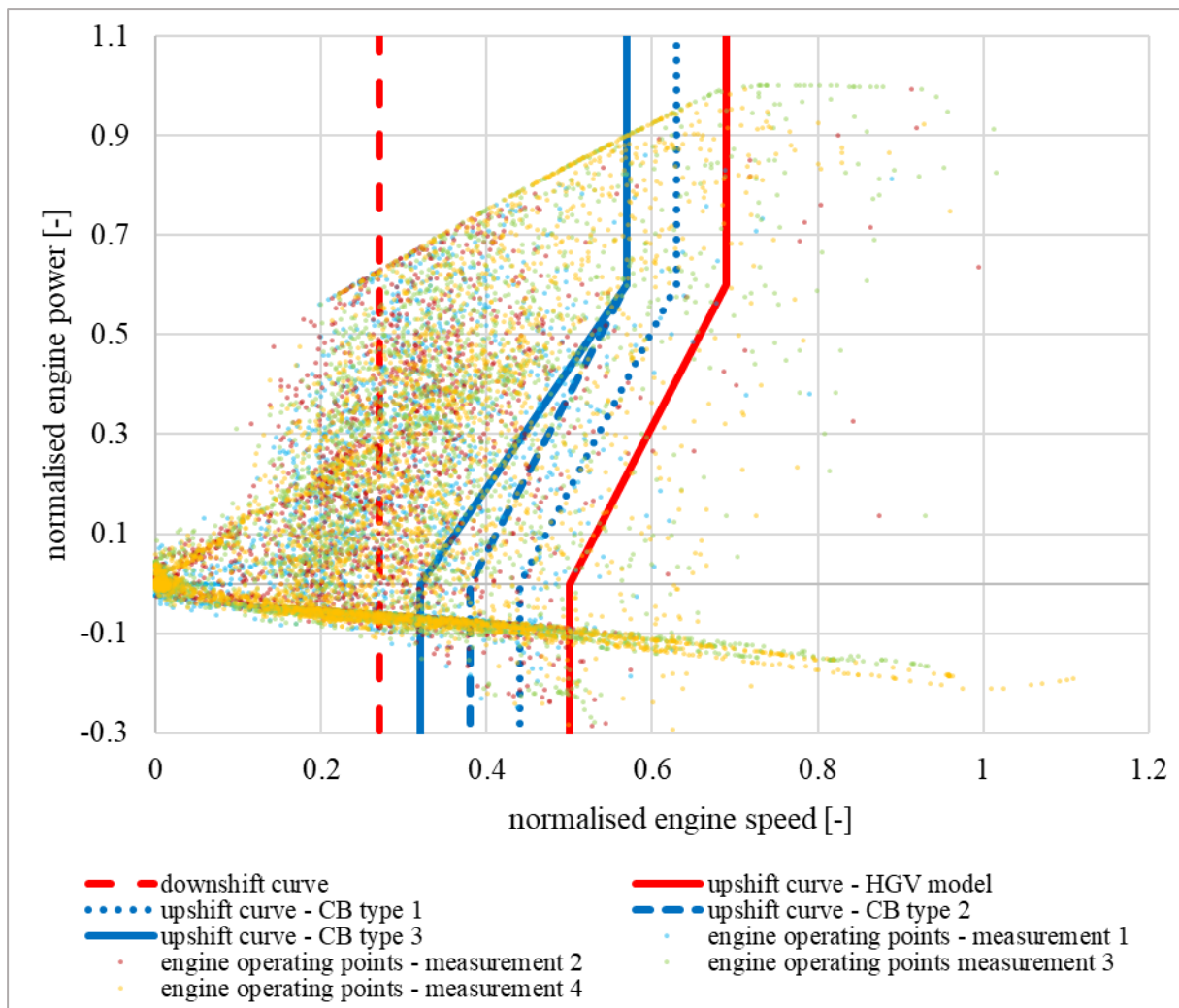


**Figure 47: Engine operating points and possible shift curves for CBs**

Figure 48 shows the deviation between the simulated (with the different gear shift models) and the measured engine operating points. As already explained in Figure 46, the new HGV model improves the result compared to the gear shift model for the HBEFA 3. This graph illustrates the results for the tests as were already shown in Figure 46 with the adapted gear shift curves in addition. Regarding the absolute mean deviation (right graph), the new curves deliver just a small benefit compared to the new HGV model, but the results for the mean deviation (left graph) show an enhancement of the balance around zero deviation between measurement and simulation of the engine operating points especially for type 2. As a consequence, upshift curve – CB type 2 is included in the gear shift model HBEFA 4.1 for city busses.

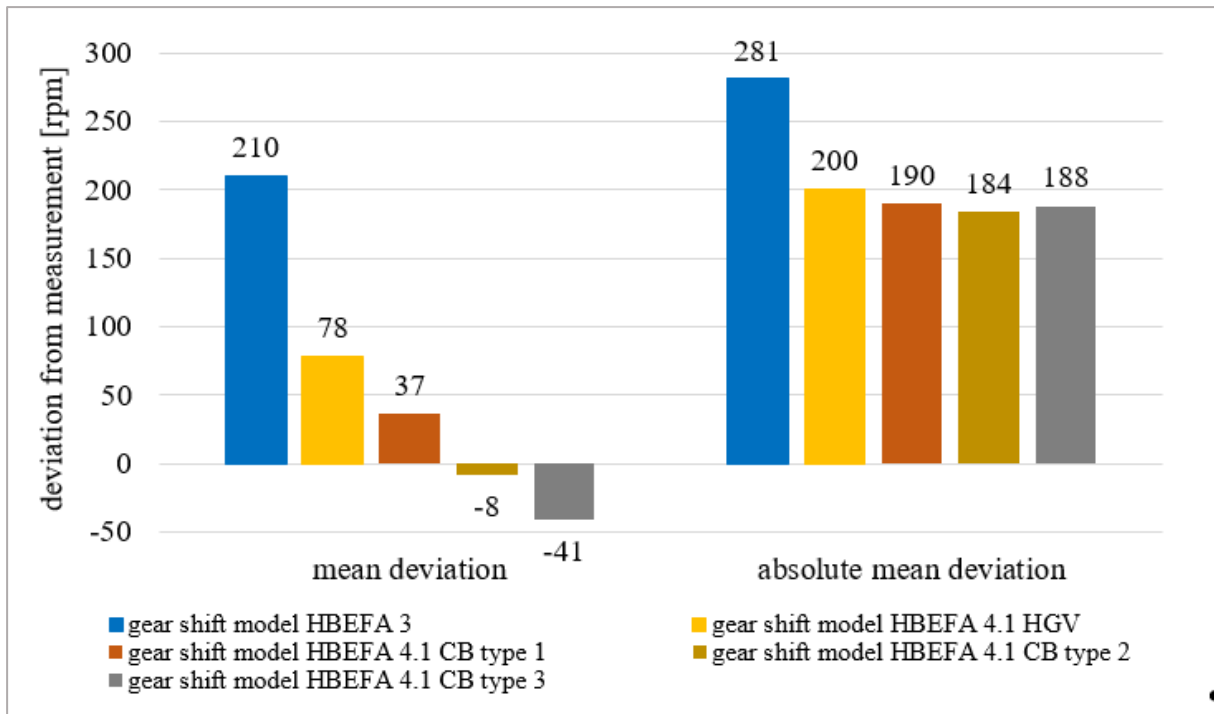


Figure 48: Engine speed simulation – comparison of adapted gear shift methods for CBs

## 7 Heavy Duty Emission Model

This chapter describes the methods for generating and calibrating vehicle models, emissions maps and exhaust after-treatment system models for all different categories of heavy duty vehicles in the current European fleet. This data works as input for the simulation tool PHEM and is the base for all HDV emission factors in the HBEFA 4.1.

### 7.1 Database

The following databases were used for the HDVs in creating the HBEFA 4.1:

- ACEA database on new HDV registrations in EU-28 for weighting the single engine emission maps with the registration numbers. [53]
- ERMES HDV database, which includes all measurement data for emission map creation, calibration and validation.

The following sections describe the 2 databases in detail.

#### 7.1.1 Database of New Vehicle Registration EU-28

The shares of brands in the new vehicle registrations of the EURO<sup>o</sup>VI fleet in EU-28 was assessed by an averaging of registrations over the last 3 years (2015–2017), see Table 9. Of course, HDVs can be split into a lot of different subcategories; however, by comparing the number of measured vehicles (14 by TUG) to existing vehicle categories (21 in HBEFA), it is obvious that a more detailed level would not be reasonable. Consequently, the shares are not specified any further. Moreover, the general engine and exhaust after-treatment technologies for HDVs are more or less similar, independent of the vehicle subcategory. Consequently, using this data as a base for the weighting regarding the average PHEM vehicles is the best way.

**Table 9: New vehicle registrations in EU-28 for HDVs [53]**

Brand	Market share							
	2015		2016		2017		average	
	#	%	#	%	#	%	#	%
DAF	43 347	13.7	44 710	13.4	38 511	12.2	42 189	13.1
Daimler	72 605	23.0	73 011	22.0	70 689	22.5	72 102	22.5
Iveco	37 732	11.9	41 286	12.4	38 845	12.4	39 288	12.2
MAN	50 372	15.9	52 925	15.9	51 399	16.3	51 565	16.1
Renault	25 343	8.0	26 152	7.9	26 793	8.5	26 096	8.1
Scania	43 670	13.8	45 721	13.7	41 978	13.4	43 790	13.6
Volvo	43 063	13.6	48 735	14.7	46 174	14.7	45 991	14.3
Total	316 132	100.0	332 540	100.0	314 389	100.0	321 020	100.0

#### 7.1.2 HDV Emission Database

The measurement data has to meet some boundary conditions before it can be included in the database and then used for the PHEM models:

- Since the emission factors exclusively represent hot emissions, the cold start part of each cold started cycle has to be cut off (first 30 minutes).
- Cycles covering common driving situations (e.g. WHVC, ISC) are used for the generation of emission maps.

- Cycles describing special driving situations (e.g. heavy Stop&Go cycles) build the base for the parametrization of special features like the NH<sub>3</sub> storage model.
- Cycles with DPF regeneration are excluded.
- Cycles with a longer recording failure (approx. >1 minute) are excluded.

Table 10 shows the total amount of vehicles and their assignment to certain functions. A minimum of 1 test per listed vehicle fulfils the given requirements for setting up and calibrating PHEM models.

**Table 10: Number of measured HDVs used for the creation of the HBEFA 4.1 simulation models**

Function	Number of vehicles						
	Total	Euro <sup>5</sup>	Euro <sup>V</sup>	Euro <sup>6</sup>	Euro <sup>VI</sup>		
		N2	N3	N2	N2	N3	M3
Total	41	1	1	1	8	26	4
Map creation	13	1	-	1	3	8	-
Map calibration	20	-	-	-	5	13	2
Deterioration function	5	-	1	-	-	4	-
CNG vehicles	3	-	-	-	-	1	2

The total number of vehicles differs from the number in Table 5, because, in addition to the new measurements for the HBEFA 4.1, this table also contains Euro<sup>VI</sup> measurement data, which was already used for the HBEFA 3.3.

## 7.2 Vehicle Data

In the HBEFA 4.1, the PHEM vehicle models have been updated for all emission standards (Euro 0 – Euro<sup>VI</sup>). Details regarding this topic can be found in [23].

Model input for typical Euro<sup>VI</sup> vehicle configurations was derived from tests and data collection performed during the development of the HDV CO<sub>2</sub> determination method (Regulation (EU) 2017/2400, “VECTO”). Table 11 gives an overview of the vehicle specifications for conventional Euro<sup>VI</sup> vehicles manufactured in 2014.

**Table 11: Vehicle specifications for averages of HDV classes Euro<sup>o</sup>VI 2014 [23]**

Vehicle category	weight category	Max. allowed total weight [t]	Vehicle weight empty [t]	Cd*A [m <sup>2</sup> ]	Engine displacement [l]	ICE Rated Power [kW]	RRC total [N/kN]	Tyre dimension	Auxiliaries base power demand [kW]
Rigid truck	<=7,5t	5.8	3.7	4.84	3.0	125	9.99	235/75 R16	1.5
Rigid truck	7.5-<=12t	11.0	6.3	5.05	4.5	151	6.62	265/70 R19.5	2.4
Rigid truck	12-<=14t	13.5	7.7	5.15	7.7	172	6.65	285/70 R19.5	2.8
Rigid truck	14-<=20t	17.2	9.3	5.30	7.7	247	6.37	315/70 R22.5	4
Rigid truck	20-<=26t	25.5	12.3	5.63	10.7	296	6.23	315/70 R22.5	4.8
Rigid truck	26-<=28t	27.0	12.9	5.85	12.7	296	6.19	315/80 R22.5	4.8
Rigid truck	28-<=32t	32.0	14.3	5.85	12.7	312	6.32	315/80 R22.5	5.0
Rigid truck	>32t	35.5	15.1	5.85	12.7	328	6.32	315/80 R22.5	5.3
Tractor trailer	<=28t	18.0	9.6	5.57	10.7	280	5.89	285/70 R19.4	3.9
Tractor trailer	28-<=34t	32.0	14.3	5.57	10.7	280	5.89	285/70 R19.5	3.9
Tractor trailer	>34-40t	39.8	15.9	5.57	12.7	327	5.78	315/70 R22.5	4.5
Tractor trailer	>40-50t	47.0	16.8	6.32	12.7	375	5.82	315/70 R22.5	5.2
Tractor trailer	>50-60t	60.0	20.4	7.07	15.6	450	5.82	315/70 R22.5	6.2
Tractor trailer	>60	90.0	25.0	10.07	15.6	510	5.82	315/70 R22.5	7.0
Urban bus midi	<15t	11.5	7.0	4.08	2.2	120	6.99	235/75 R17.5	4.8
Urban bus standard	15-18t	17.8	10.9	4.17	7.7	210	6.44	275/70 R22.5	8.4
Urban bus articulated	>18t	27.0	15.8	4.25	10.7	265	6.29	275/70 R22.5	10.6
Coach midi	<15t	10.2	6.2	3.83	4.5	120	6.99	235/75 R17.5	4.0
Coach standard	<=18t	18.0	14.4	3.91	12.7	323	6.44	295/80 R22.5	7.9
Coach 3-axes <sup>7</sup>	>18t	24.0	16.6	4.00	12.7	357	6.29	295/80 R22.5	8.5

The determination of vehicle specifications for vehicle generations from Euro<sup>o</sup>V to pre-Euro classes is based on data available at TU Graz and on these Euro<sup>o</sup>VI data sets. The following vehicle components were adapted for vehicle generations before Euro<sup>o</sup>VI:

- Vehicle weight
- Engine Power
- Air drag coefficients
- Auxiliaries
- Axle ratio

<sup>7</sup> The share of double decker busses is 10 %.

- Transmission type
- Specific fuel consumption maps

It was assumed that all vehicle generations use current tire technology, so the RRC remains the same as for Euro<sup>o</sup>VI for all older vehicle generations<sup>8</sup>.

### 7.3 Engine Maps for Fuel Consumption

The FC maps are derived from a reference engine map of a Euro<sup>o</sup>VI engine with 325 kW rated power and a displacement of 12.7 litres (see Figure 49). The impact of different engine sizes on fuel consumption is considered with a correction function. This function is described in detail in [23]. It allows using an average fuel consumption map for all engine power classes per EURO class.

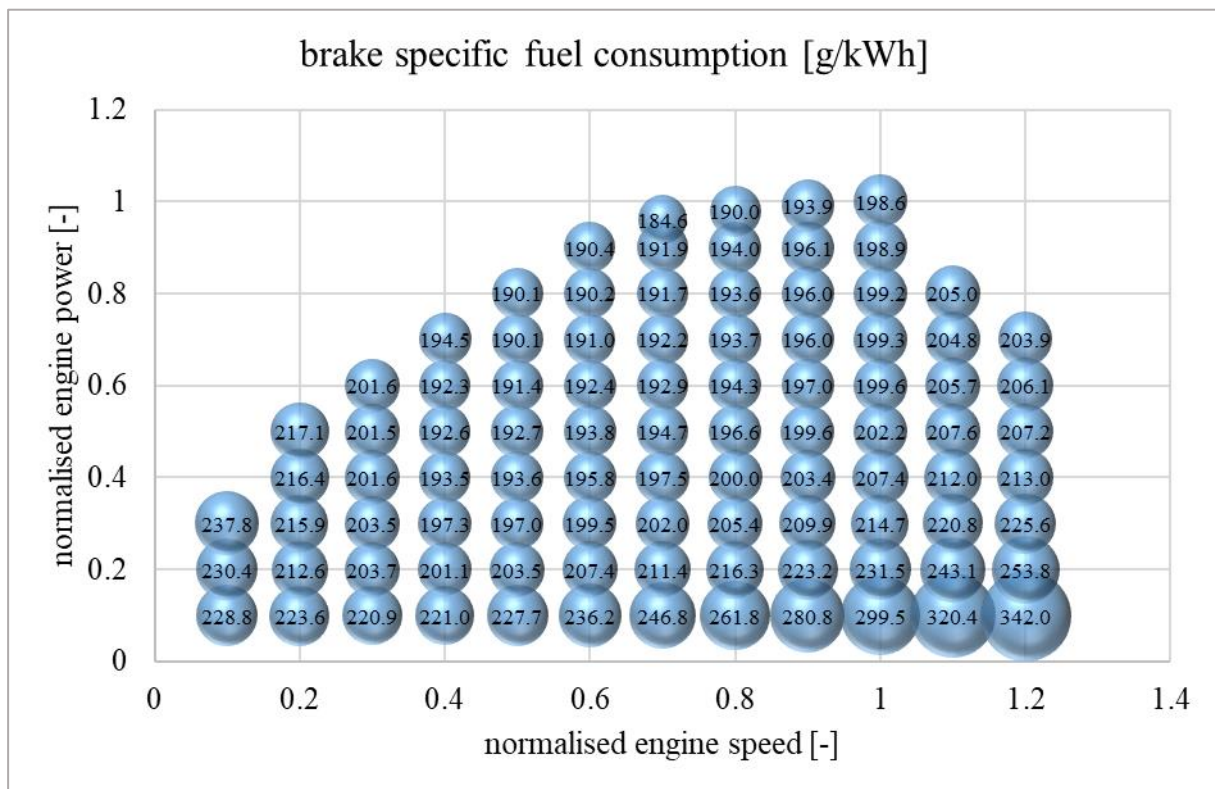


Figure 49: Euro<sup>o</sup>VI engine map, 325 kW, 12.7 litre – brake specific fuel consumption

The FC maps for Euro 0 to Euro<sup>o</sup>V vehicles were adjusted by correction factors using the reference EURO<sup>o</sup>VI map as a base. The EURO classes IV and V were further subdivided according to emission reduction technologies EGR and SCR, since these technologies imply differences in fuel consumption. Table 12 shows these fuel consumption ratios depending on the engine generation. [54]

Table 12: Fuel consumption ratios of engine generations and average model year per EURO class

Euro <sup>o</sup> VI (2014)	Euro <sup>o</sup> V SCR (2011)	Euro <sup>o</sup> V EGR (2011)	Euro IV SCR (2007)	Euro IV EGR (2007)	Euro III (2004)	Euro II (1998)	Euro I (1993.5)	Euro 0 (pre Euro)
1.000	1.000	1.020	1.033	1.043	1.030	1.024	1.059	1.095

<sup>8</sup> This may result in inaccuracies for emission factors in former years by a few percent, when older EURO classes used tires of these periods. However, adjusting the RRC values for different time periods would have led to a multiplication of the emission factors to be simulated and consequently would have exceeded the storage capacity of the HBEFA.

## 7.4 Models for Pollutant Emissions

For the creation of emission maps, PHEM uses instantaneous emission data. This data has to be time aligned (see chapter 5) correctly and needs a measured engine speed signal for engine power calculation with the CO<sub>2</sub> interpolation method [44]. Since PHEM shall produce hot emission factors, only test data in hot engine conditions was used and accordingly cold start phases were cut off.

The models described in this section are based on the vehicles measured by TUG only, because the TUG measurement program was especially designed for the development of vehicle models for the HBEFA 4.1 (see chapter 4). Additional measurement data of other laboratories is used for the adjustment of the models later on (see section 7.5).

### 7.4.1.1 Principle Generation of Emission Maps

HDV engine maps for pollutant emissions are based on chassis dyno and on-road measurements. While chassis dyno measurements contain all relevant emission components, on-road measurements do not deliver PM, PN and exhaust components recorded by FTIR analysers.

Another issue is the accuracy of the different measurement systems which are used on the chassis dyno and for on-road measurements. Comparison measurements on the chassis dyno show a notable deviation between the different systems for some emission components. Consequently, for each emission component in the PHEM emission maps only one of the two different measurement systems (either laboratory equipment or PEMS) is selected as input for the emission maps. Table 13 shows the origin of the different emission components for the PHEM model. To avoid bias effects, this approach is also used for model adjustment work, even when only on-road measurement data is available (e.g. AVL MTC measurement data, see section 7.5).

**Table 13: Source allocation per emission component for PHEM emission maps**

Emission component	CO	HC	NO <sup>9</sup>	NO <sub>x</sub> <sup>9</sup>	PM	PN
Source Used	Laboratory Equipment	Laboratory Equipment	On-road test	On-road test	Laboratory Equipment	Laboratory Equipment

The next topic is the creation of an average emission map. The following points describe all single steps in detail for one Euro class:

1. First, all appropriate cycles for emission map creation were selected from the data measured for the HBEFA 4.1. The cycles should cover all relevant driving conditions (WHVC on the chassis dyno or ISC in real world driving) and fulfil every boundary condition defined in 7.1.2.
2. The instantaneous data was prepared for emission map generation in PHEM. This includes correct time alignment (see chapter 5) and a cut off of cold start phases, because the HBEFA provides only hot emission factors.
3. Single vehicle emission maps were set up using the CO<sub>2</sub> interpolation method. This method uses instantaneously measured engine speed and CO<sub>2</sub> mass flow to interpolate the engine power from a generic CO<sub>2</sub> engine map [44]. Normalised formats (see chapter 6) allow an averaging of single emission maps later on. This engine map

<sup>9</sup> Every vehicle is measured in real world conditions (on-road), consequently measurement data of every vehicle can be used for the creation of emissions maps. Regarding the dependency of NO and NO<sub>x</sub> on cycle preconditioning, another advantage is the long duration of ISC tests compared to standard chassis dyno cycles (e.g. WHVC). This long duration minimizes the influence of the start conditions.

creation step also includes a normalisation of all pollutants based on the rated engine power.

4. The next step is the creation of brand models. For this reason, all single engine emission maps of each single brand within one EURO-class are averaged.
5. All single brand engine maps are then weighted together into one average end-of-tailpipe emission map by using the weighting factors according to the registration numbers in EU-28 (see 7.1.1).
6. The final step is merging this newly created emission map and the already existing emission map for the HBEFA 3.2. The HBEFA 3.2 emission maps are based on measurements available at the time of the HBEFA 3.2 production. The 2 emission maps are put together by weighting factors according to the number of vehicles used for the setup of each model. Of course, this merging can only be done for the emission components which exist in both emission maps.

Figure 50 shows the mean brake specific average engine emission map for CO as an example.

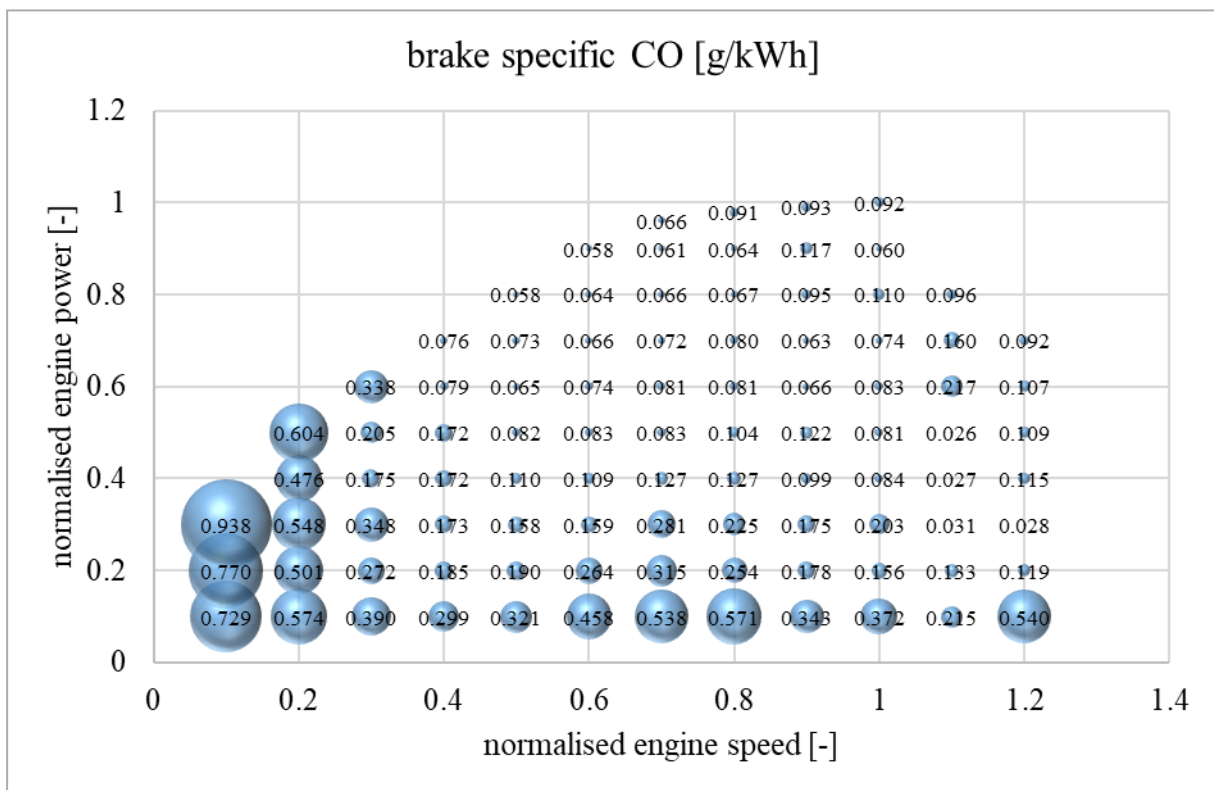


Figure 50: Average engine emission map – brake specific CO emissions for EURO VI engines

Point 5 describes the maps as end-of-tailpipe emission maps. This is valid for all emission components besides  $\text{NO}_x$ . As described in section 6.2, PHEM also offers the possibility to simulate the complete exhaust after-treatment model – next to the emission map-based standard simulation process. This after-treatment model is used for  $\text{NO}_x$  tailpipe emissions since the conversion in the SCR is mainly dependent on the catalyst temperature and space velocity (see section 3.2.2.3) and cannot be illustrated in an appropriate way by engine power and engine speed only (see section 6.2.2). However, a map for  $\text{NO}_x$  engine-out emissions was produced based on the engine map to provide the input raw emission data for the SCR model.

Since new measurement data is available only for Euro V and Euro VI, models of the other Euro classes already existing were not touched during work for the HBEFA 4.1 and were taken the way they are (see HBEFA 3).

### 7.4.1.2 Combination of EGR + SCR and SCR-only Vehicles

In general, Euro<sup>o</sup>VI vehicles use two different technologies to reduce NO<sub>x</sub> emissions. One part of the vehicles uses only SCR catalysts (SCR-only) and the other part uses both EGR and SCR. Details of the different technologies are described in section 3.2.

Of course, the use of EGR influences the combustion process and, as a consequence, also all emission components other than NO<sub>x</sub>. However, measurement data of different vehicles did not show a significant technology impact on any of the other emission components. In fact, the mean variation between vehicles based on the same technology is similar compared to all vehicles independent of their emission reduction technologies. Thus, one average emission map is sufficient for these emission components for the entire EURO<sup>o</sup>VI HDV fleet.

The main issue regarding SCR-only and EGR+SCR vehicles definitely is NO<sub>x</sub>. Figure 51 shows NO<sub>x</sub> EO ISC measurement results for different vehicles (5 EGR+SCR vehicles, 2 SCR-only vehicles, and the average for each). The NO<sub>x</sub> engine-out emissions of SCR-only vehicles are almost twice as high as those of EGR+SCR vehicles. It has to be remarked that these results illustrate the average emission results for an entire ISC cycle and not the 90 percentile results evaluated with the regulatory MAW method (see section 3.1).

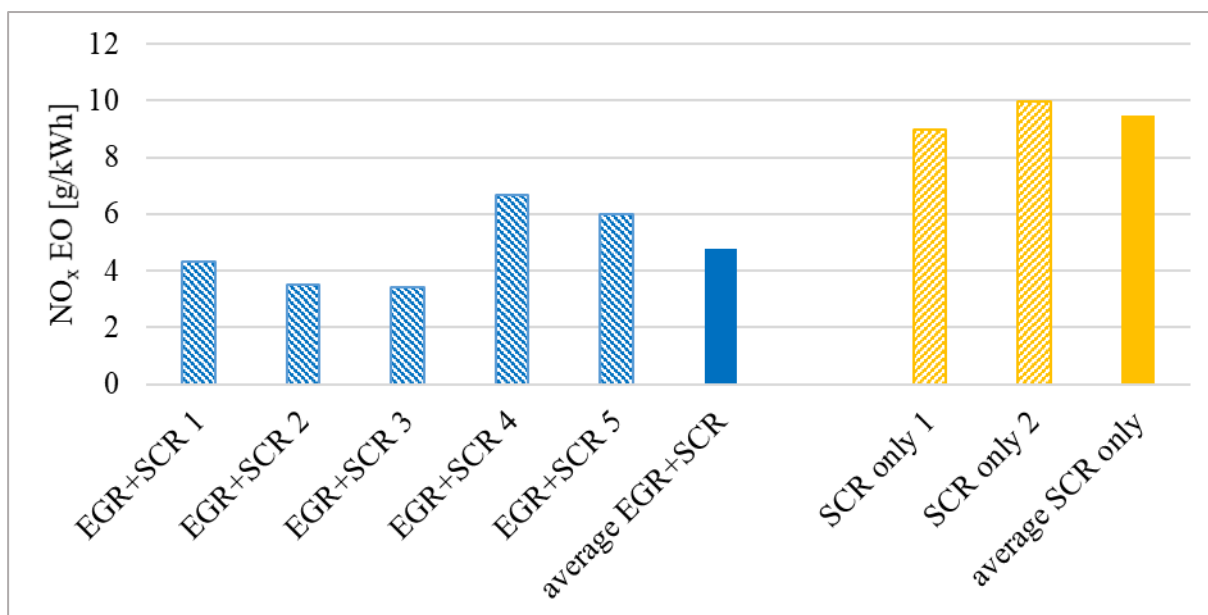


**Figure 51: Brake specific NO<sub>x</sub> EO emissions – ISC measurement results, Euro<sup>o</sup>VI**

Figure 52 and Figure 53 show the average NO<sub>x</sub> EO emission maps for EGR+SCR and SCR-only vehicles. Of course, the difference between the technologies can also be seen in these maps as they are based on the measurement data. It clearly shows that vehicles with EGR use this option even at very high loads to reduce their engine-out emissions.

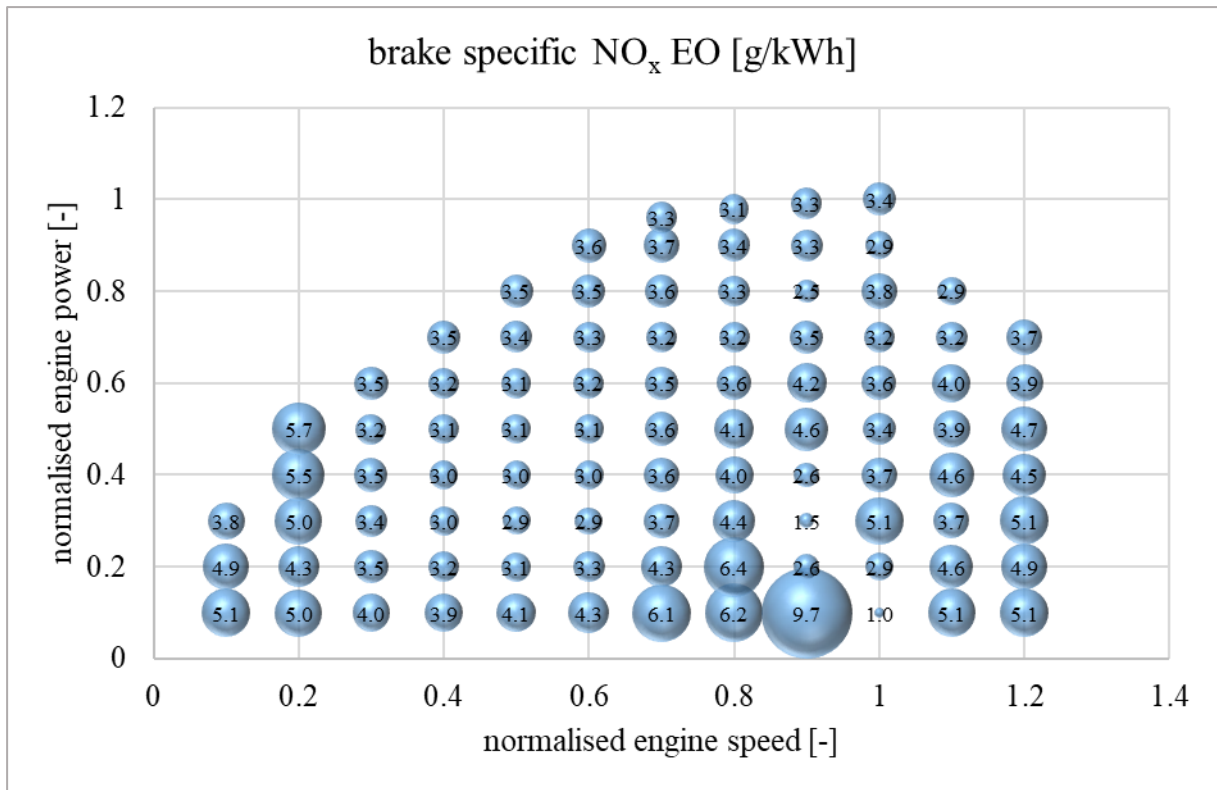


Figure 52: EGR+SCR Euro<sup>VI</sup> engine emission map – brake specific NO<sub>x</sub> EO emissions

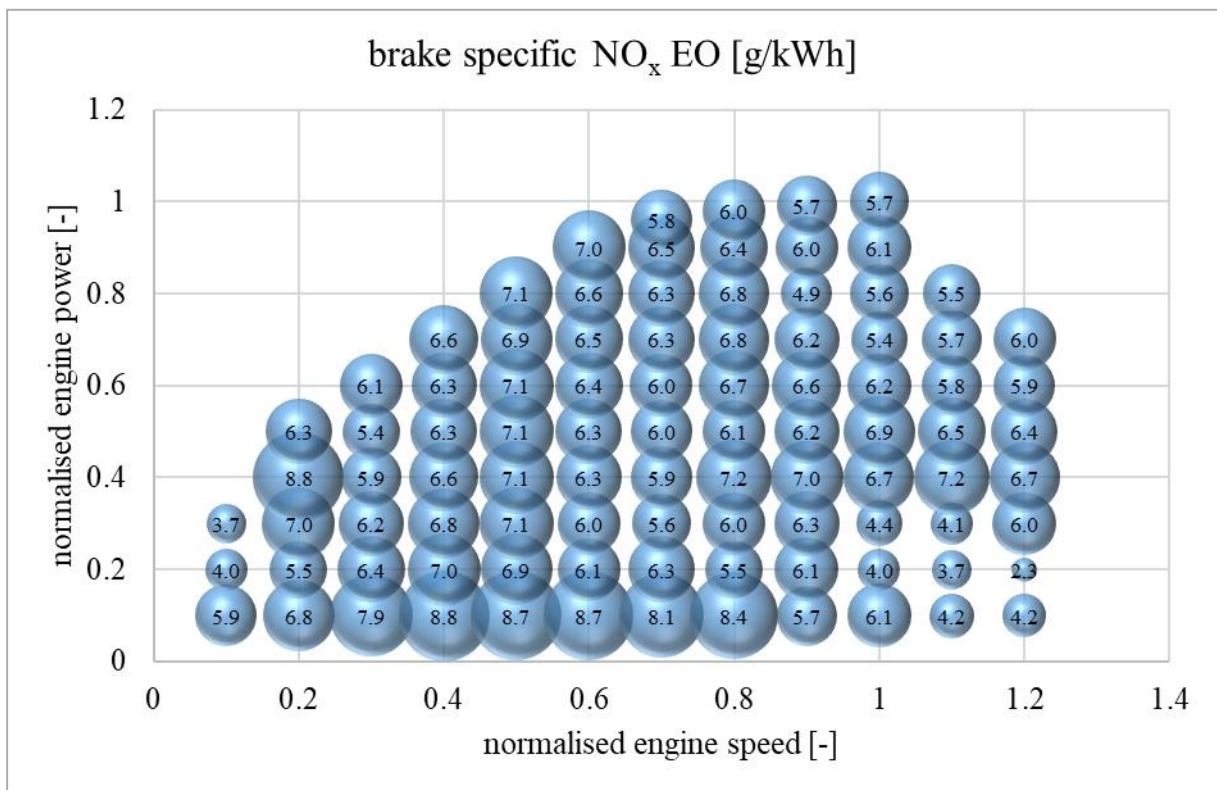
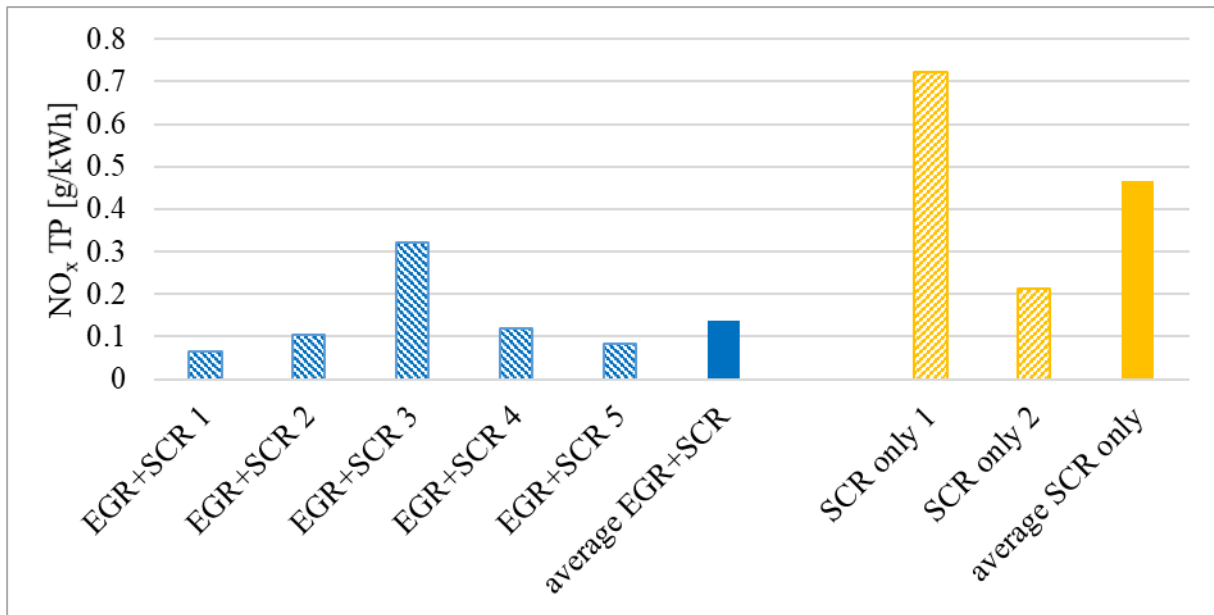


Figure 53: SCR only Euro<sup>VI</sup> engine emission map – brake specific NO<sub>x</sub> EO emissions

The variance in NO<sub>x</sub> engine-out emissions suggests principally 2 separate models for the different technologies. However, the results for ISC measurements show that the real world average NO<sub>x</sub> TP emissions are on a low level for both technologies (regulatory limit is 0.69 g/kWh). This can be seen in Figure 54.



**Figure 54: Brake specific NO<sub>x</sub> TP emissions – ISC measurement results, Euro<sup>o</sup>VI**

Since these simulation models are created for the HBEFA, it is reasonable to simulate exactly the corresponding cycles to estimate the effect on the HBEFA traffic situations. In this case, especially low load phases are crucial for the different technologies, because SCR efficiency drops with decreasing temperature. EGR+SCR vehicles can reduce tailpipe emissions in this phase by controlling engine-out emissions by using EGR; however, SCR-only vehicles do not have the possibility to change emissions at this point of the system. Consequently, they need to control the conversion of the SCR catalyst by preventing its cool down with an increase in exhaust gas temperature. For this purpose, vehicles can use late fuel injection, an exhaust throttle or extra fuel injection in the exhaust gas. Figure 55 shows the results for the two different emission models on the HBEFA cycles. The emissions are on a similar level in high speed cycles and the SCR-only emissions (yellow) are even smaller at low speed and consequently in low load phases.

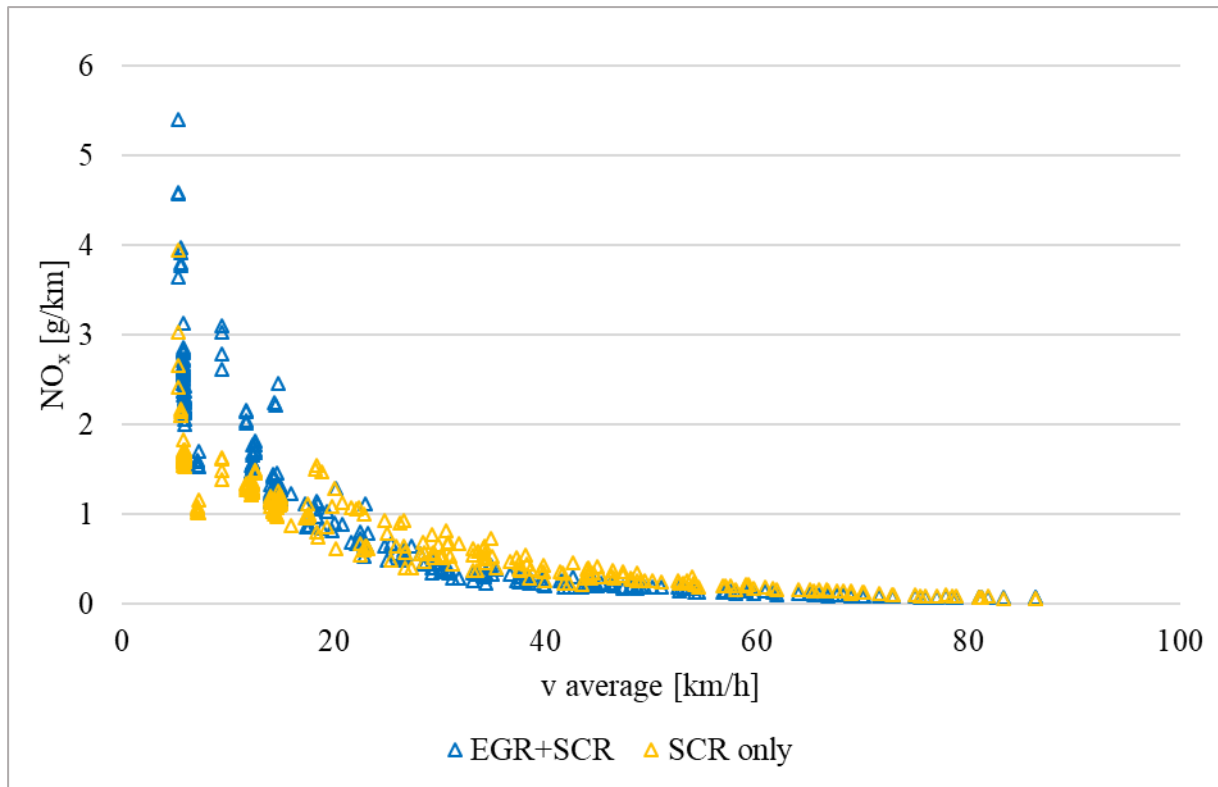


**Figure 55: NO<sub>x</sub> EO emission factors – EGR + SCR vehicles and SCR-only vehicles, Euro<sup>o</sup>VI**

These results lead to the determination that 2 different models are not necessary for the simulation of more or less similar tailpipe results regarding complexity and effort for the creation of average emission models. Consequently, all single vehicle models will be weighted together independent of their NO<sub>x</sub>-reduction technology based on the EU registration figures into one comprehensive Euro<sup>o</sup>VI model. Figure 56 illustrates the final NO<sub>x</sub> engine-out emission map.

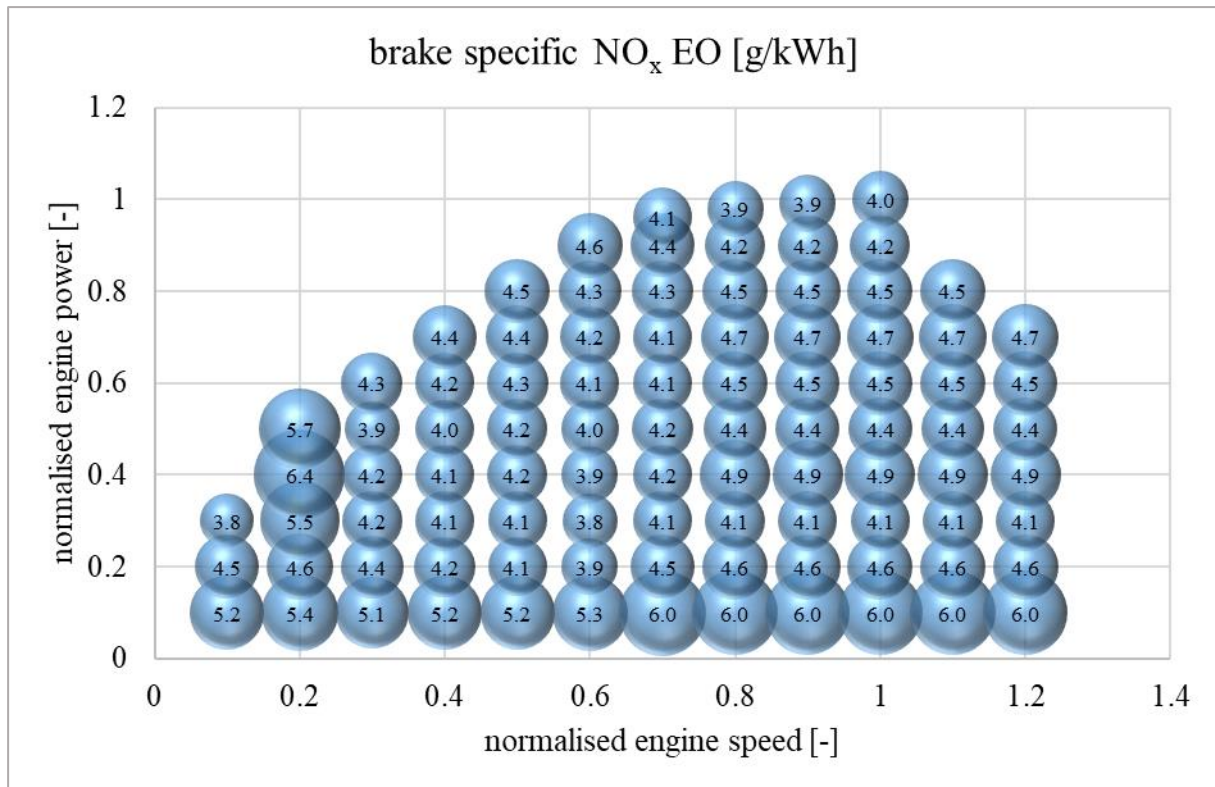
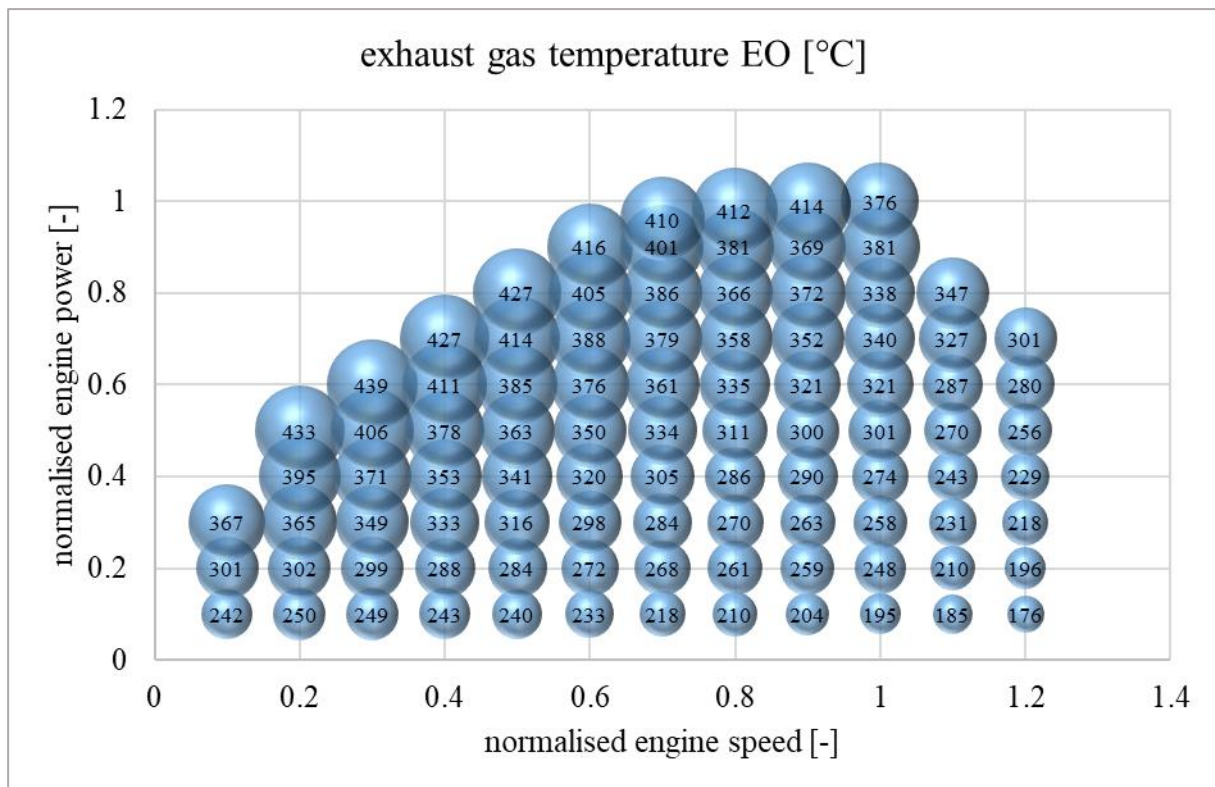


Figure 56: Average Euro<sup>VI</sup> engine emission map – brake specific NO<sub>x</sub> EO emissions

#### 7.4.1.3 Setup of Exhaust After-Treatment Model

As already mentioned, NO<sub>x</sub> tailpipe emissions are simulated by using the PHEM exhaust after-treatment model. This means that engine-out temperature maps, all different modules of the exhaust after-treatment model (e.g. DOC, SCR) and SCR conversion maps have to be averaged according to the fleet shares of the different brands.

It starts with the creation of an average Euro<sup>VI</sup> engine-out temperature map. As already described in 7.4.1.2, all different EURO<sup>VI</sup> engines get averaged to one normalised simulation model, although vehicles have different thermal management strategies according to their emission reduction systems. Figure 57 shows the average engine-out exhaust gas temperature map for Euro<sup>VI</sup> vehicles.



**Figure 57: Average engine map – exhaust gas temperature EO**

Figure 34 shows the validation of a Euro<sup>o</sup>VI temperature map for one single vehicle. For this on-road trip, the simulation of the temperature after turbocharger follows the measurement result quite well. Of course, average models cannot be finally checked because there is no measurement signal of the average vehicle.

The second point are the special characteristics of the after-treatment modules, which are split into two groups. On the one hand, the ones which are dependent on the rated engine power (e.g. mass or size) and, on the other hand, those which are independent of the rated engine power (e.g. heat capacity coefficients). This system and the fact, that all different HDV exhaust after-treatment systems are built up in the same structure (see 3.2.2), allows them to be merged together to average modules again, with respect to EU registration figures. [43]

Figure 35 illustrates one example for the check of the temperature upstream of the SCR and also at this point both signals fit together for this single vehicle model.

The last step in the exhaust after-treatment is the creation of the average SCR-efficiency map. Before putting all the data together into one average conversion map, single ones were created for each vehicle. Equation 7-1 describes how the efficiency of a SCR catalyst is calculated in principle:

$$CR = \frac{NO_x EO - NO_x TP}{NO_x EO} \quad 7-1$$

Notation:

$CR$  ... Conversion rate

$NO_x EO$  ...  $NO_x$  engine out in g

$NO_x TP$  ...  $NO_x$  tailpipe in g

The following work flow was developed to calculate the SCR conversion map:

First, 20 second mean values of all NO<sub>x</sub> engine-out data was allocated to the grid of the map (see Figure 58) and the masses were cumulated to a total NO<sub>x</sub> EO mass in each cell of the grid. The temperature upstream of the SCR catalyst and the space velocity inside the SCR catalyst were used as the axis of the grid (see section 6.2.2.1). As a second step, the NO<sub>x</sub> tailpipe emission masses were allocated to the SCR map in the same way. The next step was the calculation of the NO<sub>x</sub> conversion by using the cumulated NO<sub>x</sub> EO and TP emission masses in every cell. This method guarantees a weighting of the conversion rates dependent on the NO<sub>x</sub> emission mass in the respective time step. This means that high emission masses lead to stronger weightings compared to low ones.

The comprehensive Euro<sup>o</sup>VI conversion map is illustrated in the annex. Figure 58 shows an excerpt of the complete average SCR conversion map and points out the general trends for the conversion in a SCR catalyst.

- Dependency on temperature is more developed than on space velocity.
- Between 200 and 430 °C, efficiency is quite good; however, it drastically decreases below 200 °C and also goes down above 430 °C.
- An increasing space velocity mainly affects the conversion efficiency at low temperatures.

NOX conversion	SV 0.25	SV 0.75	SV 1.25	SV 1.75	SV 2.25	SV 2.75	SV 3.25	SV 3.75	SV 4.25	SV 4.75	SV 5.25
50	0.0%	0.0%	0.0%	0.0%	0.0%	0.0%	0.0%	0.0%	0.0%	0.0%	0.0%
90	62.7%	56.6%	53.8%	51.1%	48.6%	46.1%	43.8%	41.6%	39.6%	37.6%	35.7%
110	74.9%	70.4%	64.6%	59.6%	57.7%	56.2%	54.3%	51.5%	48.8%	46.2%	43.7%
130	87.1%	84.1%	75.3%	68.1%	66.9%	61.4%	59.0%	56.0%	53.1%	50.3%	48.6%
150	99.3%	97.9%	86.1%	76.6%	76.0%	66.7%	63.6%	60.4%	57.4%	54.5%	53.5%
170	99.6%	98.0%	90.2%	80.8%	82.9%	71.9%	68.3%	64.9%	61.7%	58.6%	58.4%
190	99.7%	97.8%	96.3%	92.1%	88.5%	84.2%	77.7%	76.3%	72.9%	70.6%	68.8%
210	97.3%	97.3%	96.2%	95.0%	94.1%	87.9%	87.1%	87.7%	84.2%	82.7%	76.5%
230	99.8%	96.9%	94.9%	96.8%	95.1%	94.8%	93.9%	86.8%	87.2%	85.1%	84.2%
250	99.3%	98.1%	95.9%	97.0%	97.4%	96.8%	95.8%	95.1%	88.2%	87.6%	87.4%
270	98.8%	97.6%	96.8%	99.0%	98.0%	97.8%	97.8%	96.7%	95.1%	90.0%	90.6%
290	98.3%	97.2%	96.1%	96.5%	97.4%	98.3%	97.1%	96.7%	97.0%	97.2%	97.5%
310	97.8%	97.7%	97.6%	99.5%	98.9%	98.3%	98.4%	97.7%	96.1%	95.5%	96.9%
330	97.3%	98.2%	99.1%	98.9%	98.6%	98.0%	98.9%	98.3%	98.4%	98.6%	96.4%
350	96.8%	97.2%	98.1%	97.9%	98.3%	99.8%	99.4%	98.7%	98.9%	99.1%	99.1%
370	96.3%	96.3%	97.2%	96.9%	98.0%	99.0%	99.1%	99.1%	99.2%	99.3%	99.4%
390	95.8%	95.3%	96.2%	95.9%	97.7%	98.2%	99.1%	99.1%	99.2%	99.3%	99.4%
410	95.3%	94.4%	95.2%	95.0%	97.5%	97.4%	99.1%	99.1%	99.2%	99.3%	99.4%
430	90.5%	89.6%	90.5%	90.2%	92.6%	92.6%	94.1%	94.2%	94.2%	94.3%	94.4%
450	86.0%	85.2%	85.9%	85.7%	88.0%	87.9%	89.4%	89.5%	89.5%	89.6%	89.7%
470	81.7%	80.9%	81.6%	81.4%	83.6%	83.6%	85.0%	85.0%	85.1%	85.1%	85.2%
490	77.6%	76.8%	77.6%	77.4%	79.4%	79.4%	80.7%	80.8%	80.8%	80.9%	81.0%
510	73.7%	73.0%	73.7%	73.5%	75.4%	75.4%	76.7%	76.7%	76.8%	76.8%	76.9%
530	70.1%	69.4%	70.0%	69.8%	71.6%	71.6%	72.8%	72.9%	72.9%	73.0%	73.1%

Figure 58: Excerpt of the Euro<sup>o</sup>VI SCR conversion map based on TUG data

This conversion efficiency map explains exactly the problems for SCR catalysts in low load cycles. The cooling down of the catalyst leads to a drop in efficiency and consequently to an increase of tailpipe emissions. High engine loads with high exhaust volumes at low SCR temperatures are the most critical situation for NO<sub>x</sub> TP emissions.

The temperature model, the SCR conversion model and the NH<sub>3</sub> storage model combined lead to a comprehensive exhaust after-treatment model and represent the average Euro<sup>o</sup>VI vehicle in all different kinds of cycles (see Figure 40).

## 7.5 Adjustment of NO<sub>x</sub> Emission Models

The creation of the basic PHEM emission models was based only on data provided by TUG for the HBEFA 4.1. This data is particularly suited for this issue due to the the measurement program, which is exactly designed for these routines, and detailed knowledge about special features of the measurements. For example, the aforementioned determination of the average

SCR efficiency map needs measured emissions up- and downstream of the SCR. In addition, special test conditions were addressed by chassis dyno measurements (e.g. low load operation).

Besides this TUG measurement data, AVL MTC provided ISC measurement data and additional data from TUG recorded for the HBEFA 3.3 was also available. However, this data does not fit the setup of the HBEFA 4.1 simulation model (e.g. some measurements like emissions upstream of the SCR are missing). Consequently, the tailpipe emission data was used for calibration of the basic model to represent the average EU vehicle fleet. In this case, the challenging points were, for example, different numbers of tests per vehicle and that the share between the measured tests per brand did not fit the brand sales numbers shares in the EU (see Table 9). Additionally, differences between the emission behaviour of HGVs, city busses and vehicles below 7.5 tons lead to 3 different NO<sub>x</sub> emission models. The following section describes the adjustment processes.

### 7.5.1 Heavy Goods Vehicles – NO<sub>x</sub> Emission Model

The data measured by AVL MTC is PEMS data. Every measured cycle follows the ISC boundary conditions and therefore covers the most relevant driving conditions; however, in detail, of course, every single cycle is unique. As already mentioned, the cold start part of the cycles was cut off for the creation of hot emission factors.

The additional TUG data recorded for the HBEFA 3.3 also contains Euro<sup>o</sup>VI measurement data. Most of the data was already processed in the emission maps besides the NO<sub>x</sub> emissions (see section 7.4.1.1). However, the NO<sub>x</sub> data was already used in the HBEFA 3.3 for the creation of an exhaust after-treatment model. Thus, this already existing average Euro<sup>o</sup>VI emission model (HBEFA 3.3) can be used for checks and, if needed, for model adjustment reasons.

The main question is how to compare the results of the different sources or how to calibrate the models by using this data. Of course, the most obvious way would be to set up emission models for each single AVL MTC vehicle and to merge all different simulation models into an average one. However, the huge effort due to the big amount of different vehicles and the lack of knowledge regarding vehicle and measurement details would probably not lead to a reasonable result. Consequently, an alternative method was created, which allows comparison between measurement and simulation results for exactly the same cycles. Since simulation models based on the HBEFA 3.3 and 4.1 dataset already exist, it is possible to simulate all AVL MTC ISC cycles and compare the results of both models with the measurement results. Consequently, each AVL MTC ISC cycle has a measurement result, a HBEFA 3.3 simulation model result and a HBEFA 4.1 simulation model result. This allows comparing the 3 different data input sources on the same cycles without setting up extra AVL MTC simulation models. This method allows a validation of the HBEFA 4.1 simulation model according to all Euro<sup>o</sup>VI measurement data and of course, it delivers the input data for possible model adjustment work. The following steps explain this process in detail:

1. The first step is the simulation of all AVL MTC ISC cycles with both existing average Euro<sup>o</sup>VI emission models (HBEFA 4.1 and HBEFA 3.3 model). The input cycles for the simulation contain the measured engine speed and engine power in normalised form. This “engine only simulation” helps to avoid uncertainties of the longitudinal dynamics (e.g. road gradient) and does not demand a calibrated vehicle model for each measured HDV. The temperatures at cycle start regarding the different modules (e.g. turbocharger, SCR) in the temperature simulation model have been estimated at 250°C. This is the average module temperature of all measured ISC cycles by TUG. Corresponding measured data was not available from the AVL MTC tests.

2. Most vehicles were tested in more than one cycle. Consequently, the second step incorporated the generation of average emission results per vehicle to ensure a balanced weighting between the different vehicles. For this reason, the brake specific emissions of each cycle were merged to average emissions according to the same share of every cycle per vehicle. To compare the measurement results, i.e. the simulation results of the HBEFA 3.3 model and the simulation results of the HBEFA 4.1, this merging was done separately for each of the 3 different datasets. Consequently, every single vehicle had one measurement and 2 different simulation results (HBEFA 3.3 and HBEFA 4.1 model).
3. The next step is to combine all these single vehicle results (measured and simulated) into average vehicle models. The introduction of adjustment factors for each vehicle helps to combine the results of the different vehicles independent of their vehicle specifications:

$$AF_{meas} = \frac{BSE_{NOx,meas}}{BSE_{NOx,sim\ HBEFA\ 4.1}} \quad 7-2$$

$$AF_{HBEFA\ 3.3} = \frac{BSE_{NOx,sim\ HBEFA\ 3.3}}{BSE_{NOx,sim\ HBEFA\ 4.1}} \quad 7-3$$

$$AF_{HBEFA\ 4.1} = \frac{BSE_{NOx,sim\ HBEFA\ 4.1}}{BSE_{NOx,sim\ HBEFA\ 4.1}} \quad 7-4$$

Notation:

$AF_{HBEFA\ 3.3}$  ... Adjustment factor for the HBEFA 3.3 model

$AF_{HBEFA\ 4.1}$  ... Adjustment factor for the HBEFA 4.1 model (always = 1)

$AF_{meas}$  ... Adjustment factor for the AVL MTC measurement results

$BSE_{NOx,meas}$  ... AVL MTC NO<sub>x</sub> measurement result in g/kWh

$BSE_{NOx,sim\ HBEFA\ 3.3}$  ... NO<sub>x</sub> simulation (HBEFA 3.3 model) result in g/kWh

$BSE_{NOx,sim\ HBEFA\ 4.1}$  ... NO<sub>x</sub> simulation (HBEFA 4.1 model) result in g/kWh

4. These adjustment factors illustrate the ratios of the measurement results, the HBEFA 3.3 simulation results or the HBEFA 4.1 simulation results to the HBEFA 4.1 simulation results per vehicle. The adjustment factors are related to the HBEFA 4.1 model, because this is the base for further model adjustment work. Of course, the AF for the HBEFA 4.1 simulation results is exactly 1 in any case. The next step is the combining of the different AFs per vehicle into one AF per brand for each model by summarising all vehicles of one brand with the same weighting factors.
5. The next step is to combine all brand specific adjustment factors into an average one, which represents the average Euro<sup>o</sup>VI vehicle. The weighting factors per brand are their market shares.

This results in a basic adjustment factor of 1.59. That means that the HBEFA 4.1 simulation model underestimates the emissions of the average Euro<sup>o</sup>VI fleet.

6. The final step is the adjustment of the HBEFA 4.1 simulation model in order to meet the average fleet emissions. For this reason, the structure of the simulation model offers different possibilities to adjust the NO<sub>x</sub> tailpipe emissions:

- a. Option 1 is the adjustment of engine-out emissions. However, the HBEFA also provides results for vehicles with non-functioning exhaust after-treatment systems, such as for tampered SCR systems. In this case, the engine-out emissions are equal to the tailpipe emissions and consequently this would lead to mistakes for this group.
- b. Option 2 is the adjustment of the conversion model of the SCR catalyst. In this case, the engine-out emissions remain on the same level, while only the tailpipe emissions change.

Regarding the characteristics of the different options, option 2 seems to be the most reasonable solution. The next question is how the conversion map can be adjusted in such a way that the principal characteristics of this map remain untouched. Figure 58 shows an excerpt of the SCR conversion map, which illustrates the characteristics as e.g. the drop of the conversion when the temperature decreases below approx. 200°C. The following equation shows how the conversion rate was adjusted in every cell of the map.

$$CR_{adj.} = 1 - (1 - CR_{TUG}) * AF_{res.} \quad 7-5$$

Notation:

$AF_{res.}$  ... Resulting adjustment factor

$CR_{adj.}$  ... Adjusted conversion rate

$CR_{TUG}$  ... Conversion rate based on TUG data

The adjustment process started with the basic adjustment factor of 1.59. This factor represents the difference of the HBEFA 4.1 simulation model to the average Euro<sup>o</sup>VI fleet; this has already been described in point 5 of this section. However, the application of this factor does not lead to a final average adjustment factor of 1.00. A final average adjustment factor of 1.00 means that the HBEFA 4.1 simulation model exactly represents the average Euro<sup>o</sup>VI fleet. The following iterative process results in an adjustment factor of 2.02. By use of this resulting adjustment factor the final average adjustment factor is 1.00 and consequently the final HBEFA 4.1 simulation model represents the average Euro<sup>o</sup>VI fleet.

Figure 59 shows an excerpt of the final adjusted SCR conversion map. Compared to the not adjusted conversion map (see Figure 58) it is obvious, that the principal characteristic is still the same.

NOx conversion	SV 0.25	SV 0.75	SV 1.25	SV 1.75	SV 2.25	SV 2.75	SV 3.25	SV 3.75	SV 4.25	SV 4.75	SV 5.25
50	0.0%	0.0%	0.0%	0.0%	0.0%	0.0%	0.0%	0.0%	0.0%	0.0%	0.0%
90	57.1%	53.2%	51.7%	50.5%	48.6%	46.1%	43.8%	41.6%	39.6%	37.6%	35.7%
110	67.5%	63.3%	58.5%	55.0%	53.9%	53.0%	52.0%	50.7%	48.8%	46.2%	43.7%
130	81.4%	77.8%	68.0%	61.3%	60.3%	56.2%	54.6%	52.9%	51.4%	50.1%	48.6%
150	98.8%	96.7%	80.2%	69.2%	68.7%	60.1%	57.8%	55.6%	53.7%	52.1%	51.6%
170	99.4%	96.9%	85.6%	73.8%	76.3%	64.6%	61.5%	58.7%	56.4%	54.4%	54.3%
190	99.6%	96.6%	94.2%	88.2%	83.3%	77.8%	70.4%	68.9%	65.6%	63.5%	61.8%
210	95.9%	95.7%	94.2%	92.3%	91.0%	82.5%	81.5%	82.2%	77.8%	76.0%	69.1%
230	99.7%	95.2%	92.2%	95.0%	92.6%	92.1%	90.8%	81.1%	81.6%	78.9%	77.9%
250	99.0%	97.0%	93.6%	95.3%	95.9%	95.0%	93.5%	92.4%	82.9%	82.0%	81.9%
270	98.2%	96.3%	95.1%	98.5%	96.8%	96.6%	96.6%	94.9%	92.5%	85.3%	86.1%
290	97.4%	95.7%	94.0%	94.6%	95.9%	97.3%	95.5%	94.9%	95.3%	95.7%	96.1%
310	96.6%	96.4%	96.3%	99.2%	98.2%	97.3%	97.5%	96.3%	94.0%	93.1%	95.3%
330	95.8%	97.2%	98.6%	98.2%	97.8%	96.8%	98.3%	97.3%	97.6%	97.7%	94.4%
350	95.1%	95.7%	97.1%	96.7%	97.4%	99.7%	99.1%	98.0%	98.3%	98.6%	98.5%
370	94.3%	94.2%	95.6%	95.2%	96.9%	98.5%	98.6%	98.6%	98.7%	98.9%	99.1%
390	93.5%	92.8%	94.1%	93.7%	96.5%	97.2%	98.6%	98.6%	98.7%	98.9%	99.1%
410	92.8%	91.4%	92.7%	92.3%	96.0%	96.0%	98.6%	98.6%	98.7%	98.9%	99.1%
430	86.0%	84.8%	85.9%	85.6%	88.9%	88.8%	91.1%	91.2%	91.2%	91.4%	91.5%
450	80.1%	79.0%	80.0%	79.7%	82.6%	82.6%	84.5%	84.6%	84.6%	84.8%	84.9%
470	74.9%	73.9%	74.8%	74.5%	77.1%	77.0%	78.7%	78.8%	78.9%	79.0%	79.1%
490	70.3%	69.5%	70.3%	70.0%	72.2%	72.2%	73.7%	73.8%	73.8%	73.9%	74.0%
510	66.4%	65.7%	66.3%	66.1%	68.0%	68.0%	69.3%	69.4%	69.4%	69.5%	69.6%
530	63.0%	62.4%	62.9%	62.8%	64.4%	64.4%	65.5%	65.6%	65.6%	65.7%	65.7%

**Figure 59: Excerpt of the EURO<sup>o</sup>VI SCR conversion map adjusted to the complete Euro<sup>o</sup>VI HGV data**

The complete EURO<sup>o</sup>VI SCR conversion map adjusted to the complete Euro<sup>o</sup>VI HGV data can be found in the annex (Figure 90).

This method allows a reasonable integration of all measurement data in a comprehensive exhaust after-treatment model for NO<sub>x</sub> simulation without changing the main characteristics of the created emission model.

Finally, the comprehensive simulation model has to be validated by means of measurements. For this reason, Figure 60 shows the NO<sub>x</sub> simulation results for the 40 tons half loaded tractor trailer combination in the respective HBEFA 4.1 cycles (red). Additionally, all measurement data of HDV tests at TU Graz (blue) and AVL MTC (yellow) are shown. Each point represents the result of either one simulation or one measurement cycle. The emissions are shown in brake specific form; consequently all measured HDV sizes can be compared in one figure independent of their vehicle and engine size. While the single measurement results show a high level of scatter, the PHEM simulation results behave in a more regular way. On the one hand, the simulation model overestimates some measurements and on the other hand it also underestimates others. In this way, the graph illustrates the big influence of variabilities in vehicle brands and models, test cycles and driving conditions on test results, which are especially obvious for on-road measurements as shown in this case. All in all, the simulation represents the mean of the measurement results.

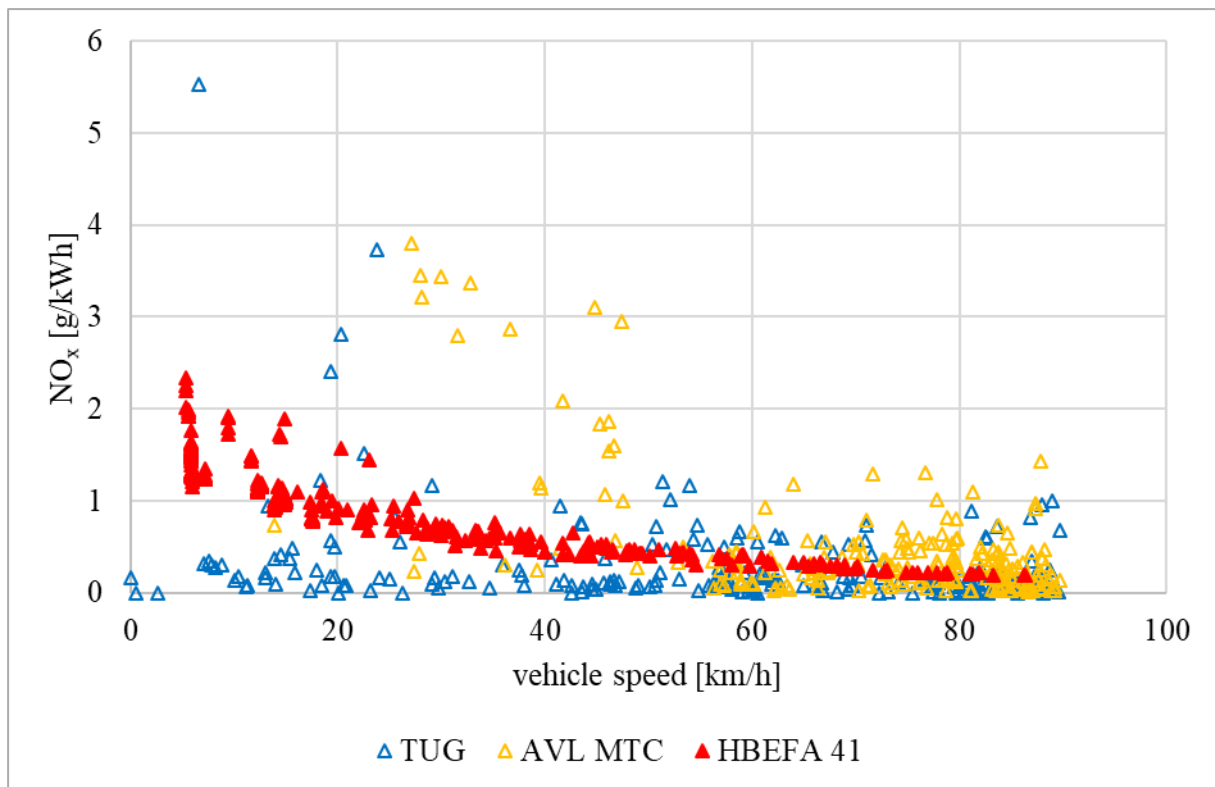


Figure 60: NO<sub>x</sub> results for HBEFA 4.1 and measurement data of TU Graz and AVL MTC

### 7.5.2 City busses – NO<sub>x</sub> Emission Model

In general, city busses have a different operating area compared to trucks. Most of the time they operate in urban areas on a low average load level with a lot of stop times. However, city bus engines also have to fulfil the Euro<sup>o</sup>VI emission regulation on the test bench and in on-road conditions<sup>10</sup>.

The available city bus data for the HBEFA 4.1 comprises just 2 vehicles from the same make and model, both measured only in on-road conditions. The measured cycles are different urban bus routes, which cover most relevant operating conditions. An emission model for PHEM adjusted to these vehicles was produced. According to Table 13, only NO<sub>x</sub> can be used for the work on the HBEFA due to on-road measurements. These 2 vehicles fulfil the current valid emission limit Euro<sup>o</sup>VI C. In addition to this data, the emission model of the HBEFA 3.3 for city busses is also available. The HBEFA 3.3 model is based on only 1 city bus, which actually was a vehicle of the first Euro<sup>o</sup>VI A generation. All in all, 2 vehicle measurements of the same make and model and an emission model based on 1 vehicle do not represent a reasonable database for setting up a completely new simulation model. Thus, the average EURO<sup>o</sup>VI HGV exhaust after-treatment model described before was used as a base for the adjustment to city busses. This seems to be a reasonable approach because the hardware of exhaust after-treatment systems of city busses is generally structured in the same way as for HGVs [55].

The SCR conversion map was calibrated in an iterative way to meet the data available from the 3 EURO<sup>o</sup>VI CBs. The resulting SCR map is shown in Figure 61.

<sup>10</sup> ISC trip boundary conditions for city busses: 70 % urban and 30 % rural driving [10]

NOX conversion	SV 0.25	SV 0.75	SV 1.25	SV 1.75	SV 2.25	SV 2.75	SV 3.25	SV 3.75	SV 4.25	SV 4.75	SV 5.25
50	0.0%	0.0%	0.0%	0.0%	0.0%	0.0%	0.0%	0.0%	0.0%	0.0%	0.0%
90	53.0%	50.8%	50.2%	50.0%	48.6%	46.1%	43.8%	41.6%	39.6%	37.6%	35.7%
110	62.2%	58.1%	54.0%	51.7%	51.1%	50.7%	50.3%	50.0%	48.8%	46.2%	43.7%
130	77.3%	73.1%	62.6%	56.3%	55.5%	52.4%	51.5%	50.6%	50.1%	50.0%	48.6%
150	98.5%	95.8%	79.7%	78.9%	78.8%	78.3%	78.1%	78.0%	78.0%	77.9%	77.9%
170	97.5%	97.3%	96.3%	95.3%	93.8%	90.5%	86.0%	81.6%	81.5%	78.9%	78.9%
190	96.1%	95.8%	95.6%	96.1%	94.8%	92.8%	93.8%	86.6%	86.4%	86.2%	86.1%
210	97.0%	96.6%	96.4%	96.8%	96.7%	95.0%	96.2%	83.0%	82.6%	82.5%	80.1%
230	97.9%	97.5%	97.2%	98.8%	99.0%	97.6%	98.7%	97.3%	96.7%	96.2%	96.2%
250	99.0%	98.8%	98.5%	98.8%	99.1%	99.2%	98.8%	98.8%	97.8%	97.0%	97.9%
270	98.1%	97.9%	97.8%	98.8%	99.2%	99.3%	99.2%	99.1%	98.7%	98.4%	98.5%
290	99.8%	99.6%	98.0%	98.8%	99.2%	99.2%	99.3%	99.3%	99.3%	99.4%	99.4%
310	99.7%	99.7%	99.7%	99.9%	99.8%	99.8%	99.8%	99.7%	99.5%	99.4%	99.6%
330	99.6%	99.8%	99.9%	99.8%	99.8%	99.7%	99.8%	99.8%	99.8%	99.8%	99.5%
350	99.6%	99.6%	99.7%	99.7%	99.8%	99.9%	99.9%	99.8%	99.8%	99.9%	99.9%
370	99.5%	99.5%	99.6%	99.6%	99.7%	99.9%	99.9%	99.9%	99.9%	99.9%	99.9%
390	96.6%	96.6%	96.7%	96.7%	96.9%	97.0%	97.1%	97.1%	97.1%	97.1%	97.1%
410	92.9%	92.7%	92.8%	92.8%	93.1%	93.1%	93.4%	93.4%	93.4%	93.4%	93.4%
430	89.5%	89.4%	89.5%	89.5%	89.7%	89.7%	89.9%	89.9%	89.9%	89.9%	90.0%
450	79.7%	79.6%	79.7%	79.7%	79.9%	79.9%	80.1%	80.1%	80.1%	80.1%	80.1%
470	69.9%	68.9%	69.8%	69.5%	72.3%	72.3%	74.2%	74.3%	74.4%	74.5%	74.6%
490	65.0%	64.2%	64.9%	64.7%	67.0%	67.0%	68.6%	68.7%	68.7%	68.8%	68.9%
510	61.0%	60.3%	61.0%	60.8%	62.7%	62.7%	64.0%	64.0%	64.1%	64.2%	64.2%
530	57.8%	57.3%	57.8%	57.6%	59.1%	59.1%	60.2%	60.2%	60.3%	60.3%	60.4%

Figure 61: Excerpt of the EURO<sup>o</sup>VI SCR conversion map adjusted to the Euro<sup>o</sup>VI CB data

The complete EURO<sup>o</sup>VI SCR conversion map adjusted to the Euro<sup>o</sup>VI CB data can be found in the annex (Figure 91).

The final simulation results of the HBEFA 4.1 CB model meet the average of the HBEFA 3.3 and the Euro<sup>o</sup>VI C model for CBs smaller than 15 tons, 2-axle CBs with a GVM between 15 and 18 tons and 3-axle CBs with a GVM higher than 18 tons. Figure 62 illustrates the final results after model adjustment.

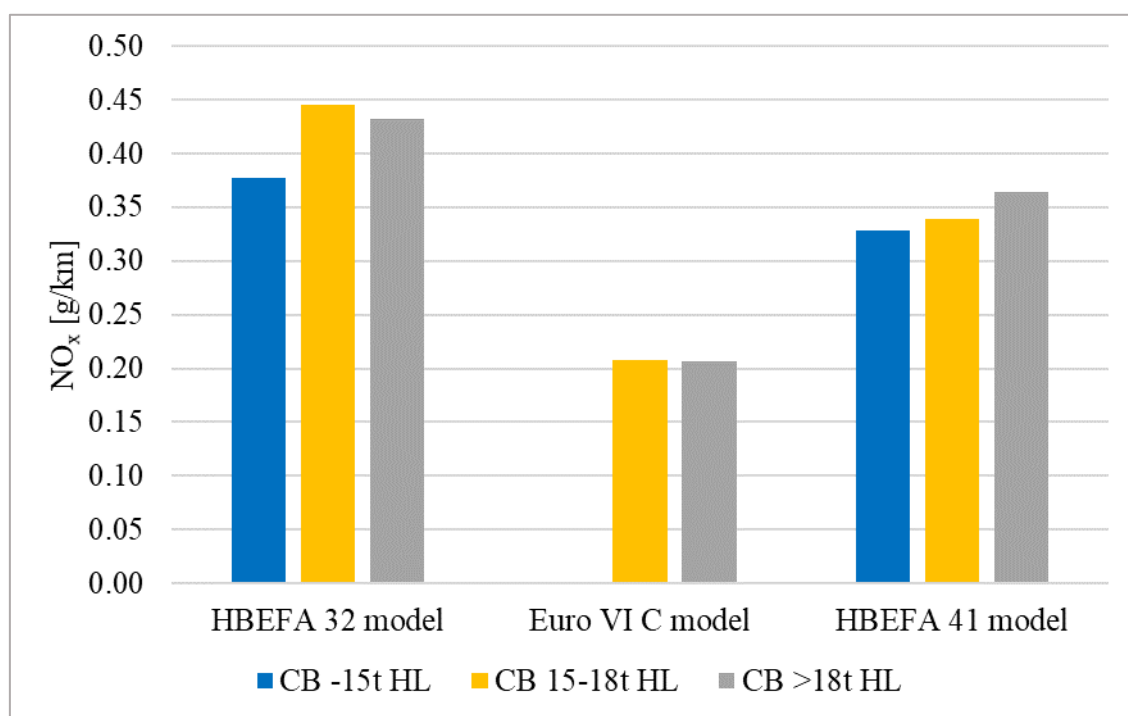


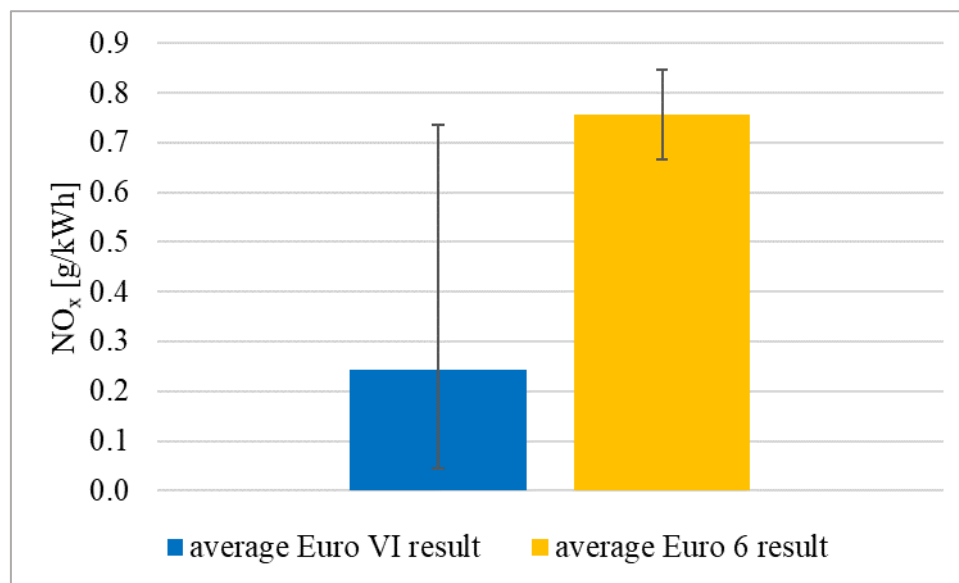
Figure 62: CB NO<sub>x</sub> emissions, aggregated traffic situation “urban driving – Germany” – HBEFA 4.1 model adjusted to CB measurements

### 7.5.3 Vehicles below 7.5 Tons – NO<sub>x</sub> Emission Model

Vehicles with a TPMLM between 3.5 and 7.5 tons are treated in a special way for the HBEFA 4.1. As they are partly certified as HDV (WHTC and WHSC test on the engine test bed, vehicle reference mass > 2610 kg) and as LDV (NEDC or WLTP test on the chassis dyno,

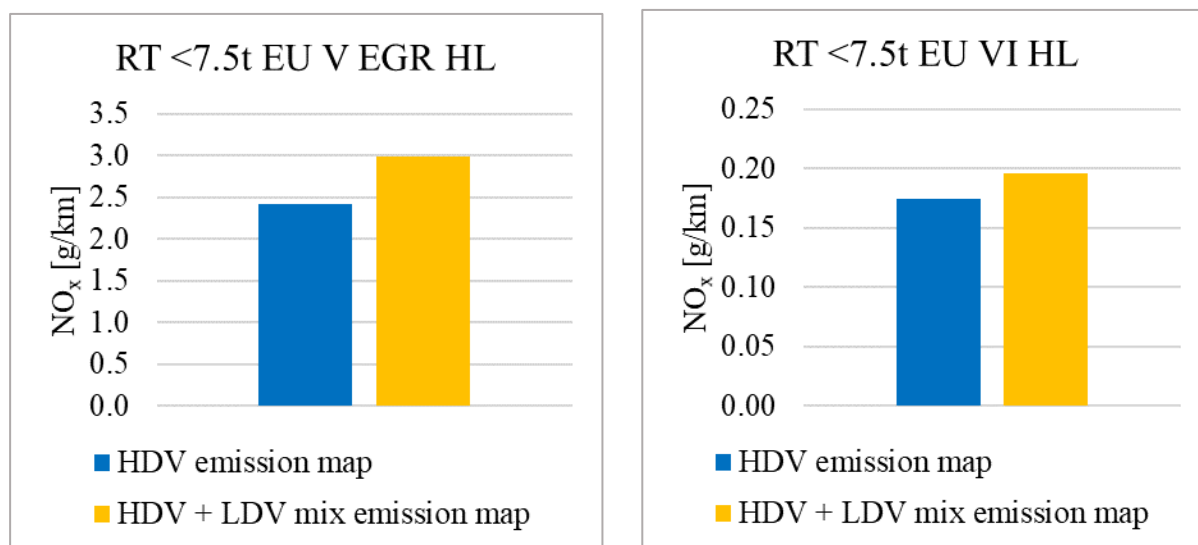
vehicle reference mass < 2610 kg), either HDV or LDV emission technology can be present in the different vehicles. The share of LDV technology in the vehicle segment below 7.5t TPMLM is assumed to be 35 % related to [56] and the rest of the vehicles use HD engines. This share is used for the creation of average emission maps and the average model for the exhaust after-treatment system for this vehicle category. This special emission map generation is done for Euro<sup>°</sup>V and Euro<sup>°</sup>VI, because the measurement campaign for HBEFA 4.1 provides LDV data for these two vehicle categories only. [23]

Figure 63 compares measurement data of Euro<sup>°</sup>6 and VI vehicles on exactly the same ISC track measured at TUG. Details regarding the single test results can be found in Table 25 in the annex. The blue bar represents the average of all HDV Euro<sup>°</sup>VI vehicles and the yellow bar illustrates the same for Euro<sup>°</sup>6 LDVs. The LDV mean NO<sub>x</sub> TP emissions are approximately three times higher compared to the HDV result; however, the variation of HDVs is quite high and the maximum values almost reach the mean LDV result. This means that NO<sub>x</sub> emissions of HDV certified vehicles are generally lower in terms of g/kWh, but single vehicles also have relatively high NO<sub>x</sub> TP emissions. In this case, it is important to mention that LDV measurement data contains only one vehicle in the maximum TPMLM category above 3.5 tons (N2 vehicles), because this vehicle could also be a high emitter. Of course, for affirmation of fleet emissions more measurement data of different vehicles would be necessary. However, the dataset does not provide more information and consequently this vehicle represents the average Euro<sup>°</sup>6 LDV in this case.



**Figure 63: Average Euro<sup>°</sup>VI (HDV) and Euro<sup>°</sup>6 (LDV) NO<sub>x</sub> results for one ISC route**

This measurement data builds the base for both a mean LDV engine emission map and a mean LDV exhaust after-treatment system. This LDV model was setup with standard routines (see section 7.4). Since only on-road test data is available for this vehicle, the model adjustment was done for NO<sub>x</sub> (see Table 13) only. As mentioned before, the LDV is weighted by 35 % and the HDV by 65 % for the final simulation models of this vehicle category. Figure 64 shows the simulation results of the 7.5 tons rigid truck (half loaded) for the HBEFA cycles weighted according to the German traffic mix. The blue bar gives the results of the HDV-only emission map and the yellow bar represents the HDV-LDV mix. The left graph shows the result for Euro<sup>°</sup>V vehicles and the right one for Euro<sup>°</sup>VI. Since Euro<sup>°</sup>5 LDVs do not use a SCR at all (all vehicles have EGR for NO<sub>x</sub> reduction), the Euro<sup>°</sup>5 model was merged with the Euro<sup>°</sup>V EGR model. Consequently, the Euro<sup>°</sup>V SCR model is left untouched. As expected, the “HDV+LDV mix emission map” model emissions exceed the “HDV emission map” NO<sub>x</sub> TP emissions in both emission classes.



**Figure 64: RT <7.5t HL Euro<sup>o</sup>V EGR and Euro<sup>o</sup>VI – NO<sub>x</sub> TP results for German traffic mix**

The complete EURO<sup>o</sup>VI SCR conversion map adjusted to the Euro<sup>o</sup>VI HGV RT <7.5t data can be found in the annex (Figure 92).

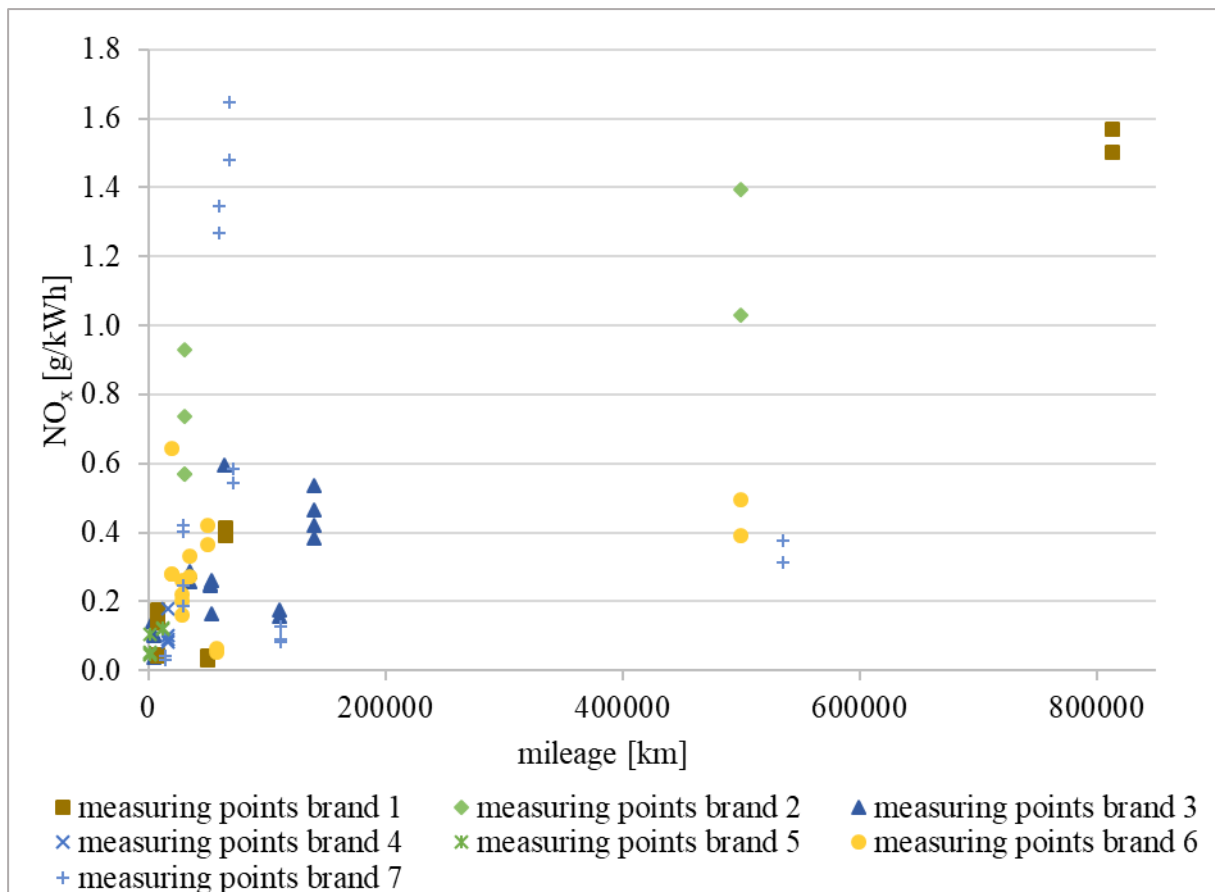
## 7.6 Deterioration Function

The elaboration of the deterioration functions for HDVs is based on single vehicle measurements. No Remote Sensing data is available for the HBEFA HDVs yet, since the location of tailpipes in HDVs is usually not at the rear of the vehicles and thus the measurement path across the street is blocked by the vehicle itself. Different vehicles of different brands with a minimum mileage of 500 000 km were measured on the chassis dyno and on on-road trips (4 of them EURO<sup>o</sup>VI and one EURO<sup>o</sup>V). The measured emission levels at the high mileages were then compared with the measurements with low mileage.

The EURO<sup>o</sup>V vehicle did not show a deterioration effect. Thus, no deterioration function for “aged” vehicles has been introduced for EURO<sup>o</sup>V HDVs. Whether this behaviour is representative for the entire fleet is open, since this one truck is most likely not representative for the entire fleet behaviour.

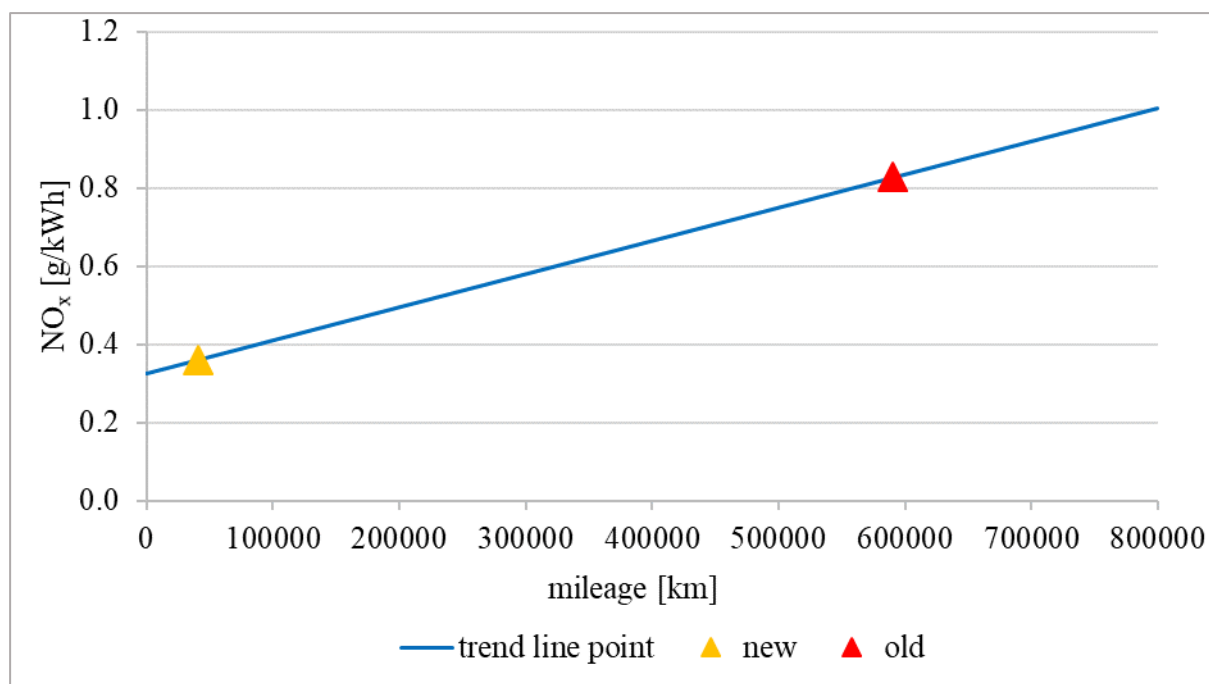
The analysis of all measured EURO<sup>o</sup>VI vehicles showed a noticeable deterioration only for NO<sub>x</sub>, while all other emission components stayed on the same level between low and high mileages. The newer measured vehicles have a mileage of approx. 50 000 km. The comprehensive measurement results are shown in Figure 8. This section will illustrate some more details, which can also be found in [57].

Figure 65 illustrates the ISC measurement results for NO<sub>x</sub> separated into different brands. Obviously 2 of the 4 “old” (more than 500 000 km) vehicles emit on a quite high level (more than 1 g/kWh), while the other 2 brands do not show any deterioration effects (lower than 0.69 g/kWh). However, also 1 “new” vehicle has rather high emissions. Note that the measurement data comprises only one “old” vehicle per brand. Of course, different “old” vehicles per brand would lead to a more reliable database.



**Figure 65: NO<sub>x</sub> TP emissions and vehicle mileage of EURO<sup>o</sup>VI HDVs separated into brands – total ISC**

For the elaboration of the Euro<sup>o</sup>VI NO<sub>x</sub> deterioration function, an average “aged” vehicle was created based on on-road test data. Therefore, ISC measurements of vehicles with high mileage from different brands were compiled into an average vehicle. The weighting of the mileage and the NO<sub>x</sub> emission mass of the single vehicles was based on the market shares of each brand (see Table 9). The second step was the creation of a “new” vehicle by measurements of vehicles with a mileage less than 150 000 km using the same weighting method as for the aged vehicle. The emission levels of the “new” and the “aged” vehicle and their corresponding average mileages provide 2 points for a linear equation, in which the grade describes the deterioration that occurs with increasing mileage. This is illustrated in Figure 66.



**Figure 66: Average „new“ and average „old“ vehicle – linear trend line**

The final models in the HBEFA 4.1 are corrected to a mileage of 50 000 km before the calculation of the emission factors. Consequently, the deterioration function is normalised to this mileage in order to apply this function to all different vehicle categories independent of their basic emission level. This normalisation is illustrated in equation 7-6:

$$Factor_{det} = \frac{k_{det} * x + d_{det}}{k_{det} * 50\,000\,km + d_{det}} \quad 7-6$$

Notation:

$d_{det}$  ... NO<sub>x</sub> TP emissions at 0 km in g/kWh

$Factor_{det}$  ... Deterioration factor

$k_{det}$  ... Deterioration gradient in g/(kWh\*km)

$x$  ... Average mileage of the vehicle fleet in km

A more detailed approach would be the determination of separate deterioration factors for different road categories (urban, rural and motorway). Figure 67 shows the variability between the particular functions including the comprehensive one.

The aging factor for the urban part has the lowest gradient. The main reason for this is the general high emission level in such operating conditions due to the long lasting low load phases. As a consequence, the relative increase of emissions based on deterioration effects is rather small compared to the other operating conditions.

The big emission increase in the category “rural” can be referred to the low emission level of “new” vehicles. In this case, the emission level increases to a relatively high level due to aging effects.

In general, the motorway sector delivers perfect conditions for a very high performance in NO<sub>x</sub> conversion due to constant high loads. This leads to a very low absolute base level

compared to urban conditions (see Figure 9 and Figure 10) and, consequently, the deterioration in the motorway part does not lead to a very high emission level.

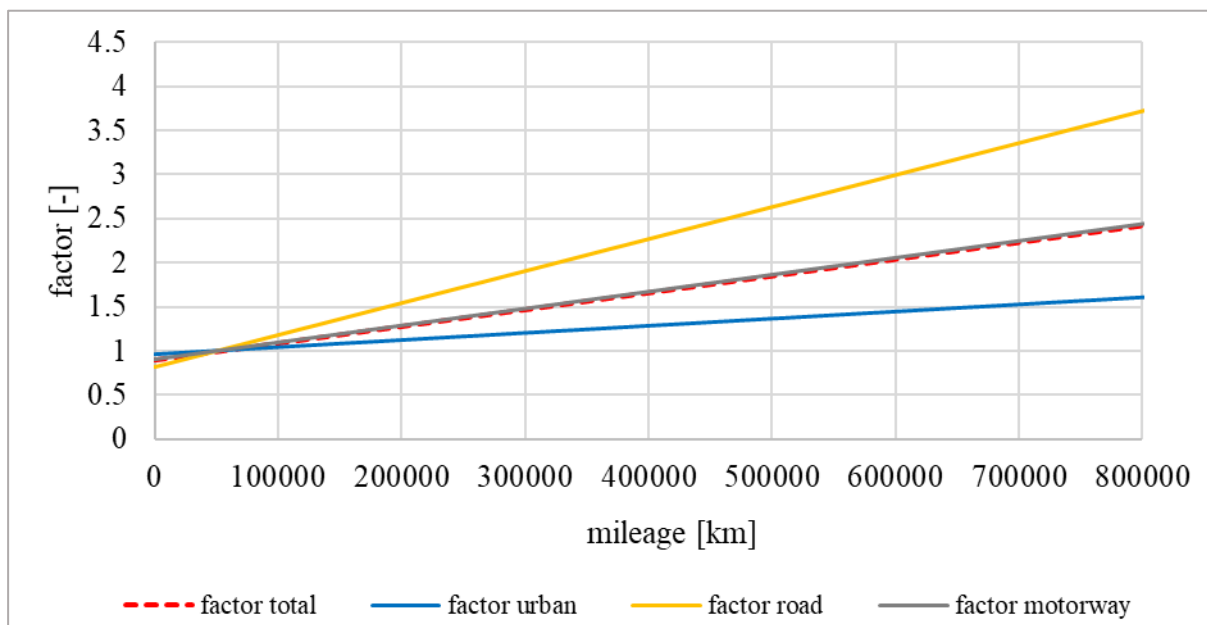


**Figure 67: Deterioration functions – urban, rural, motorway and total**

Of course, there is a difference between the deterioration functions of the various parts; however, the thin database implies quite a high risk regarding the generation of such detailed functions. For this reason, it seems to be more reasonable to integrate the total aging function into the HBEFA.

Euro<sup>o</sup>VI vehicles have to guarantee an appropriate emission performance during their entire lifetime. Every vehicle has to be checked in terms of whether the NO<sub>x</sub> emission level exceeds the allowed tolerances<sup>11</sup> at any time of their usage. For this reason, the OBD system checks every component of the engine and the exhaust after-treatment system for malfunctions. Type approval tests show which malfunctions or combinations thereof lead to an excess of the OBD emission limit in the WHTC. If such malfunctions or combinations are detected during normal usage, the vehicle has to activate the emergency operating mode. This will lead to a repair of the system(s) with malfunctions. However, as already explained, the emission limit of 1500 mg NO<sub>x</sub>/kWh refers to the WHTC and, of course, in general, on-road trips do not represent the same load conditions as the WHTC. Consequently, it is a challenge to compare an on-road trip to a WHTC and, consequently, it was assumed for HBEFA that vehicles exceed this OBD threshold up to a value of 2000 mg NO<sub>x</sub>/kWh before detection. Of course, this repair work will not eliminate all problems, but these necessary repairs will lead to an emission reduction to approximately 1500 mg NO<sub>x</sub>/kWh. An alternation between emission limit exceeding and problem fixing is assumed to keep emissions of the fleet on a constant level after a certain mileage. Determination of this mileage is based only on two brands that show obvious aging effects (brand 1 and brand 2, see Figure 65). The mileage is exactly 890 099 km, i.e. the point at which the comprehensive deterioration function for the 2 aged vehicles reaches 1750 mg NO<sub>x</sub>/kWh (see Figure 68).

<sup>11</sup> The limit is 1500 mg NO<sub>x</sub>/kWh referring to a WHTC cycle.

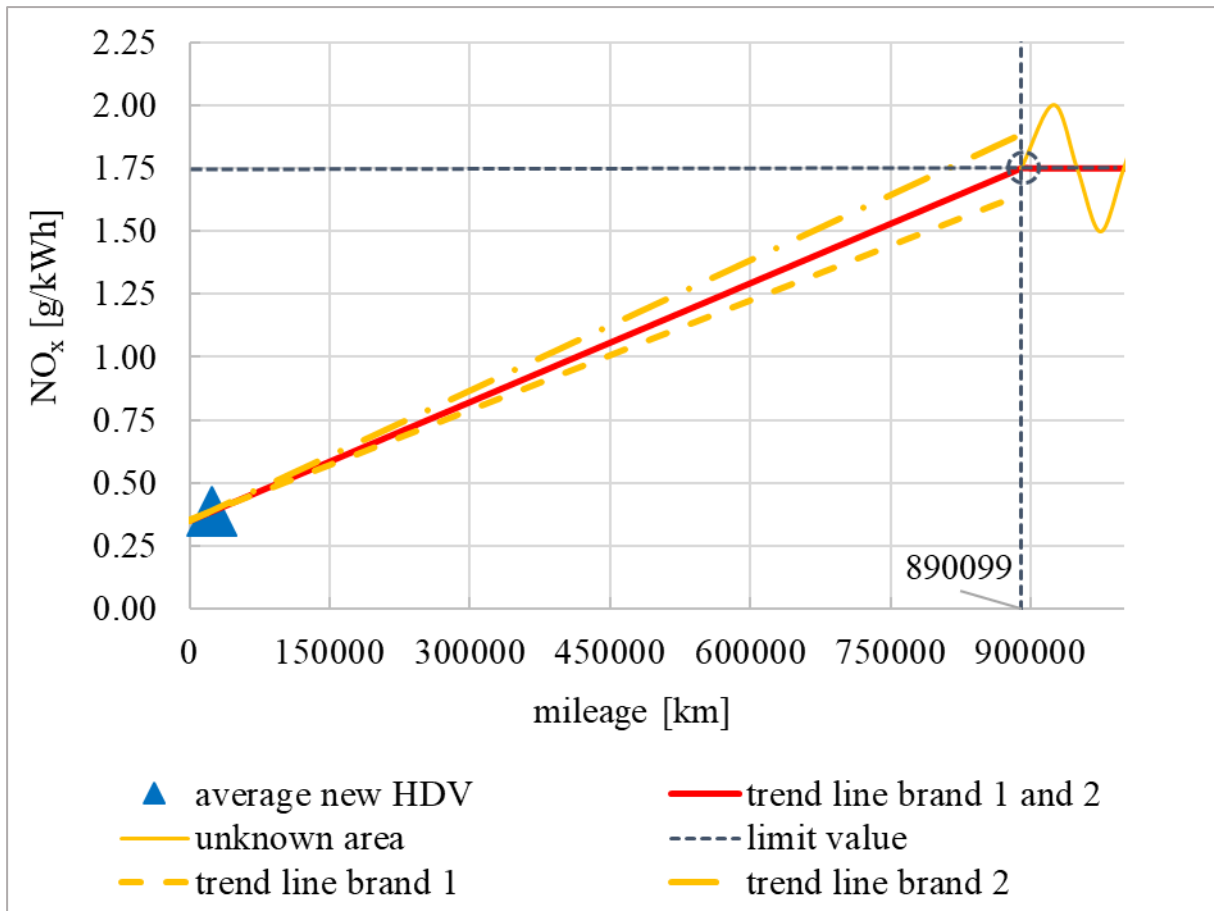


**Figure 68: NO<sub>x</sub> deterioration function – determination of the mileage at the excess of the OBD limit**

Figure 69 shows the final NO<sub>x</sub> deterioration function as emission ratio to vehicles at 50 000 km for Euro<sup>o</sup>VI HDVs.

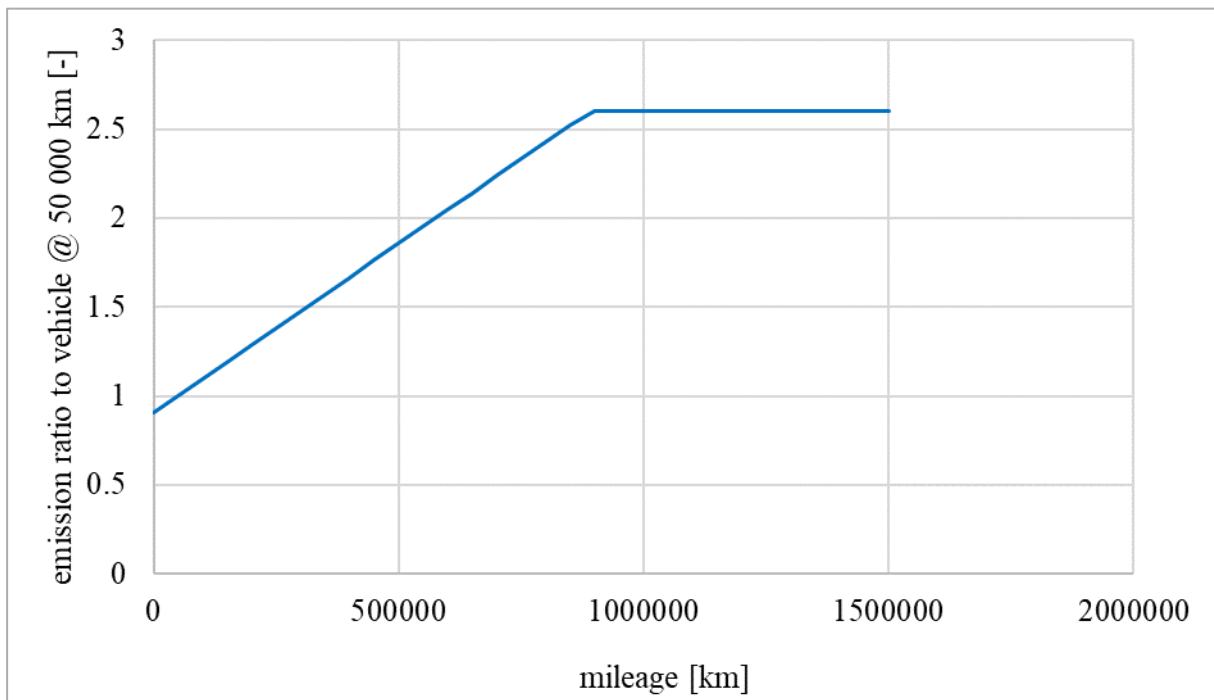


**Figure 69: NO<sub>x</sub> deterioration function for HDV**

One reason for the significant deterioration of Euro<sup>o</sup>VI compared to no deterioration for Euro<sup>o</sup>V may be the use of DOCs upstream of the SCR to increase the NO<sub>2</sub> share in NO<sub>x</sub>

towards 50 %, which is typical for Euro<sup>o</sup>VI but was not a standard for Euro<sup>o</sup>V with its less demanding type approval limits and test procedures. A 50 % NO<sub>2</sub> share leads to the fastest NO<sub>x</sub> conversion and also to higher conversion efficiency at lower temperatures. The aging of the DOC reduces the NO<sub>2</sub> production from the NO dominated raw exhaust and thus also SCR efficiency. Certainly, also other effects will contribute to the deterioration, such as the aging of NO<sub>x</sub>-sensors etc. The resulting relative increase in emissions is much higher at the low NO<sub>x</sub> levels of Euro<sup>o</sup>VI compared to the higher base NO<sub>x</sub> values of Euro<sup>o</sup>V. However, as shown in Figure 69, the deterioration of Euro<sup>o</sup>VI vehicles is limited and consequently these emissions will be below Euro<sup>o</sup>V NO<sub>x</sub> emissions in any case.

### **7.7 Elaboration of N<sub>2</sub>O and NH<sub>3</sub> EFAs for HDVs**

The HBEFA also provides emission factors for the unregulated emission components N<sub>2</sub>O and NH<sub>3</sub>. FTIR measurements of 6 Euro<sup>o</sup>VI vehicles at TU Graz' chassis dynamometer for HDV are the base for elaborating emission factors for these components.

NH<sub>3</sub> is used for the reduction of NO<sub>x</sub> in the SCR catalyst; however, if the AdBlue dosing strategy does not work properly, NH<sub>3</sub> can pass the SCR catalyst. For this reason, the exhaust after-treatment system contains a clean-up catalyst as a final module for the oxidation of excess ammonia. But in certain cases the oxidation process in this catalyst does not work accurately and not all of the NH<sub>3</sub> can be converted (details in section 3.2.2.3). Thus, NH<sub>3</sub> emissions at tailpipe are mostly dependent on AdBlue dosing and the conditions at the CUC. A standard emission map based on engine speed and engine power as used for regulated emission components seems not to be reasonable in this case. Figure 70 illustrates the application of such a standard PHEM emission map for the brake specific emissions of NH<sub>3</sub>. This irregular structure – with regard to these very high emission peaks in particular – would not lead to a meaningful result. Small changes, e.g. in the transmission ratios, would implicate completely different emission results according to the change in the engine operating point. It is unlikely that such a small change in engine operating points leads to big differences in the AdBlue dosing strategy or in the conditions at the CUC, which are relevant for NH<sub>3</sub> emissions.

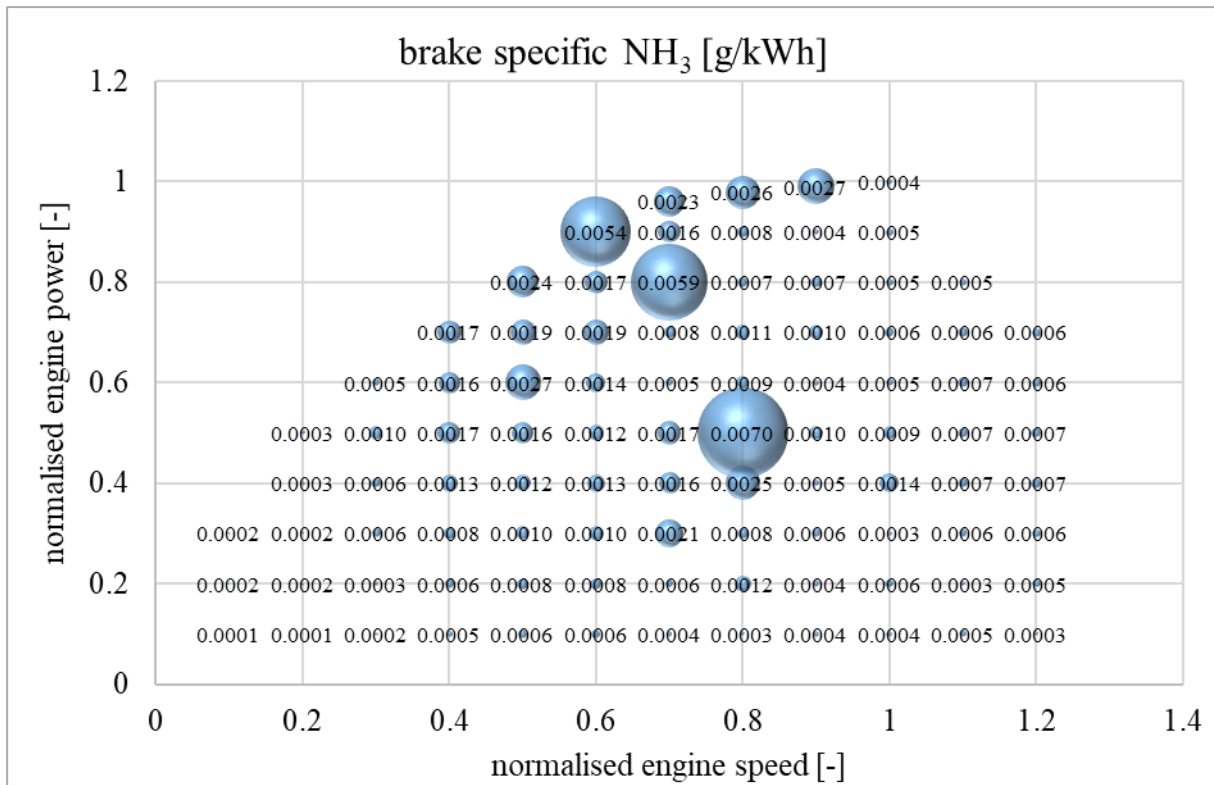


**Figure 70: Average engine map – brake specific NH<sub>3</sub> emissions (only for demonstration, not used for emission factors)**

N<sub>2</sub>O is a side product of the oxidation of NH<sub>3</sub> in the CUC due to special operating conditions in the catalyst. It is mainly high temperatures that lead to the conversion of NH<sub>3</sub> and NO<sub>x</sub> to N<sub>2</sub>O, but this process can also run at low temperatures [19]. This process is also not mainly and directly dependent on the current engine speed and engine power and, consequently, the standard PHEM simulation process is not ideal for this component either. Figure 71 shows what the engine speed and power based engine map for N<sub>2</sub>O would look like. Indeed, this emission map is more regular compared to the one of NH<sub>3</sub>; however, the setup of an engine power and speed based model according to the explanations given above is also not reasonable for this component.

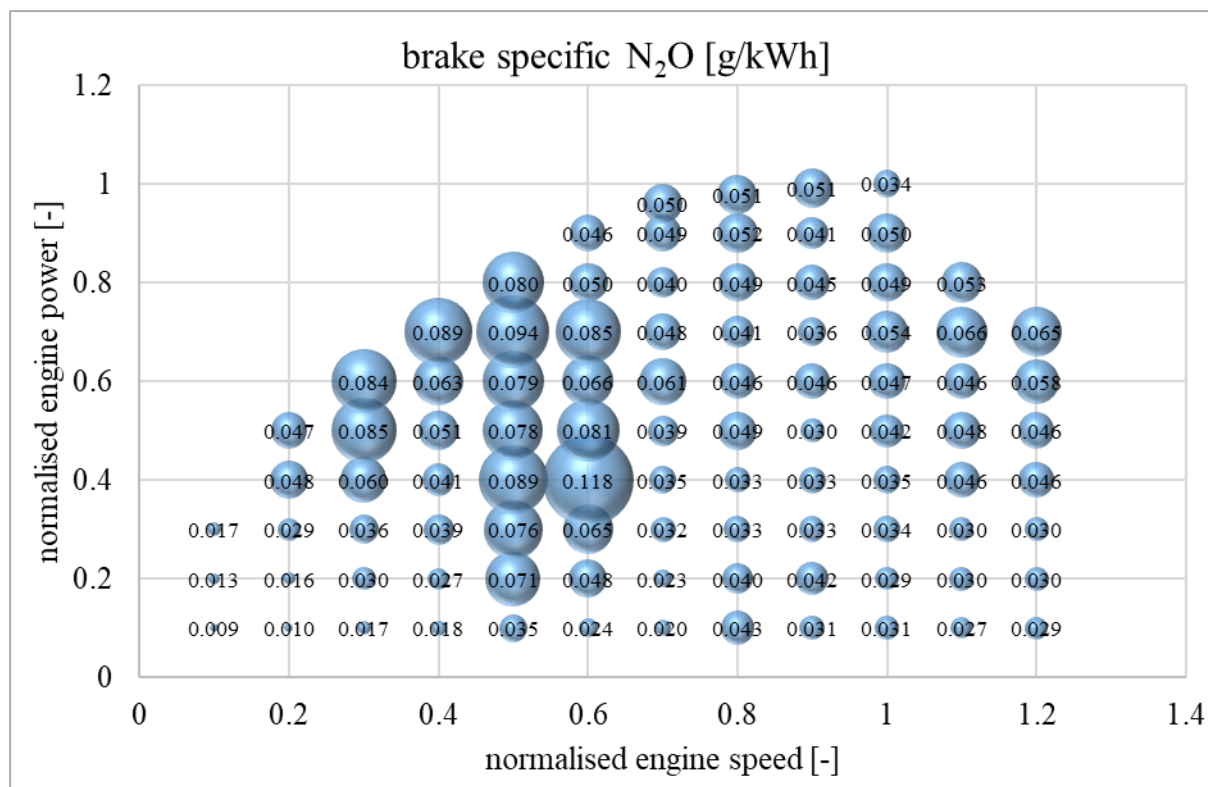


**Figure 71: Average engine map – brake specific N<sub>2</sub>O emissions (for demonstration only, not used for emission factors)**

Since standard PHEM routines do not work reasonably for these components, the creation of hot emission factors for N<sub>2</sub>O and NH<sub>3</sub> is based on brake specific test results and the energy consumption of the different vehicle categories in the HBEFA aggregated traffic situations (e.g. urban, rural or motorway). The calculation of the final emission factors is based on the following equation:

$$EFA = BSE * EnC$$

7-7

Notation:

*BSE* ... Brake specific emissions in g/kWh

*EFA* ... Emission factor in g/km

*EnC* ... Energy consumption in kWh/km

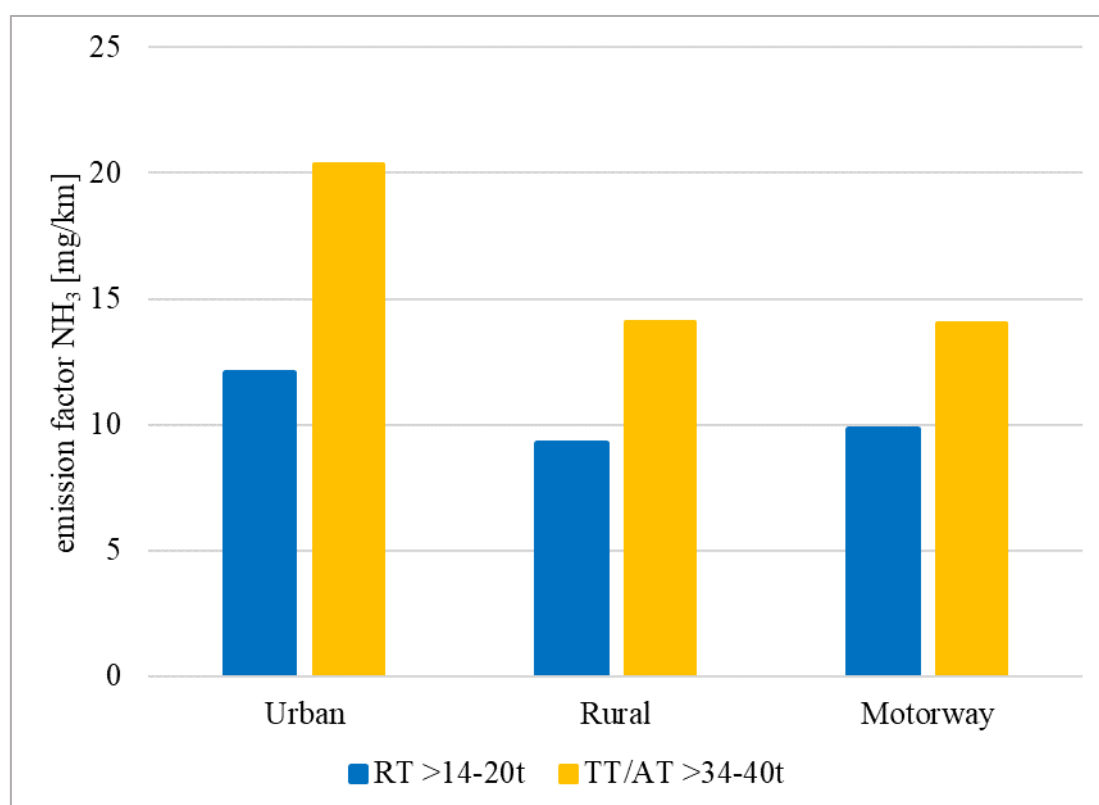
The brake specific emissions are assumed to be independent of the vehicle category, because the small database does not provide enough data for a more precise distribution. Table 14 shows all available measurement results for the WHVC (preconditioning: 10 minutes at 80 km/h). This cycle covers a wide range of different operating conditions and thus properly fits the average picture of emission behaviour. Finally, the single vehicle results are averaged to one value for each emission component (marked in orange). While the measurement results for NH<sub>3</sub> are quite low for all vehicles, the values for N<sub>2</sub>O are remarkable for some vehicles. Regarding the N<sub>2</sub>O greenhouse gas potential of 298 [36], for example, vehicle 6 shows CO<sub>2</sub> equivalent emissions of 129.0 g/kWh just from the N<sub>2</sub>O emissions. This leads to an increase of CO<sub>2</sub> equivalent emissions of approximately 15 % (CO<sub>2</sub> emissions: 741.3 g/kWh of vehicle 6 in the WHVC).

**Table 14: NH<sub>3</sub> and N<sub>2</sub>O brake specific emissions for the WHVC**

Vehicle	Mileage [km]	NH <sub>3</sub> [g/kWh]	N <sub>2</sub> O [g/kWh]
1	813 500	0.00064	0.03131
2	500 000	0.00630	0.39139
3	535 000	0.00292	0.37666
4	500 000	0.01087	0.08650
5	1 200	0.00414	0.07092
6	16 000	0.00121	0.43371
average	394 283	0.00435	0.23175

The HBEFA provides different emission factors for all vehicle categories (HGV, coaches and city busses) for the main aggregated traffic situations (urban, rural and motorway) for N<sub>2</sub>O and NH<sub>3</sub>. Since the energy consumption varies a lot regarding different vehicles and traffic situations, these values have to be calculated for each combination. This calculation was done for the German mix of traffic situations. The emission factors for each vehicle category can be found in the annex (see Table 26).

Figure 72 and Figure 73 show the final emission factors for NH<sub>3</sub> and N<sub>2</sub>O for a representative rigid truck and a tractor trailer combination. The NH<sub>3</sub> emission factors are on a low level with values up to 20 mg/km. However, for N<sub>2</sub>O, the results show values above 1 g/km for the tractor trailer combination in urban conditions.

**Figure 72: NH<sub>3</sub> emission factors for RT > 14-20t and TT/AT > 34-40t**

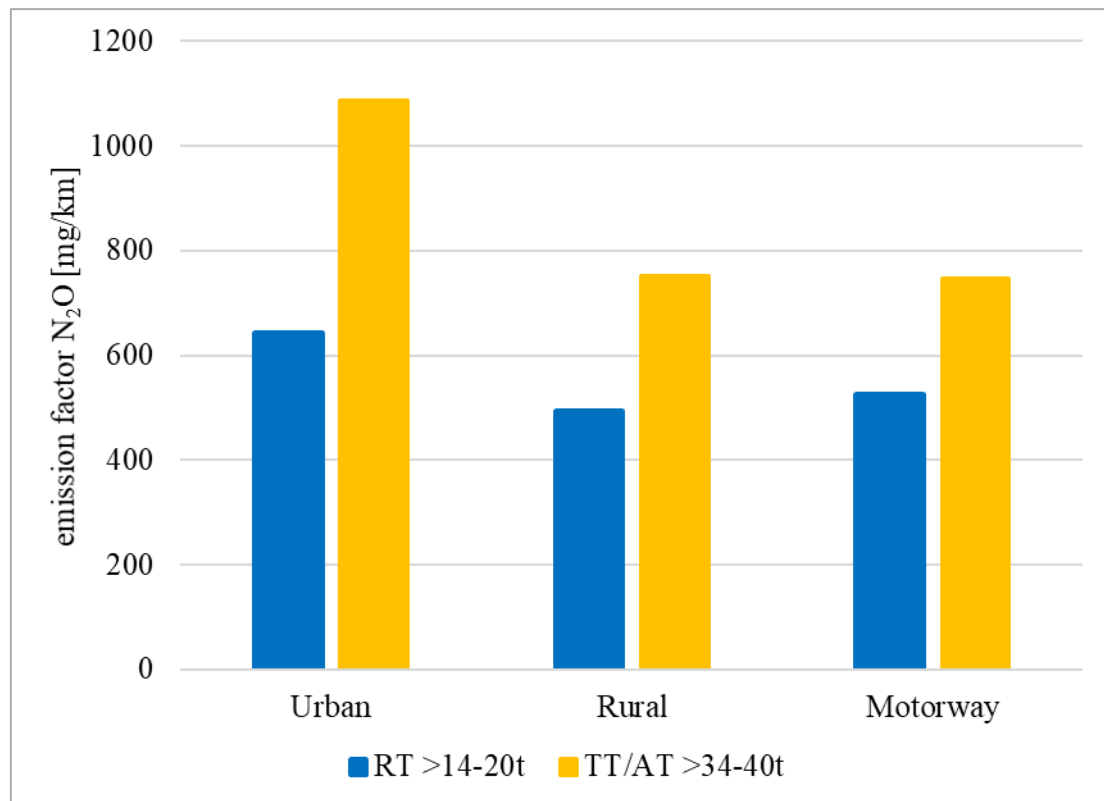


**Figure 73: N<sub>2</sub>O emission factors for RT > 14-20t and TT/AT > 34-40t**

The data set includes measurements of vehicles with a relatively low mileage (< 50 000 km) and some with a high mileage (> 500 000 km). Consequently, it implies emissions during different periods in a vehicle's lifetime. Since the available data does not show a trend on vehicle mileage (see Table 14), no deterioration function for the EFAs for N<sub>2</sub>O and NH<sub>3</sub> was introduced in the HBEFA.

The impact of these emission factors is quite high especially with regard to greenhouse gas emissions from N<sub>2</sub>O. Since the database is rather small with 6 Euro<sup>o</sup>VI vehicles measured with FTIR, these results were not introduced in HBEFA version 4.1. For extending the database and for consolidating the results, some more measurements are suggested to be performed for HBEFA version 4.2. The HBEFA 4.1 contains the results of the EMEP/EEA air pollutant emission inventory guidebook [27] for NH<sub>3</sub> and N<sub>2</sub>O.

## 8 HDV Results for the HBEFA 4.1

This chapter describes the main results of the HBEFA 4.1 for diesel driven HDVs and compares them with the results of the HBEFA 3.3. Therefore, the most representative vehicle categories like tractor trailers, rigid trucks or city busses are illustrated on the following pages.

As already described in section 3.3, the HBEFA provides emission factors for all regulated and some unregulated emission components for more than 1000 different traffic situations. These single results can be summarized into country-specific aggregated traffic situations like urban, rural or motorway driving and into one average traffic situation finally representing the real-drive-emission level of all different HDV categories. These aggregated traffic situation results are illustrated in this chapter for comparison and evaluation.

### 8.1 Introduction of New Driving and Preconditioning Cycles

The further development of emission reduction systems lead to low emissions in almost all driving situations. Only longer low load driving and the following cool down effects in the exhaust after-treatment system lead to a drop in NO<sub>x</sub> conversion efficiency of the SCR catalyst as was already explained in section 6.2.2. To distinguish exactly between Stop&Go and heavy Stop&Go situations, HBEFA 4.1 introduced a new traffic situation called “Stop & Go 2”. Compared to the traffic situation “Stop & Go” (already existing in HBEFA 3.3), this driving situation extends the low load phases.

Another point related to the topic driving cycles is the introduction of preconditioning cycles before the main cycle. These cycles take care of an appropriate temperature of the exhaust after-treatment system at the beginning of the following traffic situation and consequently affect the NO<sub>x</sub> tailpipe emissions. Equal main cycles can coexist with various preconditioning cycles and thus illustrate different traffic situations. A traffic jam, for example, can be preconditioned by free flow motorway driving or, in contrast, by Stop&Go urban driving. The impact of these different preconditioning cycles is illustrated in Figure 74 for exactly the same main cycle at 0 % gradient. The results represent the broad scatter for NO<sub>x</sub> emissions of the 34–40t tractor trailer half loaded: each bar illustrates exactly the same main cycle, but with variable preconditioning. The emission masses vary between 3.8 and 4.6 g/km.

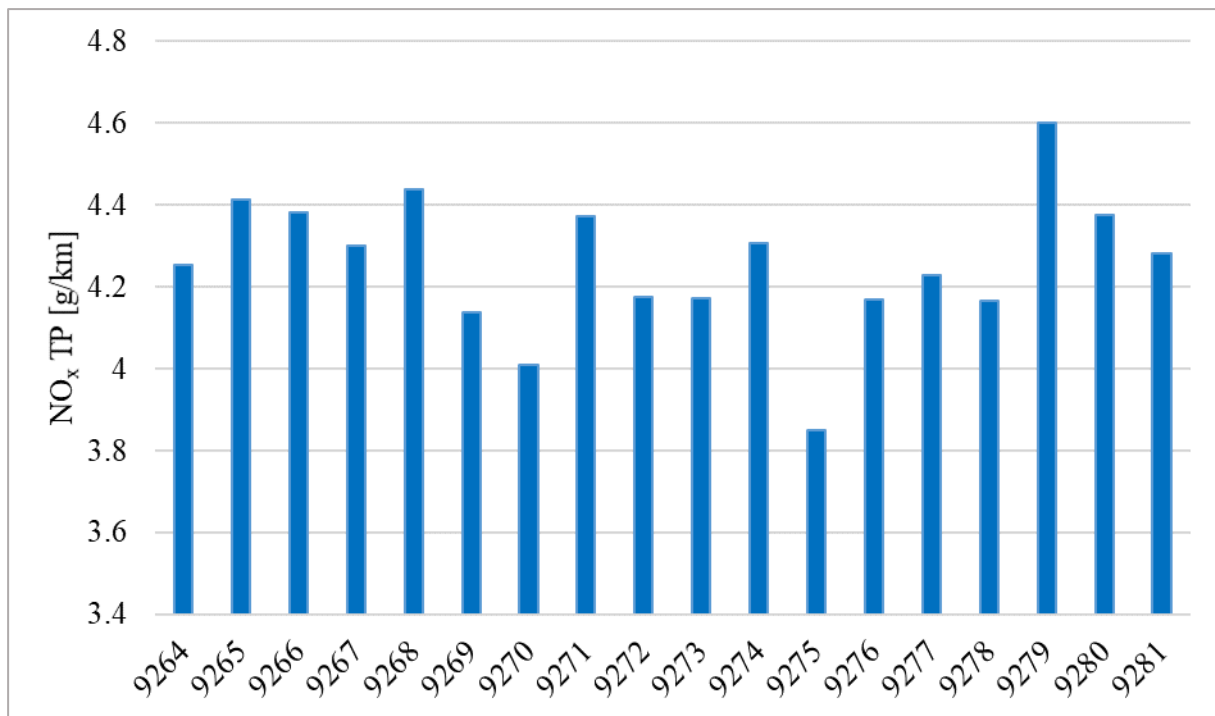


**Figure 74: NO<sub>x</sub>-TP emissions, HGV TT 34–40t half loaded, 0 % gradient – same main cycle, different preconditioning cycles**

In contrast to this, the HBEFA 3.3 does not contain any preconditioning cycles. The temperature simulation had been an iterative process until the temperature at the start of the cycle reached the same value as at the end of the cycle. This method focused only on the main cycle and did not take any preconditioning phase into account. Consequently, the same main cycle always delivered equal emission results independent of the traffic situation. Details regarding this method can be found in [43]. The HBEFA 4.1 method differentiates more precisely in this regard. All preconditioning cycles as well as the main cycles were provided by HS Consulting [58].

## 8.2 Comparison between Simulation Models for HBEFA 3.3 and HBEFA 4.1

This part describes the comparison between emission factors in the HBEFA 3.3 and the HBEFA 4.1. Of course, all innovations and updates that were introduced have an influence on the results. This section explains the details.

Before illustrating the final emission factors for the single vehicle categories, it is helpful to point out once again the main innovations introduced with the HBEFA 4.1. These are:

- Updated database: on-road and additional chassis dyno measurements (see chapter 4)
- Improvements and updates of the simulation model PHEM (explanations in chapter 6) and the heavy duty emission model (see chapter 7)
- Introduction of new driving and preconditioning cycles (see section 8.1)

Table 15 quantifies the impact of the different changes between the HBEFA 3.3 and the HBEFA 4.1 for a Euro<sup>o</sup>VI tractor trailer combination (GVM 40t, half loaded, 0 % gradient) in the German traffic mix for different emission components. Every column introduces a new feature, which is added to the changes that have already been applied in the steps before. The resulting value represents the difference coming along only with this new modification.

- **Migration to a new PHEM version:** The change of the new PHEM model, which was introduced with the HBEFA 4.1, mainly has an impact on NO<sub>x</sub> emissions, which

rise by 7 percent. As already explained, NO<sub>x</sub> is calculated by the use of a complex exhaust after-treatment model and consequently the change of the model influences the NO<sub>x</sub>-EO simulation, the temperature model and the SCR conversion.

- **Introduction of HBEFA 4.1 driving cycles:** The introduction of new driving cycles has a bigger impact. The FC rises by nearly 10 percent and NO<sub>x</sub> emissions even by more than 20 %. Obviously, the HBEFA 4.1 driving cycles are more demanding than the ones of the HBEFA 3.3. One reason is the Stop&Go 2 traffic situation which was already explained.
- **Introduction of HBEFA 4.1 vehicle data:** The HBEFA 4.1 vehicle data leads to higher fuel consumption, but decreases emissions. These values based on data of the VECTO project (see section 7.2) lead to higher driving resistances for this vehicle category and emission class. This implies higher temperature levels of the exhaust gas after-treatment systems and consequently better conversion efficiencies.
- **Introduction of HBEFA 4.1 emission data:** Of course, the introduction of new emission data (FC and emission maps) including the HBEFA 4.1 basic after-treatment calculation principle for the NO<sub>x</sub> conversion (see section 6.2.2.1) has a very big influence. While fuel consumption is lower, all pollutant emissions have clearly increased (43 to 196 %). These results are based on the measurement data already described in section 4.3. The data for the HBEFA 4.1 covers much more vehicles and additionally on-road tests. Obviously, this data leads to higher pollutant emissions.
- **Introduction of the NH<sub>3</sub> storage model:** Section 6.2.2.2 explains the demand of the NH<sub>3</sub> storage model in low load phases. This model influences only NO<sub>x</sub> emissions and the impact is rather small compared to other changes. The HBEFA low load cycles are too short for a significant intervention of the storage model.
- **Impact of aging factors (mileage = 300°000 km):** Section 7.6 illustrates the deterioration function for NO<sub>x</sub> for Euro°VI vehicles. In this chapter, a mileage of 300 000 km was assumed for an average Euro°VI truck on German roads and consequently was used for calculating the aging effects. This leads to a considerable increase in NO<sub>x</sub> emissions.
- **Total change:** Summing up all these single changes into a total value results in an increase in all components. The fuel consumption rose by nearly 4 percent while, in the case of PM, emissions more than tripled. Also NO<sub>x</sub> shows an increase of more than 150 % for a Euro°VI tractor trailer combination in the aggregated German traffic mix.

**Table 15: Impact of changes between HBEFA 3.3 and 4.1, HGVT 34–40t Euro°VI half loaded, German traffic mix**

	Migration to a new PHEM version	Introduction of HBEFA 4.1 driving cycles	Introduction of HBEFA 4.1 vehicle data	Introduction of HBEFA 4.1 emission data	Introduction of the NH <sub>3</sub> storage model	Impact of aging factors (mileage = 300°000 km)	Total change
FC	1.5 %	9.5 %	1.7 %	-8.9 %	-	-	3.9 %
CO	-0.6 %	6.4 %	-9.2 %	76.0 %	-	-	72.7 %
NO <sub>x</sub>	7.0 %	22.9 %	-9.9 %	48.8 %	5.6 %	83.1 %	157.5 %
PM	-0.3 %	13.3 %	-3.5 %	196.9 %	-	-	206.4 %
PN	-0.4 %	16.9 %	-10.1 %	43.3 %	-	-	49.8 %

Figure 75 shows some more details. It illustrates the  $\text{NO}_x$  results compared to the average cycle speed of a tractor trailer combination of 34–40 tons for all traffic situations which exist in both HBEFAs, versions 3.3 and 4.1. The HBEFA 4.1 comes along with higher emission factors in more or less every traffic situation as expected regarding the results for the aggregated German traffic mix in the previous table. However, what is interesting is the single very high emission factor at low vehicle speed in the HBEFA 3.3. This can be explained by the preconditioning phase implemented in the HBEFA 4.1, which is rather high demanding compared to the main cycle (see Figure 76). The preconditioning in HBEFA 4.1 operates on higher speed level with high accelerations. This leads to higher temperatures of the exhaust after-treatment system and consequently to more efficient conversion in the SCR at the start of the main cycle. In contrast, the iteration method to meet the same catalyst temperatures at the start and at the end of the cycles in HBEFA 3.3 simulated an extremely long Stop&Go situation. Moreover, the main cycle was fundamentally changed for this traffic situation. This driving cycle change for some traffic situations started with the introduction of the HBEFA 4.1. This can be seen in Figure 77: every point compares the average cycle vehicle speed for one traffic situation. Each point that is not on the  $45^\circ$  line implies a deviation between the cycles for this traffic situation.

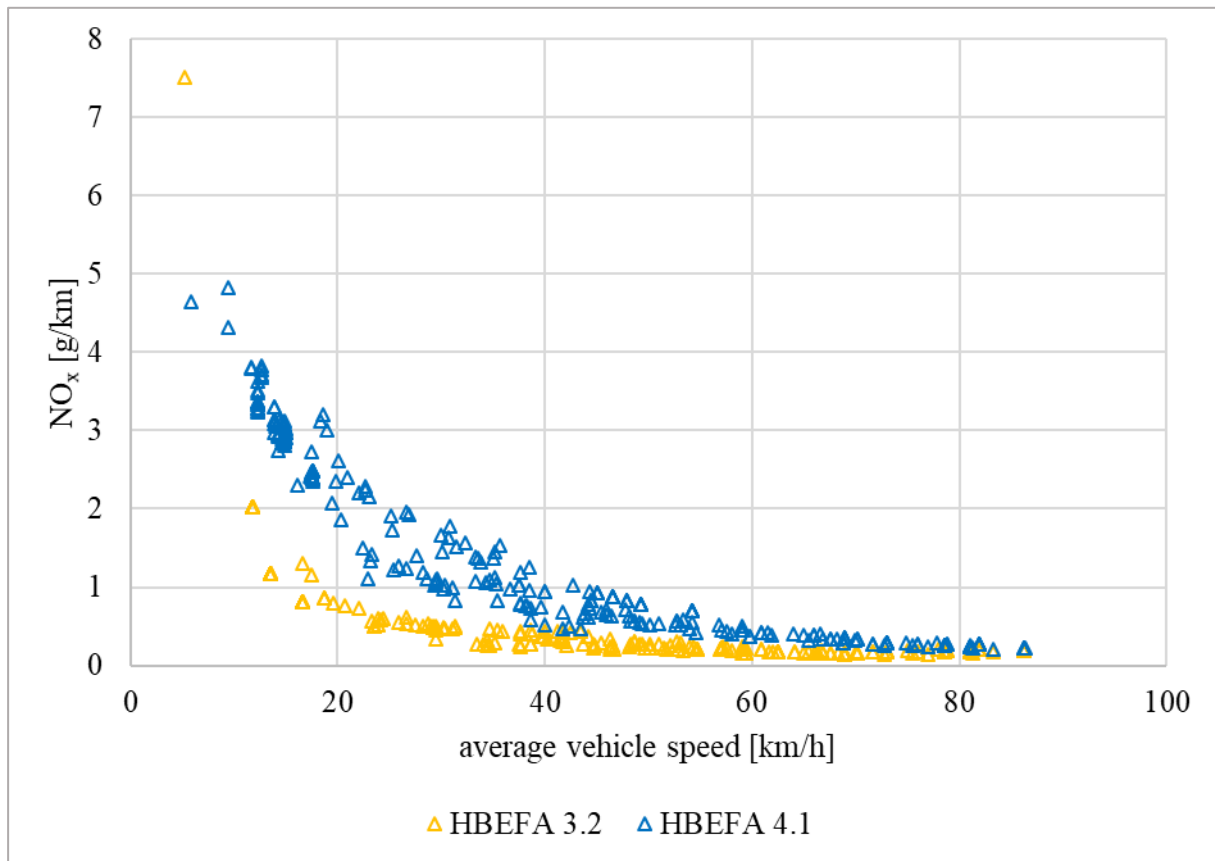


**Figure 75: Comparison of  $\text{NO}_x$  emissions in the same traffic situations in the HBEFA 3.3 and 4.1, HGV TT 34–40t Euro<sup>VI</sup> half loaded, 0 % gradient**

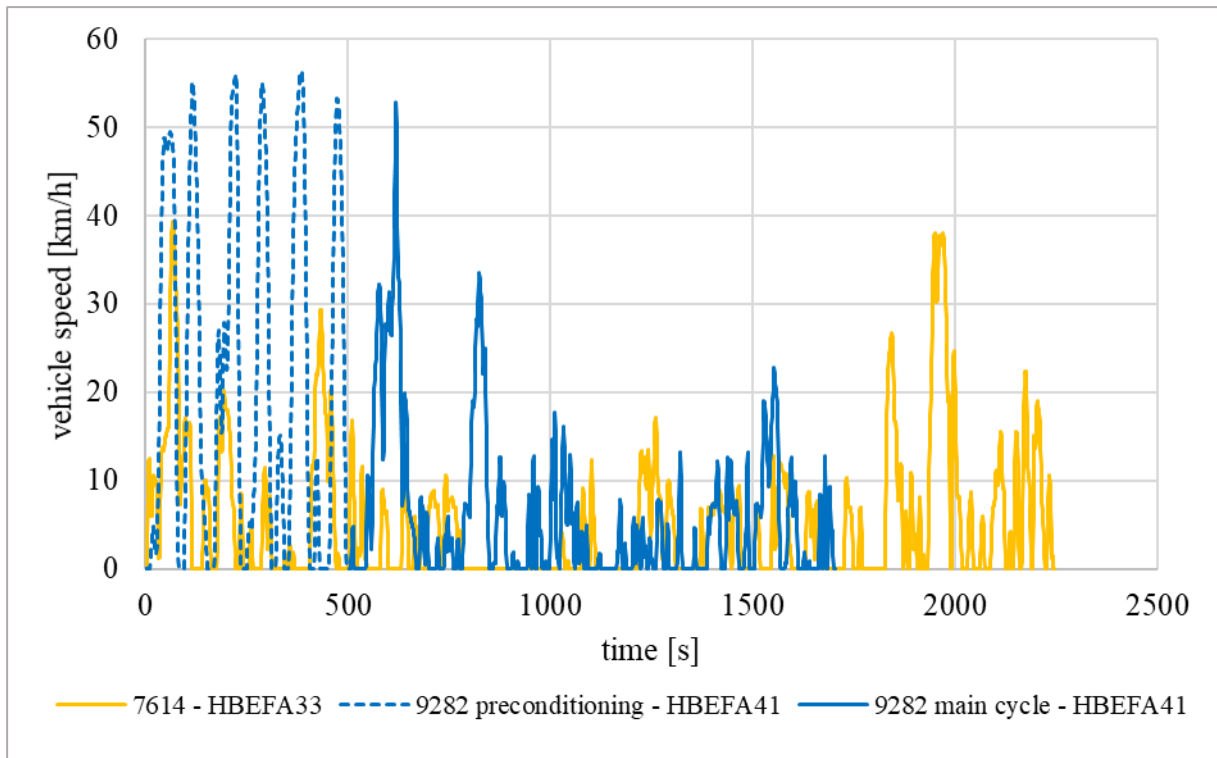


Figure 76: Comparison of vehicle speed in the traffic situations “Stop&Go\*” in the HBEFA 3.3 and the same one in the HBEFA 4.1, HGV TT 34–40t Euro<sup>o</sup>VI half loaded, 0 % gradient

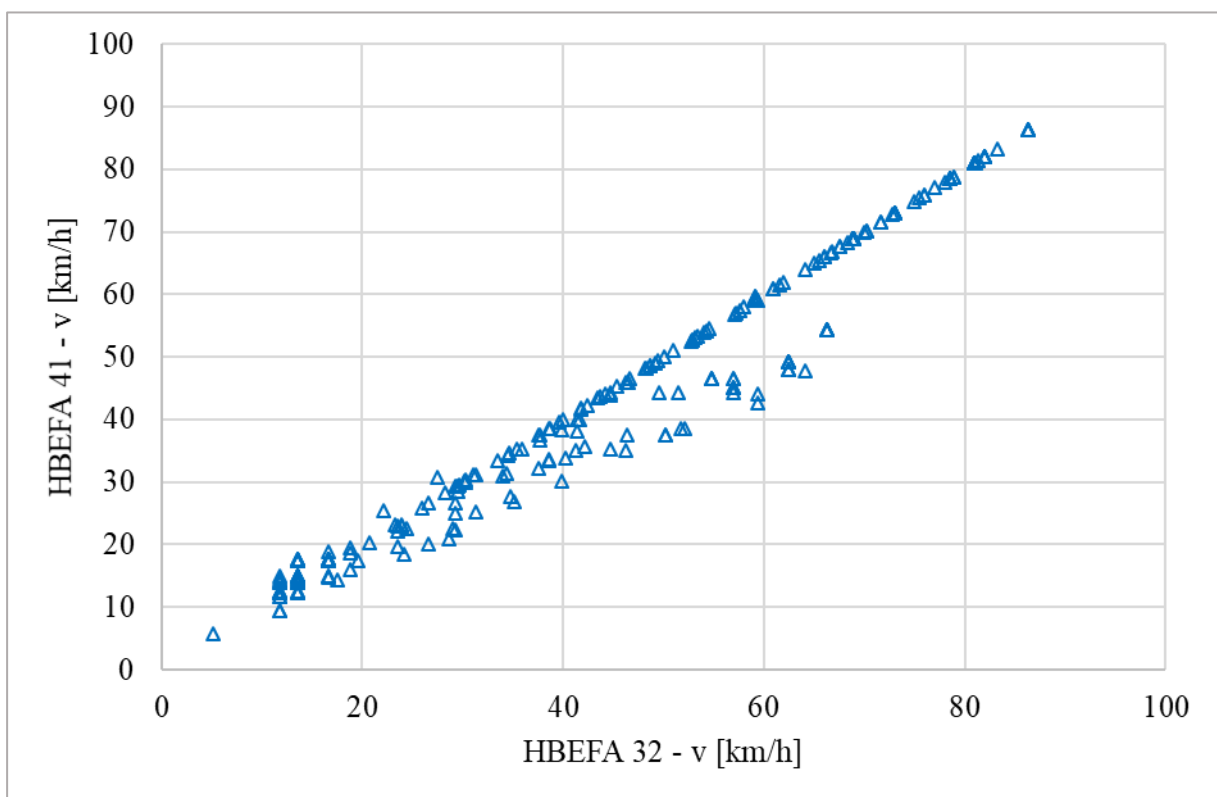


Figure 77: Comparison of the vehicle speed in the same traffic situations in the HBEFA 3.3 and 4.1, HGV TT 34–40t Euro<sup>o</sup>VI half loaded, 0 % gradient

Table 16 shows the same comparison as Table 15 on the impacts coming along with HBEFA 4.1 for a Euro<sup>o</sup>V SCR tractor trailer combination in the aggregated German traffic mix.

- **Migration to a new PHEM version:** Also in this case, the version migration has an influence mainly on NO<sub>x</sub> emissions due to the same reasons as explained for Euro<sup>o</sup>VI. All changes are on a similar level compared to the ones of Euro<sup>o</sup>VI.
- **Introduction of HBEFA 4.1 driving cycles:** The new driving cycles have a big impact on this emission class as well. Fuel consumption is increased by more than 10 percent and NO<sub>x</sub> emissions even by nearly 50 percent.
- **Introduction of HBEFA 4.1 vehicle data:** The update of the vehicle data also leads to higher fuel consumption due to higher driving resistances and consequently higher engine power demand. What is interesting is the behaviour of the pollutant emissions based on the engine power increase. While CO and PM emissions rise, NO<sub>x</sub> emissions decrease. Higher engine power leads to higher exhaust gas temperatures and consequently to an increase in after-treatment temperature. As already explained in section 3.2.2.3, this results in better conversion in the SCR catalyst. Since EURO<sup>o</sup>V most often had no DOC upstream of the SCR and no DPF, exhaust temperature effects on CO and PM are different to EURO<sup>o</sup>VI.
- **Introduction of HBEFA 4.1 emission data:** The introduction of updated fuel maps reduces the consumption by 6 percent. The principle data of the emission maps had not been changed, but the number of grid points rose. This leads to different behaviour regarding the interpolation of emissions by use of these maps. This results in a small increase in pollutant emissions.
- **Total change:** The total changes show an increase in all different components. Fuel consumption is increased by nearly 15 percent, while CO emissions rise by even more than 60 percent. NO<sub>x</sub> emissions of Euro<sup>o</sup>V SCR tractor trailer combinations are 40 percent higher in HBEFA 4.1 compared to HBEFA 3.3.

**Table 16: Impact of changes between HBEFA 3.3 and 4.1, HGV TT 34–40t Euro<sup>o</sup>V half loaded, German traffic mix**

	Migration to a new PHEM version	Introduction of HBEFA 4.1 driving cycles	Introduction of HBEFA 4.1 vehicle data	Introduction of HBEFA 4.1 emission data	Total change
FC	1.0%	12.2%	7.4%	-6.0%	14.6%
CO	-0.3%	0.5%	51.8%	12.4%	64.5%
HC	-0.6%	26.6%	-13.0%	6.1%	19.1%
NO <sub>x</sub>	7.2%	46.1%	-19.1%	5.2%	39.5%
PM	-0.5%	8.2%	26.5%	6.0%	40.2%
PN	-0.1%	21.2%	-6.0%	6.9%	22.1%

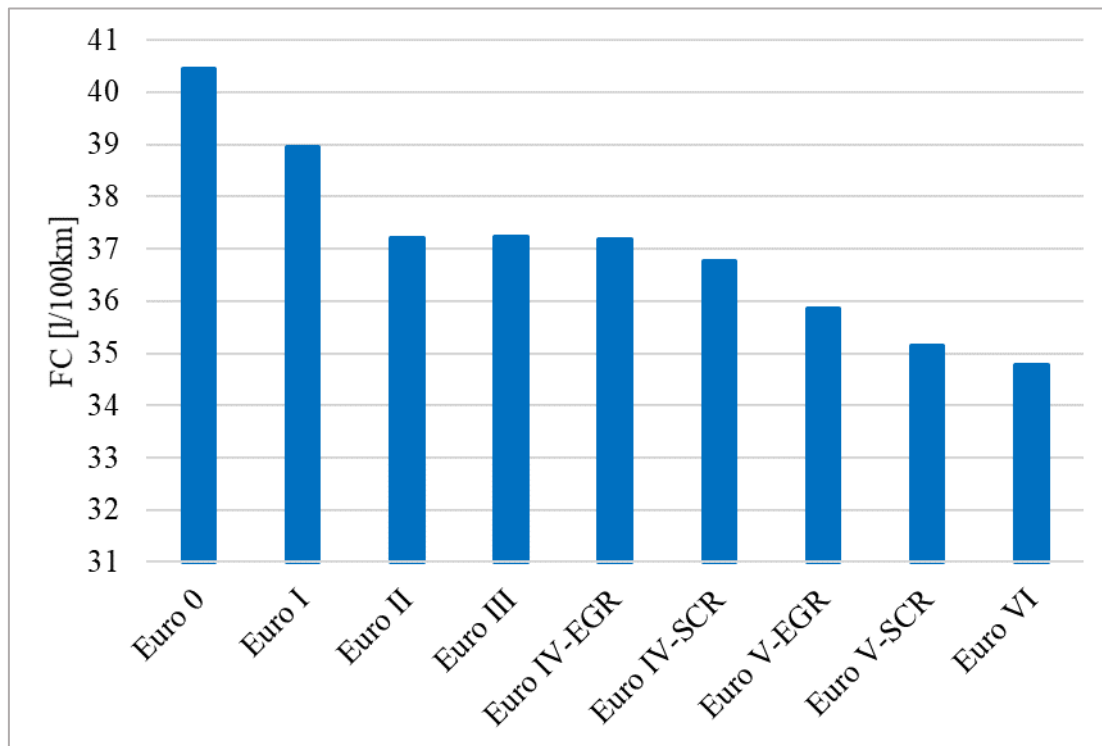
### 8.3 Results HBEFA 4.1

All of the following results correspond to the HBEFA 4.1 emission factors with average weighting for an aggregated German traffic situation, a vehicle mileage of 50 000 km, the year 2015 and half loaded vehicles independent of the vehicle category. Each graph represents the results for the Euro classes 0 to VI.

### 8.3.1 34–40t Tractor Semi-trailer Combination

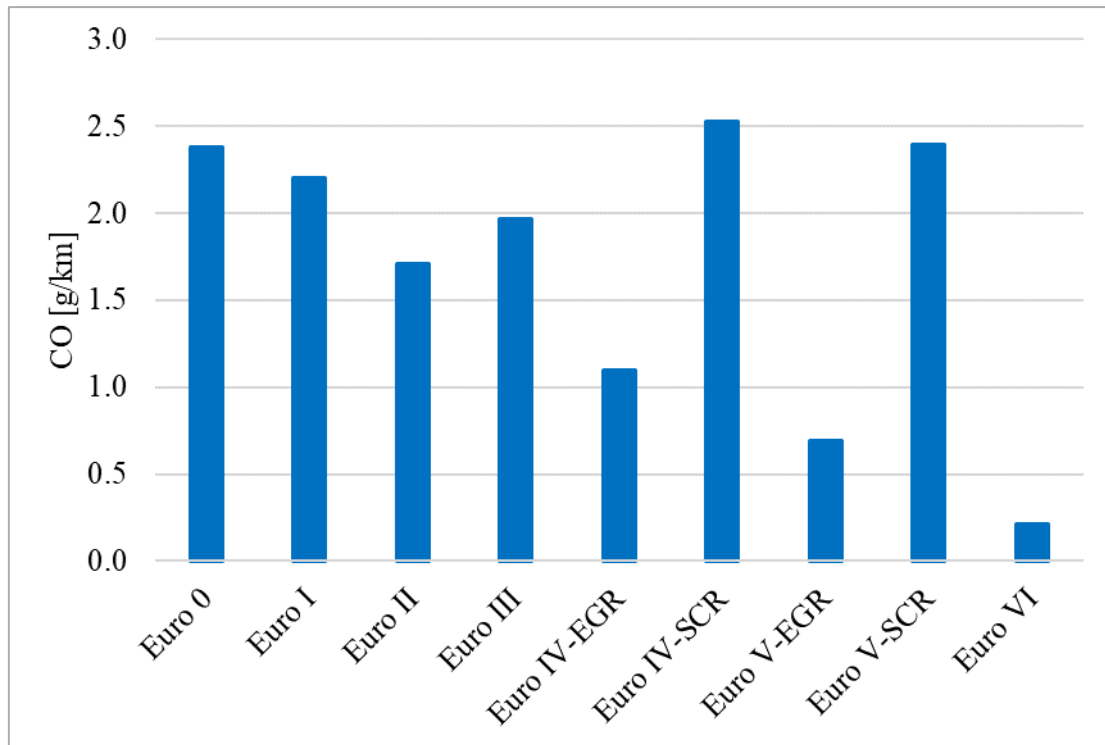
This part focuses on the results of the tractor semi-trailer combination with 34–40t GVM. This category is very representative for HGVs as it has the highest vehicle kilometres travelled of all HGVs [59].

Figure 78 summarizes fuel consumption results for all Euro classes. The technological developments from Euro<sup>0</sup> to Euro<sup>VI</sup> have a positive influence on fuel consumption, but improvements in engine technologies were most significant for Euro<sup>0</sup> to Euro<sup>II</sup> (introduction of turbocharger, charge air cooler, etc.). They lead to a reduction in fuel consumption by approximately 10 %. Due to the continuous reduction of NO<sub>x</sub> emission limits and the introduction of more demanding test procedures, fuel consumption more or less stagnated between Euro<sup>II</sup> and Euro<sup>IV</sup> despite improved vehicle specifications. Technologies used for NO<sub>x</sub> reduction, such as later injection timing or EGR, obviously showed significant negative impact on engine efficiency. The need for an inefficient setting of the combustion parameters was clearly reduced by the introduction of SCR systems from Euro<sup>V</sup> on, since these systems allow higher raw exhaust NO<sub>x</sub> emissions.



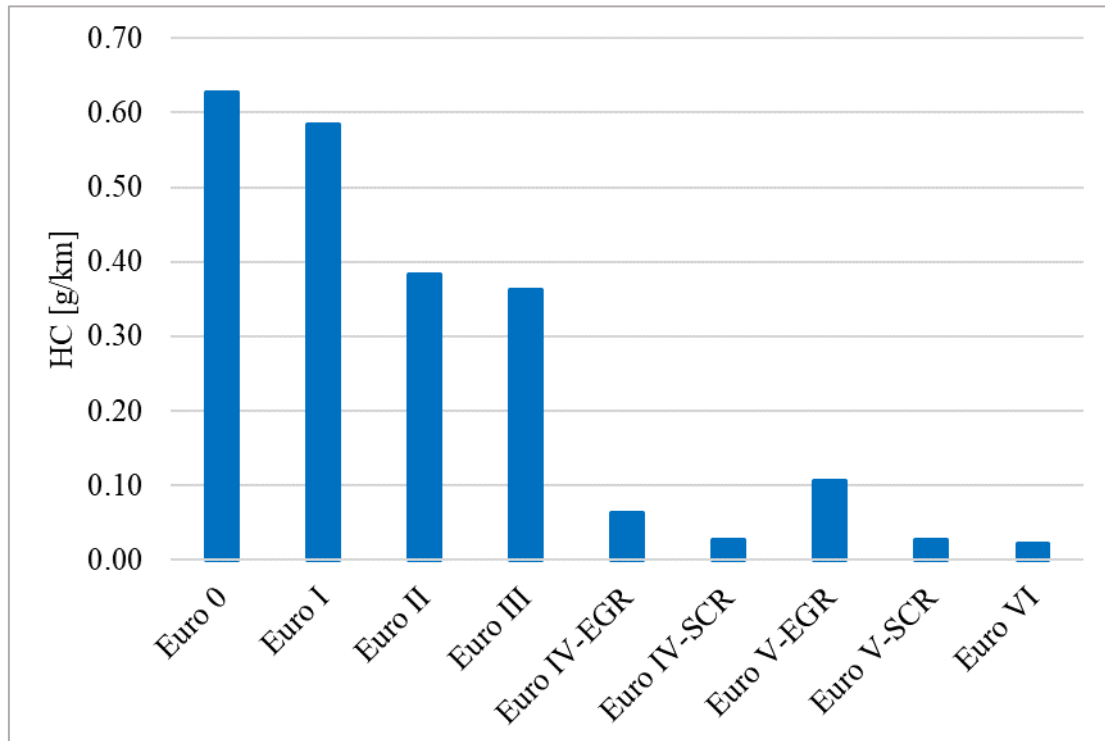
**Figure 78: FC, TT 34–40t half loaded, average German traffic situation, Euro<sup>0</sup> to Euro<sup>VI</sup>**

Figure 79 illustrates the CO results. Further development of engine technologies improved the combustion process and consequently reduced undesired side products as CO. However, the Euro<sup>IV</sup> and V SCR emissions are conspicuous. While EURO<sup>IV</sup> and V with EGR for NO<sub>x</sub> control also had DOCs to maintain HC and CO emissions coming along with low NO<sub>x</sub> combustion settings, the SCR only systems obviously had no efficient DOCs on board on average. This explains the higher CO levels. The stricter limits of Euro<sup>VI</sup> lead to a comprehensive introduction of DOCs and consequently a clear reduction in CO.



**Figure 79: CO, TT 34–40t half loaded, average German traffic situation, Euro<sup>0</sup> to Euro<sup>VI</sup>**

Figure 80 shows the HC emissions. The increase in efficiency of internal combustion engines lead to a reduction of unburned fuel. Consequently, HC emissions decrease with rising Euro classes and are on a very small level with Euro<sup>VI</sup>.



**Figure 80: HC, TT 34–40t half loaded, average German traffic situation, Euro<sup>0</sup> to Euro<sup>VI</sup>**

Figure 81 shows an example for the NO<sub>x</sub> emission factors. NO<sub>x</sub> emissions have constantly decreased over the last years due to stricter limits and the implementation of new test cycles in type approval. EURO<sup>IV</sup> and EURO<sup>V</sup> brought an effective reduction due to a widespread application of SCR catalyts. The introduction of EURO<sup>VI</sup> limits combined with the

introduction of on-road tests leads to an impressive further improvement of the NO<sub>x</sub> emission performance of EURO<sup>o</sup>VI vehicles.

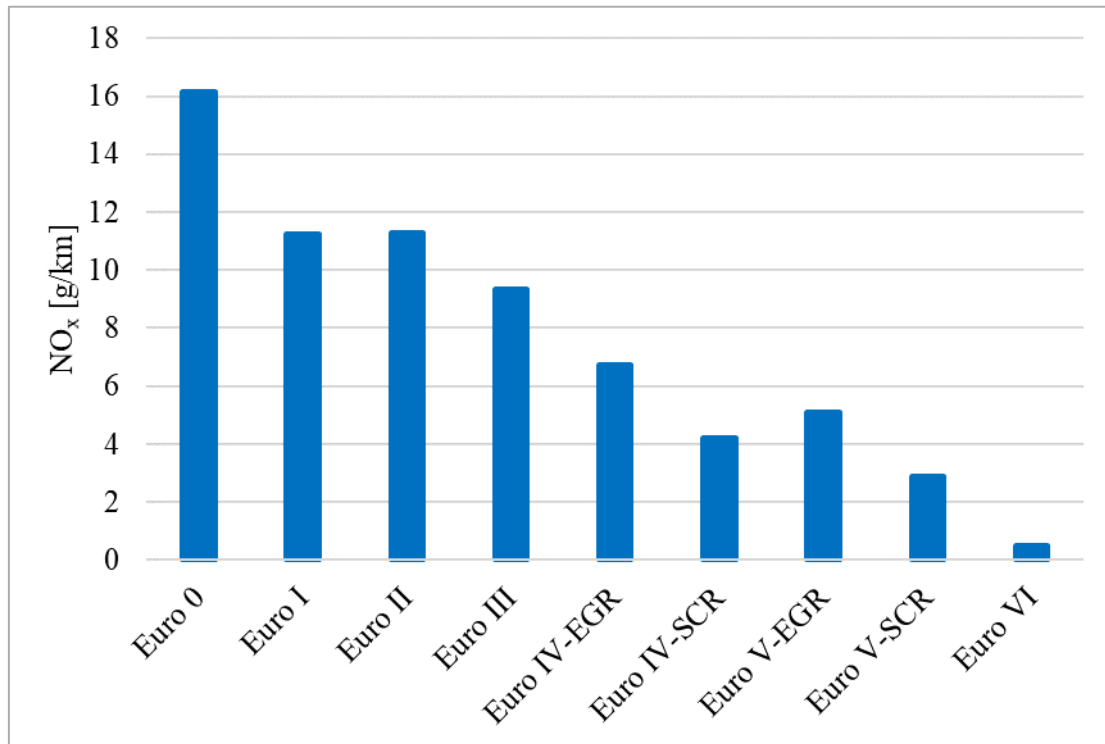


Figure 81: NO<sub>x</sub>, TT 34–40t half loaded, average German traffic situation, Euro<sup>o</sup>0 to Euro<sup>o</sup>VI

Figure 82 shows the development of PN emissions of HBEFA. Up to EURO<sup>o</sup>VI, only PM was limited and thus typically no DPF was installed on HDVs. The introduction of additional PN limits led to the application of DPF for all Diesel driven vehicles and to a decrease in PN emission levels by more than two orders of magnitude.

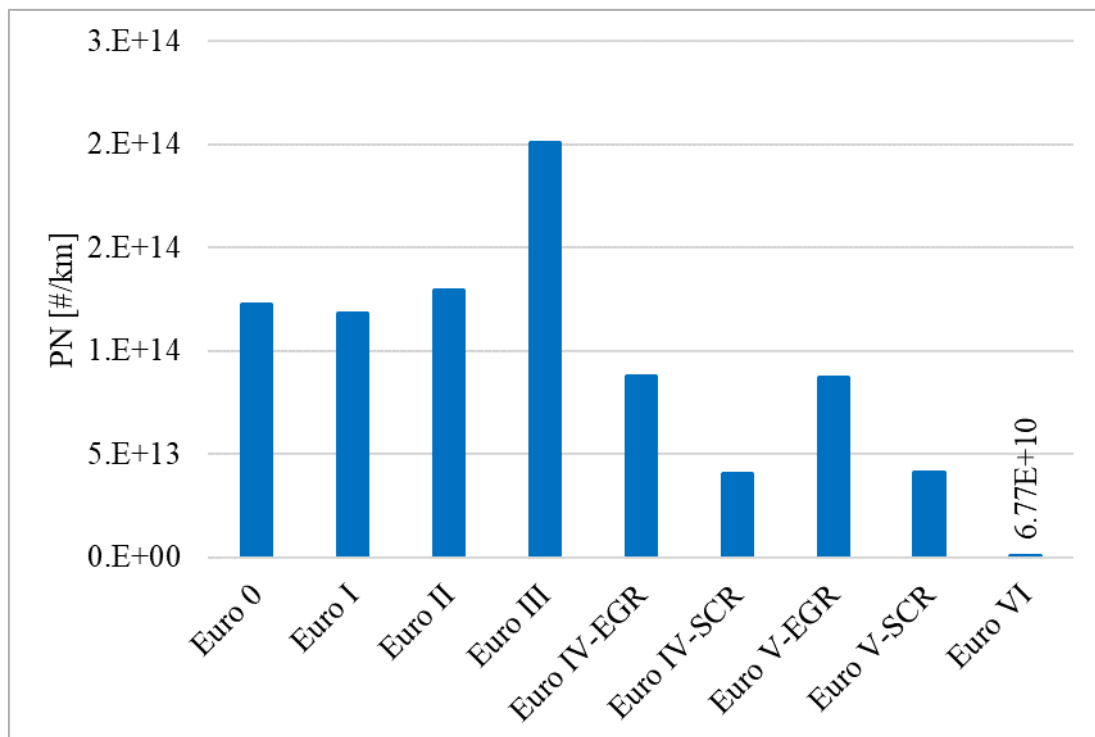
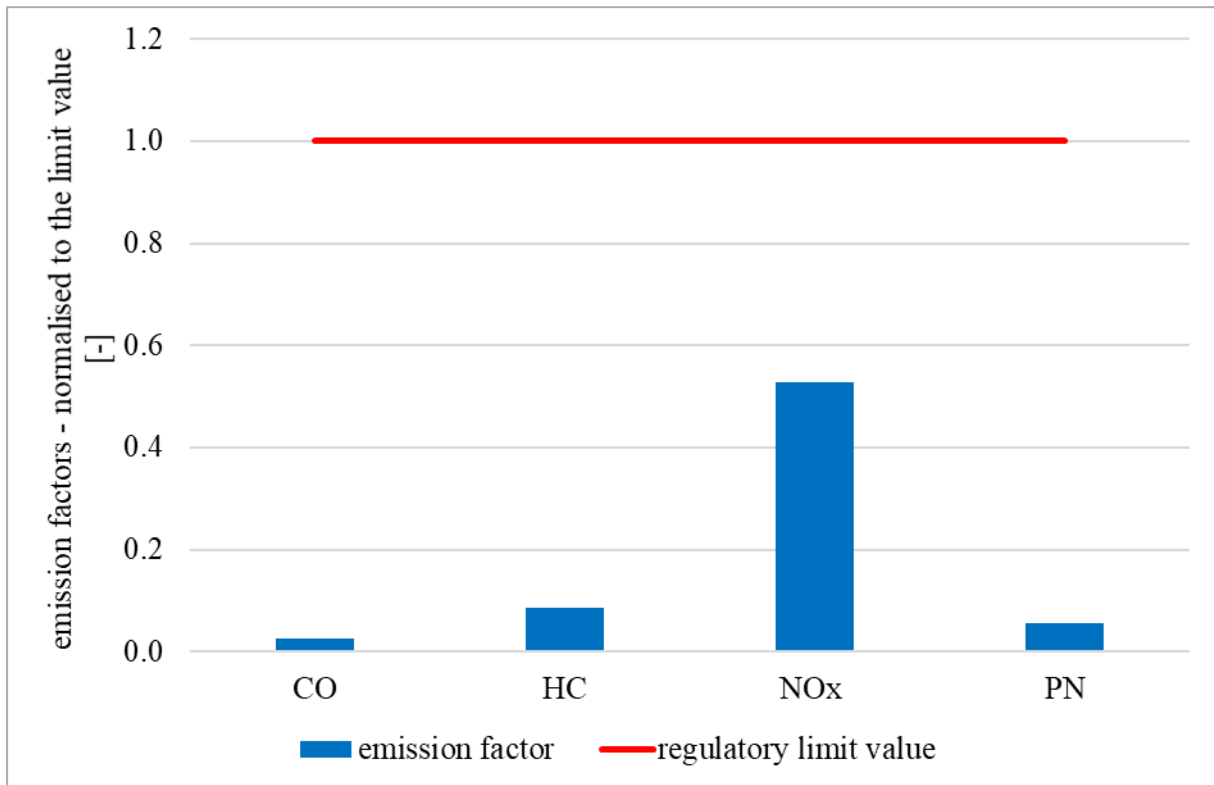


Figure 82: PN, TT 34–40t half loaded, average German traffic situation, Euro<sup>o</sup>0 to Euro<sup>o</sup>VI

Of course, all these values do not have to comply with the regulatory limits for ISC trips; however, an estimation gives a rough idea on how the emissions behave in relation to the limits for Euro<sup>o</sup>VI. The positive work provided by the engine during this aggregated German traffic situation is 54.4 kWh and the trip distance is 40.4 km. This results in a work per distance of 1.35 kWh/km. This value is needed to convert the g/km emission factors into g/kWh values, which are needed for comparison with the work based limits. The estimation in Figure 83 shows that the EFAs are below the limit multiplied with the conformity factor of 1.5 for on-road trips for all emission components in the aggregated German traffic mix. All values in this graph are normalised to their respective limit values (see section 4.3.1) for a comprehensive representation. The absolute values can be found in the annex (see Table 27).



**Figure 83: Comparison of EFAs with ISC regulatory limits, TT 34–40t half loaded, average German traffic situation, Euro<sup>o</sup>VI**

### 8.3.2 < 7.5 Tons Rigid Truck

This section illustrates the main results for the most representative<sup>12</sup> rigid truck, i.e. the one with a GVM below 7.5 tons [59].

Figure 84 and Figure 85 illustrate the FC and NO<sub>x</sub> results. It is conspicuous that Euro classes III to V do not show a decrease in fuel consumption in this category, while tractor trailers showed stagnation up to Euro<sup>o</sup>IV and a decline for Euro<sup>o</sup>V (see Figure 78). NO<sub>x</sub> emissions show the same trend, i.e. an ongoing reduction and a big step with the introduction of Euro<sup>o</sup>VI.

<sup>12</sup> Most representative is related to the driven kilometres per vehicle category.

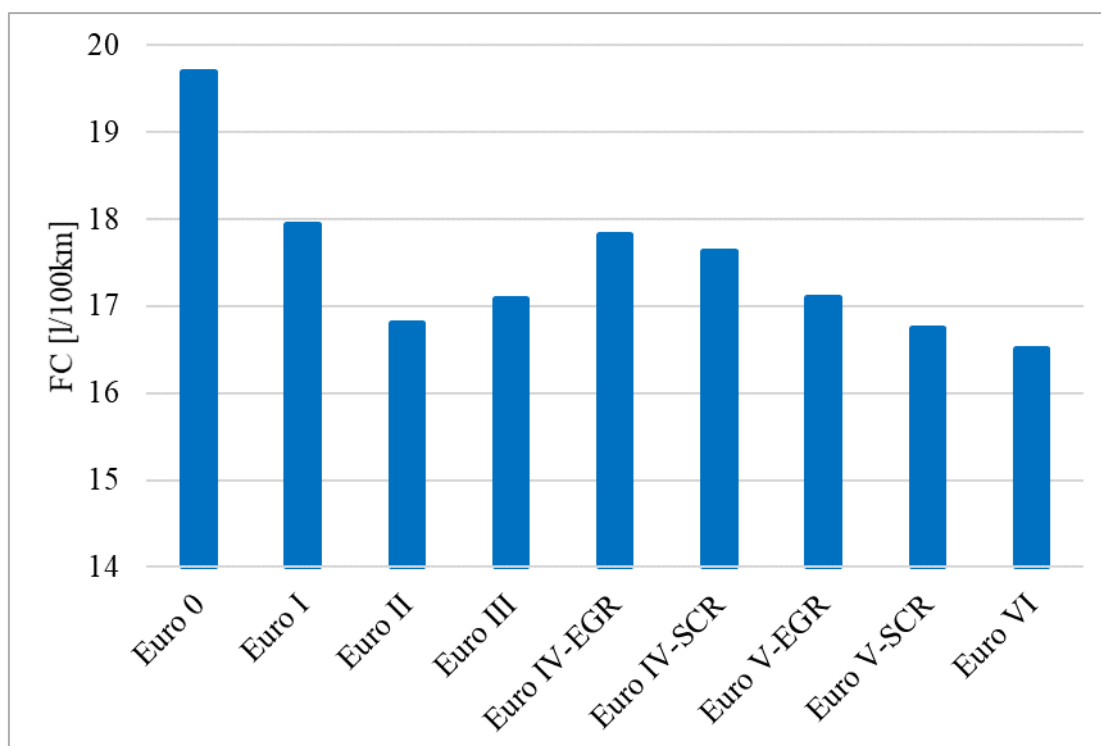


Figure 84: FC, RT < 7.5t half loaded, average German traffic situation, Euro<sup>0</sup> to Euro<sup>VI</sup>

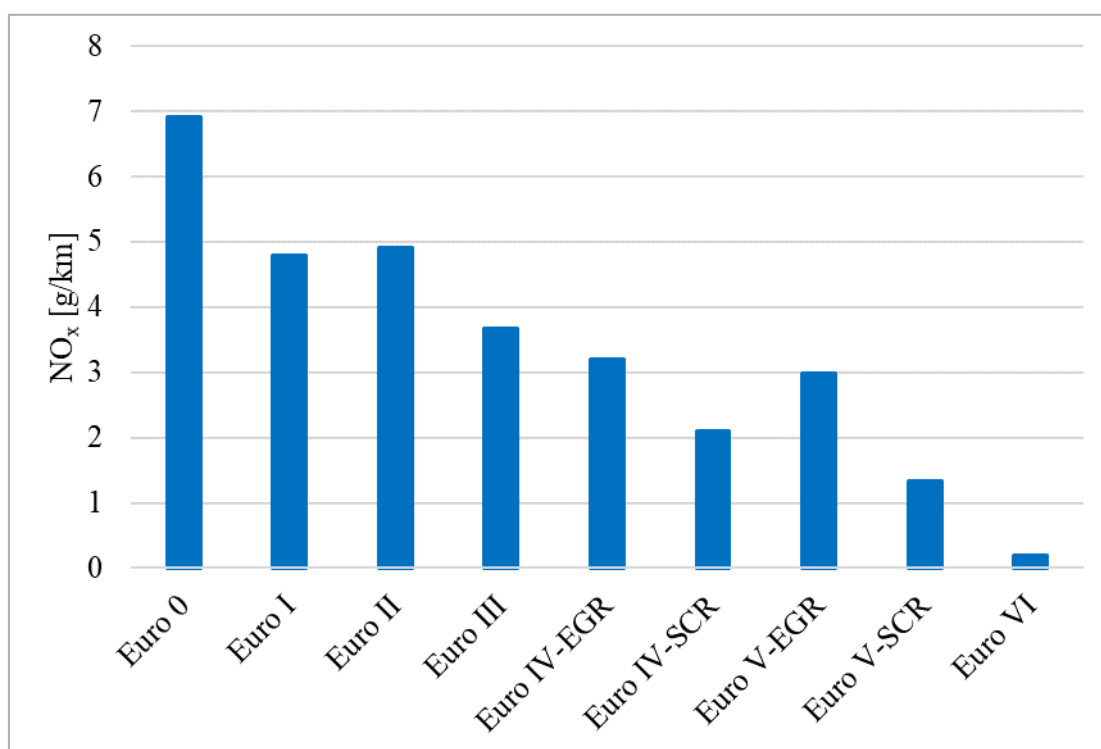


Figure 85: NO<sub>x</sub>, RT < 7.5t half loaded, average German traffic situation, Euro<sup>0</sup> to Euro<sup>VI</sup>

### 8.3.3 Coach

This section illustrates the main results for a 3-axle coach with a GVM higher than 18 tons, the most representative<sup>13</sup> coach category [59]. The decrease in fuel consumption results (see Figure 86) is similar to the one of the tractor trailer. This vehicle category is also designed for

<sup>13</sup> Most representative is related to the driven kilometres per vehicle category.

high kilometre performance and consequently low fuel costs. NO<sub>x</sub> emissions (see Figure 87) are interesting for this vehicle category. Reduction across the different Euro classes is smaller compared to the other vehicle categories, but Euro<sup>o</sup>VI<sup>14</sup> brings a big decrease.

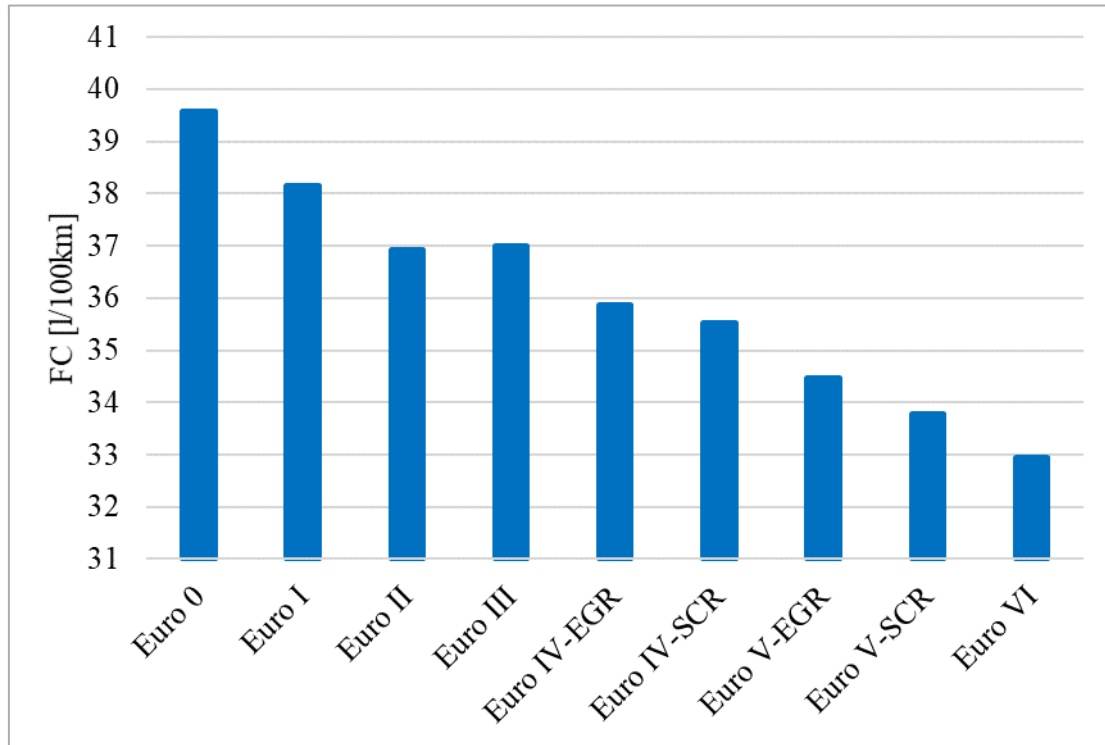


Figure 86: FC, CO > 18t half loaded, average German traffic situation, Euro<sup>o</sup>0 to Euro<sup>o</sup>VI

<sup>14</sup> On average, coaches run on a lower load compared to trucks, because of high rated engine power compared to the relatively small mass, and NO<sub>x</sub> reduction for Euro<sup>o</sup>V and older vehicles is mainly effective in high load conditions. The introduction of Euro<sup>o</sup>VI leads to high conversion rates in a broader range of load conditions.

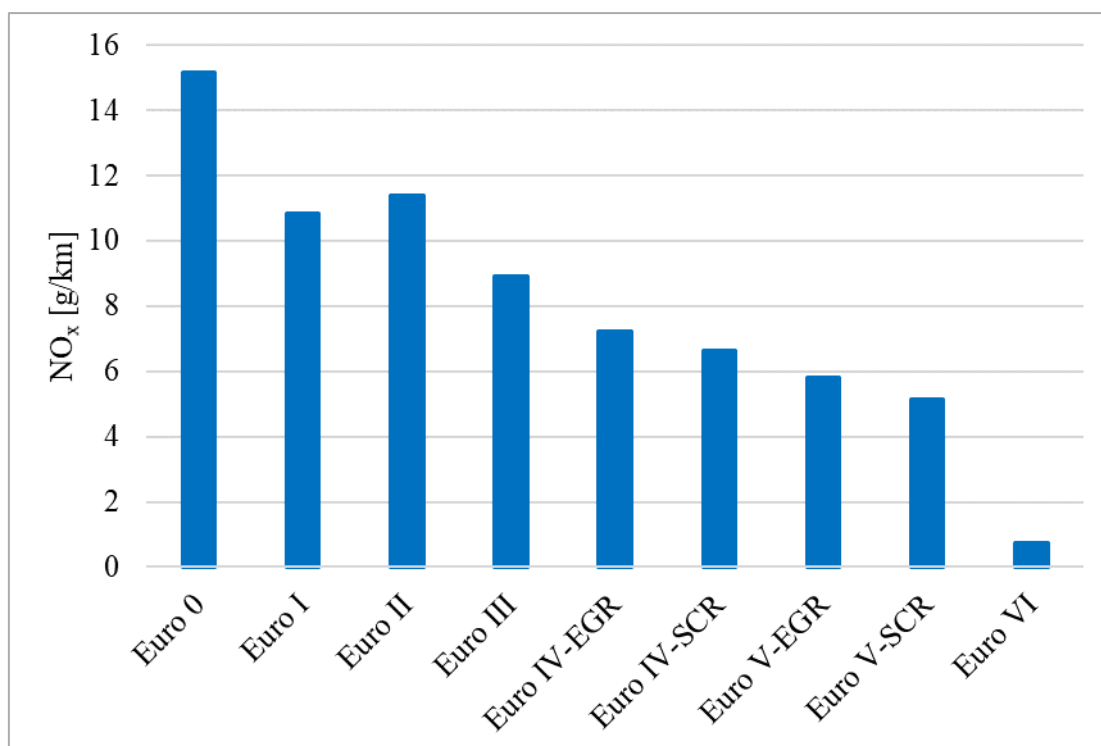


Figure 87: NO<sub>x</sub>, CO > 18t half loaded, average German traffic situation, Euro<sup>0</sup> to Euro<sup>VI</sup>

### 8.3.4 3-Axle City Bus

This part shows results for city busses and illustrates the most relevant emission factors for the 3-axle city bus with a GVM higher than 18 tons.

Figure 88 and Figure 89 show fuel consumption and NO<sub>x</sub> results. This vehicle category also has a constant decline in fuel consumption; however, the absolute values are on a higher level compared to the other categories because of low speed conditions in urban areas. Following the introduction of Euro<sup>VI</sup>, NO<sub>x</sub> emissions dropped significantly again. Special heating strategies increase the temperature in the exhaust after-treatment system and together with improved catalyst technologies lead to an effective NO<sub>x</sub> conversion in the SCR catalyst even in longer low load phases. Regarding typical operating conditions for CBs, this improvement decreases NO<sub>x</sub> emissions compared to EURO<sup>V</sup>, when the catalyst system did not work or at least worked less efficiently in these low load phases.

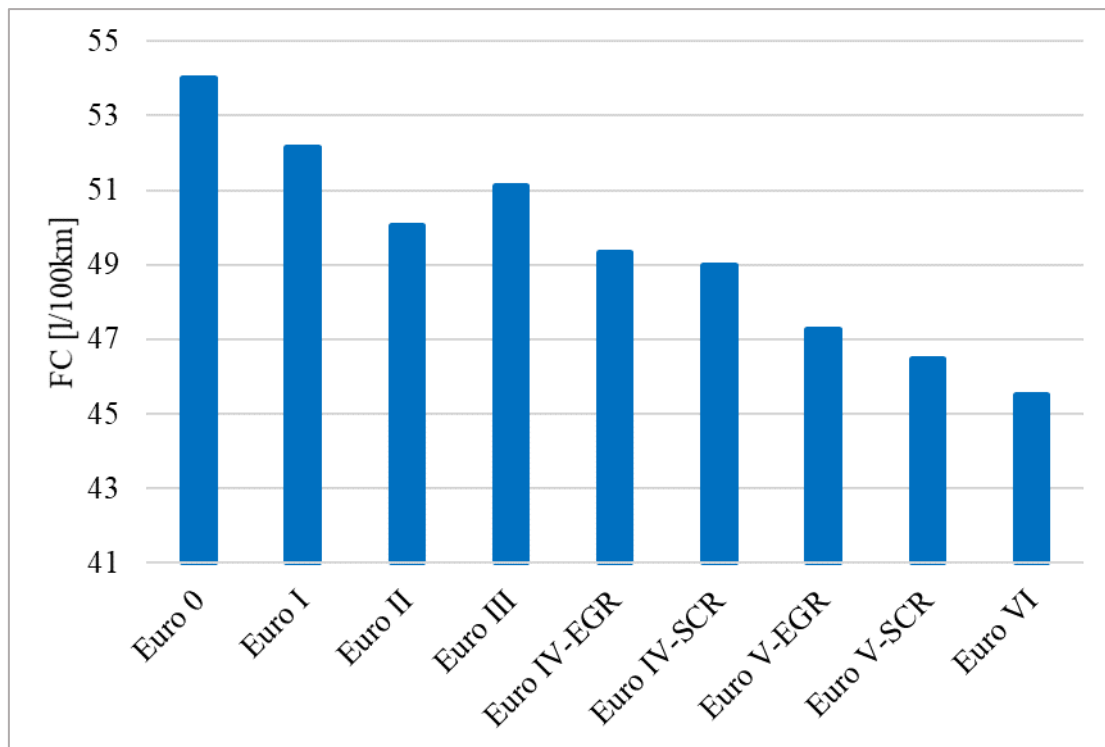


Figure 88: FC, CB > 18t half loaded, average German traffic situation, Euro<sup>0</sup> to Euro<sup>VI</sup>

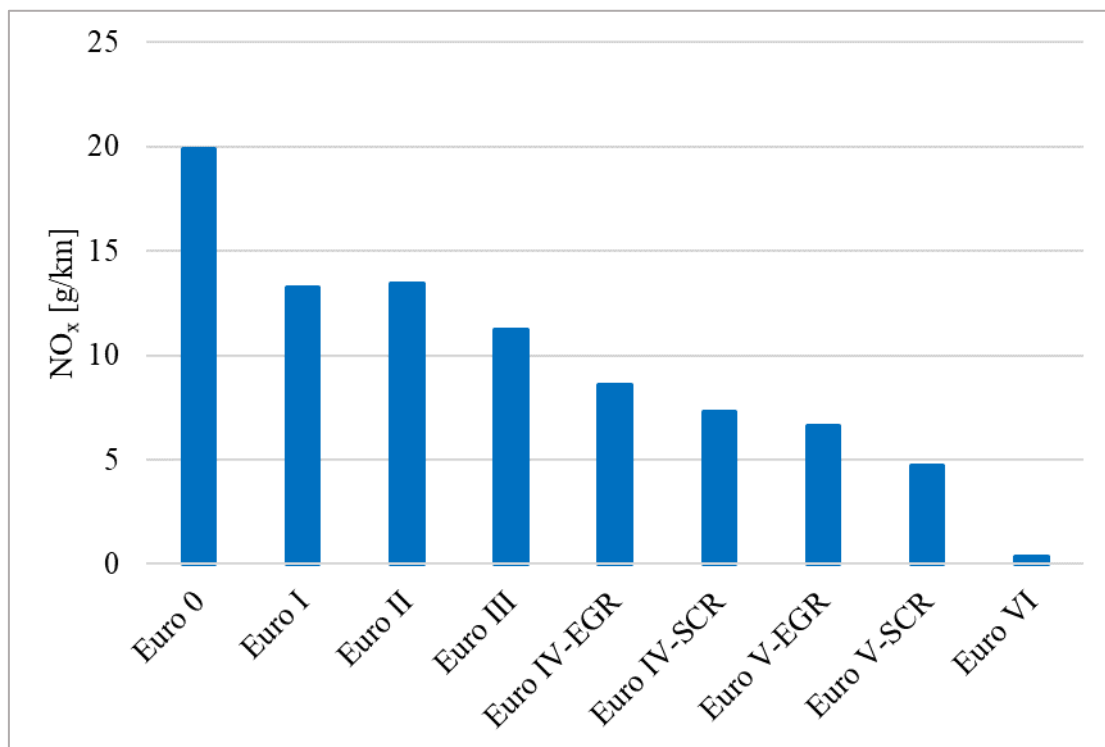


Figure 89: NO<sub>x</sub>, CB > 18t half loaded, average German traffic situation, Euro<sup>0</sup> to Euro<sup>VI</sup>

## 9 Conclusion and Outlook

This thesis describes the development of heavy duty emission factors for the HBEFA 4.1. It covers all work done starting with measurements, continuing with data evaluation and emission model setup, and ending with the final emission factors for heavy good vehicles, coaches and city busses. This chapter summarizes the results achieved in the fields of research questions defined in the ‘objective of work’ part, highlights the most important points, shows the main results and gives a short outlook on the future.

The first research question (How can the emission behaviour in any driving situation be assessed based on a limited number of on-road tests per vehicle?) is answered by combining vehicle emission simulation with a comprehensive design of the measurement program created for the HBEFA 4.1. It covers all relevant driving situations for HDVs by the use of on-road and additional chassis dyno measurements. In-service-conformity tests cover the most relevant real traffic conditions due to the split into urban, rural and motorway sections and, in combination with on-road Stop&Go tests, reflect the vehicles’ real emission behaviour. The chassis dyno tests are mainly used for special driving conditions like heavy Stop&Go and for recording particular pollutant emissions by using FTIR and particle emissions by using CPC. Of course, further advantages of test bench measurements are their repeatability and the possibility to compare vehicles with each other due to repeatable laboratory conditions. This combination of on-road and chassis dyno tests in the measurement program for the HBEFA leads to a comprehensive database for developing single vehicle simulation models. The simulation tool is designed to consider all known relevant effects on real world emission behaviour based on the data gained from the measurement program. The physical approach of the simulation method allows simulating any driving situation. The vehicle selection for the measurements regarding different brands and vehicle categories covers the European HDV fleet reasonably well to assume representative results. Some categories, such as e.g. coaches and light lorries with WLTP certification, so far have been covered by one measured vehicle only.

To answer the second research question (Do the recorded signals from a PEMS system need post-processing to be used as a model input?), an algorithm for comprehensive data evaluation was developed, which allows for the correction of variable gas transport times in the analysis of instantaneous emission measurements. The corrections are performed using a physical model based on measured exhaust mass flow as well as volumes and temperatures in the measurement system. This algorithm was implemented into the software “ERMES tool” which is capable to perform evaluations of measurement data from any kind of emission test systems (diluted from CVS, undiluted from engine dyno or PEMS measurement). The tool now provides methods to correct emission test results for effects of analyser response behaviour and transport times in diluted and undiluted parts of the measurement equipment. Main benefits of the application of the ERMES tool methods are a significantly improved quality of instantaneous emission mass signals regarding temporal allocation to the operation point of engine and exhaust after-treatment. This correction method is also applicable for chassis dyno tests and CVS tunnels. To complement external PEMS data, which most often did not include engine torque information, a new method was applied, which interpolates the engine power from the recorded engine speed and the CO<sub>2</sub> exhaust mass flow. With the help of such a post processing, all PEMS data was integrated into the database of the models.

Stricter limits and test conditions in the HDV emission regulation lead to new challenges for emission reduction systems and consequently to more complex exhaust after-treatment technologies. The simulation model PHEM which is used for the calculation of emission factors for the HBEFA was further developed within this work to overcome these new demands and consequently gives an answer to research question 3 (Can a proper method for

the use of PEMS data be implemented in the vehicle simulation tool PHEM, which in the past was used for the calculation of emission factors?). The SCR simulation part was modified and extended by a model to consider the decrease in NO<sub>x</sub> conversion rates in long low load phases. Heavy Stop&Go measurements on the chassis dyno and in real world conditions showed that this is mainly important for Euro<sup>o</sup>VI vehicles. These low load driving conditions lead to a decrease in temperature in the exhaust system and consequently to a cut off of the AdBlue injection below a certain limit temperature. The model uses the NH<sub>3</sub> stored in the catalyst for further conversion of engine-out NO<sub>x</sub> and thus reduces the ammonia storage level of the SCR. Again, this storage level affects the efficiency of the NO<sub>x</sub> conversion. The NH<sub>3</sub> storage model helps to improve the accuracy of NO<sub>x</sub> emission simulation, especially in low speed phases (e.g. Stop&Go traffic). To set up this model, emission measurements up- and downstream of the catalysts are needed. In order to include also PEMS data without engine-out emission recording in the model, a calibration method was developed which adjusts the SCR conversion maps to meet the fleet's average tailpipe emission levels. With this method, a much broader vehicle sample could be used for the development of the EU average HDV models. Additionally, a new gear shift model for HDVs was installed and increased both the quality of engine speed and emission simulation. This model provides two different gear shift strategies: one for automated manual transmission systems, e.g. trucks, and one for automatic transmission systems, e.g. city busses.

As an input for emission factor simulation of heavy duty vehicles in PHEM, new emission models were developed. For this reason, data made available from the development of the HDV CO<sub>2</sub> certification methods ("VECTO") formed the base for the setup of vehicle models and fuel consumption maps for every emission class. These models are used to calculate the correct engine power and speed to overcome all driving resistances, losses in the powertrain and auxiliary power demands. The engine operating points calculated are the base for fuel consumption and pollutant emission calculation. New pollutant maps were also setup for all relevant emission components by the use of TUG measurement data available for the HBEFA 4.1 for Euro<sup>o</sup>VI vehicles. This data is also used for adjusting the exhaust after-treatment model for the simulation of NO<sub>x</sub> emissions. First, these models were created for single vehicles of all different brands and then they were summarized into one model for average vehicles by the use of the brand specific new vehicle registrations in EU 28 as weighting factors. The final step in the development of these heavy good vehicle emission models was the adjustment to all available measurement data including data of other laboratories.

Research question 4 (Does the simulation of current EURO<sup>o</sup>VI vehicles need additional or different methods to reflect the real world emission behaviour?) can also be affirmed. Since city busses mostly run in urban operating conditions, another model was created for this vehicle category by adapting the general HDV model to appropriate measurement data. Additionally, a deterioration function for NO<sub>x</sub> dependent on the vehicle mileage and emission factors for the non-regulated emission components N<sub>2</sub>O and NH<sub>3</sub> were worked out as well.

A comparison of the final emission factors of the HBEFA 4.1 with the factors of the HBEFA 3.3 shows remarkable differences between the two versions. All models were migrated to the new version of the simulation tool, the vehicle data and the fuel consumption maps were updated and different driving cycles compared to HBEFA 3.3 were used. This results in differences e.g. for Euro<sup>o</sup>V vehicles in fuel consumption of 14.6 %, which can mainly be addressed to changes in vehicle models and the HBEFA 4.1 cycles. Changes in EURO<sup>o</sup>V emissions are smaller compared to Euro<sup>o</sup>VI (NO<sub>x</sub> + 39.5 %, PM + 40.2 %). For Euro<sup>o</sup>VI completely new emission models based on newly available test data were created. This results in an increase in all emission components, e.g. fuel consumption rose by 3.9 %, NO<sub>x</sub> by nearly 160 % and PM even by more than 200 %. To understand these huge changes, it has to be mentioned, that the Euro<sup>o</sup>VI emission factors in the HBEFA 3.3 are on a very low level.

The final HBEFA 4.1 results for a 34–40 tons tractor trailer combination show a reduction in fuel consumption starting from Euro<sup>0</sup> (40.5 l/100km) up to Euro<sup>VI</sup> (34.8 l/100km). Also, all pollutant emission components decreased until they reached Euro<sup>VI</sup>, e.g. NO<sub>x</sub> (Euro<sup>0</sup> = 16.15 g/km, Euro<sup>VI</sup> = 0.49 g/km) and PN (Euro<sup>0</sup> = 1.23 E14 #/km, Euro<sup>VI</sup> = 6.77 E10 #/km). Development across the emission classes is in a similar range for all other HGV and coach categories. These results show that emission reduction technologies have been improved effectively over the last years. City busses behave in an analogical way, but the NO<sub>x</sub> drop between Euro<sup>V</sup> SCR and VI is much bigger compared to the other vehicle categories (15–18t solo city bus: Euro<sup>V</sup> SCR = 6.07 g/km, Euro<sup>VI</sup> = 0.43 g/km). Special heating strategies and improvements in SCR catalysts lead to this big enhancement. All in all, the final Euro<sup>VI</sup> emission factors come along with emission levels below the regulatory limit for every emission component as is also illustrated by the measurements for the HBEFA 4.1.

The HBEFA 4.1 is based on a much broader database compared to all versions before and comes along with a lot of new features for improved emission factor calculation. Nevertheless, there will be some more space for improvements in the next update. The Euro<sup>VI</sup> measurements only comprise data of Euro<sup>VI</sup> A and B vehicles, but meanwhile also Euro<sup>VI</sup> C and D vehicles are on the road and in the future, Euro<sup>VI</sup> step E will enter into force as well. These vehicles also have to be taken into account for future fleet models. Regarding the slim database for coaches and city busses, further measurements would allow for more accurate adjustments of the basic emission model especially for these categories. For now, the exhaust after-treatment simulation model is on a sufficient level according to the requirements of the current fleet; however, in the future the inclusion of an additional simulation of the heating strategy could be necessary for vehicles mainly driven in urban areas (like city busses). Another point is the database for the deterioration functions. The database should also be extended by vehicles used in distribution traffic and by city busses. It is not clear, if there is the same deterioration for such mission profiles. Regarding the non-regulated emission components like NH<sub>3</sub> and N<sub>2</sub>O, more measurement and consequently research work is necessary to develop reliable emission factors.

## References

- [1] Reif, K.: Abgastechnik für Verbrennungsmotoren; Springer Vieweg, Ravensburg, 2015, ISBN 978-3-658-09521-5
- [2] <https://www.umweltbundesamt.de/daten/luft/luftbelastung-in-ballungsraeumen#textpart-1>, last accessed: 20.08.2019
- [3] <https://www.wlw.de/de/inside-business/branchen-insights/fahrzeug-und-luftfahrtbranche/transportwege-im-vergleich>, last accessed: 20.08.2019
- [4] [https://www.umweltbundesamt.at/umweltsituation/verkehr/auswirkungen\\_verkehr/verk\\_treibhausgase/](https://www.umweltbundesamt.at/umweltsituation/verkehr/auswirkungen_verkehr/verk_treibhausgase/), last accessed: 20.08.2019
- [5] [https://www.umweltbundesamt.at/umweltsituation/verkehr/auswirkungen\\_verkehr/verk\\_schadstoffe/stickoxide/](https://www.umweltbundesamt.at/umweltsituation/verkehr/auswirkungen_verkehr/verk_schadstoffe/stickoxide/), last accessed: 20.08.2019
- [6] Bürke, T., Wengenmayer, R.: Erneuerbare Energie: Konzepte für die Energiewende, 3. Auflage; WILEY-VCH, Weinheim, 2012, ISBN-13: 978-3527411085
- [7] Eichseder, H., Klell, M.: Wasserstoff in der Fahrzeugtechnik, Erzeugung, Speicherung, Anwendung; 2. Auflage, Vieweg + Teubner, Graz, 2010, ISBN 978-3-8348-1027-4
- [8] Weller, K., Lipp, S., Röck, M., Matzer, C., Bittermann, A., Hausberger, S.: Real world consumption and emissions from LDVs and HDVs, Frontiers in Mechanical Engineering, section Engine and Automotive Engineering, 2019
- [9] DELPHI, Worldwide emission standards, On and off-highway commercial vehicles, 2018
- [10] COMMISSION REGULATION (EU) No 582/2011
- [11] Merker, G., Teichmann, R.: Grundlagen Verbrennungsmotoren, 7. Auflage, Tetzlaff 2014, ISBN 978-3-658-03194-7
- [12] <https://de.statista.com/themen/735/lastkraftwagen-lkw/>, last accessed: 09.07.2019
- [13] Ladommatos, N., Abdelhalim, S.M., Zhao, H., Hu, Z.: The Dilution, Chemical and Thermal Effects of Exhaust Gas Recirculation on Diesel Engine Emissions – Part 4: Effects of Carbon Dioxide and Water Vapour, SAE Paper 971660, 1997
- [14] Schutting, E., Neureiter, A., Fuchs, C., Schatzberger, T., Klell, M., Eichseder, H., Kammerdiener, T.: Miller- und Atkinson-Zyklus am aufgeladenen Dieselmotor, Motorentchnische Zeitung, 2007/06, 480
- [15] Adolph, D., Lamping, M., Körfer, T., Kolbeck, A.: Variabler Ventiltrieb beim DI-Diesel – Eine neue Funktionalität zur gezielten Steuerung der Ladungsbewegung, Haus der Technik, Aachen, 2009
- [16] Hiroyasu, H., Kadota, T., Arai, M.: Supplementary Comments: Fuel Spray Characterization in Diesel Engines, 1980

- 
- [17] Hoepke, E.: IAA Nutzfahrzeuge in Hannover. MTZ 9, 650–656, 2004
- [18] Koebel, M., Elsener, M., Kleemann, M.: Urea-SCR: a promising technique to reduce NO<sub>x</sub> emissions from automotive diesel engines, *Catalysis Today* 59, 335–345, 2000
- [19] Devadas, M., Kröcher, O., Elsener, M., Wokaun, A., Söger, N., Pfeifer, M., Demel, Y., Mussmann, L.: Influence of NO<sub>2</sub> on the selective catalytic reduction of NO with ammonia over Fe-ZSM5. *Applied Catalysis B: Environmental* 67, 187–196, 2006
- [20] Michelitsch, P.: Simulation von EURO<sup>o</sup>VI schweren Nutzfahrzeugen in Niedriglastzyklen, Master Thesis, Graz University of Technology, 2018
- [21] Mollenhauer, K., Tschöke, H.: *Handbuch Dieselmotoren*; 3. Auflage; Springer-Verlag Berlin Heidelberg, 2007, ISBN 978-3-540-72164-2
- [22] [www.hbefa.net](http://www.hbefa.net), last accessed: 17.06.2019
- [23] Matzer, C., Weller, K., Dippold, M., Lipp, S., Röck, M., Rexeis, M., Hausberger, S.: Update of Emission Factors for HBEFA Version 4.1, Graz University of Technology, 2019
- [24] Hausberger, S., Matzer, C.: Update of Emission Factors for EURO 4, EURO<sup>o</sup>5 and EURO<sup>o</sup>6 Diesel Passenger Cars for the HBEFA Version 3.3, Graz University of Technology, 2017
- [25] Rexeis, M., Hausberger, S., Kühlwein, J., Luz, R.: Update of Emission Factors for EURO<sup>o</sup>5 and EURO<sup>o</sup>6 vehicles for the HBEFA Version 3.2, Final Report; Graz University of Technology, 2013
- [26] Hausberger, S.: Simulation of Real World Vehicle Exhaust Emissions, VKM-THD Mitteilungen Heft/Volume 82, 2003, ISBN 3-901351-74-4
- [27] European Environmental Agency: EMEP/EEA air pollutant emission inventory guidebook 2019, Technical guidance to prepare national emission inventories, Luxembourg 2019, ISBN 978-92-9480-098-5
- [28] Weller, K., Rexeis, M.: Erstellung der Emissionsfaktoren für schwere Nutzfahrzeuge (SNF) für das HBEFA Version 4, Modul 1, Graz, 2016
- [29] Weller, K., Rexeis, M.: Erstellung der Emissionsfaktoren für schwere Nutzfahrzeuge (SNF) für das HBEFA Version 4, Modul 2, Graz, 2017
- [30] Weller, K., Blassnegger, J.: Projekt 91180: Realemissionen aus Fahrzeugen und Maschinen, Los 1, Graz, 2019
- [31] Matzer, C., Weller, K., Opetnik, M., Hausberger, S., Knörr, W., Notter, B.: Feldüberwachung von Kraftfahrzeugen und Aktualisierung des HBEFA, Abschlussbericht, Graz, 2019
- [32] Amendment 3 to UN GTR No. 4 - (ECE/TRANS/180/Add.4/Amend.3)

- [33] Six, C., Silberholz, G. et al.: Development of an exhaust emission and CO<sub>2</sub> measurement test procedure for heavy-duty hybrids (HDH), Vienna University of Technology, 2014
- [34] Amendment 3 to UN GTR No. 4 - (ECE/TRANS/180/Add.4/Amend.3)
- [35] Proposal for a REGULATION OF THE EUROPEAN PARLIAMENT AND OF THE COUNCIL setting CO<sub>2</sub> emission performance standards for new heavy-duty vehicles, Brussels 2018
- [36] <https://www.umweltbundesamt.de/themen/klima-energie/klimaschutz-energiepolitik-in-deutschland/treibhausgas-emissionen/die-treibhausgase>, last accessed: 26.07.2019
- [37] Weller, K., Rexeis, M., Hausberger, S., Zach, B.: A comprehensive evaluation method for instantaneous emission measurements, Transport and Air pollution conference 2016, Lyon
- [38] Garcia, Franco V.: Evaluation and improvement of road vehicle pollutant emission factors based on instantaneous emissions data processing, PhD Thesis, Jaume University, 2014
- [39] Ajtay, D., Weilenmann, M.: Compensation of the Exhaust Gas Transport Dynamics for Accurate Instantaneous Emission Measurements. Environ. Sci. Technol. 2004, 38, 5141-5148
- [40] Geivanidis, S., Samaras, Z.: Development of a dynamic model for the reconstruction of tailpipe emissions from measurements on a constant volume sampling dilution system. Measurement Science and Technology, Volume 19, Number 1. 2007, doi:10.1088/0957-0233/19/1/015404
- [41] Luz, R., Hausberger, S.: User Guide for the Model PHEM, Version 11.2; Graz University of Technology, 2013
- [42] Hausberger, S.: Simulation of Real World Vehicle Exhaust Emissions, Graz University of Technology, VKM-THD Mitteilungen Heft/Volume 82, 2003, ISBN 3-901351-74-4
- [43] Rexeis, M.: Ascertainment of Real World Emissions of Heavy Duty Vehicles, PhD Thesis, Graz University of Technology, 2009
- [44] Matzer, C., Hausberger, S., Lipp, S., Rexeis, M.: A new approach for systematic use of PEMS data in emission simulation, Transport and Air pollution conference 2016, Lyon
- [45] Hausberger, S.: Schadstoffbildung und Emissionsminimierung bei Kfz Teil III SCR, Graz University of Technology, 2012
- [46] Koch, T.: Diesel – eine sachliche Bewertung der aktuellen Debatte, Technische Aspekte und Potenziale zur Emissionsreduzierung, Springer Vieweg, Karlsruhe, 2018, ISBN 978-3-658-22210-9

- 
- [47] Robert Bosch GmbH: Denoxtronic 6-9-Dosiersystem für AdBlue in SCR-Systemen, Stuttgart, 2014.
- [48] Kartusch, S.: Gangschaltmodell für schwere Nutzfahrzeuge, Bachelor Thesis, Graz University of Technology, 2017
- [49] Höfler, M.: Gangschaltmodell für Stadtbusse, Bachelor Thesis, Graz University of Technology, 2019
- [50] Maschinenfabrik Augsburg-Nürnberg (MAN): Fundamentals of commercial vehicle technology, Bonn, 2016, ISBN: 9783781219724
- [51] Luz, R.: Simulationsbasierte Methode zur Zertifizierung der CO2 Emissionen von schweren Nutzfahrzeugen, PhD Thesis, Graz University of Technology, 2015
- [52] Fischer, R., Jürgens, G., Küçükay, F., Najork, R., Pollak, B.: Das Getriebebuch, Springer-Verlag/Wien 2012; ISBN 978-3-7091-0876-5
- [53] <https://www.acea.be/statistics/tag/category/by-manufacturer-registrations>, last accessed: 26.02.2019.
- [54] Rexeis, M., Kies, A.: Ertüchtigung von VECTO zur Berechnung des Energieverbrauches von schweren Nutzfahrzeugen vor Erstzulassung 2018. Graz University of Technology, 2016
- [55] <https://www.youtube.com/watch?v=r18hAgMn6Ag>, last accessed: 31.07.2019
- [56] Rexeis, M., Quaritsch, M., Hausberger, S., Silberholz, G., Kies, A., Steven, H., Goschütz, M., Vermeulen, R.: VECTO tool development: Completion of methodology to simulate Heavy Duty Vehicles' fuel consumption and CO2 emissions, Upgrades to the existing version of VECTO and completion of certification methodology to be incorporated into a Commission legislative proposal. Graz University of Technology, 2017
- [57] Mörth, M.: Analyse laufeleistungsabhängiger Emissionserhöhungen von schweren Nutzfahrzeugen für das HBEFA; Bachelor Thesis, Graz, 2019
- [58] Ericsson, E., Nolinder, E., Persson, A., Steven, H.: Work programme 2016 - 2018 for HBEFA Version 4.1, Report of the work carried out for work package 2, 2019
- [59] HBEFA version 4.1

## Annex

Table 17 gives an overview of the implementation of the different steps of Euro<sup>o</sup>VI. More details regarding the single steps can be found in [10].

**Table 17: Different steps of Euro<sup>o</sup>VI and corresponding amendments for ISC tests**

Euro <sup>o</sup> VI step	Implementation dates: new types	Implementation dates: all vehicles	Power threshold	Cold start and PM number
A, B	31.12.2012	31.12.2013	20 %	-
B	1.9.2014	1.9.2015	20 %	-
C	31.12.2015	31.12.2016	20 %	-
D	1.9.2018	1.9.2019	10 %	-
E	1.1.2021	1.1.2022	10 %	Yes

Table 18 to Table 22 show specifications of all vehicle measurements used for the HBEFA 4.1 and those Euro<sup>o</sup>VI vehicle measurements which were already used in HBEFA 3.3 and are also used in HBEFA 4.1.

**Table 18: Specifications of EURO<sup>o</sup>5 Diesel vehicles used for the emission maps in PHEM**

Laboratory	Make	Model	Vehicle category	Engine capacity [l]	Rated engine power [kW]	Mileage [km]
TUG	Iveco	Daily 72C17	N2	3.0	125	5 000

**Table 19: Specifications of EURO<sup>o</sup>6 Diesel vehicles used for the emission maps in PHEM**

Laboratory	Make	Model	Vehicle category	Engine capacity [l]	Rated engine power [kW]	Mileage [km]
TUG	Iveco	Daily 72C17	N2	3.0	125	2 500

**Table 20: Specifications of EURO<sup>o</sup>VI Diesel vehicles used for the emission maps in PHEM**

Laboratory	Make	Model	Vehicle category	Engine capacity [l]	Rated engine power [kW]	Mileage [km]
TUG	MAN	TGL 12.200	N2	4.6	162	7 500
TUG	Volvo	FL 280	N3	7.7	210	4 500
TUG	Renault	Midlum 240	N2	5.1	177	16 500
TUG	DAF	LF 250	N3	6.7	180	1 100
TUG	Scania	R450	N3	12.7	331	28 000
TUG	Mercedes	Atego 1524	N3	7.7	175	30 000
TUG	Iveco	Eurocargo 75E12	N2	4.5	152	31 000
TUG	Mercedes	Actros 1845 LS	N3	12.8	330	-

Laboratory	Make	Model	Vehicle category	Engine capacity [l]	Rated engine power [kW]	Mileage [km]
TUG	Scania	R LA	N3	12.7	324	-
TUG	Iveco	Stralis	N3	11.0	353	-
TUG	Mercedes	Citaro	M3	10.7	290	-
TUG	Mercedes	Citaro	M3	10.7	290	-
TÜV Nord	Scania	R LA	N3	12.7	353	-
AVL MTC	Mercedes	Antos	N3	10.7	290	112 000
AVL MTC	MAN	TGS 26.440	N3	12.4	324	65 000
AVL MTC	Volvo	FH16	N3	16.1	552	35 400
AVL MTC	MAN	TGM 15.250	N3	6.9	184	50 000
AVL MTC	Volvo	FL	N3	7.7	188	52 000
AVL MTC	Mercedes	Atego	N2	7.7	175	60 000
AVL MTC	Scania	P280	N3	9.3	206	58 000
AVL MTC	Volvo	FH	N3	12.8	345	140 000
AVL MTC	Mercedes	Atego	N2	7.7	175	68 000
AVL MTC	Volvo	FL	N3	7.7	206	53 000
AVL MTC	Volvo	FL	N3	7.7	184	64 500
AVL MTC	DAF	LF210	N2	4.5	157	11 990
AVL MTC	Volvo	FL	N3	7.7	184	110 600
AVL MTC	Mercedes	Atego	N2	7.7	175	72 000
AVL MTC	Scania	R410	N3	12.8	302	20 000
AVL MTC	Scania	R520	N3	16.3	386	35 000
AVL MTC	Mercedes	Atego	N2	7.7	175	15 000
AVL MTC	Scania	R450	N3	12.8	331	-

**Table 21: Specifications of EURO<sup>o</sup>V EEV Diesel vehicles analysed for deterioration effects**

Laboratory	Make	Model	Vehicle category	Engine capacity [l]	Rated engine power [kW]	Mileage [km]
TUG	MAN	TGX 18.480	N3	12.4	353	620 000

**Table 22: Specifications of EURO<sup>o</sup>VI Diesel vehicles used for deterioration function**

Laboratory	Make	Model	Vehicle category	Engine capacity [l]	Rated engine power [kW]	Mileage [km]
TUG	MAN	TGX 18.400	N3	10.5	294	800 000
TUG	Iveco	Stralis AS440S42T/P	N3	11.1	309	500 000
TUG	Mercedes	Actros 1845	N3	12.8	330	535 000

Laboratory	Make	Model	Vehicle category	Engine capacity [l]	Rated engine power [kW]	Mileage [km]
TUG	Scania	R450	N3	12.7	331	500 000

Table 23 shows the WHVC results measured on the chassis dyno at TUG. The results for the regulated emission components were illustrated in Figure 6 and the unregulated ones were summed up in Table 7.

**Table 23: WHVC measurement results – chassis dyno TUG**

Vehicle	Mileage [km]	CO <sub>2</sub> [g/kWh]	CO [g/kWh]	HC [g/kWh]	NO [g/kWh]	NO <sub>x</sub> [g/kWh]	PM [g/kWh]	PN [g/kWh]	N <sub>2</sub> O [g/kWh]	NH <sub>3</sub> [g/kWh]
MAN TGL 12.200	7 500	771.6	0.080	0.000	0.240	0.260	0.004	2.0E11	-	-
Scania R450	28 000	636.7	0.022	0.006	0.613	0.727	0.004	2.7E10	-	-
Renault Midlum	16 500	754.8	0.183	0.001	0.083	0.368	0.000	4.2E10	0.25991	0.00104
DAF LF250	1 100	761.9	0.012	0.065	0.808	0.828	0.007	5.3E11	0.06600	0.02200
MAN TGX	800 000	742.7	0.222	-	1.465	1.607	0.006	6.2E10	0.03848	0.00092
Iveco Stralis	500 000	767.2	1.794	-	1.945	3.024	0.009	1.6E11	0.21008	0.00095
Mercedes Actros	535 000	676.0	0.242	0.002	0.420	0.531	0.001	2.8E10	0.32084	0.00553
Scania R450	500 000	652.9	0.028	0.001	0.948	1.021	0.002	6.8E11	0.08449	0.00585

Table 24 illustrates the single measurement and simulation results for the validation of the different SCR simulation models (see Figure 37 and Figure 40). The measurement program was not identical for every vehicle and consequently the measured cycles are different for each vehicle.

**Table 24: Single NO<sub>x</sub> test and simulation results – validation of SCR simulation models**

Vehicle	Cycle	NO <sub>x</sub> measurement [g/kWh]	NO <sub>x</sub> simulation standard model [g/kWh]	NO <sub>x</sub> simulation NH <sub>3</sub> storage model [g/kWh]
Iveco Daily	ISC	0.53	0.49	0.49
Iveco Daily	Stop&Go – on-road	0.93	0.51	0.61
Renault Midlum	ISC	0.18	0.13	0.58
Renault Midlum	Stop&Go – chassis dyno	4.77	0.15	4.45
DAF LF 250	ISC	0.05	0.07	0.07
DAF LF 250	Stop&Go – chassis dyno	2.07	0.09	1.97
MAN TGL 12.220	ISC	0.11	0.07	0.08
MAN TGL 12.220	Stop&Go – chassis dyno	5.90	1.27	4.87
MB Atego 1524	ISC	0.45	0.37	0.39

Vehicle	Cycle	NO <sub>x</sub> measurement [g/kWh]	NO <sub>x</sub> simulation standard model [g/kWh]	NO <sub>x</sub> simulation NH <sub>3</sub> storage model [g/kWh]
Iveco Eurocargo	ISC	0.58	0.51	0.62
Iveco Eurocargo	Stop&Go – on-road	1.23	0.77	0.80
Scania R450	ISC	0.20	0.21	0.21
Scania R450	Stop&Go – on-road	1.20	0.51	1.71
Scania R450	Stop&Go – chassis dyno	13.27	1.05	10.82
Volvo FL280	ISC	0.11	0.08	0.13
Volvo FL280	Stop&Go – on-road	0.16	0.09	0.65

Figure 90 to Figure 92 show the complete SCR conversion maps, which are used for the final emission factor calculation in the HBEFA 4.1 (see section 7.5.1 to 7.5.3).

NOx conversion	all SV	SV 0.25	SV 0.75	SV 1.25	SV 1.75	SV 2.25	SV 2.75	SV 3.25	SV 3.75	SV 4.25	SV 4.75	SV 5.25	SV 5.75	SV 6.25	SV 6.75	SV 7.25	SV 7.75
all temperatures		81.2%	79.6%	77.4%	76.0%	76.6%	75.0%	74.7%	73.6%	72.4%	71.4%	70.8%	69.7%	69.3%	68.6%	66.8%	65.3%
50	0.0%	0.0%	0.0%	0.0%	0.0%	0.0%	0.0%	0.0%	0.0%	0.0%	0.0%	0.0%	0.0%	0.0%	0.0%	0.0%	0.0%
90	40.7%	53.0%	50.8%	50.2%	50.0%	48.6%	46.1%	43.8%	41.6%	39.6%	37.6%	35.7%	33.9%	32.2%	30.6%	29.1%	27.6%
110	46.8%	62.2%	58.1%	54.0%	51.7%	51.1%	50.7%	50.3%	50.0%	48.8%	46.2%	43.7%	41.2%	38.8%	36.5%	34.2%	32.0%
130	52.1%	77.3%	73.1%	62.6%	56.3%	55.5%	52.4%	51.5%	50.6%	50.1%	50.0%	48.6%	46.5%	44.4%	41.7%	37.9%	35.7%
150	58.6%	98.5%	95.8%	95.8%	95.9%	93.3%	93.3%	93.5%	92.0%	91.0%	90.3%	90.2%	90.0%	89.9%	87.0%	81.6%	79.4%
170	61.4%	99.3%	96.1%	96.1%	96.7%	94.4%	94.4%	94.5%	94.2%	92.5%	91.3%	91.3%	90.9%	90.5%	90.1%	85.3%	83.1%
190	68.0%	99.5%	95.7%	92.7%	92.7%	90.4%	85.4%	85.1%	83.6%	80.3%	78.3%	76.8%	72.7%	72.7%	71.5%	68.6%	66.4%
210	73.7%	94.8%	94.6%	94.0%	92.7%	88.7%	78.5%	77.4%	78.2%	73.2%	71.2%	73.2%	67.8%	63.3%	59.6%	54.6%	51.5%
230	78.2%	99.7%	94.0%	90.3%	93.7%	90.7%	90.1%	88.5%	76.9%	77.5%	74.4%	73.2%	67.8%	63.3%	59.6%	56.7%	54.4%
250	82.3%	98.7%	96.2%	92.0%	94.1%	94.8%	93.7%	91.8%	90.5%	79.0%	78.0%	77.8%	71.6%	66.4%	65.3%	65.2%	61.4%
270	88.7%	97.7%	95.4%	93.8%	98.0%	96.0%	95.6%	95.7%	93.5%	90.7%	81.9%	82.8%	83.0%	83.1%	83.3%	77.2%	71.7%
290	93.4%	96.7%	94.5%	92.4%	93.2%	94.9%	96.6%	94.4%	93.5%	94.1%	94.6%	95.1%	95.7%	94.0%	95.3%	87.8%	81.0%
310	95.6%	95.7%	95.5%	95.3%	98.9%	97.8%	96.6%	96.8%	95.4%	92.5%	91.4%	94.0%	92.2%	98.5%	98.0%	96.5%	95.0%
330	96.4%	94.7%	96.5%	98.2%	97.7%	97.2%	96.0%	97.9%	96.6%	96.9%	97.1%	93.0%	92.1%	97.5%	98.0%	96.8%	95.4%
350	97.2%	93.8%	94.6%	96.3%	95.6%	96.7%	99.6%	98.9%	97.4%	97.8%	98.2%	98.1%	97.9%	98.0%	98.7%	97.2%	95.8%
370	97.1%	92.8%	92.7%	94.4%	93.9%	96.1%	98.1%	98.2%	98.3%	98.4%	98.6%	98.8%	99.0%	98.9%	98.8%	98.7%	98.6%
390	96.6%	91.9%	91.0%	92.6%	92.1%	95.0%	96.5%	98.2%	98.3%	98.4%	98.6%	98.8%	99.0%	98.9%	98.8%	98.7%	98.6%
410	96.1%	91.0%	89.2%	90.8%	90.3%	95.0%	95.0%	98.2%	98.3%	98.4%	98.6%	98.8%	99.0%	98.9%	98.8%	98.7%	98.6%
430	87.1%	82.7%	81.3%	82.6%	82.2%	86.2%	86.1%	88.8%	88.9%	89.0%	89.2%	89.4%	89.5%	89.4%	89.4%	89.3%	89.2%
450	79.4%	75.7%	74.5%	75.6%	75.3%	78.6%	78.6%	80.9%	81.0%	81.1%	81.2%	81.4%	81.5%	81.4%	81.4%	81.3%	81.2%
470	73.0%	69.9%	68.9%	69.8%	69.5%	72.3%	72.3%	74.2%	74.3%	74.4%	74.5%	74.6%	74.7%	74.6%	74.6%	74.5%	74.5%
490	67.0%	65.0%	64.2%	64.9%	64.7%	67.0%	67.0%	68.7%	68.7%	68.7%	68.8%	68.9%	69.0%	68.9%	68.9%	68.8%	68.8%
510	63.1%	61.0%	60.3%	61.0%	60.8%	62.7%	62.7%	64.0%	64.0%	64.1%	64.2%	64.3%	64.3%	64.3%	64.2%	64.2%	64.2%
530	59.5%	57.8%	57.3%	57.8%	57.6%	59.1%	59.1%	60.2%	60.2%	60.3%	60.3%	60.4%	60.4%	60.4%	60.4%	60.4%	60.3%

Figure 90: SCR conversion map – Euro<sup>o</sup>VI HGV

all temperatures	NOx conversion	all SV	SCR conversion map – Euro <sup>o</sup> VI CBs														
			SV 0.25	SV 0.75	SV 1.25	SV 1.75	SV 2.25	SV 2.75	SV 3.25	SV 3.75	SV 4.25	SV 4.75	SV 5.25	SV 5.75	SV 6.25	SV 6.75	SV 7.25
50	0.0%	82.5%	81.4%	79.8%	78.8%	79.2%	78.0%	77.6%	76.7%	76.2%	75.7%	75.3%	74.8%	74.4%	73.4%	71.2%	68.9%
90	40.7%	53.0%	50.8%	50.2%	50.0%	48.6%	46.1%	43.8%	41.6%	39.6%	37.6%	35.7%	33.9%	32.2%	30.6%	29.1%	27.6%
110	46.8%	62.2%	58.1%	54.0%	51.7%	51.1%	50.7%	50.3%	50.0%	48.8%	46.2%	43.7%	41.2%	38.8%	36.5%	34.2%	32.0%
130	52.1%	77.3%	73.1%	62.6%	56.3%	55.5%	52.4%	51.5%	50.6%	50.1%	50.0%	48.6%	46.5%	44.4%	41.7%	37.9%	35.7%
150	58.6%	98.5%	95.8%	75.9%	63.9%	63.3%	55.3%	53.5%	52.0%	51.0%	50.3%	50.2%	50.0%	49.9%	47.0%	41.6%	39.4%
170	76.5%	97.9%	97.0%	92.8%	88.8%	88.3%	82.8%	82.8%	74.9%	74.4%	72.1%	72.1%	72.0%	63.8%	62.1%	58.4%	55.9%
190	84.0%	96.9%	95.8%	94.9%	92.0%	91.0%	86.9%	86.7%	80.9%	79.9%	79.3%	78.9%	77.6%	77.6%	77.3%	75.1%	72.5%
210	85.1%	97.6%	96.2%	95.2%	95.2%	94.7%	90.9%	91.4%	81.8%	80.3%	79.7%	76.0%	74.9%	79.2%	78.5%	76.1%	73.2%
230	89.9%	98.3%	96.6%	95.5%	97.5%	96.9%	95.8%	96.1%	92.3%	91.9%	90.8%	90.5%	88.9%	87.5%	85.9%	83.3%	80.3%
250	93.8%	98.9%	98.2%	96.9%	97.6%	98.0%	97.9%	97.1%	96.8%	93.1%	92.3%	92.9%	91.5%	89.8%	89.5%	87.4%	83.4%
270	95.7%	98.0%	97.3%	96.8%	98.6%	98.4%	98.4%	97.7%	96.7%	94.3%	94.3%	94.6%	94.9%	94.7%	95.0%	91.1%	86.6%
290	97.3%	99.0%	98.4%	96.6%	97.4%	98.1%	98.6%	98.0%	97.8%	98.0%	98.2%	98.3%	98.7%	98.1%	98.6%	94.2%	89.4%
310	98.2%	98.7%	98.7%	98.6%	99.7%	99.3%	99.0%	99.0%	98.6%	97.7%	97.4%	98.2%	98.7%	98.5%	99.4%	96.8%	93.6%
330	98.5%	98.4%	98.9%	99.5%	99.3%	99.2%	98.8%	99.4%	99.0%	99.1%	99.1%	97.9%	97.6%	99.3%	99.4%	97.0%	93.7%
350	98.7%	98.1%	98.4%	98.9%	98.7%	99.0%	99.9%	99.7%	99.2%	99.4%	99.5%	99.4%	99.4%	99.4%	99.6%	97.1%	93.8%
370	98.7%	97.8%	97.8%	98.3%	98.2%	98.8%	99.4%	99.5%	99.5%	99.5%	99.6%	99.6%	99.7%	99.7%	99.6%	97.5%	94.7%
390	96.5%	95.5%	95.2%	95.7%	95.5%	96.6%	96.9%	97.4%	97.4%	97.4%	97.5%	97.5%	97.6%	97.6%	97.5%	95.5%	92.7%
410	93.5%	92.4%	91.9%	92.3%	92.2%	93.6%	93.6%	94.6%	94.6%	94.6%	94.7%	94.7%	94.8%	94.8%	94.7%	92.8%	90.1%
430	88.7%	87.8%	87.4%	87.8%	87.7%	88.8%	88.8%	89.7%	89.7%	89.7%	89.8%	89.8%	89.9%	89.8%	89.8%	87.9%	85.4%
450	79.5%	78.7%	78.4%	78.7%	78.6%	79.6%	79.6%	80.3%	80.3%	80.3%	80.4%	80.4%	80.4%	80.4%	80.4%	78.7%	76.4%
470	73.0%	69.9%	68.9%	69.8%	69.5%	72.3%	72.3%	74.2%	74.2%	74.4%	74.5%	74.6%	74.7%	74.6%	74.6%	74.5%	74.8%
490	67.6%	65.0%	64.2%	64.9%	64.7%	67.0%	67.0%	68.6%	68.7%	68.7%	68.8%	68.9%	69.0%	68.9%	68.9%	68.9%	68.5%
510	63.1%	61.0%	60.3%	61.0%	60.8%	62.7%	62.7%	64.0%	64.0%	64.1%	64.2%	64.2%	64.3%	64.3%	64.2%	64.2%	64.2%
530	59.5%	57.8%	57.3%	57.8%	57.6%	59.1%	59.1%	60.2%	60.2%	60.3%	60.3%	60.4%	60.4%	60.4%	60.4%	60.4%	60.3%

Figure 91: SCR conversion map – Euro<sup>o</sup>VI CBs

NOx conversion	all SV	SCR conversion map – Euro <sup>o</sup> VI HGV < 7.5 tons																	
		SV 0.25	SV 0.75	SV 1.25	SV 1.75	SV 2.25	SV 2.75	SV 3.25	SV 3.75	SV 4.25	SV 4.75	SV 5.25	SV 5.75	SV 6.25	SV 6.75	SV 7.25	SV 7.75	8.25	9.75
all temperatures		81.0%	79.1%	78.5%	77.7%	76.4%	76.8%	75.8%	74.9%	74.8%	73.3%	71.6%	71.3%	70.9%	71.1%	68.6%	67.1%	65.8%	62.2%
50	0.0%	0.0%	0.0%	0.0%	0.0%	0.0%	0.0%	0.0%	0.0%	0.0%	0.0%	0.0%	0.0%	0.0%	0.0%	0.0%	0.0%	0.0%	0.0%
90	42.1%	53.0%	50.8%	50.5%	50.2%	50.0%	48.6%	47.3%	46.1%	43.8%	41.6%	39.6%	38.6%	37.6%	35.7%	33.9%	32.2%	31.4%	27.6%
110	48.4%	62.2%	58.1%	56.1%	54.0%	51.7%	51.1%	50.9%	50.7%	50.3%	50.0%	48.8%	47.5%	46.2%	43.7%	41.2%	38.8%	37.6%	32.0%
130	53.9%	77.3%	73.1%	67.8%	62.6%	56.3%	55.5%	54.0%	52.4%	51.5%	50.6%	50.1%	50.1%	50.0%	48.6%	46.5%	44.4%	43.1%	35.7%
150	60.7%	98.5%	95.8%	85.9%	75.9%	63.9%	63.3%	59.3%	55.3%	53.5%	52.0%	51.0%	50.6%	50.3%	50.2%	50.0%	49.9%	48.5%	39.4%
170	68.2%	97.5%	92.6%	88.6%	84.7%	74.4%	76.0%	70.1%	67.2%	63.8%	62.0%	60.6%	60.6%	60.1%	59.9%	57.9%	55.7%	53.5%	43.1%
190	73.1%	97.6%	95.0%	92.2%	91.6%	85.3%	81.3%	77.2%	76.5%	69.4%	68.0%	65.7%	65.6%	64.9%	64.0%	59.3%	57.3%	54.8%	50.1%
210	77.3%	94.9%	92.7%	92.7%	91.7%	88.8%	87.4%	82.0%	80.3%	77.4%	77.6%	74.1%	74.2%	73.6%	69.1%	64.3%	60.2%	57.3%	51.5%
230	80.8%	98.4%	93.0%	93.0%	91.4%	90.6%	90.6%	90.1%	88.1%	84.6%	76.7%	76.9%	76.9%	76.0%	75.8%	69.5%	64.4%	61.1%	54.4%
250	83.8%	97.4%	94.8%	94.3%	93.5%	94.5%	94.8%	93.1%	89.0%	91.4%	86.1%	78.0%	78.8%	78.7%	79.3%	72.2%	66.6%	64.1%	61.4%
270	88.8%	95.9%	94.8%	94.8%	94.7%	97.8%	96.7%	95.9%	94.7%	95.3%	91.3%	88.4%	81.5%	81.5%	83.0%	79.8%	77.6%	75.4%	71.7%
290	91.7%	96.5%	94.0%	93.4%	93.7%	94.6%	95.1%	96.0%	95.8%	93.9%	93.9%	90.9%	94.3%	90.1%	91.6%	88.2%	84.9%	83.0%	81.0%
310	92.8%	95.3%	94.9%	95.4%	95.0%	97.8%	97.7%	97.0%	96.0%	96.6%	94.5%	90.2%	90.2%	88.8%	90.7%	86.2%	80.1%	89.7%	85.0%
330	93.5%	94.6%	94.4%	94.4%	96.6%	97.3%	97.3%	96.3%	94.5%	96.4%	93.6%	90.9%	92.4%	95.1%	91.4%	91.0%	90.9%	87.5%	85.0%
350	94.0%	94.0%	93.3%	93.3%	95.6%	95.3%	93.9%	94.9%	96.2%	97.5%	95.3%	93.9%	92.3%	94.2%	98.5%	91.7%	91.8%	92.1%	85.0%
370	93.9%	93.4%	92.3%	92.3%	94.1%	94.7%	95.4%	97.0%	96.6%	98.1%	96.5%	94.0%	93.0%	92.8%	96.0%	95.8%	91.8%	87.8%	85.0%
390	92.7%	92.8%	91.3%	91.3%	93.0%	93.5%	93.0%	96.7%	97.2%	97.4%	95.7%	93.2%	90.3%	91.4%	95.1%	90.8%	88.7%	86.6%	85.0%
410	92.1%	92.2%	90.3%	91.8%	92.4%	96.1%	96.1%	96.0%	97.2%	97.1%	95.7%	93.2%	90.4%	91.4%	95.2%	88.6%	87.1%	85.6%	85.0%
430	86.5%	82.7%	81.3%	81.9%	82.2%	86.2%	86.1%	86.1%	86.1%	88.8%	88.9%	89.0%	89.1%	89.2%	89.4%	89.5%	89.4%	89.4%	85.0%
450	79.1%	75.7%	74.5%	75.1%	75.6%	78.6%	78.6%	78.6%	78.6%	80.9%	81.0%	81.1%	81.2%	81.2%	81.4%	81.5%	81.4%	81.4%	81.2%
470	72.7%	69.9%	68.9%	69.3%	69.8%	72.3%	72.3%	72.3%	72.3%	74.2%	74.3%	74.4%	74.5%	74.5%	74.6%	74.7%	74.6%	74.6%	74.5%
490	67.4%	65.0%	64.2%	64.6%	64.9%	67.0%	67.0%	67.0%	67.0%	68.0%	68.7%	68.7%	68.8%	68.8%	68.9%	69.0%	69.0%	69.0%	68.8%
510	63.0%	61.0%	60.3%	60.7%	60.8%	62.7%	62.7%	62.7%	62.7%	64.0%	64.0%	64.1%	64.2%	64.2%	64.3%	64.3%	64.3%	64.3%	64.2%
530	59.4%	57.8%	57.3%	57.8%	57.6%	59.1%	59.1%	59.1%	59.1%	60.2%	60.2%	60.3%	60.3%	60.3%	60.4%	60.4%	60.4%	60.4%	60.3%

Figure 92: SCR conversion map – Euro<sup>o</sup>VI HGV < 7.5 tons

Table 25 shows the NO<sub>x</sub> results for the ISC route “Ries” for all Euro<sup>o</sup>VI and Euro<sup>o</sup>6 vehicles measured on this route. These results were illustrated in Figure 63.

**Table 25: Single test NO<sub>x</sub> ISC-Ries results – comparison Euro<sup>o</sup>6 and Euro<sup>o</sup>VI**

Vehicle	Cycle	Euro class	NO <sub>x</sub> [g/kWh]
Iveco Daily	ISC-Ries	Euro <sup>o</sup> 6	0.846
Iveco Daily	ISC-Ries	Euro <sup>o</sup> 6	0.666
Renault Midlum	ISC-Ries	Euro <sup>o</sup> VI	0.180
Renault Midlum	ISC-Ries	Euro <sup>o</sup> VI	0.100
DAF LF 250	ISC-Ries	Euro <sup>o</sup> VI	0.052
DAF LF 250	ISC-Ries	Euro <sup>o</sup> VI	0.106
MAN TGL 12.220	ISC-Ries	Euro <sup>o</sup> VI	0.153
MAN TGL 12.220	ISC-Ries	Euro <sup>o</sup> VI	0.045
MB Atego 1524	ISC-Ries	Euro <sup>o</sup> VI	0.403
MB Atego 1524	ISC-Ries	Euro <sup>o</sup> VI	0.419
Iveco Eurocargo	ISC-Ries	Euro <sup>o</sup> VI	0.736
Iveco Eurocargo	ISC-Ries	Euro <sup>o</sup> VI	0.570
Scania R450	ISC-Ries	Euro <sup>o</sup> VI	0.220
Scania R450	ISC-Ries	Euro <sup>o</sup> VI	0.259
Volvo FL280	ISC-Ries	Euro <sup>o</sup> VI	0.141
Volvo FL280	ISC-Ries	Euro <sup>o</sup> VI	0.038

Table 26 illustrates the emission factors for all vehicle categories elaborated for the non-regulated pollutants N<sub>2</sub>O and NH<sub>3</sub> for the HBEFA 4.1 (see section 7.7).

**Table 26: Emission factors elaborated for non-regulated pollutants N<sub>2</sub>O and NH<sub>3</sub> for the HBEFA 4.1**

Size class	Road Category	Energy consumption [kWh/km]	Emission factor N <sub>2</sub> O [mg/km]	Emission factor NH <sub>3</sub> [mg/km]
RT < 7.5t	MW	1.8	406.1	7.6
RT > 7.5–12t	MW	2.0	455.0	8.5
RT > 12-14t	MW	2.1	479.0	9.0
RT > 14-20t	MW	2.3	524.6	9.8
RT > 20-26t	MW	2.7	617.6	11.6
RT > 26-28t	MW	3.0	701.7	31.2
RT > 28-32t	MW	3.3	756.4	14.2
RT > 32t	MW	3.4	791.7	14.9
TT/AT > 20-28t	MW	2.4	544.8	10.2
TT/AT > 28-34t	MW	2.9	678.9	12.7
TT/AT > 34-40t	MW	3.2	747.2	14.0
RT < 7.5t	Rural	1.5	351.1	6.6
RT > 7.5–12t	Rural	1.7	404.8	7.6

Size class	Road Category	Energy consumption [kWh/km]	Emission factor N <sub>2</sub> O [mg/km]	Emission factor NH <sub>3</sub> [mg/km]
RT > 12-14t	Rural	1.9	441.3	8.3
RT > 14-20t	Rural	2.1	493.9	9.3
RT > 20-26t	Rural	2.6	599.5	11.2
RT > 26-28t	Rural	2.9	668.1	12.5
RT > 28-32t	Rural	3.2	731.4	13.7
RT > 32t	Rural	3.3	772.6	14.5
TT/AT > 20-28t	Rural	2.2	514.8	9.7
TT/AT > 28-34t	Rural	2.9	676.7	12.7
TT/AT > 34-40t	Rural	3.2	751.2	14.1
RT < 7.5t	Urban	1.5	340.0	6.4
RT > 7.5-12t	Urban	1.9	448.1	8.4
RT > 12-14t	Urban	2.3	524.7	9.8
RT > 14-20t	Urban	2.8	642.6	12.1
RT > 20-26t	Urban	3.6	831.2	15.6
RT > 26-28t	Urban	3.9	901.6	16.9
RT > 28-32t	Urban	4.4	1010.6	19.0
RT > 32t	Urban	4.7	1083.4	20.3
TT/AT > 20-28t	Urban	2.9	667.5	12.5
TT/AT > 28-34t	Urban	4.1	941.1	17.7
TT/AT > 34-40t	Urban	4.7	1086.4	20.4
TT/AT > 40-50t	MW	3.7	852.3	16.0
TT/AT > 40-50t	Rural	3.7	856.9	16.1
TT/AT > 40-50t	Urban	5.3	1239.3	32.2
TT/AT > 50-60t	MW	4.6	1056.1	19.8
TT/AT > 50-60t	Rural	4.7	1086.5	20.4
TT/AT > 50-60t	Urban	7.0	1621.9	30.4
TT/AT ≤7,5t	MW	1.8	406.1	7.6
TT/AT >7,5t-14t	MW	2.1	479.0	9.0
TT/AT >14-20t	MW	2.3	524.6	9.8
TT/AT ≤7,5t	Rural	1.5	351.1	6.6
TT/AT >7,5t-14t	Rural	1.9	441.3	8.3
TT/AT >14-20t	Rural	2.1	493.9	9.3
TT/AT ≤7,5t	Urban	1.5	340.0	6.4
TT/AT >7,5t-14t	Urban	2.3	524.7	9.8
TT/AT >14-20t	Urban	2.8	642.6	12.1
Coach Std ≤18t Euro-VI	MW	2.6	599.4	11.2
Coach 3-Axes >18t Euro-VI	MW	2.9	674.1	12.6

Size class	Road Category	Energy consumption [kWh/km]	Emission factor N <sub>2</sub> O [mg/km]	Emission factor NH <sub>3</sub> [mg/km]
Coach Std <=18t Euro-VI	Rural	2.3	543.2	10.2
Coach 3-Axes >18t Euro-VI	Rural	2.7	625.7	11.7
Coach Std <=18t Euro-VI	Urban	3.5	807.9	15.2
Coach 3-Axes >18t Euro-VI	Urban	4.1	950.8	17.8
UBus Midi <=15t Euro-VI	MW	2.1	493.7	9.3
UBus Std >15-18t Euro-VI	MW	2.5	584.0	11.0
UBus Artic >18t Euro-VI	MW	3.1	728.5	13.7
UBus Midi <=15t Euro-VI	Rural	2.4	555.2	10.4
UBus Std >15-18t Euro-VI	Rural	3.0	702.2	13.2
UBus Artic >18t Euro-VI	Rural	4.1	944.0	17.7
UBus Midi <=15t Euro-VI	Urban	3.0	696.5	13.1
UBus Std >15-18t Euro-VI	Urban	4.0	937.2	17.6
UBus Artic >18t Euro-VI	Urban	5.5	1285.1	24.1

Table 27 illustrates the emission limits and emission factors in g/km and in g/kWh for a Euro<sup>o</sup>VI tractor trailer combination half loaded in the German aggregated traffic situation. These values were illustrated in normalised form in Figure 83.

**Table 27: EFAs, TT 34–40t half loaded, average German traffic situation, Euro<sup>o</sup>VI**

Objective	CO	HC	NO <sub>x</sub>	PN	Work per distance [kWh/km]
Limit value ISC	6	0.24	0.69	6.0E11	-
EFA [g/km]	0.215	0.027	0.491	6.77E10	1.35
EFA [g/kWh]	0.160	0.020	0.364	5.01E10	-

## Index of figures

Figure 1: Principle scheme of an exhaust after-treatment system of HDVs .....	8
Figure 2: NO <sub>x</sub> emission factors for a EURO <sup>o</sup> VI tractor trailer combination 34-40t HL .....	10
Figure 3: Workflow for the creation of emission factors for the HBEFA .....	11
Figure 4: Engine operating points – WHVC and ISC cycle .....	14
Figure 5: Vehicle speed and road gradient – ISC measurement on the “Ries” route .....	15
Figure 6: Regulated pollutants compared to the respective limit value – WHVC measurement results of 8 Euro <sup>o</sup> VI vehicles .....	17
Figure 7: NO <sub>x</sub> TP emissions and normalised engine power of EURO <sup>o</sup> VI HDVs – total ISC. 18	
Figure 8: NO <sub>x</sub> TP emissions and vehicle mileage of EURO <sup>o</sup> VI HDVs – total ISC .....	19
Figure 9: NO <sub>x</sub> TP emissions and normalised engine power of EURO <sup>o</sup> VI HDVs – urban part of ISC .....	20
Figure 10: NO <sub>x</sub> TP emissions and normalised engine power of EURO <sup>o</sup> VI HDVs – motorway part of ISC .....	20
Figure 11: NO <sub>x</sub> TP emissions and normalised engine power of 8 different EURO <sup>o</sup> VI HDVs – HBEFA Stop&Go measurements, 30 minutes idling and 10 minutes at 80 km/h as preconditioning.....	21
Figure 12: NO <sub>x</sub> EO and TP emissions of EURO <sup>o</sup> VI HDVs – HBEFA Stop&Go measurements, 30 minutes idling as preconditioning .....	22
Figure 13: CVS system of the dynamometer of the IVT Graz.....	24
Figure 14: Test case, emission mass flow at position E (engine outlet) .....	24
Figure 15: Test case, emission mass flow at position C (mixing point with dilution air).....	25
Figure 16: Test case, emission mass flow at position B (sampling point in CVS tunnel) .....	25
Figure 17: Test case, emission concentration as measured by an analyser at position A .....	26
Figure 18: Principle of pushing packets through the undiluted section .....	28
Figure 19: Division into partial volume sections .....	28
Figure 20: Mass curve, illustration of various packet volumes in the undiluted system .....	29
Figure 21: Overlapping of packets while dynamic time shift .....	30
Figure 22: Assignment of emission masses for volume packets only partly released out of the pipe .....	30
Figure 23: Assignment of emission masses with variable time shift .....	32
Figure 24: Evaluation of a test measurement representing a step response test .....	33
Figure 25: Comparison of CO <sub>2</sub> emission mass flow with engine power for an emission test at a chassis dyno with emission sampling in diluted exhaust (CVS system).....	33
Figure 26: Engine power – CO <sub>2</sub> regression for an emission test at a chassis dyno with emission sampling in diluted exhaust (CVS system).....	34
Figure 27: Comparison of CO <sub>2</sub> emissions on the drag curve.....	35
Figure 28: Comparison of variable and constant time shift method for a PEMS measurement .....	35

Figure 29: Volume determination (exhaust system + CVS connection pipe) based on the results of the short test.....	36
Figure 30: Coherence of response characteristic.....	37
Figure 31: Scheme of the PHEM model .....	39
Figure 32: Scheme of the PHEM model for temperature simulation in the exhaust after-treatment.....	40
Figure 33: Quasi-stationary temperatures at turbocharger .....	41
Figure 34: Temperature downstream TC – simulation and measurement .....	41
Figure 35: Temperature upstream SCR – simulation and measurement.....	42
Figure 36: Principle of the standard SCR model in PHEM .....	43
Figure 37: Standard SCR model – comparison of measurement and simulation.....	44
Figure 38: On-road trip – AdBlue dosing and temperature upstream of the SCR.....	45
Figure 39: Principle of the SCR model with NH <sub>3</sub> storage function in PHEM.....	48
Figure 40: Standard SCR and NH <sub>3</sub> storage model – comparison of measurement and simulation.....	48
Figure 41: Exhaust gas temperature and vehicle speed – on-road Stop&Go cycle .....	49
Figure 42: Exhaust gas temperature and vehicle speed – HBEFA Stop&Go cycle.....	49
Figure 43: Comparison of engine speed – measurement and simulation.....	51
Figure 44: Gear shift curves – gear shift model HBEFA 4.1 .....	52
Figure 45: Deviation in gear selection – gear shift model HBEFA 3 and 4.1 .....	53
Figure 46: Engine speed simulation – comparison of existing gear shift methods for CBs ....	54
Figure 47: Engine operating points and possible shift curves for CBs .....	55
Figure 48: Engine speed simulation – comparison of adapted gear shift methods for CBs ....	56
Figure 49: Euro <sup>o</sup> VI engine map, 325 kW, 12.7 litre – brake specific fuel consumption.....	60
Figure 50: Average engine emission map – brake specific CO emissions for EURO <sup>o</sup> VI engines.....	62
Figure 51: Brake specific NO <sub>x</sub> EO emissions – ISC measurement results, Euro <sup>o</sup> VI .....	63
Figure 52: EGR+SCR Euro <sup>o</sup> VI engine emission map – brake specific NO <sub>x</sub> EO emissions....	64
Figure 53: SCR only Euro <sup>o</sup> VI engine emission map – brake specific NO <sub>x</sub> EO emissions.....	64
Figure 54: Brake specific NO <sub>x</sub> TP emissions – ISC measurement results, Euro <sup>o</sup> VI.....	65
Figure 55: NO <sub>x</sub> EO emission factors – EGR + SCR vehicles and SCR-only vehicles, Euro <sup>o</sup> VI .....	66
Figure 56: Average Euro <sup>o</sup> VI engine emission map – brake specific NO <sub>x</sub> EO emissions.....	67
Figure 57: Average engine map – exhaust gas temperature EO .....	68
Figure 58: Excerpt of the Euro <sup>o</sup> VI SCR conversion map based on TUG data .....	69
Figure 59: Excerpt of the EURO <sup>o</sup> VI SCR conversion map adjusted to the complete Euro <sup>o</sup> VI HGVS data.....	73
Figure 60: NO <sub>x</sub> results for HBEFA 4.1 and measurement data of TU Graz and AVL MTC ..	74

Figure 61: Excerpt of the EURO <sup>0</sup> VI SCR conversion map adjusted to the Euro <sup>0</sup> VI CB data	75
Figure 62: CB NO <sub>x</sub> emissions, aggregated traffic situation “urban driving – Germany” – HBEFA 4.1 model adjusted to CB measurements .....	75
Figure 63: Average Euro <sup>0</sup> VI (HDV) and Euro <sup>6</sup> (LDV) NO <sub>x</sub> results for one ISC route .....	76
Figure 64: RT <7.5t HL Euro <sup>0</sup> V EGR and Euro <sup>0</sup> VI – NO <sub>x</sub> TP results for German traffic mix .....	77
Figure 65: NO <sub>x</sub> TP emissions and vehicle mileage of EURO <sup>0</sup> VI HDVs separated into brands – total ISC.....	78
Figure 66: Average „new“ and average „old“ vehicle – linear trend line.....	79
Figure 67: Deterioration functions – urban, rural, motorway and total .....	80
Figure 68: NO <sub>x</sub> deterioration function – determination of the mileage at the excess of the OBD limit.....	81
Figure 69: NO <sub>x</sub> deterioration function for HDV .....	81
Figure 70: Average engine map – brake specific NH <sub>3</sub> emissions (only for demonstration, not used for emission factors) .....	83
Figure 71: Average engine map – brake specific N <sub>2</sub> O emissions (for demonstration only, not used for emission factors) .....	84
Figure 72: NH <sub>3</sub> emission factors for RT > 14-20t and TT/AT > 34-40t.....	85
Figure 73: N <sub>2</sub> O emission factors for RT > 14-20t and TT/AT > 34-40t.....	86
Figure 74: NO <sub>x</sub> -TP emissions, HGV TT 34–40t half loaded, 0 % gradient – same main cycle, different preconditioning cycles.....	88
Figure 75: Comparison of NO <sub>x</sub> emissions in the same traffic situations in the HBEFA 3.3 and 4.1, HGV TT 34–40t Euro <sup>0</sup> VI half loaded, 0 % gradient .....	90
Figure 76: Comparison of vehicle speed in the traffic situations “Stop&Go*” in the HBEFA 3.3 and the same one in the HBEFA 4.1, HGV TT 34–40t Euro <sup>0</sup> VI half loaded, 0 % gradient.....	91
Figure 77: Comparison of the vehicle speed in the same traffic situations in the HBEFA 3.3 and 4.1, HGV TT 34–40t Euro <sup>0</sup> VI half loaded, 0 % gradient.....	91
Figure 78: FC, TT 34–40t half loaded, average German traffic situation, Euro <sup>0</sup> to Euro <sup>0</sup> VI	93
Figure 79: CO, TT 34–40t half loaded, average German traffic situation, Euro <sup>0</sup> to Euro <sup>0</sup> VI	94
Figure 80: HC, TT 34–40t half loaded, average German traffic situation, Euro <sup>0</sup> to Euro <sup>0</sup> VI	94
Figure 81: NO <sub>x</sub> , TT 34–40t half loaded, average German traffic situation, Euro <sup>0</sup> to Euro <sup>0</sup> VI .....	95
Figure 82: PN, TT 34–40t half loaded, average German traffic situation, Euro <sup>0</sup> to Euro <sup>0</sup> VI	95
Figure 83: Comparison of EFAs with ISC regulatory limits, TT 34–40t half loaded, average German traffic situation, Euro <sup>0</sup> VI.....	96
Figure 84: FC, RT < 7.5t half loaded, average German traffic situation, Euro <sup>0</sup> to Euro <sup>0</sup> VI.	97
Figure 85: NO <sub>x</sub> , RT < 7.5t half loaded, average German traffic situation, Euro <sup>0</sup> to Euro <sup>0</sup> VI	97
Figure 86: FC, CO > 18t half loaded, average German traffic situation, Euro <sup>0</sup> to Euro <sup>0</sup> VI..	98
Figure 87: NO <sub>x</sub> , CO > 18t half loaded, average German traffic situation, Euro <sup>0</sup> to Euro <sup>0</sup> VI	99

---

Figure 88: FC, CB > 18t half loaded, average German traffic situation, Euro <sup>0</sup> to Euro <sup>VI</sup>	100
Figure 89: NO <sub>x</sub> , CB > 18t half loaded, average German traffic situation, Euro <sup>0</sup> to Euro <sup>VI</sup> .....	100
Figure 90: SCR conversion map – Euro <sup>VI</sup> HGV .....	112
Figure 91: SCR conversion map – Euro <sup>VI</sup> CBs .....	113
Figure 92: SCR conversion map – Euro <sup>VI</sup> HGV < 7.5 tons .....	114

## Index of tables

Table 1: Emission limits for HDVs [9] .....	5
Table 2: Chassis dyno test program at TU Graz .....	13
Table 3: On-road test program at TU Graz .....	14
Table 4: ISC trip – share of road categories [10] .....	15
Table 5: Number of conventional HDVs with instantaneous test data used for setup and calibration of PHEM models (numbers: new data for HBEFA 4.1, numbers in brackets: measured HDV already included in HBEFA 3.2 [25]) .....	16
Table 6: Overview of Euro <sup>o</sup> VI regulatory emission limits in the WHTC .....	16
Table 7: Unregulated pollutants – WHVC measurement results .....	22
Table 8: Definition of the gear shift curves for the HBEFA 4.1 .....	52
Table 9: New vehicle registrations in EU-28 for HDVs [53] .....	57
Table 10: Number of measured HDVs used for the creation of the HBEFA 4.1 simulation models .....	58
Table 11: Vehicle specifications for averages of HDV classes Euro <sup>o</sup> VI 2014 [23] .....	59
Table 12: Fuel consumption ratios of engine generations and average model year per EURO class .....	60
Table 13: Source allocation per emission component for PHEM emission maps .....	61
Table 14: NH <sub>3</sub> and N <sub>2</sub> O brake specific emissions for the WHVC .....	85
Table 15: Impact of changes between HBEFA 3.3 and 4.1, HGV TT 34–40t Euro <sup>o</sup> VI half loaded, German traffic mix .....	89
Table 16: Impact of changes between HBEFA 3.3 and 4.1, HGV TT 34–40t Euro <sup>o</sup> V half loaded, German traffic mix .....	92
Table 17: Different steps of Euro <sup>o</sup> VI and corresponding amendments for ISC tests .....	108
Table 18: Specifications of EURO <sup>o</sup> 5 Diesel vehicles used for the emission maps in PHEM108	
Table 19: Specifications of EURO <sup>o</sup> 6 Diesel vehicles used for the emission maps in PHEM108	
Table 20: Specifications of EURO <sup>o</sup> VI Diesel vehicles used for the emission maps in PHEM .....	108
Table 21: Specifications of EURO <sup>o</sup> V EEV Diesel vehicles analysed for deterioration effects .....	109
Table 22: Specifications of EURO <sup>o</sup> VI Diesel vehicles used for deterioration function .....	109
Table 23: WHVC measurement results – chassis dyno TUG .....	110
Table 24: Single NO <sub>x</sub> test and simulation results – validation of SCR simulation models ...	110
Table 25: Single test NO <sub>x</sub> ISC-Ries results – comparison Euro <sup>o</sup> 6 and Euro <sup>o</sup> VI .....	115
Table 26: Emission factors elaborated for non-regulated pollutants N <sub>2</sub> O and NH <sub>3</sub> for the HBEFA 4.1 .....	115
Table 27: EFAs, TT 34–40t half loaded, average German traffic situation, Euro <sup>o</sup> VI .....	117